

# **Geomorphic Landform Design to Optimize Impoundment Closure**

OSMRE Cooperative Agreement Number: S21AC10058

Draft Final Report

## **Principle Authors**

Dr. John D. Quaranta, P.E., Principal Investigator

Dr. Leslie Hopkinson., Co-Principal Investigator

Jason Fillhart, Co-Principal Investigator

## **Graduate Students**

Zainab Jawad, MSCE

Amanda Rodrigues Silva, MSCE

Titus Smith, MSCE

(April 2024)

Wadsworth Department of Civil and Environmental Engineering  
Benjamin M. Statler College of Engineering and Mineral Resources  
West Virginia University  
P.O. Box 6103  
Morgantown, WV 26506-6103

## **DISCLAIMER**

This report was prepared as an account of work sponsored by an agency of the United States Government. Neither the United States Government nor any agency thereof, nor any of their employees, makes any warranty, express or implied, or assumes any legal liability or responsibility for the accuracy, completeness, or usefulness of any information, apparatus, product, or process disclosed, or represents that its use would not infringe privately owned rights. Reference herein to any specific commercial product, process, or service by trade name, trademark, manufacturer, or otherwise does not necessarily constitute or imply its endorsement, recommendation, or favoring by the United States Government or any agency thereof. The views and opinions of authors expressed herein do not necessarily state or reflect those of the United States Government or any agency thereof.

## **ABSTRACT**

Restoration of abandoned mine lands from bond forfeited mining permits and pre-law sites is ongoing in Appalachia and across the United States. One potential reclamation technique to reclaim these areas is geomorphic landforming also termed geomorphic landform design (GLD). The geomorphic approach attempts to approximate the long-term, steady state landform condition, leading to reduced erosional adjustment as compared to standard engineered designs. The objectives of this research were to apply geomorphic landform design principles to investigate closure design alternatives at an abandoned high hazard water impounding coal refuse facility. Multiple design variations were applied to two existing impoundments identified with the help of the WVDEP. The designs were evaluated, considering geotechnical stability and hydrologic function. In addition, field evaluations of coal impoundment were conducted and geotechnical material classifications of impoundment tailings were determined.

# GRAPHICS MATERIAL LIST

## Table of Contents

Disclaimer .....	2
Abstract .....	3
Graphics Material List .....	4
Introduction.....	11
Executive Summary .....	12
Experimental .....	14
Coal impoundment site evaluation.....	14
Tailings geotechnical material classifications .....	16
Carlson Natural Regrade.....	16
Finite Element Modeling using PLAXIS LE.....	16
Material Properties for Modeling.....	17
Time Rate of Consolidation .....	18
Federal No. 2 FCR Material Classification.....	19
Model Geometry .....	21
Groundwater Analysis .....	21
Slope Stability Analysis.....	21
Consolidation Analysis .....	23
Geomorphic reclamation and evaluation for Century Impoundment .....	24
Area Description .....	24
Geomorphic landform design .....	24
Hydrologic Analysis .....	26
Geomorphic reclamation and evaluation for Federal Mine #2 .....	28
Study Area .....	28
Series of Conceptual Reclamation Designs .....	29
Evaluation of reclamation designs.....	33
Results and Discussion .....	36
Coal impoundment site evaluation.....	36
Site Visit- Century Impoundment.....	37
Site Visit- Federal No. 2 .....	41
Site Visit- Rockcamp Branch, Peerless Eagle, & #1 Refuse Area .....	44
Site Visit- Knight Ink, Cowen Trench, & North Point .....	51



Tailings geotechnical material classifications .....	58
Finite Element Modeling for Century Impoundment .....	63
Century Pre-reclamation Impoundment.....	63
Century Reclaimed Impoundment .....	69
GLD Reclaimed Impoundment.....	76
Finite Element Modeling for Federal No. 2.....	82
Federal No. 2 Active Impoundment.....	82
Federal No. 2 GLD Reclaimed Impoundment.....	89
Geomorphic reclamation and evaluation for Century Impoundment .....	104
One-basin impoundment designs .....	104
Two-basin impoundment designs .....	108
Three-subbasin impoundment designs.....	111
Watershed designs .....	114
Hydrologic analysis .....	117
Discussion.....	123
Geomorphic reclamation and evaluation for Federal Mine No. 2 .....	125
Conceptual Reclamation Designs .....	125
Slope Analysis .....	129
Material Movement.....	130
Hydrologic Response Evaluation.....	132
Conclusion .....	133
Coal impoundment site evaluation.....	133
Finite Element Modeling of Century Impoundment.....	136
Geomorphic reclamation and evaluation for Century Impoundment .....	136
Geomorphic reclamation and evaluation for Federal Mine #2 .....	137
References.....	139

## List of Tables

Table 1. Field Check List (Constructed but unused in this research).	15
Table 2. Soil tests and the corresponding ASTM Standard.	16
Table 3. Initial material property inputs.	17
Table 4. Final Material Properties.	18
Table 5. Air-dried FCR summary.	19
Table 6. Oven dried FCR summary.	19
Table 7. Design description summary.	24
Table 8. Input values by design criteria.	26
Table 9. Channels information summary for channel routing of the 3-subbasins models.	28
Table 10. Natural Regrade Input Parameters.	31
Table 11. Summary of Conceptual Reclamation Designs.	33
Table 12. Visited Impoundments.	36
Table 13. FCR Sample 1 Properties.	59
Table 14. FCR Sample 2 Properties.	59
Table 15. CCR Sample 1 Properties.	60
Table 16. CCR Sample 2 Properties.	60
Table 17. FCR and CCR Average Sample Properties.	60
Table 18. Results comparison.	62
Table 19. Pre-reclamation model results.	67
Table 20. WVDEP Reclaimed model results, factor of safety.	71
Table 21. GLD reclamation model results (2 subbasin DePriest).	79
Table 22. GLD reclamation model results (3 subbasin DePriest).	81
Table 23. Active impoundment modeling results.	85
Table 24. Case 1 modeling results.	94
Table 25. Case 2 modeling results.	95
Table 26. Case 3 modeling results.	96
Table 27. Case 4 modeling results.	97
Table 28. Case 5 modeling results.	101
Table 29. Summary of designs for 1 subbasin in the impoundment area.	105
Table 30. Summary of designs for 2 subbasins in the impoundment area.	109
Table 31. Summary of results for 3 subbasins in the impoundment area.	112
Table 32. Summary of designs for the watershed-based designs.	115
Table 33. Hydrologic analysis summary results for impoundment designs.	118
Table 34. Hydrologic analysis summary results for watershed area designs.	118
Table 35. Design characteristics for sub-basins 1 for all created designs.	129
Table 36. Design characteristics for sub-basins 2 for all created designs.	129
Table 37. Slope analysis of six created designs.	130
Table 38. Earthmoving quantities summary.	130
Table 39. Hydrologic analysis summary 100-year, 24-hr. storm event: sub-basins 1 and 2, and 500-year, 24-hr. storm event: sub-basins 1 and 2.	132
Table 40: Observations across site visits.	135

## Table of Figures

Figure 1. e log p curve for Fine Coal Refuse.....	18
Figure 2. Grain Size Distribution of Air-dried FCR.....	20
Figure 3. Grain Size Distribution of Oven dried FCR.....	20
Figure 4. Toe Grid and Tangent.....	22
Figure 5. Mid-slope Grid and Tangent .....	22
Figure 6. Crest Grid and Tangent. ....	22
Figure 7. Upstream Grid and Tangent. ....	23
Figure 8. Deep Foundation Grid and Tangent. ....	23
Figure 9. Impoundment area subbasins layouts: (a) one subbasin, (b) two subbasins, and (c) three subbasins.....	25
Figure 10. a) Location and b) aerial image of the study site (source: Google Earth). ....	29
Figure 11. Design area footprint used for the following design iterations: a) conventional design (i.e., Conventional and Conventional-GLD), and b) geomorphic design iterations (i.e., Uniform-50, Uniform-90, Two-elevated areas).....	30
Figure 12. A hypothetical mid-ridgeline extending from the headwater to the other end close to the dam with surface elevations in ft. ....	31
Figure 13. a) A soil map for the area surrounding the slurry impoundment; b) drainage area (boundary) defined in the hydrologic computer analysis; and c) runoff pathways within the defined two sub-basins.....	35
Figure 14. Visited Impoundments.....	37
Figure 15. Aerial Image from 2013 showing Century Impoundment prior to reclamation.....	38
Figure 16. Aerial Image from 2020 showing Century Impoundment during reclamation. ....	38
Figure 17. Filled-in slurry pool.....	39
Figure 18. Reclaimed downstream embankment.....	40
Figure 19. View of downstream embankment.....	40
Figure 20. Aerial Image from 2022 showing impoundment prior to reclamation.....	42
Figure 21. Slurry impoundment reservoir.....	42
Figure 22. Beach of fine and course coal refuse pushout on upstream face. ....	43
Figure 23. Interface between beach and reservoir. ....	43
Figure 24. Aerial Image from 1990 showing impoundment prior to reclamation.....	44
Figure 25. Aerial Image from 2022 showing impoundment after reclamation. ....	45
Figure 26. O002184 Reclaimed impoundment.....	45
Figure 27. Aerial Image from 2022 showing active impoundment. ....	46
Figure 28. O301286 Active impoundment. ....	46
Figure 29. Aerial Image from 1997 showing impoundment prior to reclamation.....	47
Figure 30. Aerial Image from 2022 showing impoundment after reclamation. ....	47
Figure 31. R070700 Reclaimed impoundment. ....	48
Figure 32. R070700 Access Road.....	49
Figure 33. R070700 Access Road and vegetated contact ditch. ....	49
Figure 34. R070700 Differential settlement of impoundment cap. ....	50
Figure 35. R070700 Grouted riprap.....	50
Figure 36. ARCH Resources base map.....	51
Figure 37. Aerial Image from 2010 showing impoundment prior to reclamation.....	52
Figure 38. Aerial Image from 2022 showing impoundment after reclamation. ....	52
Figure 39. S201988 reclaimed impoundment.....	53

Figure 40. Aerial Image from 1997 showing impoundment prior to reclamation.....	53
Figure 41. Aerial Image from 2022 showing impoundment after reclamation. ....	54
Figure 42. S003576 reclaimed impoundment.....	54
Figure 43. Aerial Image from 2016 showing impoundment prior to reclamation.....	55
Figure 44. Aerial Image from 2022 showing impoundment after reclamation. ....	55
Figure 45. S024076 reclaimed impoundment.....	56
Figure 46. S003576 Standing water.....	57
Figure 47. S024076 Eroded hillside adjoining open channel ditch. ....	58
Figure 48. FCR and CCR grain size distribution.....	61
Figure 49. Grain size distribution of coal refuse comparison.....	63
Figure 50. Top view of historical impoundment. ....	64
Figure 51. Historical impoundment parameters.....	65
Figure 52. Additional design specification of historical impoundment.....	65
Figure 53. Pre-reclamation impoundment centerline cross section. ....	66
Figure 54. Century pre-reclamation singular 100-year seepage output.....	68
Figure 55. Century pre-reclamation auto singular 100-year.....	68
Figure 56. Century pre-reclamation repeating 100-year seepage output.....	69
Figure 57. Century pre-reclamation auto repeating 100-year.....	69
Figure 58. WVDEP reclaimed impoundment layout.....	70
Figure 59. Cut and fill design cross section for reclaimed site.....	70
Figure 60. Reclaimed impoundment centerline cross section. ....	71
Figure 61. WVDEP reclaimed singular 100-year seepage output. ....	72
Figure 62. WVDEP reclaimed auto singular 100-year.....	72
Figure 63. WVDEP reclaimed repeating 100-year seepage output.....	72
Figure 64. WVDEP reclaimed auto repeating 100-year.....	73
Figure 65. 5-ft mound load on top of fine coal refuse.....	73
Figure 66. y-displacement results for 5-ft mound after 2000 days.....	74
Figure 67. y-displacement results for 15-ft mound after 2000 days.....	74
Figure 68. y-displacement for 30-ft mound after 2000 days.....	74
Figure 69. y-displacement with 5-ft pressure head.....	75
Figure 70. y-displacement with 15-ft pressure head.....	75
Figure 71. y-displacement with 30-ft pressure head.....	76
Figure 72. GLD 1 subbasin design.....	77
Figure 73. GLD 2 subbasin design.....	77
Figure 74. GLD 3 subbasin design.....	78
Figure 75. GLD 2 and 3 subbasin design profiles.....	78
Figure 76. 2 subbasin DePriest singular 100-year seepage output.....	79
Figure 77. 2 subbasin DePriest deep foundation singular 100-year.....	80
Figure 78. 2 subbasin DePriest repeating 100-year seepage output.....	80
Figure 79. 2 subbasin DePriest deep foundation repeating 100-year.....	80
Figure 80. 3 subbasin DePriest singular 100-year seepage output.....	81
Figure 81. 3 subbasin DePriest deep foundation singular 100-year.....	81
Figure 82. 3 subbasin DePriest repeating 100-year seepage output.....	82
Figure 83. 3 subbasin DePriest deep foundation repeating 100-year.....	82
Figure 84. Overall base map.....	83
Figure 85. Zoomed in base map.....	84

Figure 86. Base map with contour data. ....	84
Figure 87. Federal No. 2 centerline existing ground profile and model. ....	85
Figure 88. Active Federal No. 2 singular 100-year seepage output.....	86
Figure 89. Active Federal No. 2 auto singular 100-year.....	86
Figure 90. Active Federal No. 2 repeating 100-year seepage output.....	86
Figure 91. Active Federal No. 2 auto repeating 100-year.....	87
Figure 92. 5-ft mound load on top of fine coal refuse. ....	87
Figure 93. y-displacement for 5-ft mounded after 2,000 days.....	88
Figure 94. y-displacement for 15-ft mounded after 2,000 days.....	88
Figure 95. y-displacement for 30-ft mounded after 2,000 days.....	88
Figure 96. y-displacement for 5-ft of water head after 2,000 days.....	89
Figure 97. y-displacement for 15-ft of water head after 2,000 days.....	89
Figure 98. y-displacement for 30-ft of water head after 2,000 days.....	89
Figure 99. GLD 2 subbasin ridge design (Case 1).....	90
Figure 100. GLD 2 subbasin impoundment design (Case 2).....	91
Figure 101. GLD Profile Cases (Part 1).....	92
Figure 102. GLD Profile Cases (Part 2).....	93
Figure 103. Case 1 singular 100-year seepage output. ....	94
Figure 104. Case 1 auto singular 100-year. ....	94
Figure 105. Case 1 repeating 100-year seepage output. ....	94
Figure 106. Case 1 auto repeating 100-year. ....	95
Figure 107. Case 2 singular 100-year seepage output. ....	95
Figure 108. Case 2 auto singular 100-year. ....	95
Figure 109. Case 2 repeating 100-year seepage output. ....	96
Figure 110. Case 2 auto repeating 100-year. ....	96
Figure 111. Case 3 singular 100-year seepage output. ....	96
Figure 112. Case 3 auto singular 100-year. ....	97
Figure 113. Case 3 repeating 100-year seepage output. ....	97
Figure 114. Case 3 auto repeating 100-year. ....	97
Figure 115. Case 4 singular 100-year seepage output. ....	98
Figure 116. Case 4 auto singular 100-year. ....	98
Figure 117. Case 4 auto singular 100-year along mound. ....	98
Figure 118. Case 4 auto singular 100-year along dam.....	99
Figure 119. Case 4 repeating 100-year seepage output. ....	99
Figure 120. Case 4 auto repeating 100-year. ....	100
Figure 121. Case 4 auto repeating 100-year along mound. ....	100
Figure 122. Case 4 auto repeating 100-year along dam.....	101
Figure 123. Case 5 singular 100-year seepage output. ....	101
Figure 124. Case 5 auto singular 100-year. ....	102
Figure 125. Case 5 auto singular 100-year along mound. ....	102
Figure 126. Case 5 auto singular 100-year along dam.....	102
Figure 127. Case 5 repeating 100-year seepage output. ....	103
Figure 128. Case 5 auto repeating 100-year. ....	103
Figure 129. Case 5 auto repeating 100-year along mound. ....	103
Figure 130. Case 5 auto repeating 100-year along dam.....	104
Figure 131. I-Def-1 designed contour lines. ....	105

Figure 132. Three-dimensional geomorphic design: I-Def-1. ....	106
Figure 133. I-DP-1 designed contour lines. ....	107
Figure 134. Three-dimensional geomorphic design: I-DP-1. ....	108
Figure 135. I-Def-2 designed contour lines. ....	109
Figure 136. Three-dimensional I-Def-2 design view.....	110
Figure 137. I-DP-2 designed contour lines. ....	110
Figure 138. Three-dimensional I-DP-2.....	111
Figure 139. I-Def-3 designed contour lines. ....	112
Figure 140. Three-dimensional I-Def-3 design view.....	113
Figure 141. I-DP-3 designed contour lines. ....	113
Figure 142. Three-dimensional I-DP-3 design view.....	114
Figure 143. W-Def-1 designed contour lines.....	115
Figure 144. Three-dimensional W-Def-1 design view. ....	116
Figure 145. Three-dimensional W-DP-1 design.....	116
Figure 146. Three-dimensional geomorphic design: W-DP-1.....	117
Figure 147. Runoff hydrograph for impoundment area design considering 1 subbasin. (a)100-yr storm; (b) 500-yr storm. ....	119
Figure 148. Runoff hydrograph for the impoundment area design considering 2 subbasin. (a)100-yr storm; (b) 500-yr storm.....	120
Figure 149. Runoff hydrograph for the impoundment area design considering 3 subbasins. (a)100-yr storm; (b) 500-yr storm. ....	121
Figure 150. Runoff hydrograph for design considering the whole watershed area. (a)100-yr storm; (b) 500-yr storm. ....	122
Figure 151. Alternative designs keeping embankment structure. (a) 2-subbasins; and (b) 4-subbasins. ....	124
Figure 152. Designed surface with contour elevations in ft.: a) Uniform-200, b) Uniform-50, c) Uniform-90, d) T-E, e) Conventional, and f) Conventional-GLD.....	128
Figure 153. Cut (red hatches) and fill zones (blue hatches): a) Uniform-50, b) Uniform-90, c) T-E, d) Conventional, and e) Conventional-GLD. ....	131
Figure 154. Runoff hydrographs: 100-year storm event a) sub-basin 1 and b) sub-basin 2 and for the 500-year storm event c) sub-basin 1 and d) sub-basin 2.....	133

## INTRODUCTION

Most of the disposed refuse material resulting from the preparation of coal mining is deposited in these refuse tailings impoundments. Coarse refuse is the waste material used to construct dam structure embankments. The fine coal refuse is a waste which is deposited in the impoundment basin in a wet, slurry form (Michael et al., 2013). In Appalachia, impoundments are usually positioned in headwaters with a community situated downstream (NRC, 2002). Often, these impoundments are redesigned during construction to accommodate additional waste, resulting in increased embankment heights and slurry depths (Michael et al., 2013).

Coal impoundment design and inspection are regulated by 30 § CFR 77.216, 30 § CFR 780.225 and engineering design guidance is documented by D'Appolonia (2009). Monitoring frequency of coal impoundments decrease as the impoundment moves through the stages of active (i.e., receiving waste), inactive (reactivation planned), and abandoned (after closure and reclamation) (Michael et al., 2013; NRC, 2002). During the phase of closure and reclamation, the impoundment surface is graded to shed precipitation towards the perimeter to prevent pool formation and minimize infiltration into the saturated fine coal tailings. The surface is then covered and vegetated, typically with a grass mixture.

Restoration of abandoned mine lands from bond forfeited mining permits and pre-law sites is ongoing in Appalachia and across the United States. One potential reclamation technique to reclaim these areas is geomorphic landforming also termed Geomorphic Landform Design (GLD). The geomorphic approach attempts to approximate the long-term, steady state landform condition, leading to reduced erosional adjustment as compared to standard engineered designs (Toy and Chuse 2005). Reclaimed locations have a series of channels that mimic dendritic drainage of the natural condition. The intent in these acid producing regions is to use the landforming technique to channelize surface water quickly and reduce infiltration, resulting in less acid water that requires long-term treatment.

Since 2010, our team at WVU (Civil and Environmental Engineering and West Virginia Water Research Institute) has been researching the approach of geomorphic landform design for application in Central Appalachia. Recent research accomplishments includes the following: i) conceptual geomorphic landform designs completed on a permitted valley fill; ii) the characterization of mature landforms in southern West Virginia to inform landform design processes; iii) a geotechnical slope stability evaluation of geomorphic landform designs for mountainous terrain; iv) an evaluation of differences in groundwater seepage between conventional and geomorphic landform designs; v) a comparison of hydrologic response; and, vii) applications at a coarse coal refuse pile. (Snyder, 2013; Buckley et al., 2013; Quaranta et al., 2013; Russell and Quaranta, 2013; Sears et al., 2013; DePriest et al., 2014; Hopkinson et al., 2014; O'Leary, 2014; Sears et al., 2014; DePriest et al., 2015; Michael et al., 2015; Hopkinson et al., 2015; Hopkinson et al., 2017; Santos et al., 2023).

The objective of this research was to apply geomorphic landform design (GLD) principles to investigate closure design alternatives at an abandoned high hazard water impounding coal refuse facility. To meet this overall, field evaluations of coal impoundment were conducted, geotechnical material classifications of impoundment tailings were determined, finite element modeling was completed for two sites, and conceptual geomorphic designs for two impoundments were created and evaluated.

## **EXECUTIVE SUMMARY**

Restoration of abandoned mine lands from bond forfeited mining permits and pre-law sites is ongoing in Appalachia and across the United States. One potential reclamation technique to reclaim these areas is geomorphic landforming also termed geomorphic landform design (GLD). The geomorphic approach attempts to approximate the long-term, steady state landform condition, leading to reduced erosional adjustment as compared to standard engineered designs. The objective of this research was to apply geomorphic landform design (GLD) principles to investigate closure design alternatives at an abandoned high hazard water impounding coal refuse facility. To meet this overall, field evaluations of coal impoundment were conducted, geotechnical material classifications of impoundment tailings were determined, finite element modeling was completed for two sites, and conceptual geomorphic designs for two impoundments were created and evaluated.

### Coal impoundment site evaluation

Through contact with the WVDEP, six reclaimed refuse impoundments, one active freshwater impoundment, and one active impoundment were visited to observe site conditions. It was observed that historical reclamation designs and practices work at maintaining a steady slope but are hydraulically imbalanced. Sites more recently reclaimed experience fewer issues but are not defect free. In the years after closure, the unchecked wet zones and differential settlement of the cap, lead to more issues. After losing the ability to retain water, erosion is raised due to the reduced infiltration promoting runoff to an under designed drainage system.

Recommendations for these observations would be subsurface drainage consisting of a corrugated pipe with a geosynthetic to prevent the transportation of fines. Mounded material placed along the cap would also reduce the saturation of the refuse by promoting runoff. Any infiltrated water would have a more delayed release than that of a saturated impoundment. Additional drainage and more robust construction of contact ditches around the perimeter are needed to divert and release water, preventing re-saturation of refuse.

### Tailings geotechnical material classification

The test results were compared to previous work regarding Fine Coal Refuse (FCR) and Coarse Coal Refuse (CCR). Material tests were performed for FCR and CCR from Federal Site #2. There were also several other sources (Smith 2023, Stawovy 2011, Tolikonda 2010, Zeng et al. 2008, Hegazy et al. 2004, and Genes et al. 2000) that indicated the FCR and CCR specimens are comparable.

### Finite element modeling

Conclusions from this work indicate that saturation of the impoundment is the key element in starting and developing issues on site. The application of GLD helps reduce infiltration within the impoundment cap but should be evaluated to ensure the slope does not exceed the angle of response of the material. Carlson Natural Regrade will generate models based on the user inputs and will not maintain slope stability of the material as such. A 3H:1V slope has been proven to maintain the best slope stability across all modeling parameters in this study and would be recommended as the maximum slope grade allowed. Cutting into the existing dam structure



should also be prevented due to the low factor of safety experienced along the downstream toe of the dam. While the failure is shallow, any failure plane will lead to a larger one or the loss of material. Overall, GLD may not be a viable option as compared to the traditional impoundment closure process.

#### Geomorphic reclamation and evaluation for Century Impoundment

Geomorphic landform design principles were applied to impoundment reclamation was applied to a slurry impoundment in Barbour County, West Virginia, USA. A total of eight designs were created by considering the design area, design criteria, and number of basins. The hydrologic response was evaluated and compared with the traditional reclamation method. Different channel configurations were analyzed. The hydrologic response was compared with the traditional reclamation method showing variation in peak flow rate, time to peak, and runoff duration. No large variation in runoff amounts were observed.

#### Geomorphic reclamation and evaluation for Federal Mine #2

Geomorphic landform design principles were applied to a coal mine slurry impoundment structure located in Monongalia County, West Virginia, USA, to generate a design that is stable, hydraulically balanced, and aesthetically appealing. A series of geomorphic designs were created and later submitted to slope analysis, earthwork balance, and hydrologic response analyses. The geomorphic approach to reclaim the reservoir area generated uniform contour lines that resulted in less amount of backfill material needed for the design compared to the conventional reclamation approach. However, no substantial difference in peak runoff discharge was observed when comparing the hydrologic response of the created designs.

## **EXPERIMENTAL**

### **Coal impoundment site evaluation**

Field visits were conducted to assess how the current reclamation process has left many of these structures years after reclamation. These visits reflected the design criteria used at the time of reclamation and the durability of each impoundment as the years passed. Site characterization was determined based on visual observations made from walking reclaimed impoundments and accessing current conditions. A field inspection sheet (Table 1) was developed to indicate measured results in the field but was limited due to the vast space required to cover with each visit.

After reviewing each site visit, a comprehensive analysis and field writeup was performed to state and address the observations made. Speculation of each observation was done after careful review of photographs and site characteristics before any conclusions were drawn. From the conclusions, some alternative design ideas could be implemented with GLD components.

Table 1. Field Check List (Constructed but unused in this research).

Site Conditions						
2	Visit Date:	County:		Company:		
3	Time:	Latitude:		Permit No.:		
4	Weather:	Longitude:		Status:		
Impoundment Dimensions:						
6	Berm Length (ft.):	Impoundment Slope (H:V):		Last Used:		
7	Berm Width (ft.):	Embankment Slope (H:V):		Reclaimed (Y/N):		
Location		Rating System				
Impoundment		Yes/No/Unknown:	Low:	Moderate:	High:	Severe:
10	Tension crack length? (ft.)		0.0-5.0'	5.1-10.0'	10.1-20.0'	20.0'+
11	Settlement distance? (in.)		0.5-1.0"	1.1-2.0"	2.1-3.0"	3.0'+
12	Scarps or slope movement? (ft.)		0.5-2.0'	2.1-4.0'	4.1-8.0'	8.0'+
13	Surface erosion (ft.)		0.0-5.0'	5.1-10.0'	10.1-20.0'	20.0'+
14	Rills/Gullies depth? (in.)		0.5-2.0"	2.1-4.0"	4.1-6.0"	6.0'+
15	Evidence of piping formation?		0.5-2.0"	2.1-4.0"	4.1-6.0"	6.0'+
16	Evidence of seeps with soil loss?		Clear water	Grey water	Murky water	Observed flow rate
17	Wet zones?		1	2	3	4+
18	Ponding water? (ft.)		0.5-5.0'	5.1-10.0'	10.1-25.0'	25.0'+
19	Animal burrows?		1	2	3	4+
20	Trees, tall weeds, or other vegetation?		Grass	Tall Weeds	Brush	Trees
21	Out of place material?		Soil	Garbage	Drainage	Refuse
Embankment		Yes/No:	Low:	Moderate:	High:	Severe:
23	Tension crack length? (ft.)		0.0-5.0'	5.1-10.0'	10.1-20.0'	20.0'+
24	Settlement distance? (in.)		0.5-1.0"	1.1-2.0"	2.1-3.0"	3.0'+
25	Scarps or slope movement? (ft.)		0.5-2.0'	2.1-4.0'	4.1-8.0'	8.0'+
26	Surface erosion (ft.)		0.0-5.0'	5.1-10.0'	10.1-20.0'	20.0'+
27	Rills/Gullies depth? (in.)		0.5-2.0"	2.1-4.0"	4.1-6.0"	6.0'+
28	Depressions, sinkholes, or slides into the impoundment?		1	2	3	4+
29	Evidence of piping formation? (in.)		0.5-2.0"	2.1-4.0"	4.1-6.0"	6.0'+
30	Evidence of seeps with soil loss?		Clear water	Grey water	Murky water	Observed flow rate
31	Wet zones?		1	2	3	4+
32	Animal burrows?		1	2	3	4+
33	Trees, tall weeds, or other vegetation?		Grass	Tall Weeds	Brush	Trees
34	Out of place material?		Soil	Garbage	Drainage	Refuse
35	Emergency spillway drainage system blockage?		0-10%	11-25%	26-35%	35%+
Impoundment Rim		Yes/No:	Low:	Moderate:	High:	Severe:
37	Tension crack length? (ft.)		0.0-5.0'	5.1-10.0'	10.1-20.0'	20.0'+
38	Settlement distance? (in.)		0.5-1.0"	1.1-2.0"	2.1-3.0"	3.0'+
39	Scarps or slope movement? (ft.)		0.5-2.0'	2.1-4.0'	4.1-8.0'	8.0'+
40	Surface erosion (ft.)		0.0-5.0'	5.1-10.0'	10.1-20.0'	20.0'+
41	Rills/Gullies depth? (in.)		0.5-2.0"	2.1-4.0"	4.1-6.0"	6.0'+
42	Depressions, sinkholes, or slides into the impoundment?		1	2	3	4+
43	Evidence of piping formation? (in.)		0.5-2.0"	2.1-4.0"	4.1-6.0"	6.0'+
44	Evidence of seeps with soil loss?		Clear water	Grey water	Murky water	Observed flow rate
45	Wet zones?		1	2	3	4+
46	Animal burrows?		1	2	3	4+
47	Trees, tall weeds, or other vegetation?		Grass	Tall Weeds	Brush	Trees
48	Out of place material?		Soil	Garbage	Drainage	Refuse
Spillway (N/A if reclaimed)		Yes/No:	Low:	Moderate:	High:	Severe:
50	Tension crack length? (ft.)		0.0-5.0'	5.1-10.0'	10.1-20.0'	20.0'+
51	Settlement distance? (in.)		0.5-1.0"	1.1-2.0"	2.1-3.0"	3.0'+
52	Scarps or slope movement? (ft.)		0.5-2.0'	2.1-4.0'	4.1-8.0'	8.0'+
53	Surface erosion (ft.)		0.0-5.0'	5.1-10.0'	10.1-20.0'	20.0'+
54	Rills/Gullies depth? (in.)		0.5-2.0"	2.1-4.0"	4.1-6.0"	6.0'+
55	Evidence of undercuts?		1	2	3	4+
56	Depressions, sinkholes, or slides into the impoundment?		1	2	3	4+
57	Evidence of piping formation? (in.)		0.5-2.0"	2.1-4.0"	4.1-6.0"	6.0'+
58	Evidence of seeps with soil loss?		Clear water	Grey water	Murky water	Observed flow rate
59	Wet zones?		1	2	3	4+
60	Animal burrows?		1	2	3	4+
61	Trees, tall weeds, or other vegetation?		Grass	Tall Weeds	Brush	Trees
62	Out of place material?		Soil	Garbage	Drainage	Refuse

### Tailings geotechnical material classifications

Tests were performed on four different coal refuse samples from Federal Site #2, two of which were fine coal refuse (FCR) and two of which were coarse coal refuse (CCR). Water content, specific gravity, grain size distribution, and soil classification were performed in triplicates on the four samples. All of the testing procedures were carried out in accordance with the referenced, current ASTM tests. The only note here is that ASTM D854-14 *Standard Test Methods for Specific Gravity of Soil Solids by Water Pycnometer* was withdrawn in 2023 without a replacement issued to present. Table 2 details ASTM tests utilized for each parameter.

**Table 2. Soil tests and the corresponding ASTM Standard.**

Water Content	ASTM D2216-19
Specific Gravity	ASTM D854-14
Grain Size Distribution	ASTM D6913/D6913M-17
Soil Classification	ASTM D2487-17e1
Atterberg Limits	ASTM D4318-17e1

### Carlson Natural Regrade

Carlson Natural Regrade is a computer modeling design package extension of Autodesk Civil 3D to create geomorphic landform designs. These models work to establish a balanced site, both hydraulically and geotechnically, with the use of a fluvial geomorphic algorithm (Bugosh, 2004). Common GLD practices look at the specific details of the region, such as climate, rainfall intensity and duration, topography, and materials. These methods help reduce problems such as revegetation, post-land use, maintenance costs, and reclamation compliance. This is primarily done by reducing precipitation runoff to select regions with mature channel geometry. These changes are noted for being minimal as to not significantly increase the cost and reduce long-term compliance and maintenance costs. Input parameters for the software evaluate the use of slope, runoff coefficient, discharge velocity, area, and other parameters. Parameters such as drainage density, channel pattern and sinuosity, longitudinal profile, channel cross-section, ridges, slopes, and volumes.

### Finite Element Modeling using PLAXIS LE

PLAXIS LE is a finite element software for geotechnical engineering problem solving. The program can solve 1D, 2D, and 3D analytical models to provide viable simulations and solutions to remove the ambiguity of geotechnical engineering. Within PLAXIS LE models may be created a conceptual model, review slope stability, estimate consolidation, monitor groundwater, and evaluate dynamic conditions. Across each modeling condition there are options to optimize the solution based on the principals and theories of different codes and practices. Different models can also be linked, or coupled, with one another to produce a more holistic result.

Geometry can be shared across platforms such as Civil 3D, ArcGIS, and text files with easy import of complex data.

*Material Properties for Modeling*

Initial material properties for the site were divided into five distinct components: clay, gravel, shale, FCR and CCR (Table 3). These materials were based on geotechnical field reports of the site and subsequently properties were determined through literature review or engineering judgement. Input parameters focus on hydraulic conductivity, cohesion, internal friction angle, and unit weight. Material properties for FCR and CCR were mixed from the Century Impoundment O-26-84 Technical Specifications and missing values parameters reference. Additional soil parameters for the clay, gravel, and shale layers were devised as per engineering guidance and judgement. Table 3 was used for material properties in early models of the Century impoundment; these parameters were used for the pre-reclamation and WVDEP reclaimed models.

**Table 3. Initial material property inputs.**

Name	Strength Type	Unit Weight (lb/ft <sup>3</sup> )	Cohesion (psf)	Phi (deg)	k <sub>sat</sub> (ft/day)	VWC Sat
FCR	Mohr Coulomb	81.12	0	39	5.90E-02	0.5
CCR	Mohr Coulomb	153.504	0	31.5	1.43E+00	0.5
Clay	Mohr Coulomb	145	0	30	2.83E-03	0.5
Gravel	Mohr Coulomb	145	0	45	2.83E+06	0.5
Shale	Mohr Coulomb	137	0	20	2.83E-09	0.5

After the implementation and use of the Century impoundment original permit file, it was determined that some material properties were inaccurate. Values such as hydraulic conductivity, established at 10<sup>-2</sup> cm/sec with laboratory test results from the permit file, for both fine and coarse coal refuse. Such conditions were not representative of onsite materials. With the two materials being two distinct particle size ranges, different hydraulic conductivity values should be used to prevent instantaneous drainage. Values from D’Appolonia (2009) Table 6.6 were used to determine a hydraulic conductivity range acceptable for FCR. It was also noted that the hydraulic conductivity of FCR varies drastically based on site conditions, and thus lower values were selected for worst case analysis. The Unified Soil Classification System (USCS) does not have a means to classify coal refuse, due to this variability of material. As such, it was assumed that the CCR had properties closest to that of a clayey gravels, poorly graded gravel-sand-clay (GC) and FCR to inorganic clay of high plasticity (CH).

Material parameters were updated in Table 4. These parameters were used for the GLD Century impoundment design and all Federal No. 2 designs. Critical changes were made in the reduction of phi, lower hydraulic conductivity values, and a revised void ratio.

**Table 4. Final Material Properties.**

Name	Strength Type	Unit Weight (lb/ft <sup>3</sup> )	Cohesion (psf)	Phi (deg)	k <sub>sat</sub> (ft/day)	VWC Sat
FCR	Mohr Coulomb	80	0	20	2.83E-04	0.13
CCR	Mohr Coulomb	120	0	31.5	2.83E-03	0.33
Clay	Mohr Coulomb	123	180	30	2.83E-05	0.34
Shale	Mohr Coulomb	137	0	30	2.83E-05	0.05

One of the parameter inputs required for consolidation involves the stress/void ratio plot. Since this information is not provided in the permit file, a typical  $e \log p$  curve was selected from the MSHA Engineering and Design Manual. Figure 4 shows the  $e \log p$  curve used for the fine coal refuse. The method used in the software was the Logarithmic Function Fit (Figure 1).

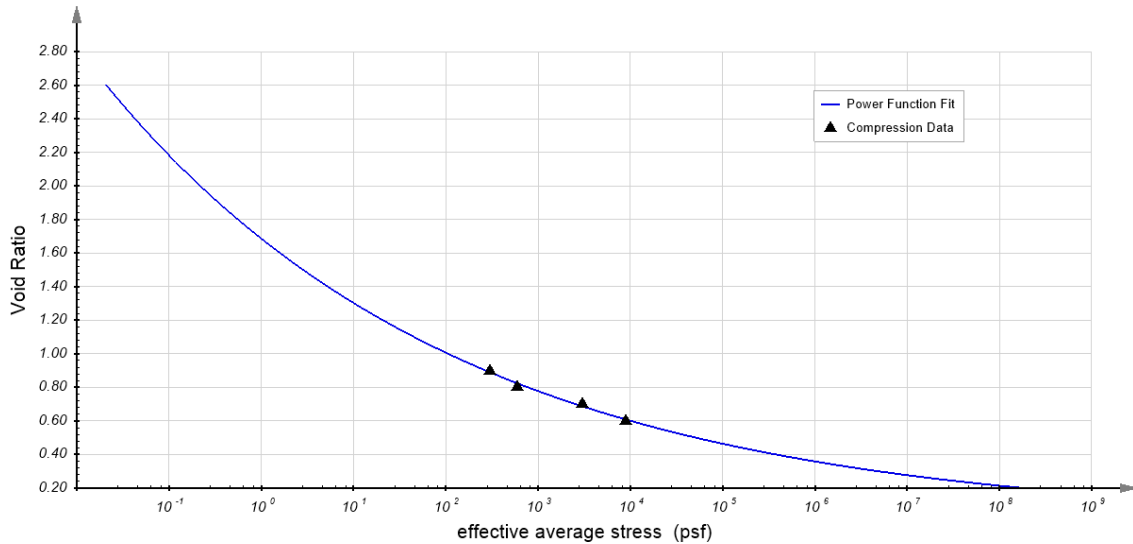


**Figure 1.  $e \log p$  curve for Fine Coal Refuse.**

*Time Rate of Consolidation*

Fine coal refuse placed by slurry piping has been reviewed to have a varied time rate of consolidation ( $C_v$ ) as performed by work done by Jedari et al. (2022). The assumptions of time rate of consolidation are that the excess pore water pressure is equal to overburden load and ignoring the self-weight of the material; this does not apply directly with fine grained materials which remain in suspension for longer. As such finite strain theory can be used to determine a resultant  $C_v$  for a material with a moving boundary such as the variable depth of material in a slurry impoundment. The study concluded that the hydraulically placed material was under consolidated, with an over consolidation ratio anywhere between 0.08 and 0.55. With reporting values like these, the material may not reach full consolidation for years to come. As such, any fieldwork requires careful consideration of site-specific material parameters and the  $C_v$  may not accurately represent site conditions.



*Federal No. 2 FCR Material Classification*

Material testing on FCR from the Federal No. 2 impoundment included particle grain size distribution (ASTM D422), hydrometer (ASTM D7928), specific gravity (ASTM D854) and Atterberg limits (ASTM D4318). Before conducting material classification, the samples had to be dried to be workable. Two drying methods were used: air-dried and oven dried. Air-dried FCR results are in Table 5 and Figure 2. Oven dried FCR results are in Table 6 and Figure 3.

**Table 5. Air-dried FCR summary.**

<b>Air-dried FCR</b>	
<b>Moisture Content (w)</b>	0.27%
<b>Specific Gravity (G<sub>s</sub>)</b>	1.578
<b>Liquid Limit</b>	37
<b>Plastic Limit</b>	28
<b>Plasticity Index</b>	9

**Table 6. Oven dried FCR summary.**

<b>Oven-dried FCR</b>	
<b>Moisture Content (w)</b>	0.20%
<b>Specific Gravity (G<sub>s</sub>)</b>	1.753
<b>Liquid Limit</b>	35
<b>Plastic Limit</b>	26
<b>Plasticity Index</b>	9

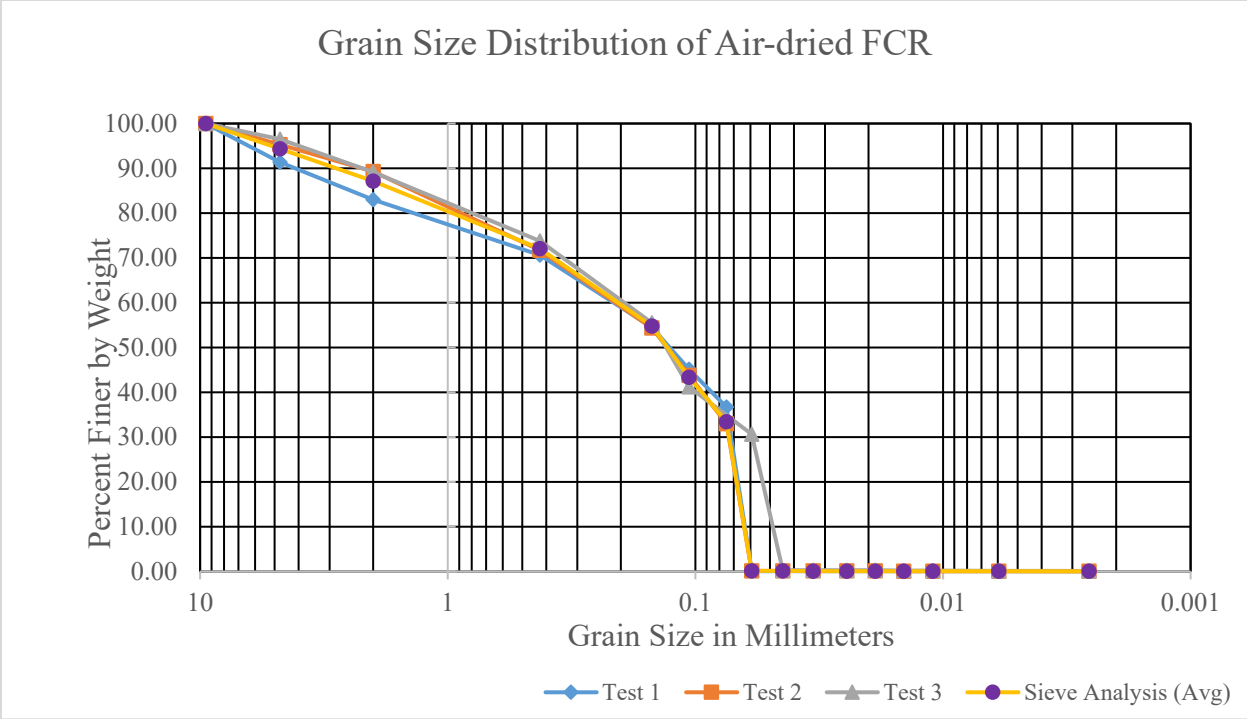


**Figure 2. Grain Size Distribution of Air-dried FCR.**

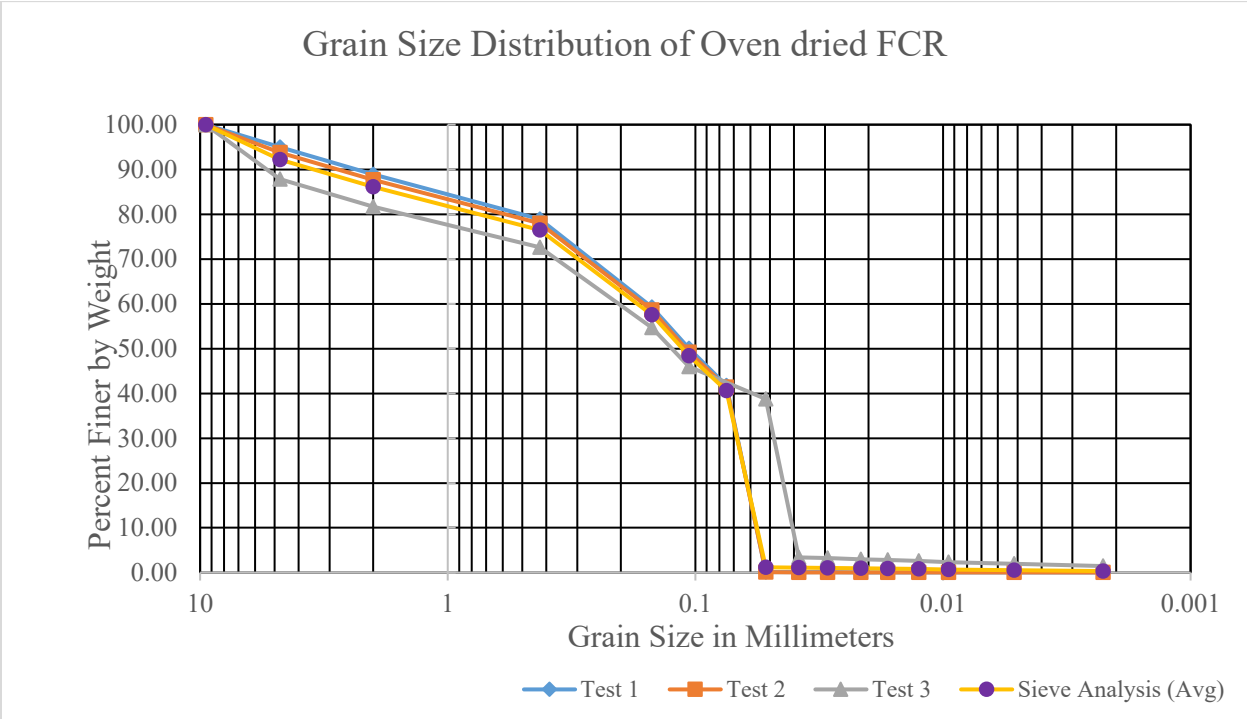


**Figure 3. Grain Size Distribution of Oven dried FCR.**



### *Model Geometry*

Each model focused on four regions: clay core, dam, foundation, and slurry. Each region was drawn through as-built drawings, pre- and post-reclamation, or through best effort. In early reeditions of the model, a drain was also considered but removed to assume worst case scenario. Each model's geometry was drawn using Civil 3D and was exported into PLAXIS LE, for convenience. The geometry of each model was extended past the extents of the impoundment to allow evaluation of potential failure modes outside of the expected area.

### *Groundwater Analysis*

Groundwater modeling consists of establishing the profile geometry, material properties, a storm event, boundary conditions, and initial conditions, such as groundwater level. After the profile was imported into PLAXIS LE and material properties were assigned to the associated regions, different boundary conditions can be included in the model to develop different conditions and limitations within a dam. These boundaries typically include climate, excess pore pressure, gradient, head, review, flux, and zero flux. Only one boundary condition may be assigned to a region at a time. Groundwater was assigned at the height of the refuse material and exited through the downstream toe of the dam.

Prior to any design storm, a 5-day inundation period was allowed for steady state flow to be achieved within the dam. Steady state allows the seepage through the dam to equate with the defined environment without large variability in the pore pressure, flow rate, and degree of saturation. A climate boundary was placed along the ground surface across all regions. Two different storm events were considered, a single storm and two storms one day apart. Models were run under transient conditions, allowing changes in the output relative to time.

Precipitation intensity data was determined through the National Oceanic and Atmospheric Administration (NOAA) Precipitation Frequency Data Server (PFDS) and was site specific for each impoundment (US Department of Commerce, 2023). A 100-year storm over a period of 24 hours was chosen as a reasonable storm to design due to its frequency and intensity.

After calculating a seepage model, outputs were reviewed for errors or considerations in the model. Changes in pore pressure, water table, and degree of saturation can be viewed at various stages in the model. Brown colors are indicated of regions without water, while blue indicates water with some pore pressure. Flux lines may be set within specific areas to monitor water as it flows vertically or horizontally through a section. After viewing the results, the output files were coupled to a slope stability model.

### *Slope Stability Analysis*

Within each slope stability analysis, multiple slope stability calculation methods can be applied within a single model. Bishop's method and general limit equilibrium (GLE) methods were selected as the limit equilibrium methods for this research. Slope search methods were selected to be grid and tangent method and automated slope search method.

With the grid and tangent method, failure locations are determined based on user input. The tangential lines are used as the bounds of the failure location, while the grid is set as anywhere the center of rotation may occur. The user specified regions of failure were divided into toe, mid-

slope, crest, upstream slope, and deep foundation. An example of each method may be seen below in Figure 4 through Figure 8.

The slope search method applies the slope search to the entire structure but can be reduced to sections of the structure based on the x-axis. Only one resultant slope search was used to determine a slope failure across the impoundment structure. The automated case was the lowest factor of safety that the computer software would generate based on the defined conditions.

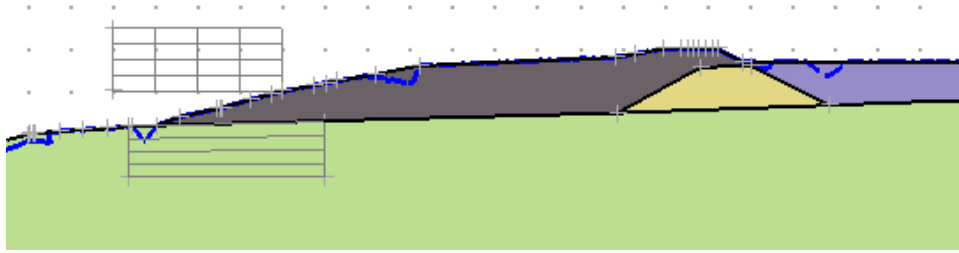


**Figure 4. Toe Grid and Tangent.**

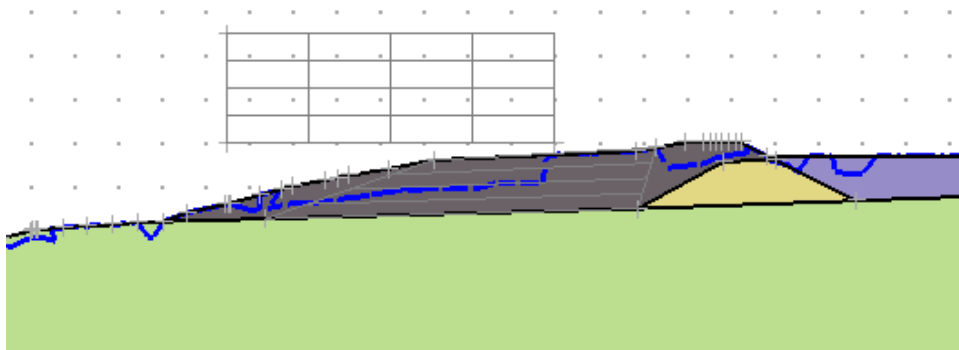


**Figure 5. Mid-slope Grid and Tangent**

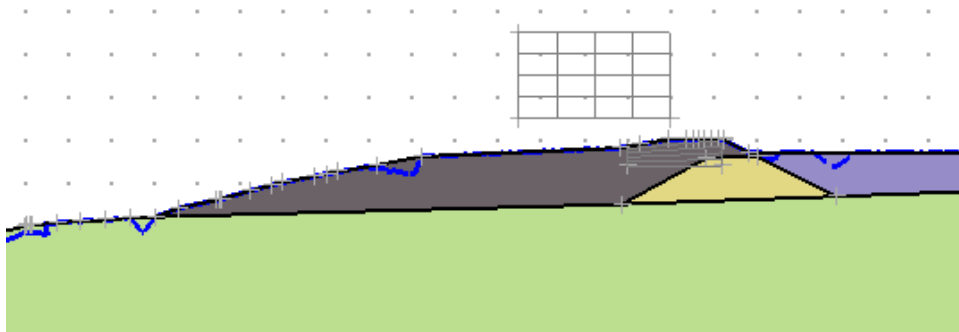


**Figure 6. Crest Grid and Tangent.**

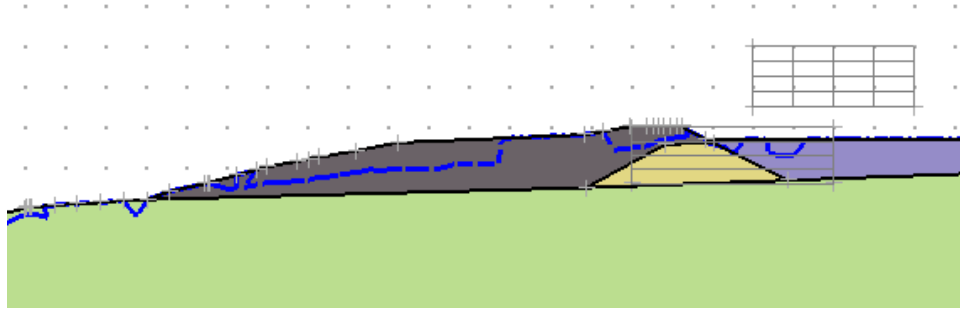


**Figure 7. Upstream Grid and Tangent.**

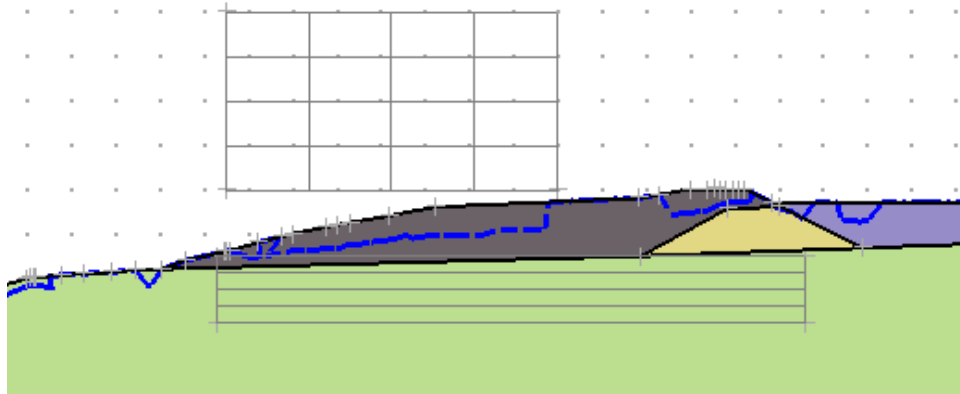


**Figure 8. Deep Foundation Grid and Tangent.**

### *Consolidation Analysis*

Consolidation models were considered to estimate the deformation when the FCR was loaded with additional material. Self-weight consolidation of FCR from being hydraulically placed, typically occurs within the first few years. Additional loading can cause considerable deformation or localized failures as the bearing capacity is too low. Modeling of these cases was limited due to unforeseen issues within the Bentley Software, in which 2D consolidation was removed after an updated version of the software. An older version of the software was reinstalled, and outputs were produced. Due to the recall of these modeling conditions however, limited research was conducted within this realm.

Input parameters changed between models were the groundwater level, the length a distributed load being applied, and the regions which were evaluated. Deformation of all regions and of only the slurry was analyzed, but deformation of the slurry was found to be the more critical concern. Additionally, groundwater level had negligible effect on the deformation.

Initial modeling concluded that only two parameters had major influence: distribution of load and pressure head along the headwater. The distributed load resembled the additional of soil to the slurry, with an additional trapezoidal mass to resemble mounding. Placement of this load also varied within the models. The pressure head was intended to determine the influence of water from the surrounding terrain during a storm event. Water was only added at the end of the impoundment to allow ensure the longest flow path.

## Geomorphic reclamation and evaluation for Century Impoundment

### *Area Description*

The study area is a slurry impoundment located in Barbour County, West Virginia (39° 6' 14.31" N, 80° 11' 7.37" W). The site is part of the West Virginia Land Stewardship Corporation for the West Virginia Department of Environmental Protection (WVDEP) in the Division of Land Restoration and the Office of Special Reclamation. The site was revoked in February 2013 and WVDEP became responsible for it in June of the same year. The property area is approximately 94 acres, of which 58 acres were disturbed. The impoundment area is approximately 34 acres, with a mean elevation of 1,540 ft, and an annual precipitation of 48 in (Dalen, 2021; WVDEP, 2022).

The area was reclaimed in 2020. The reclamation consisted of draining the pooling area and grading it by creating a crest at the center longitudinally. From the crest, the area was graded with a 2.4% slope to the sides. The crest was made by spreading coarse coal refuse over the fine refuse. Finally, the area was seeded with mixed seeds for vegetation reestablishment (Dalen, 2021).

### *Geomorphic landform design*

A series of geomorphic landform designs (GLD) was completed for the study area using GeoFluv™ (Carlson® Natural Regrade® 2021). A total of eight designs were created by considering the design area, design criteria, and number of basins indicated on Table 7.

**Table 7. Design description summary.**

Design iteration	Name	Design area	Design criteria	Number of subbasins
1	I-Def-1	Impoundment	Default	1
2	I-DP-1	Impoundment	DePriest <i>et al.</i> (2015)	1
3	I-Def-2	Impoundment	Default	2
4	I-DP-2	Impoundment	DePriest <i>et al.</i> (2015)	2
5	I-Def-3	Impoundment	Default	3
6	I-DP-3	Impoundment	DePriest <i>et al.</i> (2015)	3
7	W-Def-1	Watershed	Default	1
8	W-DP-1	Watershed	DePriest <i>et al.</i> (2015)	1

The impoundment area designs were created from a base map provided by WVDEP (WVDEP, 2020) consisting of the as-built layout of the impoundment closure. The models considered this area as only one basin, and as divided into two subbasins (17.2 acres and 16.8 acres) and three subbasins (15.6 acres, 9.6 acres, and 8.8 acres) as shown in Figure 9.

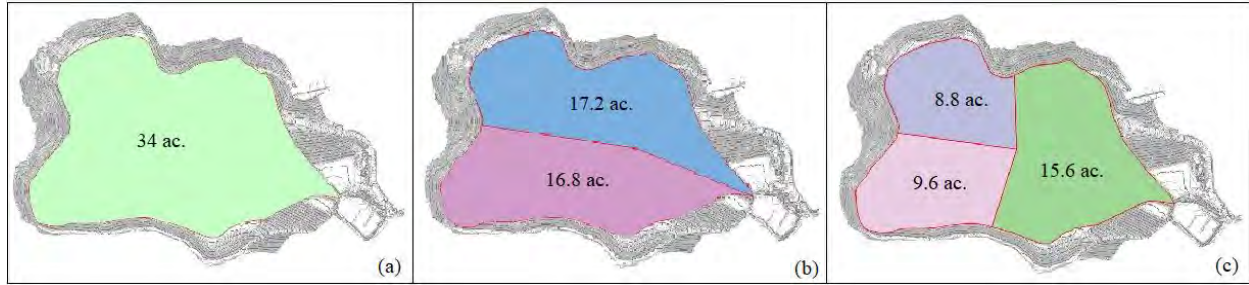


**Figure 9. Impoundment area subbasins layouts: (a) one subbasin, (b) two subbasins, and (c) three subbasins.**

For the watershed area models, a 1-ft contours geodatabase was sourced from FEMA (2020), available at WVU GIS Technology Center. The watershed was delineated using the hydrology toolbox in ArcGIS Pro and transferred to AutoCAD. The models were created considering only one subbasin in the whole watershed area.

One of the challenges in applying GLD is that the criteria vary and must be measured locally (DePriest *et al.*, 2015), such as maximum distance from ridge line to channel's head and target drainage density. The maximum distance from ridge line to channel's head is the shortest distance from a ridge line to the head of a stable channel, and drainage density is the extent to which a drainage network will develop to achieve stability compared to surrounding areas, calculated as the ratio between total channel length and basin area. Both these criteria depend on local soil cohesiveness, vegetation, climate factors, and topographic relief (TIP, 2010).

As we lack on-site information, the GeoFluv™ models were created by using two sets of input values which varied for distance from ridgeline to head of the channel, and drainage density target and variance. One set of values were the GeoFluv™ default values, referred to as "Default" on Table 2. Although these values were defined for the southwestern region of the United States (TIP, 2010), they were previously used by Sears (2012) to analyze the feasibility of GLD principles application to surface coal mine reclamation in Central Appalachia. Similar values were applied by Hopkinson *et al.* (2017) to an abandoned coal refuse pile in Central Appalachia with a small variation in the target drainage density value. The second set of values was defined by DePriest *et al.* (2015) specifically for Central Appalachia region (Table 5).

For this location, the 2-year, 1-hour rainfall depth, and the 50-year, 6-hour rainfall depth were 1.38 in. and 3.50 in., respectively, based on National Oceanic and Atmospheric Administration (NOAA, 2022) precipitation frequency estimates. Besides the values referenced on Table 8, other input information includes the maximum convex portion of subridge, 'A' channel reach, angle from subridge to channel's perpendicular, north or east straight-line slopes, maximum straight-line slopes, maximum and minimum cut/fill, cut swell factor, fill shrink factor, and maximum distance between connecting channels settings. For these additional inputs the default values were used for both design criteria analyzed (Default and DePriest *et al.*, 2015). The head elevation and head slope tolerance settings were defined as 10 ft and 5%, respectively. A slope zone analysis of the GLD models was also completed using Carlson® Natural Regrade® for checking for slopes bigger than 50%.

**Table 8. Input values by design criteria.**

GeoFluv Settings	Default	DePriest <i>et al.</i> (2015)
Max distance from ridgeline to channel's head (ft)	80	408
Target drainage density (ft/ac)	100	62
Target drainage density variance (%)	± 20	± 23
2-yr, 1-h rainfall depth (in)	1.38	1.38
50-yr, 6-h rainfall depth (in)	3.50	3.50

### *Hydrologic Analysis*

After completion, the designs and baselines were submitted to a hydrological analysis that was made using the Carlson® Hydrology module. The SCS curve number and TR-55 methods (USDA, 2004) were used to find the hydrographs for 100-yr and 500-yr storms.

### Curve Number (CN)

The ground cover assigned for the impoundment area was “pasture grassland range – fair”, and the hillside area was classified as “woods (fair)”, sourced from the SCS TR-55, Urban hydrology for small watersheds (USDA, 1986). The hydrologic soil group was defined by using the USDA Web Soil Survey (WSS) (USDA, 2019). The WSS classified the soil of the whole area of study as hydrological group D, meaning the soil has a high runoff potential and water movement through it is very restricted (NEH630.7). This classification was also verified by the observation of poor drainage on site and was a conservative value analysis. Therefore, the curve numbers chosen for this analysis were 84 and 79, for the impoundment area and hillside area, respectively. The GeoFluv™ models for the whole watershed area required a weighted CN, once the water flows through two areas with different ground cover. The weighted curve number is calculated using areas as weights (Equation 1) and, for this study, had a value of 81.

$$CN_w = \frac{CN_1 A_1 + CN_2 A_2}{A_1 + A_2} \quad (\text{Eq. 1})$$

Where:

$CN_w$  = area-weighted curve number

$A_1$  = impoundment area

$CN_1$  = curve number of impoundment area

$A_2$  = hillside area

$CN_2$  = curve number for hillside area

### Time of concentration

A flow path was defined by using the runoff tracking command. This command creates 3D polylines that simulate the way a water drop would follow based on the surface topography. The longest tracking was chosen for the time of concentration (TC) calculation and the average slope is calculated as an average of the slope of each segment of the selected 3D polyline.

The time of concentration was calculated by using the SCS curve number method (CN) for all the study cases excepting the 3-subbasins designs. The SCS method utilizes the curve number, the length of the flow, and the average land slope. For the baseline cases using the whole watershed (woods and as-built), the water would flow through existing lateral channels. The average land slope was calculated by using a weighted average. The length of the flow per area with a different slope – hillside, grassed channel, and rip-rap channel – were used as weights for the weighted average slope calculation.

The regrade designs with 3-subbasins included existing lateral channels that vary from grassed to rip-rap channels. In these cases, TC was calculated by combining the SCS method as discussed before for the water flowing over the impoundment area and the TR-55 channel flow method for the portion of the flow through the channels. The TC for each area was calculated individually and added together. The final value was the TC used for the runoff calculation.

The TR-55 channel flow method uses Manning’s roughness coefficient,  $n$ , which represents the loss of energy in open channels, channel cross-section flow area, wetted perimeter, and flow length and land slope. Manning’s coefficient used for the grassed channel was 0.025 (Earth, Uniform, Grass/GR.) and for the rip-rap channel was 0.040 (12-inch Rock Rip-rap), and were obtained from Chow (1959). Both channels had a triangular shape with a wetted perimeter of 3.35 feet, and a cross-section flow of 4.5 square feet (WVDEP, 2018).

### Runoff volume

The runoff hydrographs for all the models and baselines were calculated by using the SCS method and Carlson<sup>®</sup> Natural Regrade<sup>®</sup> 2021. Zero baseflow and the antecedent moisture condition level 2 (the mid-value) was assumed for all cases. The storm type was Type II 24-hour, following the Natural Resources Conservation Service (NRCS) storm type classification. Hydrographs were created for a return period of 100-year and 500-year for each model.

For the 3-subbasin case, additionally to the hydrograph created by the SCS methods for the top subbasins (8.8 ac. and 9.6 ac.), it was necessary the application of a channel routing method to calculate the effects of a channel on the hydrograph’s peak flow and travel time through the lateral existing channels. The Modified Att-Kin (attenuation-kinematic) method was used (USDA, 1985). The inputs for this method were the following: reach length, route coefficient  $x$ , and route coefficient  $m$ . The reach length was considered the channel length from the head of the grassed channel to the main outlet. The  $x$  coefficient was estimated by using Manning’s formula (Equation 2), and for the  $m$  coefficient was assumed the default value of 5/3 (1.6). Channels geometry and coefficients used for the hydrological analysis are summarized in Table 9.

$$x = \frac{s^{1/2}}{nP^{2/3}}, \quad (\text{Eq. 2})$$

where:

$S$  = average slope of the channel  
 $n$  = Manning's n value  
 $P$  = wetted perimeter of the flow

Following the water flow, the hydrographs resulting from the SCS method were used as inflow for the grassed channel routing, and the outflow from the grassed channel routing was used as inflow for the rip-rap channel routing. Finally, the outflow hydrographs from the two rip-rap channels and the hydrograph from the bottom subbasin were added to generate the design runoff volume hydrograph.

**Table 9. Channels information summary for channel routing of the 3-subbasins models.**

	Channel 1		Channel 2	
	Grassed	Rip-rap	Grassed	Rip-rap
Length (ft)	994	561	900	325
Width (ft)	6.0	6.0	6.0	6.0
Height (ft)	1.5	1.5	1.5	1.5
Area (s.f.)	4.5	4.5	4.5	4.5
Wetter perimeter (ft)	3.35	3.35	3.35	3.35
Average lope (%)	1.5	13	2.0	27.08
$n$	0.0245	0.0395	0.0245	0.0395
$x$	3.3179	6.0585	3.8312	8.7441
$m$	1.6	1.6	1.6	1.6

*Note: length, width, height, area, and wetted perimeter determined from WVDEP (2018).*

## Geomorphic reclamation and evaluation for Federal Mine #2

### *Study Area*

The study area is a coal mine slurry impoundment located near Blacksville in Monongalia County, WV (39° 39' 32.65" N, 80° 16' 45.79" W) (Figure 10a). The mean annual precipitation in the area is 44 inches, and monthly average temperature ranges from 28°F to 71°F (NOAA, 2023; Weather in Blacksville, WV). The coal mine operated during 1986-2018. While considered active, no slurry has been added to the impoundment since mining operations ended. The impoundment area is 57 ac. (Figure 10, Figure 9b) and is located at an average elevation of 1,281 ft. (EGM96). Water in the reservoir meets a beach of fines (elevation = 1,340 ft.) that has formed close to the dam, suggesting that the area has finished settling (WVDEP personal communication).

Through geotechnical lab testing, the moisture content of the FCR was determined to be 24% to 27% (ASTM D2216). Specific gravity, liquid limit, and plastic limit were 1.6-1.7, 35-37, and 26-28, respectively (ASTM D854, ASTM D4318). The material was classified as poorly graded sand with silt (SP-SM) (ASTM- D2487) and had a median grain size of 0.21 inches (5.21 mm) (ASTM D422).



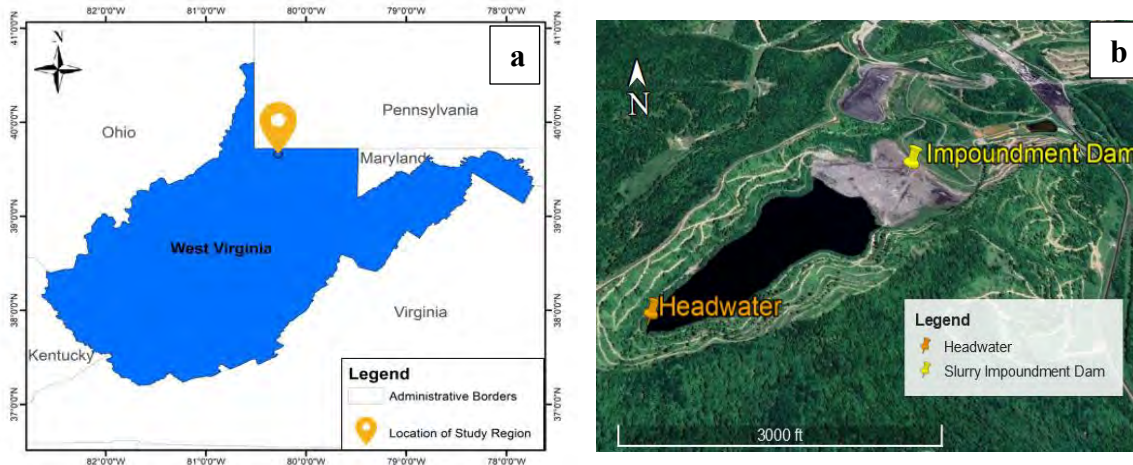


**Figure 10. a) Location and b) aerial image of the study site (source: Google Earth).**

### *Series of Conceptual Reclamation Designs*

A series of six reclamation designs were created. A conventional design followed the typical guidance of reclamation. Then, a series of five geomorphic designs followed geomorphic reclamation methods: i) Uniform-200, ii) Uniform-50, iii) Uniform-90, iv) Two-elevated areas (T-E), and v) Conventional-GLD. The methods are described in the following sections. All the units are reported in the U.S. customary system (USCS) because the topographic data on which the design iterations were based were in the USCS system. In addition, the agency that may utilize the designs work within the USCS system.

### Conventional Design

The Conventional design was created in accordance with guidelines of impoundment reclamation (D'Appolonia, 2009). This approach involves backfilling the impoundment with approved material and topsoil and grading the fill to meet the perimeter ditch (D'Appolonia, 2009). A detailed contour map (contour interval = 40 ft) provided by WVDEP showed that the beach of fines, formed by particles settling at the end of the reservoir close to the dam (Figure 10b), was located at an elevation of 1,340 ft. The height of the backfill was estimated as the difference between the elevation of the lowest point of the reservoir and the elevation of the beach of fines plus the amount needed to make a slope of less than 5% to the perimeter groin ditch. The backfill in this design slopes down toward the end of the reservoir that is close to the dam. The area of disturbance in this design was 89.66 ac., which represents the area of the reservoir and surrounding ridgelines (elevation = 1,340 ft). The area included in the design was divided into two sub-basins (sub-basin 1 area = 46.7 ac., sub-basin 2 area = 42.98 ac., Figure 11a). Design work was completed using AutoCAD Civil 3D 2022 (Version 13.4.214.0).

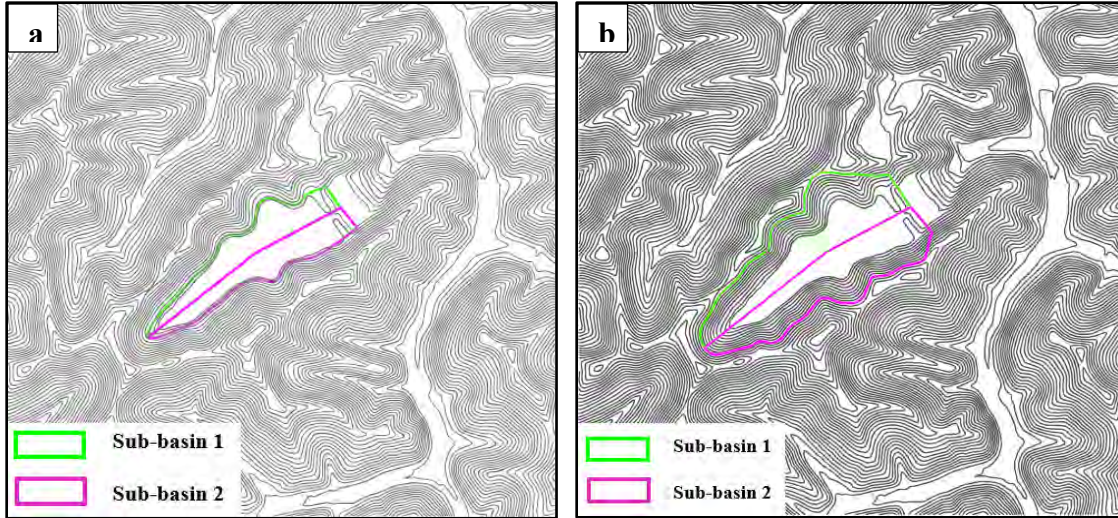


**Figure 11. Design area footprint used for the following design iterations: a) conventional design (i.e., Conventional and Conventional-GLD), and b) geomorphic design iterations (i.e., Uniform-50, Uniform-90, Two-elevated areas).**

### Geomorphic Approach

A geomorphic approach was used to develop a series of conceptual reclamation designs following guidance from previous research completed in Central Appalachia (Hancock et al. 2019, 2020, Hopkinson et al. 2017, Michael et al., 2015; Sears et al., 2014; DePriest et al., 2015). The design area included the valley ridge and the extent of the active impoundment from the headwater (the farthest point of the reservoir) to the crest of the dam (Figure 10b and Figure 11b). Ridgelines surrounding the impoundment with an elevation of 1,500 ft. were included in the layout, resulting in a total design area of 184.3 ac. The design area was divided into two sub-basins (sub-basin 1 area = 97.57 ac., sub-basin 2 area = 86.70 ac., Figure 11b). The two sub-basins drained to two different points close to the crest of the dam (Figure 10b). Different channel configurations were created for the two sub-basins. A hypothetical mid-ridgeline (mounded material) was designed by creating a line of points extending across the length of the impoundment with elevations varying among design iterations (Figure 12).

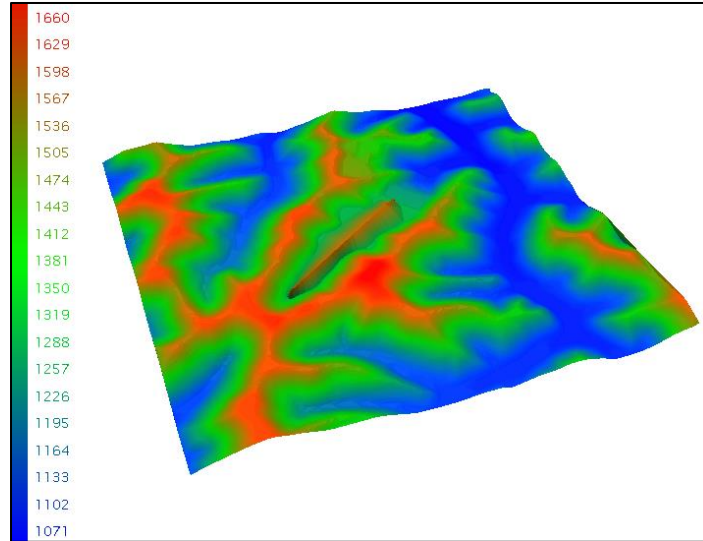


**Figure 12. A hypothetical mid-ridgeline extending from the headwater to the other end close to the dam with surface elevations in ft.**

Major design input parameters included: i) maximum distance between connecting channels (10 ft.); ii) maximum distance from ridgeline to channel head (80 ft.); iii) slope at the mouth of the main valley bottom channel (-2%); and iv) drainage density ( $D_d = 120 \text{ ft./ac.} \pm 20\%$ ). The 2-yr, 1-hr and 50-yr, 6-hr storm rain depth values of 1.2 and 3.44 in., respectively, were used (NOAA, 2023). Additional design input parameters (Table 10) were informed by studies utilizing a geomorphic approach in the Central Appalachia region (Hopkinson et al. 2017, Sears et al., 2014; Lorimer, 2016; Silva, 2022).

**Table 10. Natural Regrade Input Parameters.**

<b>Input Parameters</b>	<b>Value</b>
Maximum distance from ridgeline to channel head (ft.)	80
Slope at the mouth of the main valley bottom channel (%)	-2
“A” channel reach length (ft.)	50
Target drainage density, $D_d$ (ft./ac.)	120
Target drainage density variance (%)	20
Maximum distance between connecting channels (ft.)	10
North or East straight-line slopes (%)	20
Maximum straight-line slopes (%)	33
Maximum cut/fill variance (%)	125
Minimum cut/fill variance (%)	80
Cut swell factor	1
Fill shrink factor	1
Head elevation (ft.)	10
Head slope tolerance (%)	5

## Conceptual Reclamation Designs

A series of GLD iterations were completed for the first and second sub-basins using GeoFluv™ (Carlson Natural Regrade® module 2022). Five different models were developed with different mounded material (mid-ridgeline) elevations, as described in the following paragraphs. The first completed design was Uniform-200, and this design influenced the development of design features in subsequent designs. The height of the mounded material is uniform at 200 ft, resulting in a center ridgeline elevation of 1,500 ft. (Table 11). The area covered in the design included the valley ridge and the extent of the active impoundment from the headwater to the other end of the impoundment close to the dam (Figure 10b). Ridgelines surrounding the impoundment that have an elevation of 1,500 ft. were included in the layout to make a total design area of 195.7 ac. The design area was divided into two sub-basins. Sub-basin 1 (110.7 ac.) had a main channel with five tributaries, and sub-basin 2 (85.0 ac.) had a main channel with three tributaries. Model (Uniform-200) was subjected to seepage and slope stability analysis by Smith (2023) and the subsequent designs were built based on the results and recommendations of the analysis.

The second design was Uniform-50. The height of the mounded material was 50 ft. and was uniform across the extent of the impoundment (Table 11). A slope of 3H:1V was maintained as the maximum slope within the reservoir area. The area covered in the design included the valley ridge and the extent of the active impoundment from the headwater to the crest of the dam. Ridgelines surrounding the impoundment that have an elevation of 1,500 ft. were included in the layout to make a total area of 184.27 ac. (Figure 10b and Figure 11b). Sub-basin 1 had a main channel with ten tributaries, and sub-basin 2 had a main channel with nine tributaries.

The third design was Uniform-90. The height of the mounded material was 90 ft. and was uniform across the extent of the impoundment at an elevation of 1,390 ft. with a maximum slope of 3H:1V (Table 11). The design area was the same as for Uniform-50 (Figure 10b and Figure 11b). Sub-basin 1 had a main channel with ten tributaries, and sub-basin 2 had a main channel with eight tributaries.

The fourth design (Two-elevated (T-E) areas) was created with two elevated areas connected by a saddle. This model represents the extreme case compared to the other design iterations. The height of the first and the second elevated areas were 100 and 125 ft., with elevations of 1,400 and 1,425 ft., respectively (Table 11). The design area was the same as for Uniform-50 and Uniform-90 (Figure 10b and Figure 11b). Sub-basin 1 had a main channel with nine tributaries, and sub-basin 2 had a main channel with eight tributaries. In this design, the created main channels were pushed further from the center of the impoundment (approximately 100 ft. away from the location of channels in previous designs) to maintain a buildable slope.

The Conventional-GLD model was developed following the same calculations that were made in the conventional model to determine the amount of filling material needed for the impoundment; however, Carlson® Natural Regrade® was used to generate the layout for this design. The design area was the same as the Conventional design (Figure 10b and Figure 11a). Mounded material was designed to slope down toward the dam with an elevation decreasing from 1,390 ft. at the headwater to 1,300 ft. close to the dam (Table 11). No tributaries were added to main channels 1 and 2 in this design.

**Table 11. Summary of Conceptual Reclamation Designs.**

Name	Description	Ground slope	Height of mounded material
Uniform-200	Uniform elevation of mounded material across the extent of the impoundment	1.7H:1V	200 ft.
Uniform-50	Uniform elevation of mounded material across the extent of the impoundment	3H:1V	50 ft.
Uniform-90	Uniform elevation of mounded material across the extent of the impoundment	3H:1V	90 ft.
Two-elevated areas (T-E)	Two elevated areas and a saddle	2H:1V and 3H:1V	100 ft. - 125 ft. and a saddle of 50 ft.
Conventional	Mounded material slopes down toward the dam.	3H:1V	90 ft. at the headwater and gradually decreases toward the dam
Conventional- GLD	Mounded material slopes down toward the dam.	3H:1V	90 ft. at the headwater and gradually decreases toward the dam

*Evaluation of reclamation designs.*

Geomorphic reclamation iterations (Uniform-50, Uniform-90, T-E, and Conventional-GLD) were submitted to a slope analysis study and also evaluated for earth movement and hydrologic response. Results were compared to the response of the conventional design.

Slope Analysis

The created designs were submitted to a slope analysis study through AutoCAD Civil 3D 2022 (Version 13.4.214.0) to quantify the slopes used to build the designs by area. The total area that was included in the analysis was approximately 184 ac. regardless of the disturbance area included in each design.

Material Movement

Cut-fill maps were created using AutoCAD Civil 3D 2022 (Version 13.4.214.0) to compare the original ground to the designed surface, following the methods of Raji et al. (2017). No swell of the excavated material was assumed; therefore, a value of 1.0 was assigned for both cut and fill factors Ismael et al. (2021).

Hydrologic Response

The hydrologic response of each created design was evaluated using the Carlson Hydrology® Module to estimate peak discharge, time to peak, and runoff volume. The SCS Curve Number



method (SCS-CN method) was used. In this method, the runoff is determined based on taking into consideration precipitation losses through basic hydrologic cycle components, such as evaporation, transpiration, surface storage, and absorption Bedient et al. (2013).

The cover type for the impoundment area in the current research work was classified as “pasture grassland range” with a fair hydrologic condition. In contrast, the hillside area was defined as “woods” with a fair hydrologic condition (USDA). The hydrologic soil group (HSG) was determined by using the USDA Web Soil Survey. Gilpin-Culleoka-Upshur silt loam covers 100% of the soil surrounding the slurry reservoir. The HSG was type C, which consists of 20% to 40% clay, less than 50% sand, and loam. The CNs selected for the impoundment area and hillside were 79 and 73, respectively (Web Soil Survey, n.d.). A weighted CN was applied for the hydrologic analysis. The Antecedent Moisture Conditions were assumed to be level II (Tailor and Shrimali, 2016).

The time of concentration ( $T_c$ ) was determined from the longest flow path. Runoff tracking was used to define the flow paths of raindrops in the watershed. Then, a three-dimensional polyline was constructed by tracking the longest path of a water drop to the main channel headed toward the outlet. The created flow path followed the surface terrain.

The drainage area (boundary) shown in Figure 13b) was defined when performing the hydrologic computer models of the created designs; the area was then further divided into two sub-basins (Figure 13c). Sub-basin 1, where any raindrop can drain into main channel 1 and its tributaries, and sub-basin 2, where any raindrop can drain into main channel 2 and its tributaries. The hydrograph was created assuming a baseflow of zero. The hydrologic analysis was performed for the 100-year, 24-hr storm and the 500-year, 24-hr storm.

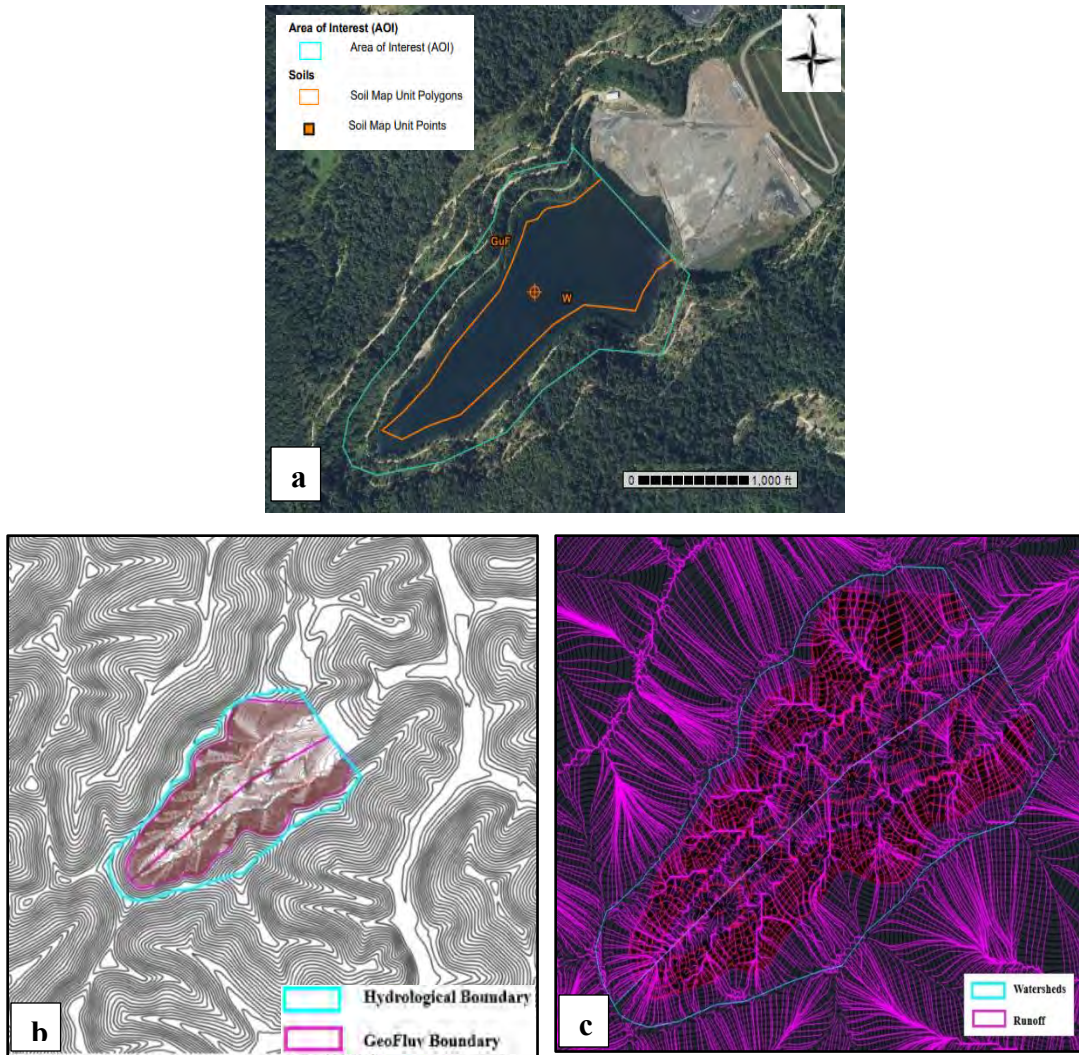


**Figure 13. a) A soil map for the area surrounding the slurry impoundment; b) drainage area (boundary) defined in the hydrologic computer analysis; and c) runoff pathways within the defined two sub-basins.**

## RESULTS AND DISCUSSION

### Coal impoundment site evaluation

A dam inventory list from the WVDEP indicated that there are 143 dams across the state of WV. Of the 143 dams, 95 dams fall under the classification of refuse impoundment. Of these, only 23 dams fall into the category of capped/non-impounding or complete/abandoned. The distinctions are the relative conditions of their WVDEP permit status. The classification of completed/abandoned refers to the condition when the impoundment is no longer in active permit status and the Dam License has been terminated by the WVDEP Division of Dam Safety. The dam closure process may last for 5 years after reclamation.

Of these sites, 8 were selected for investigation; 6 reclaimed refuse impoundments, 1 freshwater impoundment, and 1 active impoundment were visited. A detailed GLD design was conducted on the Century Impoundment and the Federal No. 2 Impoundment. A summary of all sites is provided in Table 12 and an aerial map of the sites in Figure 14.

**Table 12. Visited Impoundments.**

Permit No.:	Status	Description	County	Name	Latitude	Longitude
O002684	Capped/Non-impounding	Refuse Impoundment	Barbour	Energy Marketing North Hollow Impoundment	39.102	80.183
O101086	Active/Impounding	Refuse Impoundment	Monongalia	BUILDING RUN SLURRY IMPOUNDMENT	39.663	80.273
O002184	Capped/Non-impounding	Refuse Impoundment	Nicholas	ROCKCAMP BRANCH #1 COAL REFUSE IMPOUNDMENT	38.271	80.902
O301286	Active/Impounding	Freshwater Impoundment	Nicholas	Peerless Eagle Freshwater Impoundment	38.276	80.900
R070700	Capped/Non-impounding	Refuse Impoundment	Nicholas	#1 REFUSE AREA/SITE A IMPOUNDMENT	38.274	80.679
S201988	Capped/Non-impounding	Refuse Impoundment	Webster	Knight Ink No. 1 Mine Pit	38.432	80.644
S003576	Complete/Abandoned	Refuse Impoundment	Webster	Cowen Trench Area	38.424	80.610
S024076	Capped/Non-impounding	Refuse Impoundment	Webster	North Point Surface Impoundment	38.446	80.592



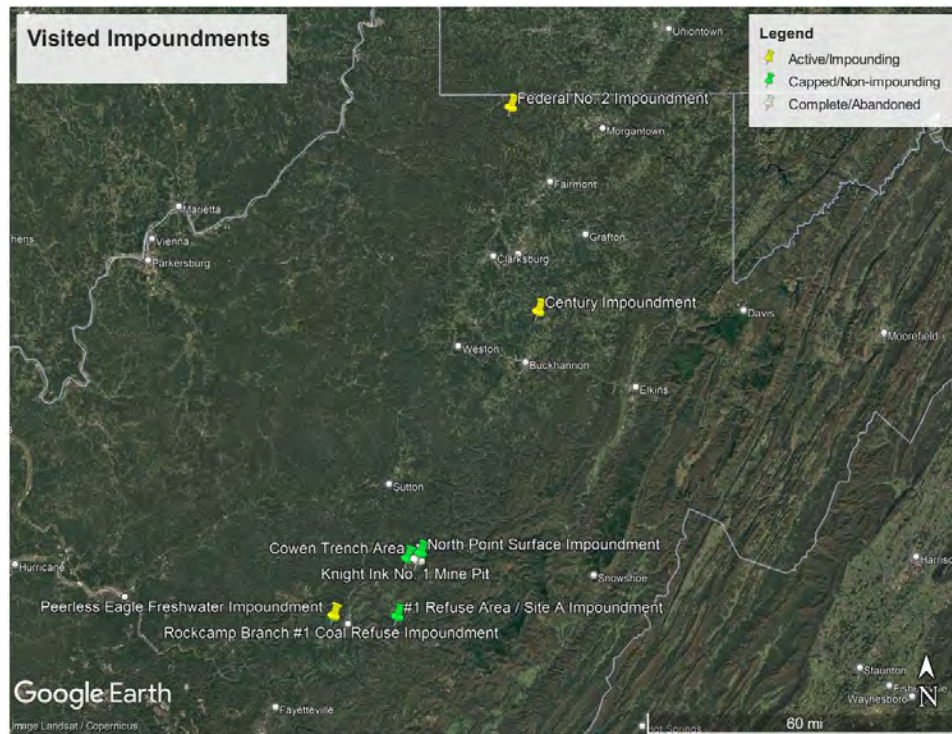


**Figure 14. Visited Impoundments.**

Initial site visits were conducted with the aid of a field observation impoundment inspection sheet. With different iterations of the inspection sheet tested, it was ultimately removed from the final report due to immeasurable parameters and inconsistencies with each of the sites. Each dam is like a snowflake, no two are the same. As such, handwritten notes and photos were taken of any observation that would be used in reclamation revisions. It is noted that none of the impoundments visited were in violation of any law.

*Site Visit- Century Impoundment*

A site visit was conducted on September 22, 2021, near Century, WV. The site visit consisted of a recently reclaimed FCR impoundment. The Energy Marketing North Hollow fine coal refuse impoundment, permit number O002684, operated from 1984 to 2009. After permit forfeiture to the West Virginia Department of Environmental Protection Office of Special Reclamation, the site was reclaimed, starting in 2013 and completed in 2020. The reclamation of this site was entirely based on available funding at the time of reclamation. Aerial images of the site prior to and after reclamation are illustrated in Figure 15 and Figure 16.

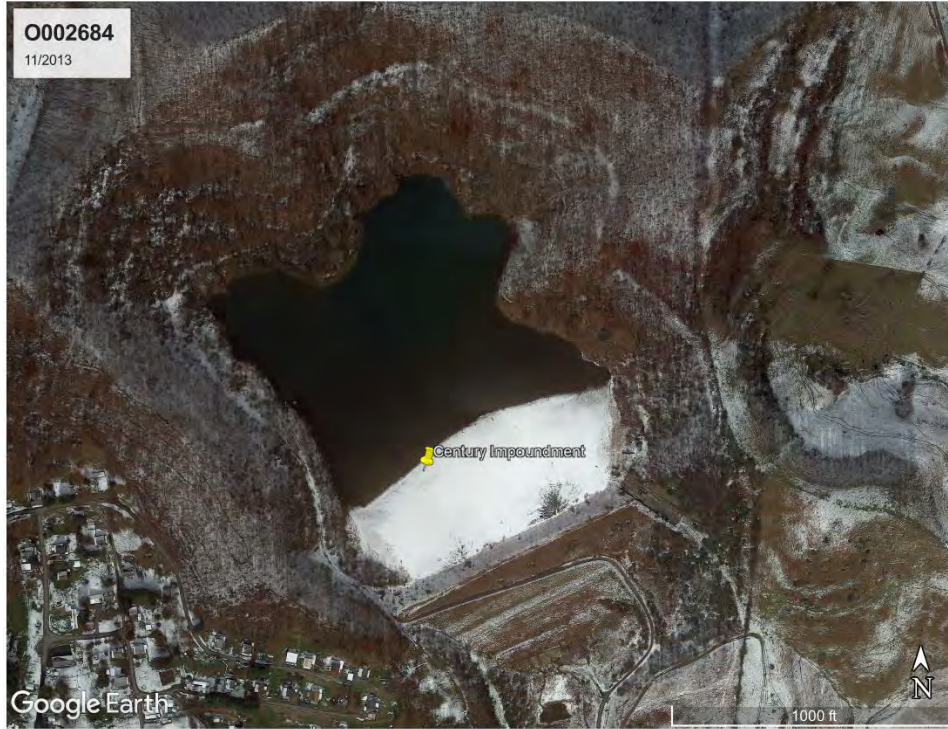


**Figure 15. Aerial Image from 2013 showing Century Impoundment prior to reclamation.**



**Figure 16. Aerial Image from 2020 showing Century Impoundment during reclamation.**



The impoundment was reclaimed as a cut and fill operation; the dam structure and surrounding terrain were cut and backfilled into the FCR. The remainder of the dam was set at a 2H:1V slope (Figure 18) to maintain geotechnical stability and a minimum 2% slope cap cover (Figure 17) was placed atop the backfilled impoundment. The depth of the cover varied based on the bearing capacity of the material beneath it. A perimeter drain was added to reduce infiltration to the FCR, and precipitation infiltration was limited to that of the cap.

With the limited vegetation on the cap, observations on site were easy and concise. Limited settlement had occurred since reclamation. There were no observed low spots, but the ground was still soft. No migration of sediment or clogging of the perimeter drain was observed. The hillside along the end of the impoundment had experienced slope failure, efforts were being made to reclaim it. The planar slope of the cutback dam had no issues at the time of the visit (Figure 19).



**Figure 17. Filled-in slurry pool.**



**Figure 18. Reclaimed downstream embankment.**



**Figure 19. View of downstream embankment.**

### *Site Visit- Federal No. 2*

A site visit was conducted on October 4, 2021, near Blacksville, WV. The site visit focused on walking and collecting FCR samples from an active impoundment. The Crown Coal of West Virginia fine coal refuse impoundment, permit number O101086, has been in operation from 1986 to present. This site was selected based on the location convenience and the expectation that it will go for bond forfeiture in the coming years.

Mining operations stopped around 2018. As such, no additional slurry has been added to the impoundment. The current reservoir, around 57 acres, is comprised entirely of rainwater and is in equilibrium with the surrounding environment. The seepage rate through the impoundment is like that of annual rainfall since the pool elevation has not changed; an annual rainfall of 41 inches.

The upstream slope of the impoundment is a mix of compacted fine and course refuse. It is an estimated 50-75' of water atop 50-75' of FCR, but this cannot be confirmed without a bathometric survey. AMD for the site was running heavily without treatment and without rain. Terrain was level at top of site and heavy weathering on slope faces. WVDEP officials claimed that the "evidence of a beach of fines indicates that an area is done settling, typically between 6 months and a year". Construction of the impoundment is speculated to be comprised of both upstream and downstream construction methods but is not known for sure.

The existing reclamation plan would be to backfill the impoundment and grade to a minimum of a 2% slope to the existing groin ditch along the perimeter of the impoundment. The estimate for reclamation may range between \$16 to 21 million.

An additional site visit was conducted May 12, 2022. During the site visit, it was observed that much of the surrounding property was being timbered. The water level in the impoundment was around 6" lower than typical pool elevation. Not all of the site was explored due to limited access. There was prevalent vegetation which may have obscured some of the otherwise obvious visual issues along the site, shown in Figure 20 through Figure 23.





**Figure 20. Aerial Image from 2022 showing impoundment prior to reclamation.**



**Figure 21. Slurry impoundment reservoir.**





**Figure 22. Beach of fine and course coal refuse pushout on upstream face.**



**Figure 23. Interface between beach and reservoir.**

*Site Visit- Rockcamp Branch, Peerless Eagle, & #1 Refuse Area*

A site visit on July 21, 2022, was conducted near Summersville, WV. The purpose of these site visits was to observe the environmental sustainability of the reclamation regarding surface erosion and general landform stability to gain information to benefit future site reclamation. Aerial imagery from Google Earth Pro was used to review the area of disturbance and potential site conditions prior to walking the impoundments, shown in Figure 24, Figure 25, Figure 26, Figure 27, Figure 29 and Figure 30.

Three impoundments were visited, these are referenced by the WVDEP Impoundment numbers: O002184, O301286, and R070700. Site O002184 (Figure 26) and R070700 (Figure 31) were a reclaimed coal refuse impoundment, closed prematurely due to recession in the coal industry. O301286 (Figure 28) was an active freshwater impoundment. Each reclaimed site had an abundance of vegetation, primarily trees and grasses, growing in all regions of the impoundment pool and previous embankment. Measurable parameters were difficult to observe, with many deemed “not measurable.” Instead, documentation of observations was conducted and documented with field notes and photos.

Erosion was observed across all sites, in various levels of degradation. In O002184, erosion was reduced due to the heavy vegetation to limit soil loss. O301286 had developed erosion channels from the inflow of rainfall and the pumping of water into the reservoir. R070700 had the worst erosion observed across all sites due to the saturation of the impoundment cap and channelization of runoff down the access road.

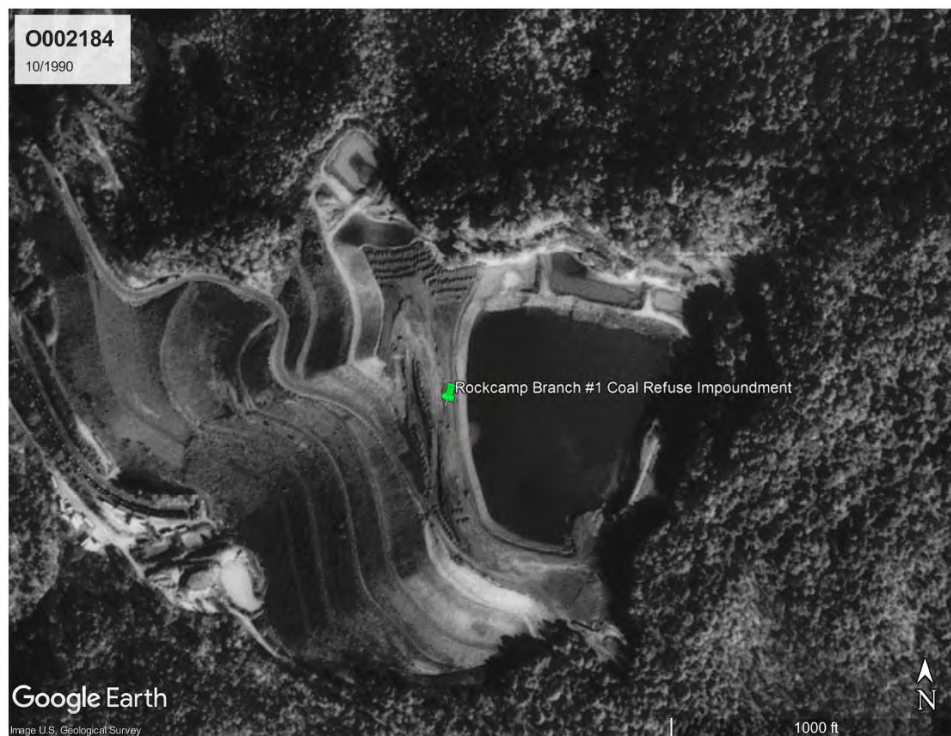


**Figure 24. Aerial Image from 1990 showing impoundment prior to reclamation.**





**Figure 25. Aerial Image from 2022 showing impoundment after reclamation.**



**Figure 26. O002184 Reclaimed impoundment.**





**Figure 27. Aerial Image from 2022 showing active impoundment.**



**Figure 28. O301286 Active impoundment.**





**Figure 29. Aerial Image from 1997 showing impoundment prior to reclamation.**

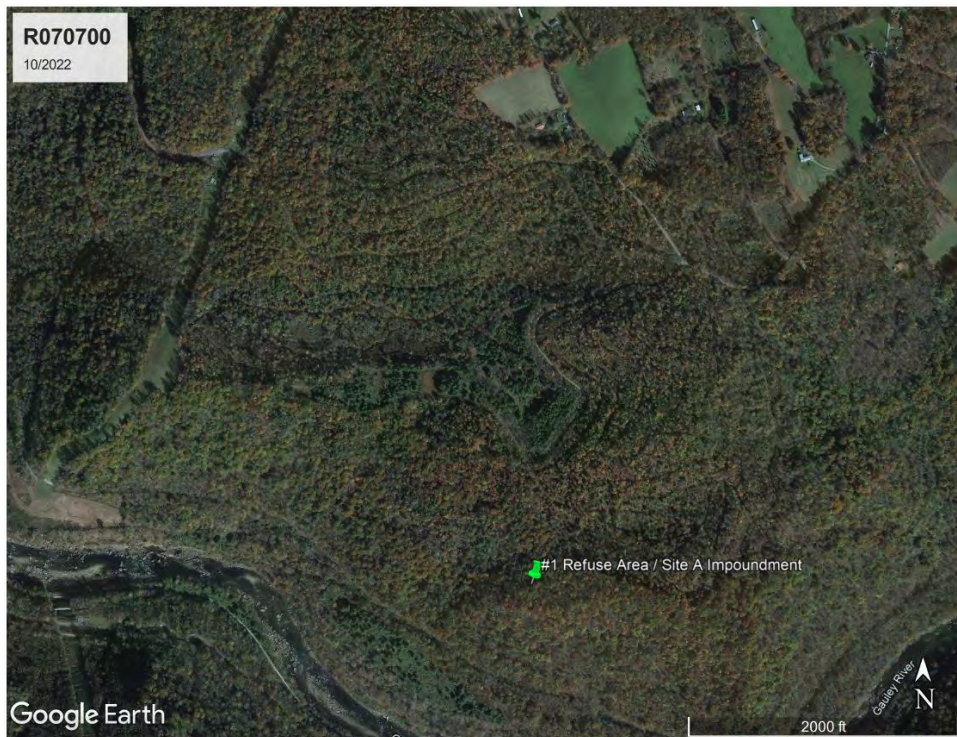


**Figure 30. Aerial Image from 2022 showing impoundment after reclamation.**



**Figure 31. R070700 Reclaimed impoundment.**

Observations at R070700 were summarized to be the best indication of measurable parameters and observations available among the sites. Driving along the access road (Figure 32), the road nearing the impoundment had developed various levels of rills and gullies. In one region, the gullies reached a depth too large for the vehicle to cross, estimated over 3 feet deep and over 4 feet wide. Walking the remainder of the road, it was observed that the gullies changed in width and depth relative to the slope. At the time of the visit, water was flowing within these gullies down the length of the road (Figure 33). Upon inspecting the open channel of grouted riprap (Figure 35) beside the access road, it was completely dry and silted up near the crest.

Reaching the crest of the hill, the reclaimed slurry impoundment outline became evident. Along the impoundment, the slurry material had been covered with coarse coal refuse. Some differential settlement and wet zones were observed within the cap (Figure 34). No indication of geotechnical instability within the impoundment was observed. The surrounding impoundment rim was covered with thick vegetation, primarily trees and brush, which made observations difficult. It was noted that only one gully of meaningful size was observed around the rim. Observations indicated that the perimeter ditch had accumulated fine coal particulate and soil covering the entire perimeter.

From the site visit, these conclusions were drawn. Recent rains in the area contributed to the water within the impoundment. However, the vegetation within the impoundment was that of a marsh. This combination of events indicates that the impoundment is often saturated, potentially permanent. Constant saturation limits additional surface water infiltration, promoting surface runoff from the site. This allows the excess water to flow and bypass the contact ditch to the steeper and slightly lower grade roadway. The roadway thus experienced gullies, in which the cross-section area changed with the slope.





**Figure 32. R070700 Access Road.**



**Figure 33. R070700 Access Road and vegetated contact ditch.**





**Figure 34. R070700 Differential settlement of impoundment cap.**



**Figure 35. R070700 Grouted riprap.**



*Site Visit- Knight Ink, Cowen Trench, & North Point*

A site visit was conducted near Birch River, WV on July 28<sup>th</sup>, 2022. Three impoundments were visited, these are referenced by the WVDEP Impoundment numbers: S201988, S003576, and S024076. All three sites were reclaimed coal refuse impoundments owned by ICG Eastern. Almost all backfill material covering the slurry impoundments was coarse coal refuse (CCR). At some locations, the CCR was estimated at 60 feet of cover. In each site there was an abundance of vegetation, primarily grass and brush. Figure 32 is a mine map of all the mining locations and impoundments. Aerial imagery from Google Earth Pro was used to determine the area of disturbance shown in Figure 37-Figure 41, Figure 43, and Figure 44. Site photos of each impoundment are provided in Figure 39, Figure 42, and Figure 45.



**Figure 36. ARCH Resources base map.**





**Figure 37. Aerial Image from 2010 showing impoundment prior to reclamation.**



**Figure 38. Aerial Image from 2022 showing impoundment after reclamation.**





**Figure 39. S201988 reclaimed impoundment.**



**Figure 40. Aerial Image from 1997 showing impoundment prior to reclamation.**



**Figure 41. Aerial Image from 2022 showing impoundment after reclamation.**



**Figure 42. S003576 reclaimed impoundment.**





**Figure 43. Aerial Image from 2016 showing impoundment prior to reclamation.**



**Figure 44. Aerial Image from 2022 showing impoundment after reclamation.**



**Figure 45. S024076 reclaimed impoundment.**

In all reclaimed areas, topsoil ground cover was minimal. This observation was based on the presence of CCR exposed on the surface. None of the sites had a clear indication of the reclaimed slurry area experiencing erosion. At the time of visiting there was no straightforward evidence to indicate that there was the migration of CCR or FCR from the reclaimed structure. However, many of the leveled slurry impoundments were observed to have differential ground surface contouring. Within these lower lying regions, standing water was observed (Figure 46); recent rain events contributed to this however the magnitude is unknown. There were no observations of geotechnical related slides or ground movement.





**Figure 46. S003576 Standing water.**

With the compacted CCR material placed over the slurry, precipitation was observed to infiltrate the fine coal refuse slurry. This effect saturates the slurry and results in isolated areas of ponding surface water. Once the ground surface was saturated, surface runoff was observed to be effective in areas of high-grade relief and at other areas of no grade the water was stagnant. Without monitoring the groundwater level, it is difficult to know the discharge rate of the impoundments. However, the differential settlement of these areas did have standing water in many regions without observed soil movement.

These observations tend to indicate that the perimeter drainage culvert systems may not have sufficient slope to promote free drainage. Along the downstream reach of the drainage culvert a washout occurred, and debris blocked the flow (Figure 47). The area had standing water and marsh like vegetation prior to the culvert. The culvert had large granular particles and was absent of fines.

From the site visit, these conclusions were drawn. The cap used at each site was effective in preventing the migration of fine through the structure. With an unlevel surface, water was observed to pond in low lying areas. These observations indicate that the refuse is saturated and re-impounding water.



**Figure 47. S024076 Eroded hillside adjoining open channel ditch.**

### **Tailings geotechnical material classifications**

Grain size distribution for all collected samples (Fine and Coarse) is shown in Figure 48. Table 13 through Table 16 summarize Sieve Analysis data for the FCR and CCR samples, respectively. Table 17 shows the FCR and CCR Average Sample Properties. Hydrometer tests were not performed on these samples because the percent of material that passed through the No. 200 sieve was lower than the 5% required by ASTM D7928-21e1. For the CCR samples, the percent of material passing through the No. 200 sieves was 1.3% (Table 15 and Table 16). Furthermore, the FCR samples contained a percent of material passing the No. 200 sieve of 5.13% and 8.06% (Table 13 and Table 14). While these percentages are above the 5% lower limit set by ASTM, the material that passed through the No. 200 sieve is not considered natural clay particles but rather as crushed aggregate residue from the sieve shaking process.

Atterberg limit tests were carried out on the material in order to be able to perform a USCS soil classification. During these tests, the material was unable to reach a 25 blow count after multiple trials at different moisture levels. As per ASTM D4318-17e1, the material was deemed “nonplastic,” and the liquid limit and plastic limits tests were not able to be performed on it. Therefore, the material does not have a plasticity index (PI), so its PI is zero for classification purposes. Following the ASTM guidelines and while utilizing  $C_u$  and  $C_c$ , the classification for the FCR and CCR samples is silty sand with gravel (SM) and well-graded gravel with sand (GW), respectively.

The test results were compared to previous work regarding FCR and CCR as shown in Table 18 and Figure 49. Smith (2023) performed material tests for FCR and CCR from Federal Site #2 as well, which had specific gravity and moisture content that were similar to the results that the



team obtained. There were also several other sources (Smith 2023, Stawovy 2011, Tolikonda 2010, Zeng et al. 2008, Hegazy et al. 2004, and Genes et al. 2000) provided to our team regarding material tests on similar material and are included in the results of this report. These sources were published between 2000 to 2023 and are collected at a variety of locations but nonetheless provide a benchmark for the test results of our material.

There are some discrepancies, minor and major, that exist between the tests performed by our team and prior authors, but these discrepancies are to be expected given the nature of the material. Because this is coal mine refuse, each sample taken from a pile is likely to be different due to the variability in the contents. One sample may contain more shale, coal, slate, etc. than another. It is by definition “refuse”- a mixture of everything that is rejected by the mine. Therefore, no two samples would be exactly the same unless it came from the same dump, at the same time, with the same conditions. The samples should all be similar to a degree, but it is unlikely that they would have the exact same material properties.

The grain size distributions (GSD) and the variation in the results mirror the expected variation in results due to lack of control over the base material sample. Results from all authors show similar profiles for FCR with the results of Stawovy (2011) and Tolikonda and Quaranta (2011) being especially close until D<sub>10</sub>, after which, results diverge slightly. No other author reviewed provided full GSD plots for CCR, and as such comparisons cannot be drawn between results. However, results for CCR reported by the reviewed authors differ significantly, as is expected based on variations in the sampled material.

**Table 13. FCR Sample 1 Properties.**

<b>Property</b>	<b>Average</b>	<b>Standard Deviation</b>
Specific Gravity, G <sub>s</sub>	1.685	0.057
Water Content (%)	27.408	1.005
D10 (mm)	0.155	-
D30 (mm)	1.127	-
D50 (mm)	8.973	-
D60 (mm)	17.101	-
Passing No. 200 (%)	5.130	-

**Table 14. FCR Sample 2 Properties.**

<b>Property</b>	<b>Average</b>	<b>Standard Deviation</b>
Specific Gravity, G <sub>s</sub>	1.562	0.071
Water Content (%)	24.278	2.607
D10 (mm)	0.092	-
D30 (mm)	0.390	-
D50 (mm)	1.465	-
D60 (mm)	2.815	-
Passing No. 200 (%)	8.060	-

**Table 15. CCR Sample 1 Properties.**

<b>Property</b>	<b>Average</b>	<b>Standard Deviation</b>
Specific Gravity, $G_s$	2.106	0.071
Water Content (%)	11.946	0.655
D10 (mm)	1.009	-
D30 (mm)	2.719	-
D50 (mm)	4.695	-
D60 (mm)	6.723	-
Passing No. 200 (%)	1.300	-

**Table 16. CCR Sample 2 Properties.**

<b>Property</b>	<b>Average</b>	<b>Standard Deviation</b>
Specific Gravity, $G_s$	1.974	0.075
Water Content (%)	11.227	0.603
D10 (mm)	0.866	-
D30 (mm)	2.614	-
D50 (mm)	4.970	-
D60 (mm)	7.181	-
Passing No. 200 (%)	1.300	-

**Table 17. FCR and CCR Average Sample Properties.**

<b>Property</b>	<b>CCR</b>	<b>FCR</b>
Specific Gravity, $G_s$	0.938	0.123
Water Content (%)	2.666	0.758
D10 (mm)	4.832	5.219
D30 (mm)	6.952	9.958
D50 (mm)	1.300	6.595
D60 (mm)	2.040	1.624
Passing No. 200 (%)	11.587	25.843



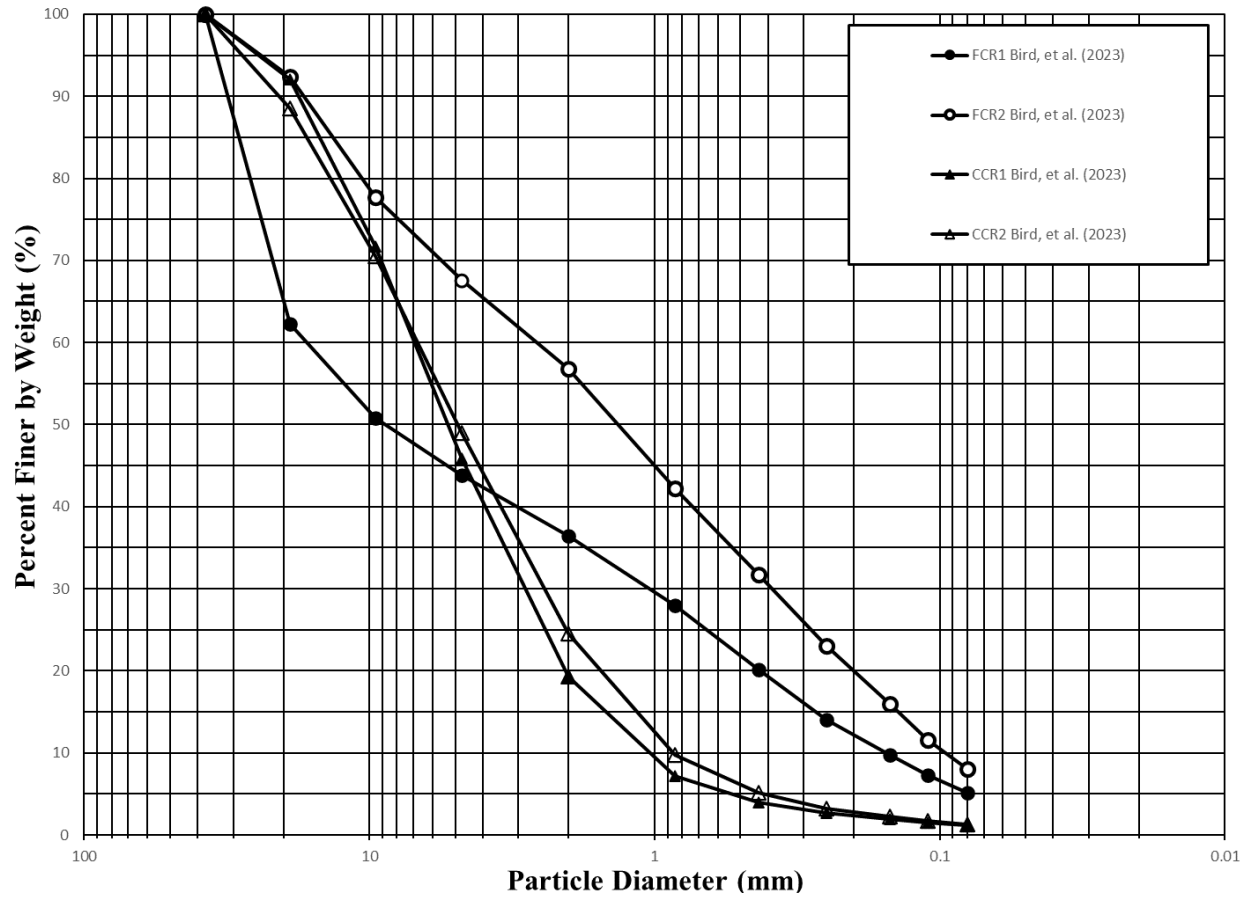


**Figure 48. FCR and CCR grain size distribution.**

**Table 18. Results comparison.**

<b>Reference</b>	<b>Specific Gravity, G<sub>s</sub></b>	<b>Water Content (%)</b>	<b>D10 (mm)</b>	<b>D30 (mm)</b>	<b>D50 (mm)</b>	<b>D60 (mm)</b>	<b>Passing #200 sieve (%)</b>
<b>Fine Coal Refuse</b>							
<i>Sample 1</i>	<i>1.685</i>	<i>27.41</i>	<i>0.155</i>	<i>1.127</i>	<i>8.973</i>	<i>17.101</i>	<i>5.13</i>
<i>Sample 2</i>	<i>1.562</i>	<i>24.28</i>	<i>0.092</i>	<i>0.39</i>	<i>1.465</i>	<i>2.815</i>	<i>8.06</i>
Smith (2023)	1.578	27.00 (air-dried)	-	-	-	-	-
Stawovy FCR 1A (2011)	2.07	3.51%	-	0.525	1.1	1.55	0.175
Stawovy FCR 2A (2011)	1.72	0.106%	0.15	0.24	0.43	0.59	6.60
Stawovy FCR 3A (2011)	1.62	0.106%	-	-	-	-	-
Tolikonda (2010)	1.875	-	-	-	-	-	-
Zeng et al. (2008)	2.02-2.16	-	-	-	-	-	-
Hegazy et al. (2004)	1.52	-	0.01	0.037	0.127	0.196	57.70
Genes et al. (2000)	1.44-2.37	-	-	-	-	-	-
<b>Coarse Coal Refuse</b>							
<i>Sample 1</i>	<i>2.106</i>	<i>11.946</i>	<i>1.009</i>	<i>2.719</i>	<i>4.695</i>	<i>6.723</i>	<i>1.30</i>
<i>Sample 2</i>	<i>1.974</i>	<i>11.227</i>	<i>0.866</i>	<i>2.614</i>	<i>4.97</i>	<i>7.181</i>	<i>1.30</i>
Smith (2023)	1.753	20.00 (Air-Dried)	-	-	-	-	-
Tolikonda (2010)	2.54	4.20%	-	3.65	6.5	8.45	1.00
Zeng et al. (2008)	2.5	-	-	-	-	-	-
Hegazy et al. (2004)	2.02	6.4	<0.075	0.35	1.23	2.02	19.76

Note: Italicized values are those completed for this work in the WVU Geotechnical Laboratory.

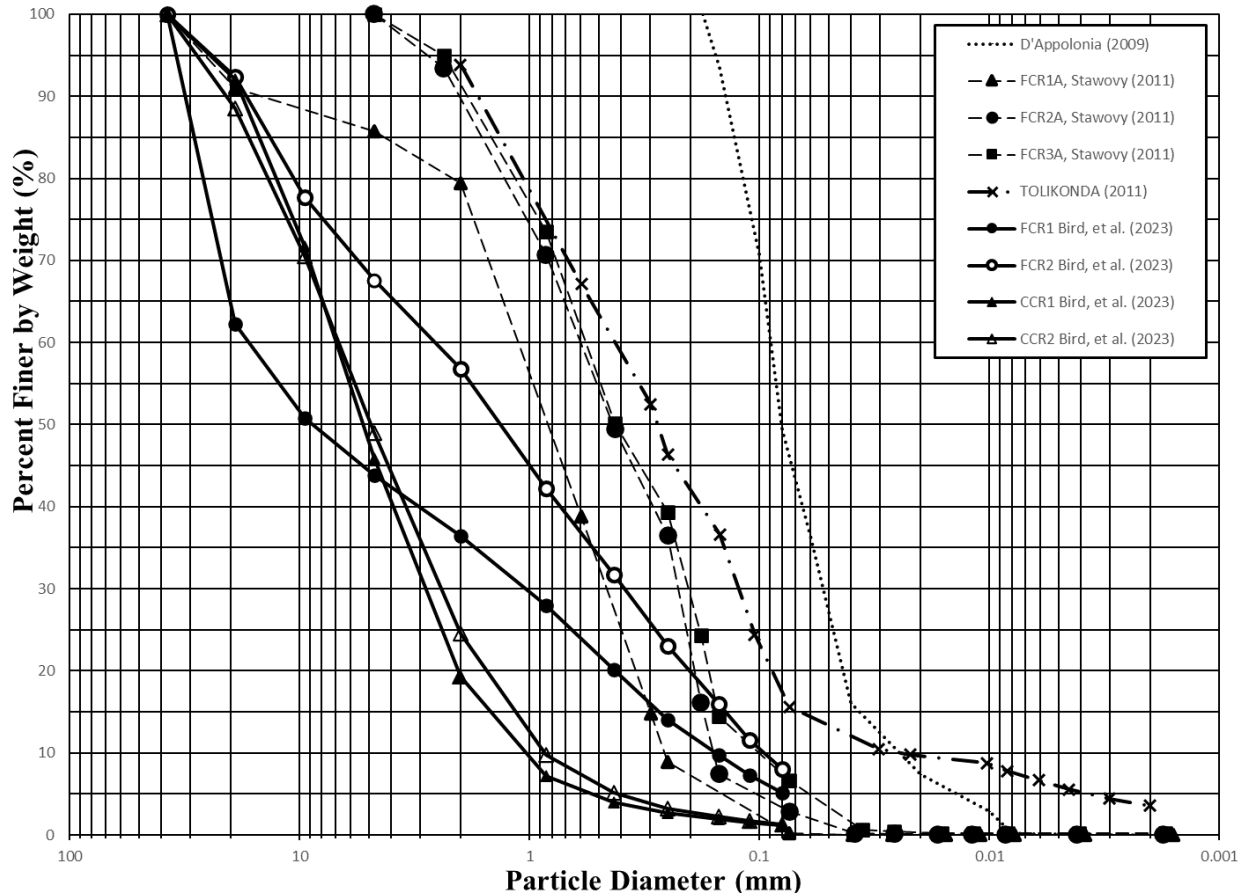


Figure 49. Grain size distribution of coal refuse comparison.

### Finite Element Modeling for Century Impoundment

Input parameters for the model geometry were based on pre-reclamation as-built drawings and reclaimed as-built drawings. Data was referenced from engineering drawings, permits, site visits, inspection reports, and publicly available data. The product of this research was to develop and assess the geotechnical stability of the structure relative to design storms in the region.

The focus of these models outlines the results of coupled seepage and slope stability analysis. All models were conducted along the centerline of the impoundment for the highest summation of forces exerted. Two design storm events were considered in the seepage analysis: a 100-year storm and repeating 100-year storms, one day apart. The design precipitation event for the area was 5.24 inches in 24 hours, as defined by US Department of Commerce, (2023). Various failure locations were considered, and the resultant factors of safety were condensed into a table.

#### *Century Pre-reclamation Impoundment*

The impoundment geometry was established through the documentation provided from as-built drawings when the dam was first constructed (Figure 50). A cross section of the dam from 1983 was used for the pre-reclamation design. The drawings show an earthen dam with a clay core. Stages of CCR were used to build up and around the clay core, separated with drains at critical points. Overall, the dam is 130 feet tall and has a crest width of 51 feet. Using the original

engineering drawings from 1983 (Figure 51 and Figure 52), the geometry of the dam was drawn into AutoCAD and exported to PLAXIS LE (Figure 53).

FCR slurry was used to determine the impoundments slope stability. With a slurry level set to 101 feet above the toe of the dam, this was a more accurate representation of site conditions. This elevation was determined by the maximum allowable slurry content based on construction drawings.

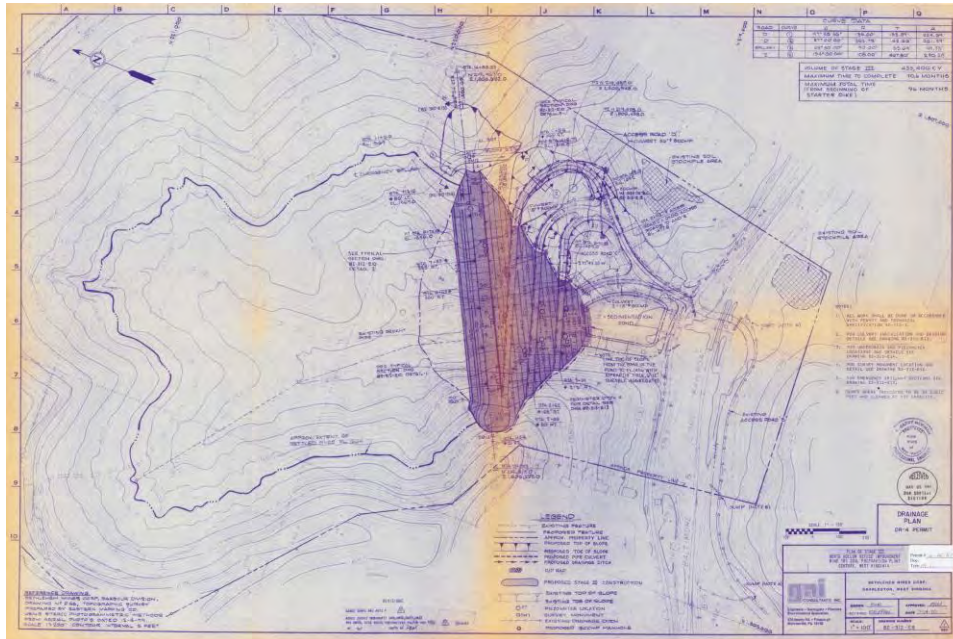


**Figure 50. Top view of historical impoundment.**

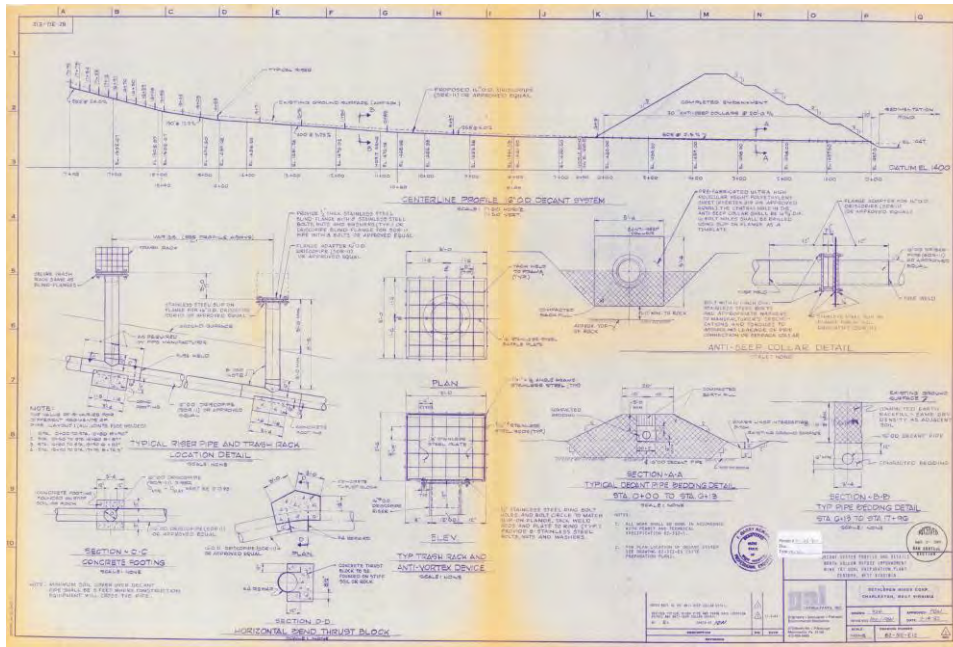


Figure 51. Historical impoundment parameters.

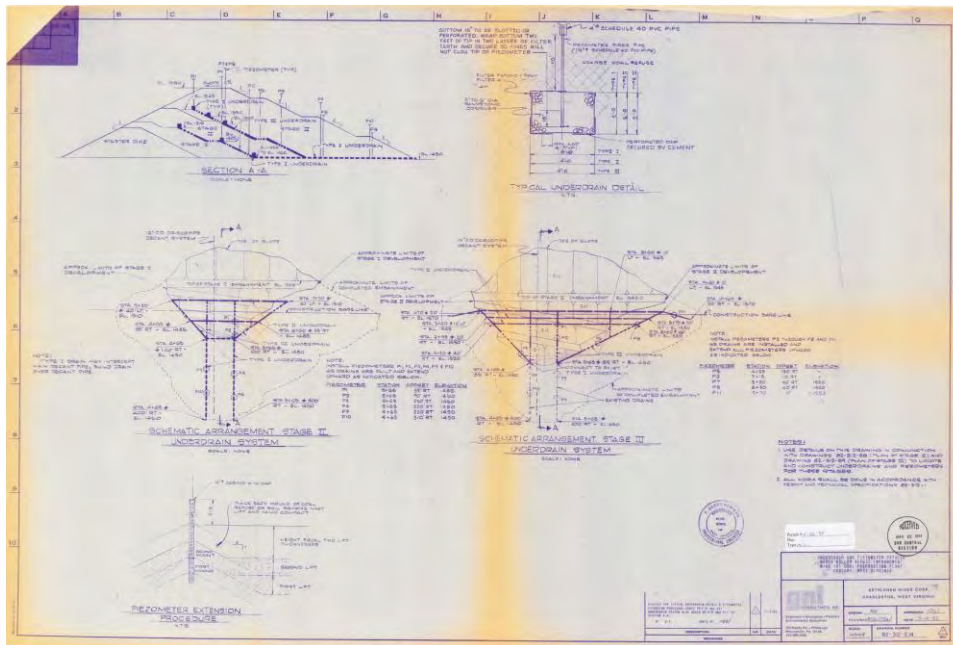
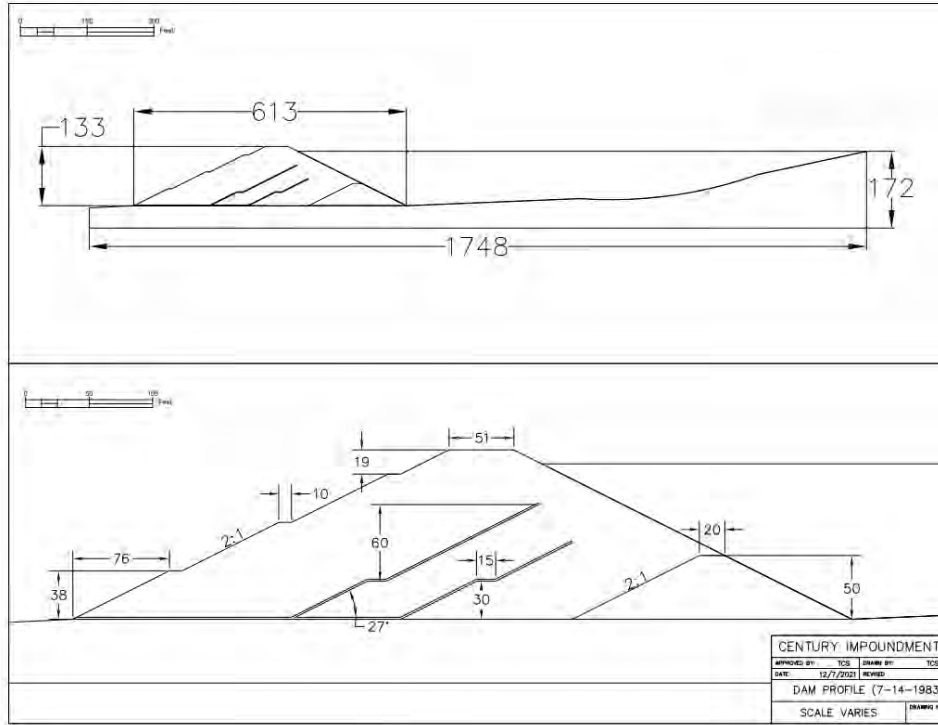


Figure 52. Additional design specification of historical impoundment.



**Figure 53. Pre-reclamation impoundment centerline cross section.**

### Century Pre-reclamation Impoundment Results

The results of the pre-reclamation modeling indicate that the impoundment structure would maintain a minimum factor of safety under all cases except for the slope search method, as seen in Table 19. Figure 54 shows the 100-year storm event seepage output and Figure 56 is the repeating 100-year storm event seepage output. Pore water pressures increased with the additional storm event but was able to dissipate some pressure within the dry period assigned. As the driving forces increase with the addition of saturated FCR, the resultant factors of safety are lower but do not fail.

Failures through the foundation layer are an indication that the geometry of the material may not be thick enough or poor assumption of material strength. Due to the unknown top of rock and existing ground, these foundation failures are very unlikely. Likewise, the automated slope search methods produced results that did not match with that of other modeling consideration with the failure plane passing through the foundation. The lowest factor of safety from each design storm were recorded with Figure 55 and Figure 57.

**Table 19. Pre-reclamation model results.**

<b>Pre-reclamation model results</b>						
<b>Location:</b>	<b>Toe</b>	<b>Mid-slope</b>	<b>Crest</b>	<b>Upstream Slope</b>	<b>Deep Foundation</b>	<b>Slope Search</b>
<b>100-year storm</b>	1.233	1.272	1.229	1.232	1.208	0.848
<b>Repeating 100-year storm</b>	1.229	1.251	1.237	1.232	1.201	0.931



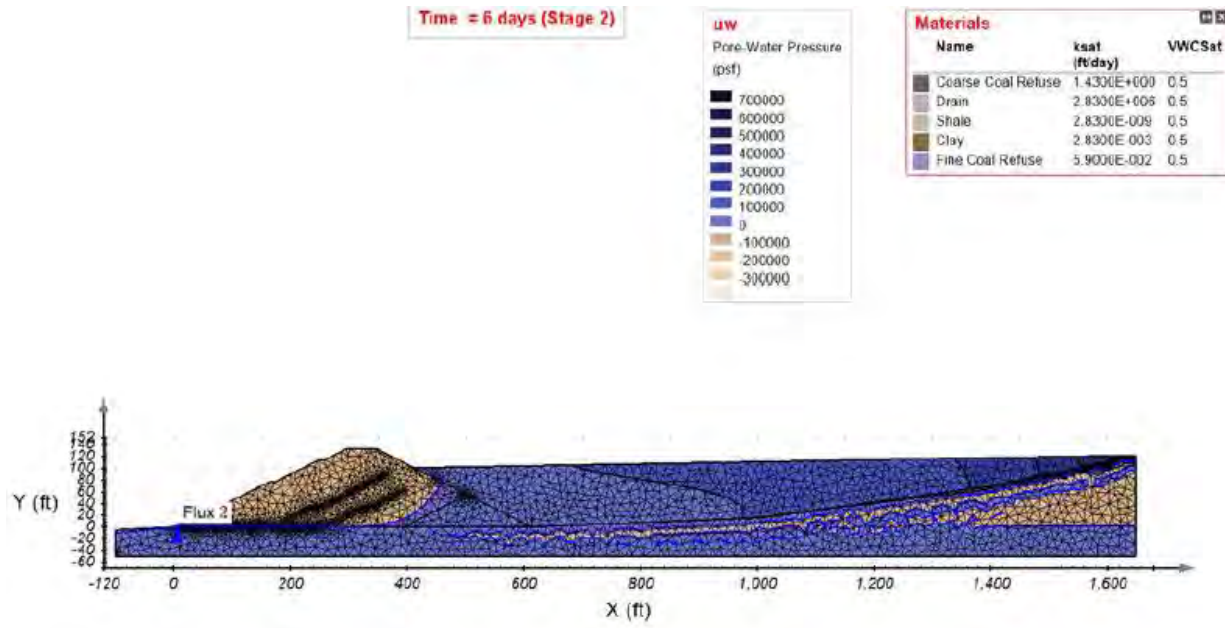


**Figure 54. Century pre-reclamation singular 100-year seepage output.**

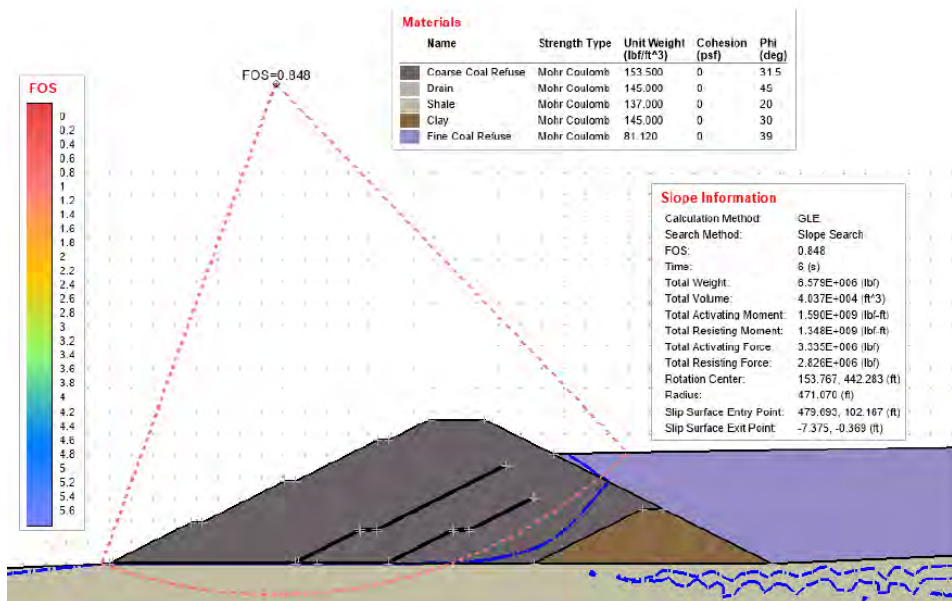


**Figure 55. Century pre-reclamation auto singular 100-year.**



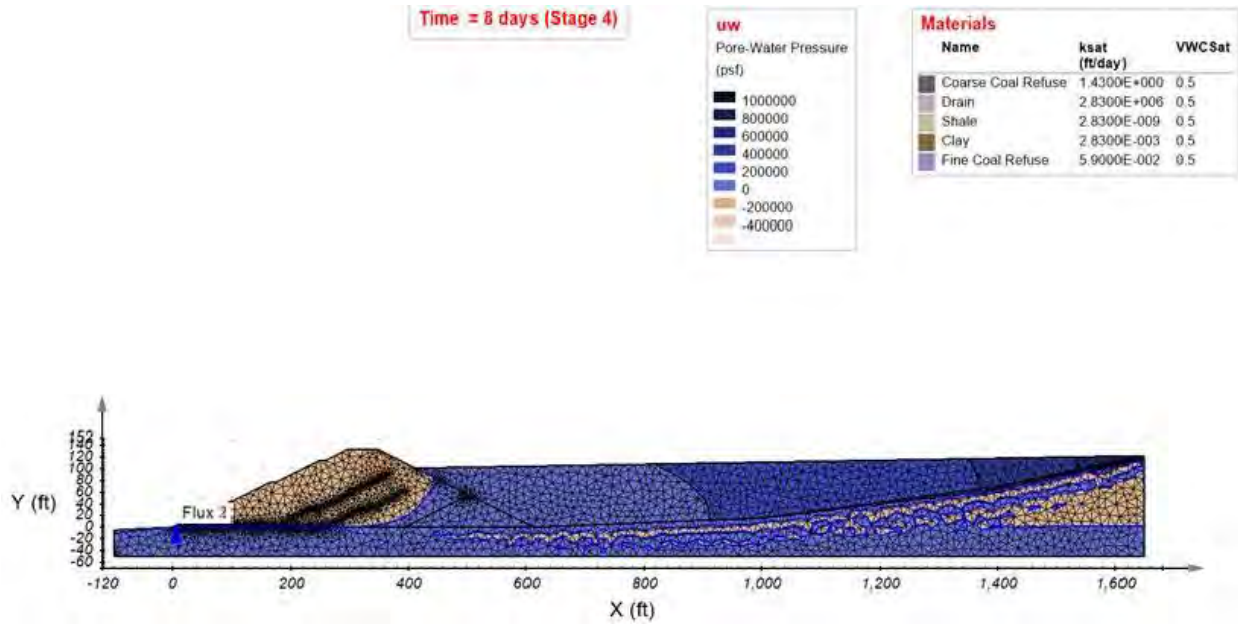


**Figure 56. Century pre-reclamation repeating 100-year seepage output.**

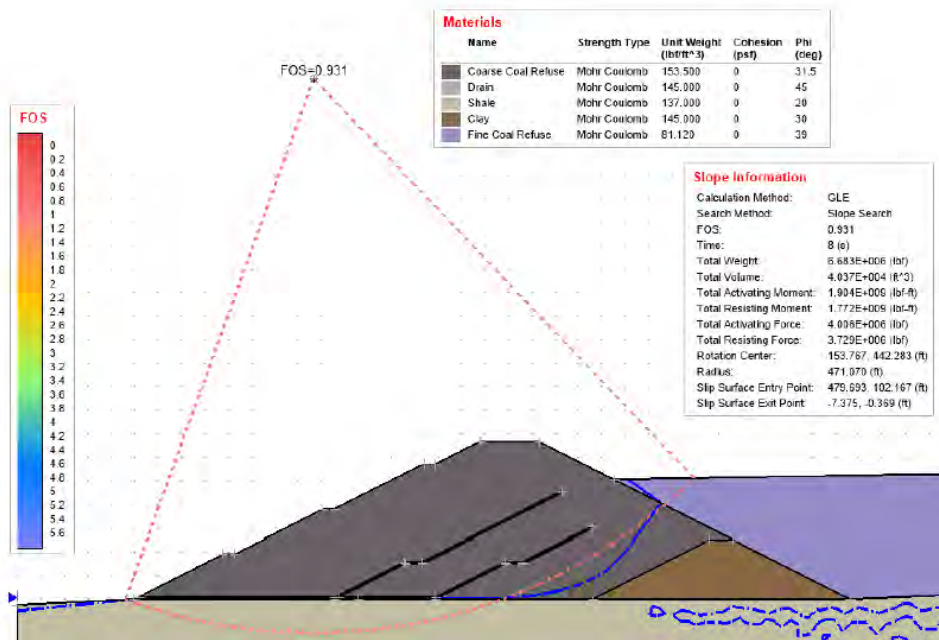


**Figure 57. Century pre-reclamation auto repeating 100-year.**

### *Century Reclaimed Impoundment*

After completing the analysis of the pre-reclaimed site, the reclaimed site was evaluated. The cross-section geometry was outlined as per the available WVDEP as-built drawings and plan sheets (Figure 58 and Figure 59). Some elements for the impoundment were clearly outlined, however some additional engineering judgement was required to infer the final design relative to the 1983 construction. As discussed, the dam crest was cut and pushed back covering the slurry.

While the slurry material has an existing topsoil cap placed above it only FCR was used when designing the reclaimed model, as the depth of material is unknown based on the differential settlement of the FCR. Additionally, the drain was omitted from these models and labeled as additional CCR to assume a clogged drain. Figure 60 shows the final cross section of the WVDEP reclaimed impoundment.



Figure 58. WVDEP reclaimed impoundment layout.

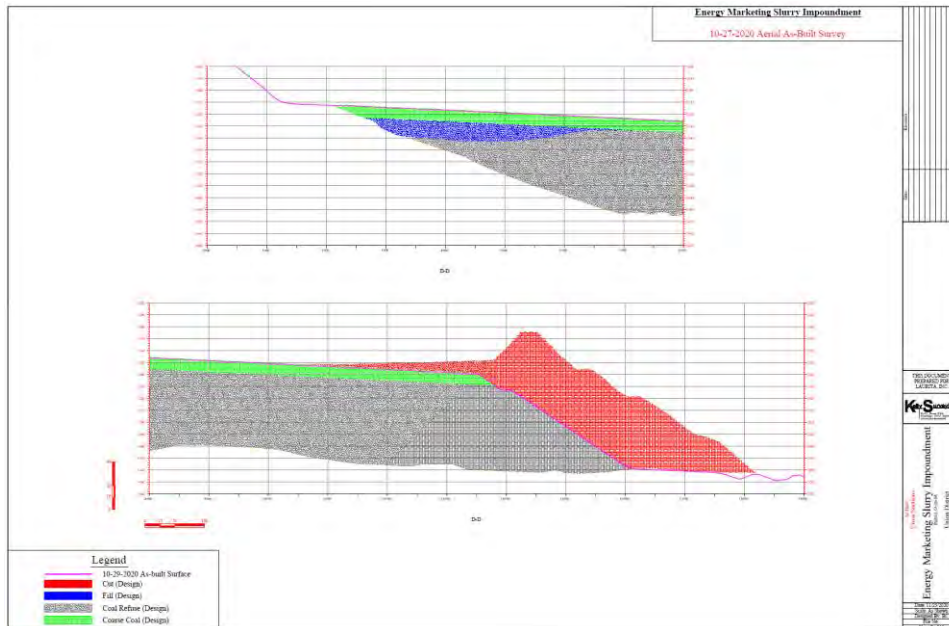
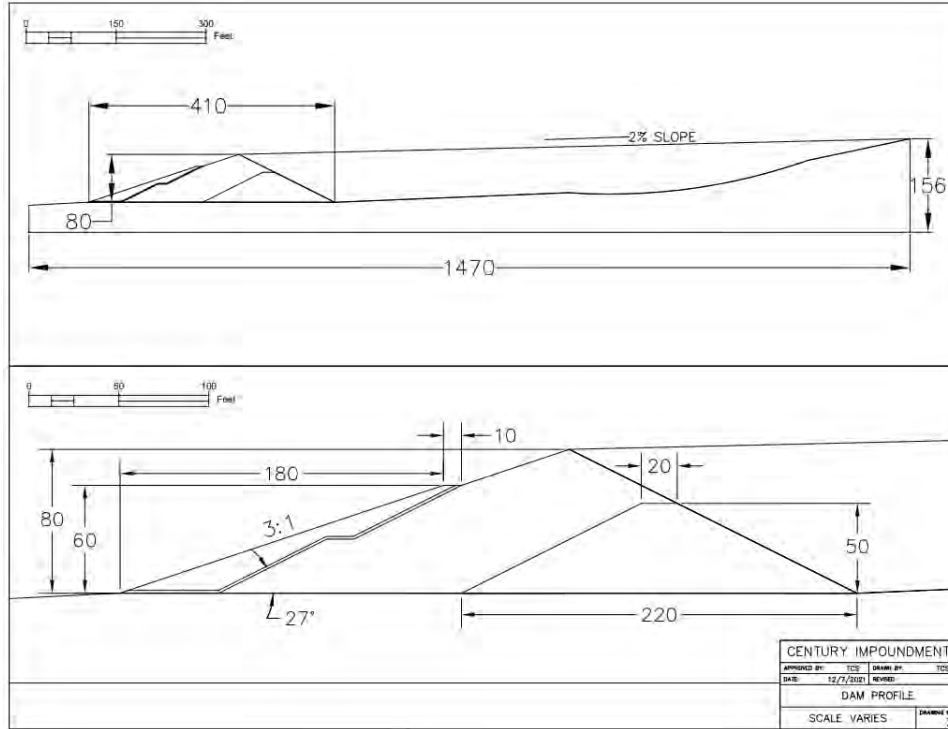


Figure 59. Cut and fill design cross section for reclaimed site.



**Figure 60. Reclaimed impoundment centerline cross section.**

Century Reclaimed Impoundment Results

The reclaimed model indicated that the overall structure has an improved factor of safety. The slope search method still produced lower factors of safety in which the failure was in the toe of the impoundment and into the foundation layer. The 100-year and repeating 100-year storm seepage outputs are outlined in Figure 61 and Figure 63, respectively. The lowest factor of safety from each design storm were recorded with Figure 62 and Figure 64.

**Table 20. WVDEP Reclaimed model results, factor of safety.**

WVDEP reclaimed model results						
Location:	Toe	Mid-slope	Crest	Upstream Slope	Deep Foundation	Slope Search
<b>100-year storm</b>	1.859	1.843	1.854	N/A	1.368	0.476
<b>Repeating 100-year storm</b>	1.859	1.843	1.854	N/A	1.368	0.462

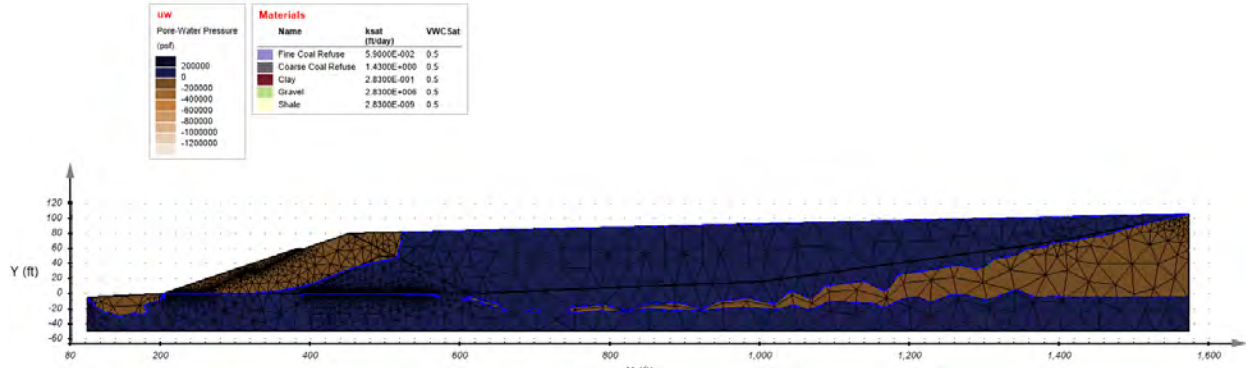


Figure 61. WVDEP reclaimed singular 100-year seepage output.

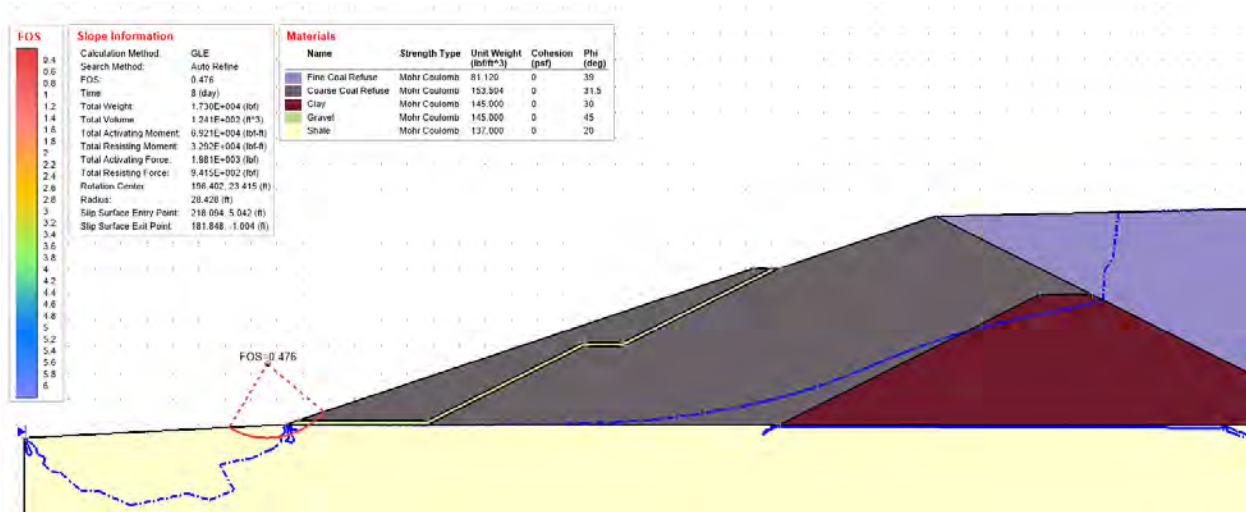


Figure 62. WVDEP reclaimed auto singular 100-year.

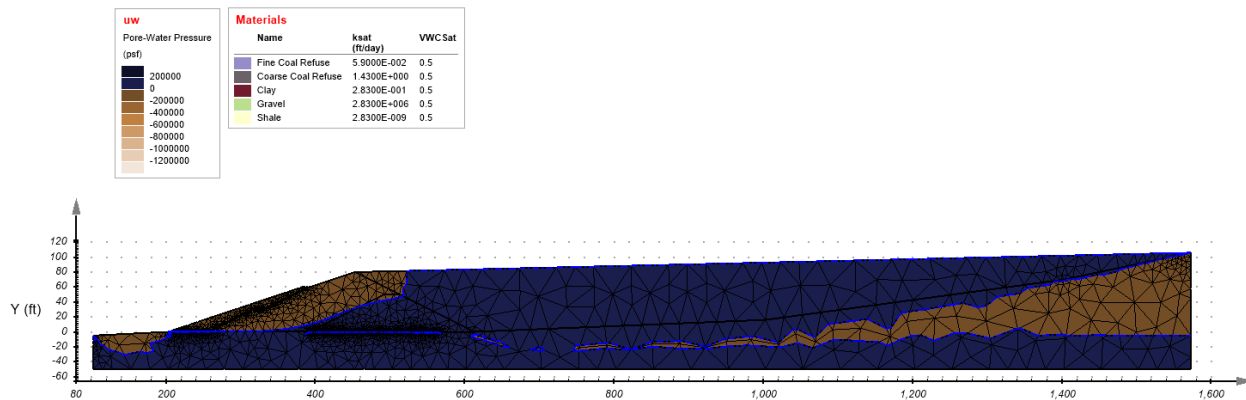


Figure 63. WVDEP reclaimed repeating 100-year seepage output.



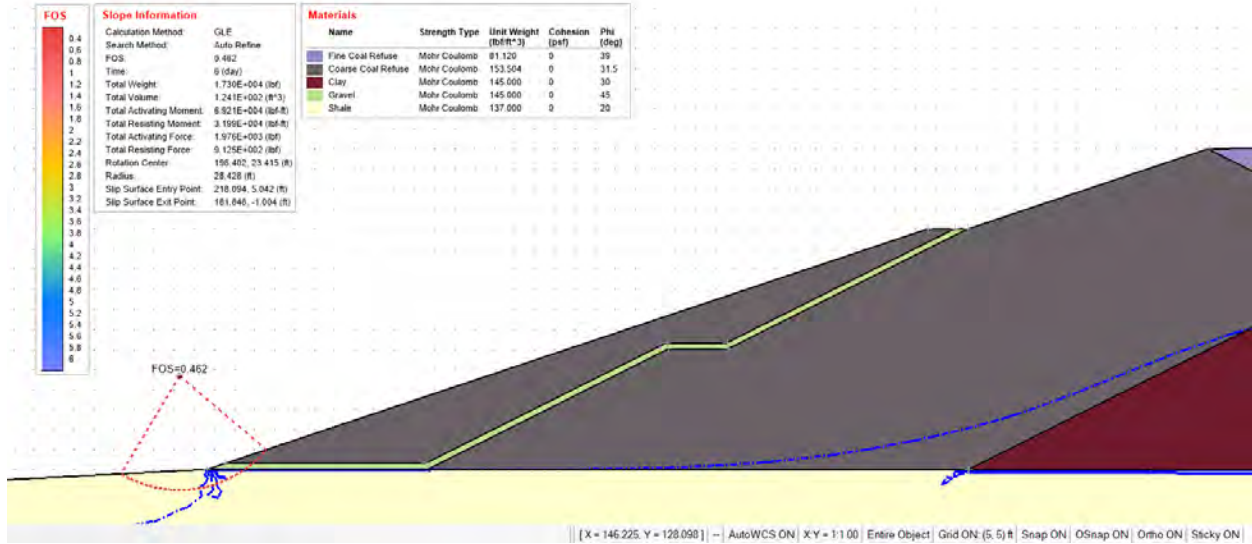


Figure 64. WVDEP reclaimed auto repeating 100-year.

After the slope stability analysis, deformation of the FCR was evaluated. FCR has been observed to have a low bearing capacity when backfilling the impoundment and can be difficult to work with. In each model the lower boundaries were fixed point, not allowing deformation past them, like the existing ground or bedrock. The exposed top surface was allowed to displace horizontally and vertically as a free boundary. Groundwater conditions in the model was set at 60 feet. Water was also allowed to dissipate through the upstream face.

Loads were applied to the model to simulate the addition of mounded material atop the FCR. Two loads were applied to the refuse, a distributed 10-foot-thick layer of CCR and a mounded 5-foot-thick layer of CCR (Figure 65). These loads were the 1200 lbf/ft<sup>2</sup> and the trapezoidal load of 600 lbf/ft<sup>2</sup>, respectively. Additional models changed the load with the addition of mounded CCR, to a height of 15 and 30 feet. Models were allowed to consolidate and deform over a period of 2000 days, or about 5.5 years.

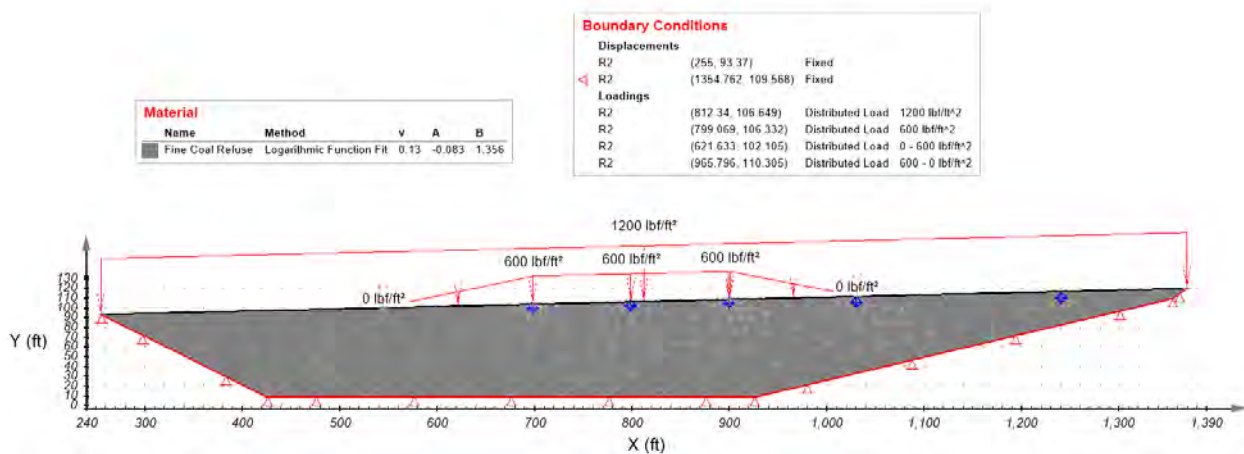
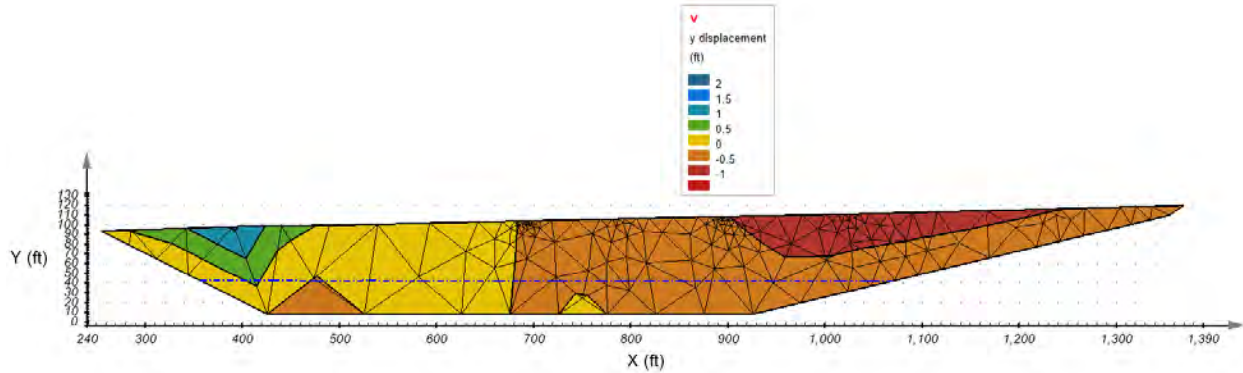


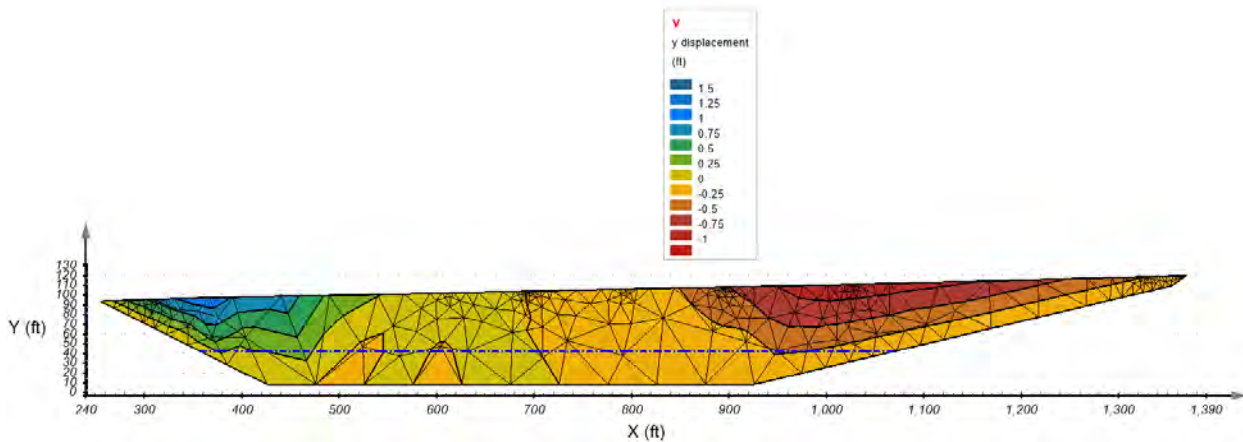
Figure 65. 5-ft mound load on top of fine coal refuse.



Figure 66, Figure 67, and Figure 68, show the deformation in the y direction after the application of a 5, 15, and 30 feet of mounded CCR. The results for all models indicate that the load causes some consolidation around 400 feet and heave around 1,000 feet. However, the difference in load has minimal to no effect on the displacement of material as it is a nearly identical output from 15 to 30 feet.



**Figure 66. y-displacement results for 5-ft mound after 2000 days.**



**Figure 67. y-displacement results for 15-ft mound after 2000 days.**

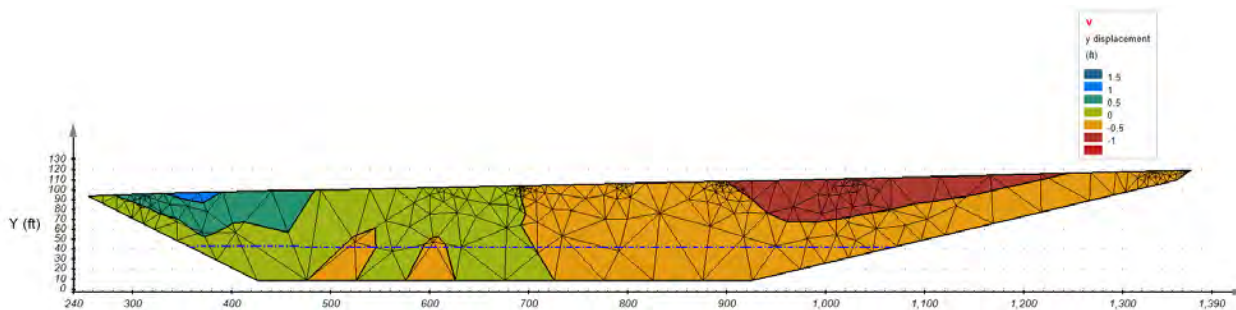


**Figure 68. y-displacement for 30-ft mound after 2000 days.**

Additional models were conducted with a pressure head applied to the top right of the model, a length of 15 feet. The pressure head was modeled to imitate that of water runoff from the surrounding hillside and not contained by the perimeter drainage ditch. The pressure heads applied were 5, 15, and 30 feet. The resultant vertical deformation can be seen in Figure 69, Figure 70, and Figure 71, respectively. These models also included a mounded 10-foot-thick layer of CCR.

Results from these loading cases produced nearly identical results across all models. Again, consolidation around 400 feet and heaving around 1,000 feet.

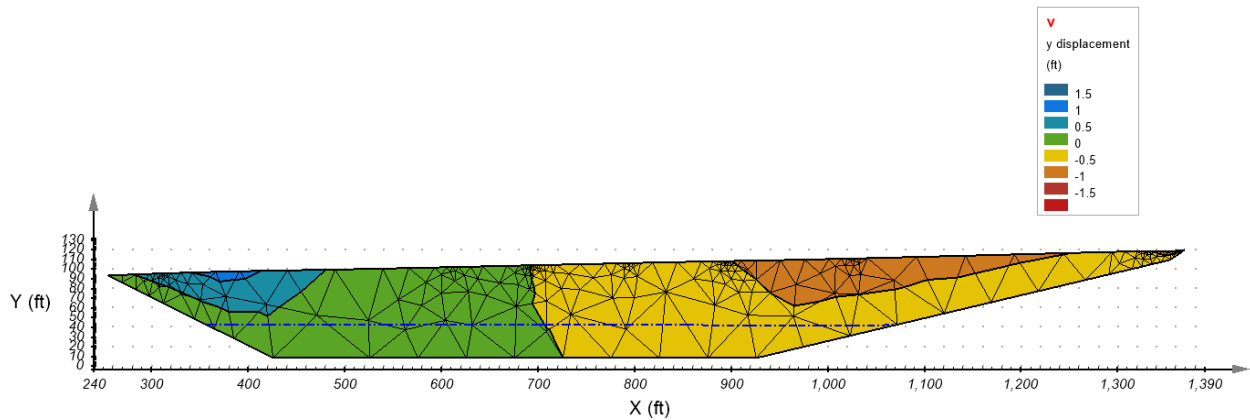


**Figure 69. y-displacement with 5-ft pressure head.**

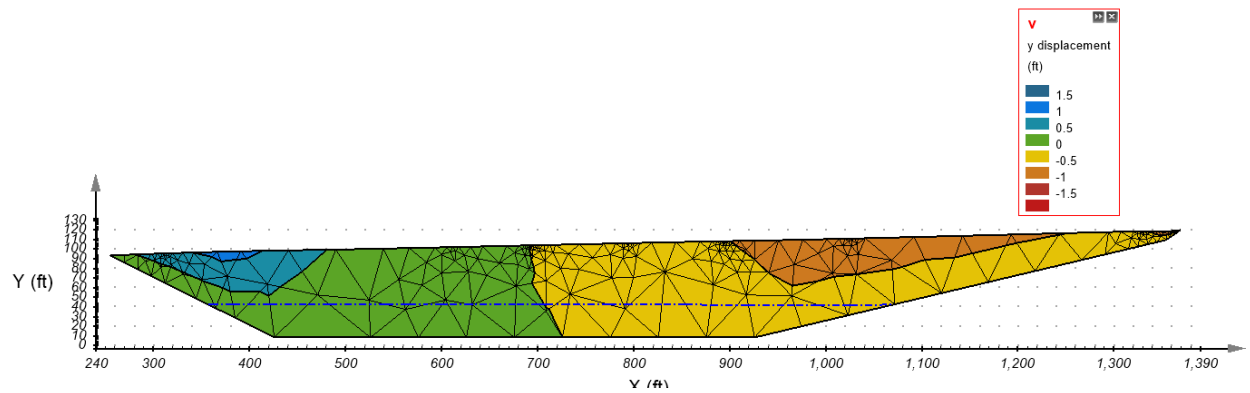


**Figure 70. y-displacement with 15-ft pressure head.**

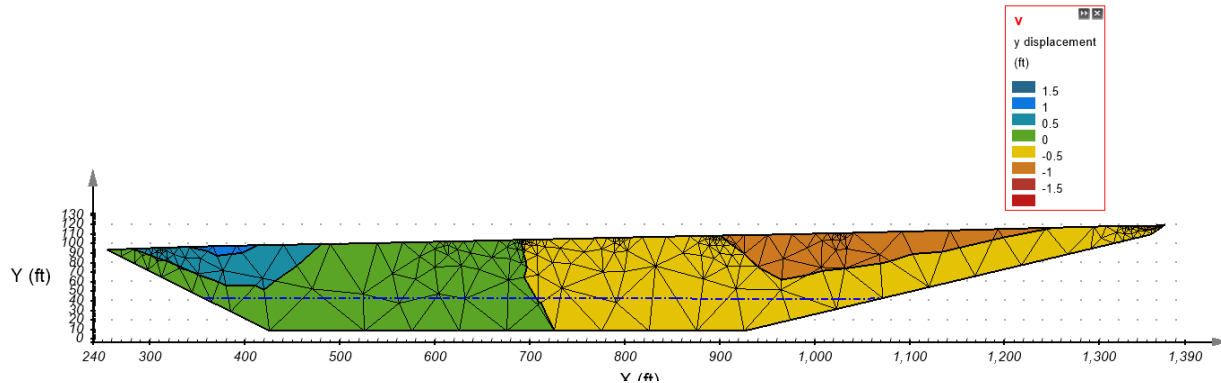


**Figure 71. y-displacement with 30-ft pressure head.**

### *GLD Reclaimed Impoundment*

After evaluating the pre-reclamation and WVDEP reclamation, a GLD reclamation of the Century impoundment was conducted. These efforts seek to answer what conditions could be changed or prevented with GLD. Models for GLD were produced using Carlson Natural Regrade and were performed by Amanda Rodrigues (Rodrigues, 2022). Of the different modeling outputs generated, the primary difference was the number of subbasins considered when creating a GLD model. After defining the number of subbasins, design criteria for the drainage density were either modeled based on default parameters for the western US or based on the work done by DePriest et al. (2015) for the Central Appalachia region.

Models that used only one subbasin (Figure 72) removed most of the dam structure to establish the desired drainage channel down the centerline of the impoundment. Models of 1 basin were also scaled improperly, resulting in meaningless results when trying to create cross section profiles as the stationing and scale could not be determined. The outputs for the 2 and 3 subbasin designs were drafted into a profile view, Figure 73 and Figure 74, respectively. Upon further comparison of the contours generate and the subsequent profiles, there was minor difference between any of the models. A mounded zone in the center of 8 to 9 feet was added, but the profile was less than a foot different between all models (Figure 75). Due to this limited difference across the models, only the DePriest cases were models.

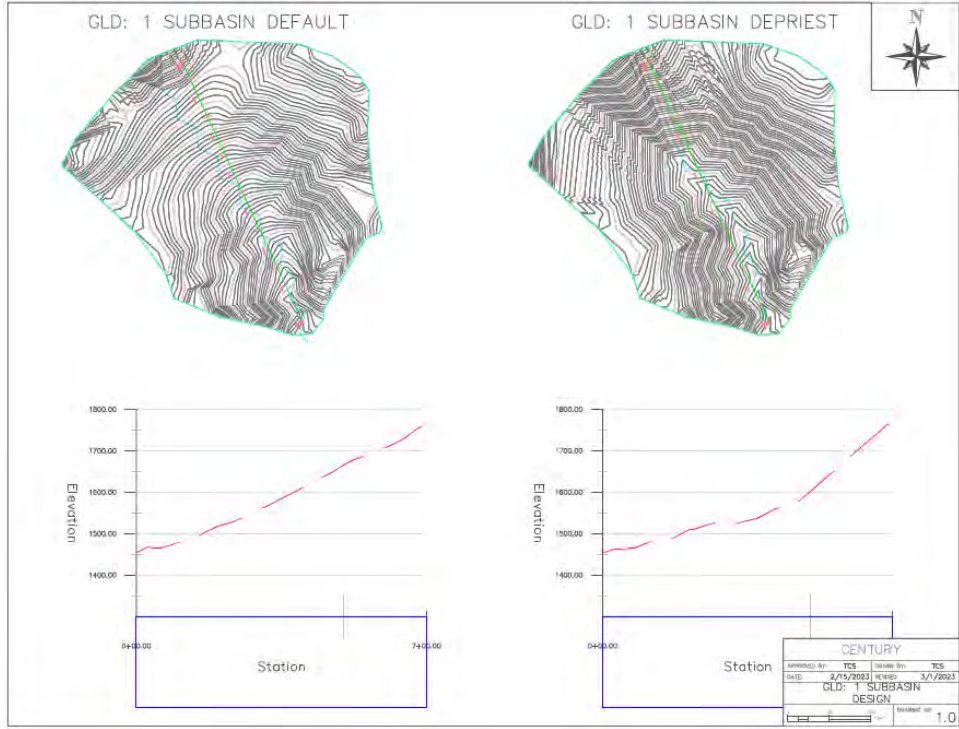


**Figure 72. GLD 1 subbasin design.**

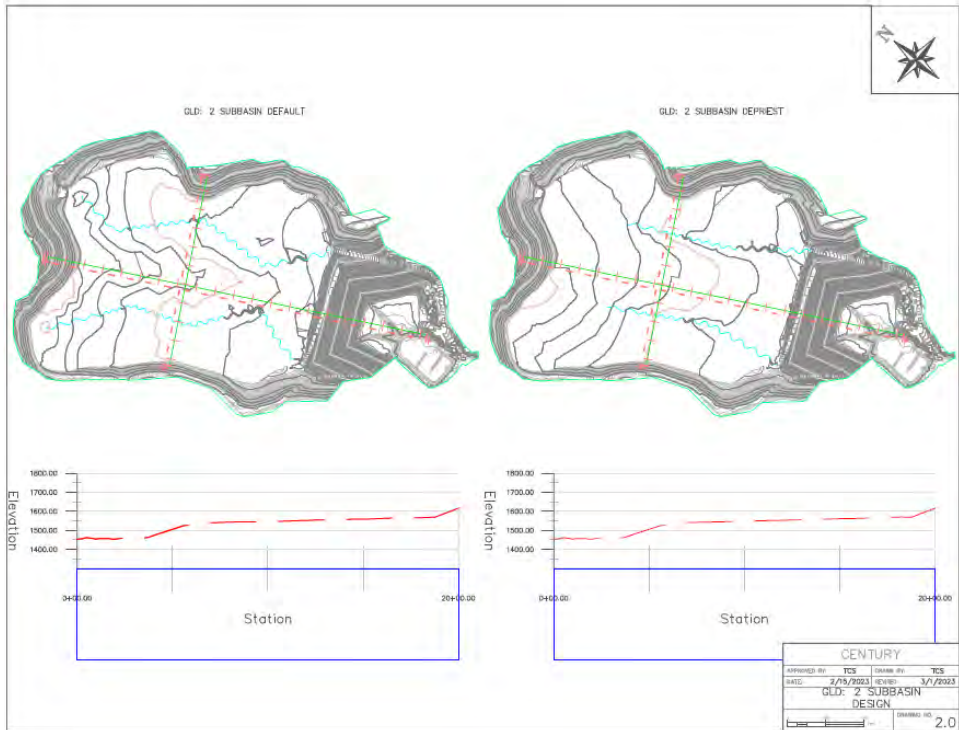


**Figure 73. GLD 2 subbasin design.**



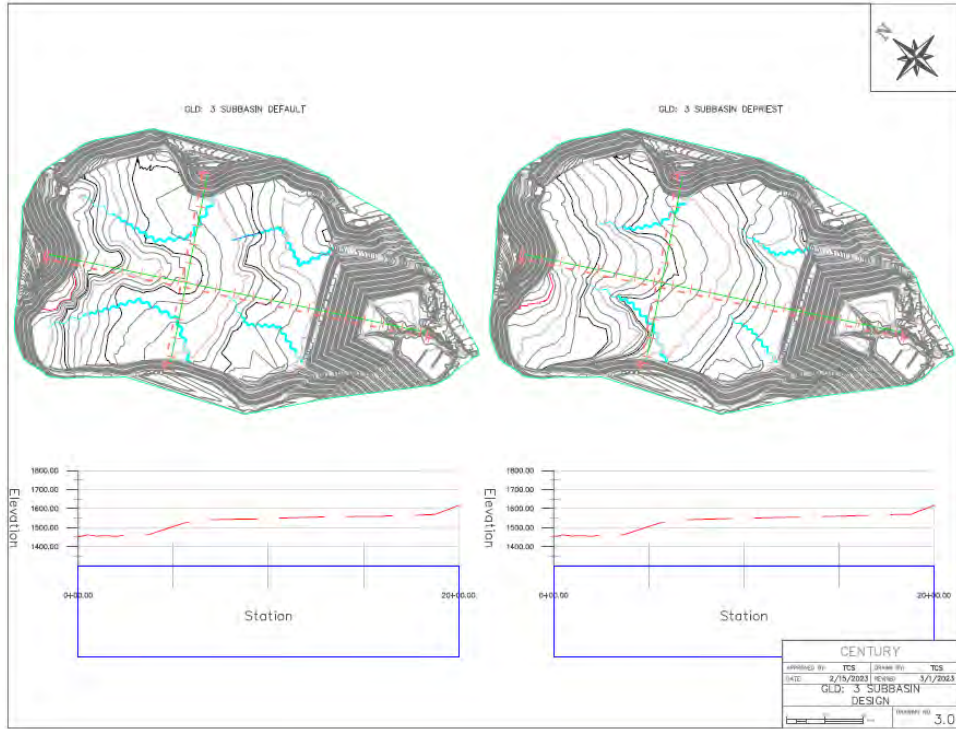


**Figure 74. GLD 3 subbasin design.**

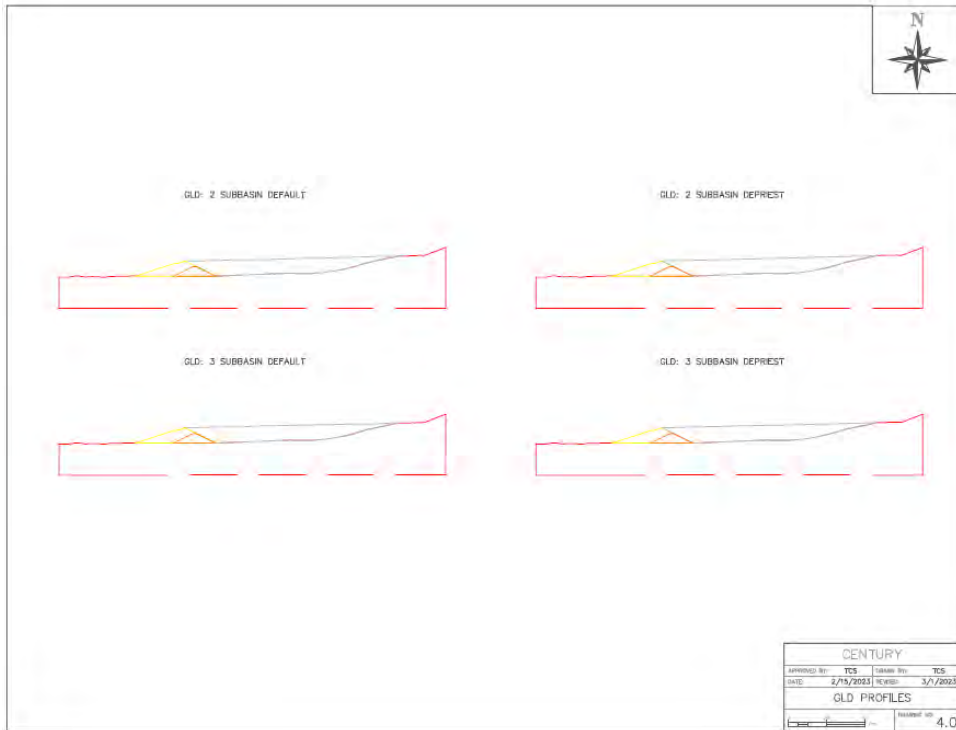


**Figure 75. GLD 2 and 3 subbasin design profiles.**

GLD Reclaimed Impoundment

**The results of the GLD reclamation are with the addition of the revised material parameters from the earlier cases; this involved changes in the seepage models and the slope stability modeling. Both GLD reclaimed models, 2 subbasin DePriest and 3 subbasin DePriest, were evaluated and summarized with**

Table 21 and Table 22, respectively. The seepage outputs for the 100-year and repeating 100-year storm are shown in Figure 76 and Figure 78 for the 2 subbasin DePriest design. The 3 subbasin DePriest seepage model outputs are illustrated in Figure 80 and Figure 82. With an increase in pore pressure from the repeating 100-year storm, the resultant factor of safety was lowered. The lowest factor of safety from each design storm were recorded with Figure 77, Figure 79, Figure 81, and Figure 83. It is noted that in this case the lowest factor of safety was produced by the deep foundation failure plane set with the grid and tangent method.

**Table 21. GLD reclamation model results (2 subbasin DePriest).**

GLD reclaimed model results (2 subbasin DePriest)						
Location:	Toe	Mid-slope	Crest	Upstream Slope	Deep Foundation	Slope Search
100-year storm	0.996 (B)	1.097	1.594	N/A	0.935	1.238 (B)
Repeating 100-year storm	0.926	0.948	1.343 (B)	N/A	0.886 (B)	1.216 (B)

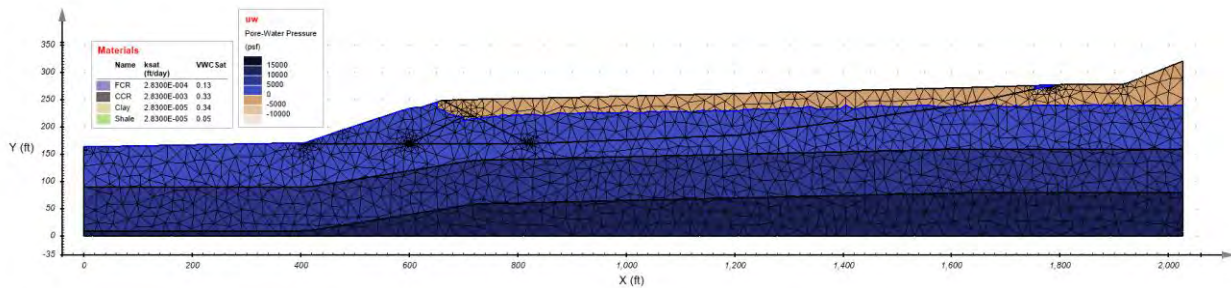


**Figure 76. 2 subbasin DePriest singular 100-year seepage output.**

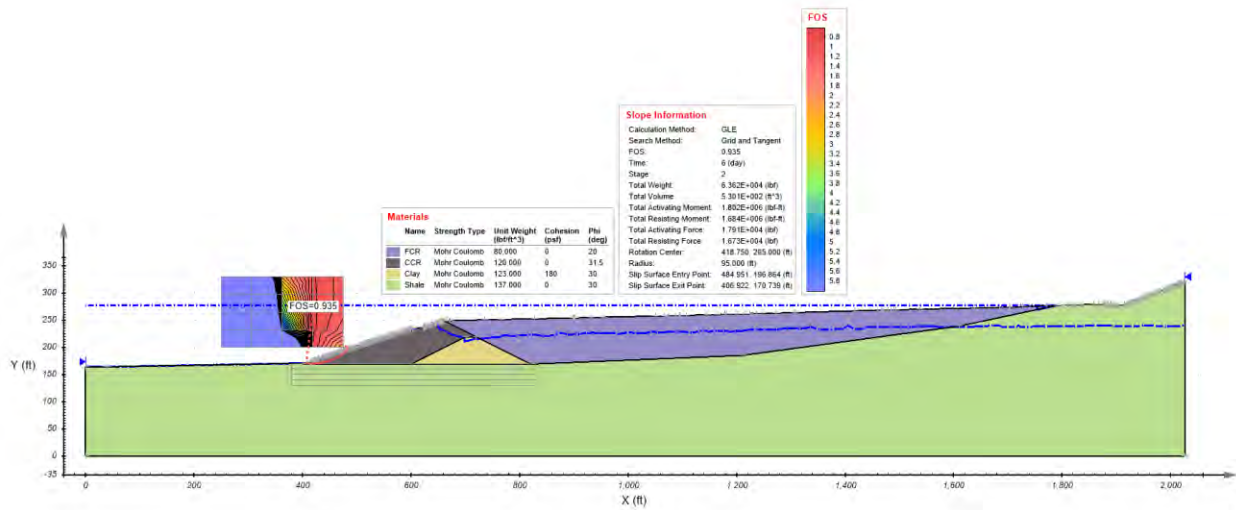


Figure 77. 2 subbasin DePriest deep foundation singular 100-year.

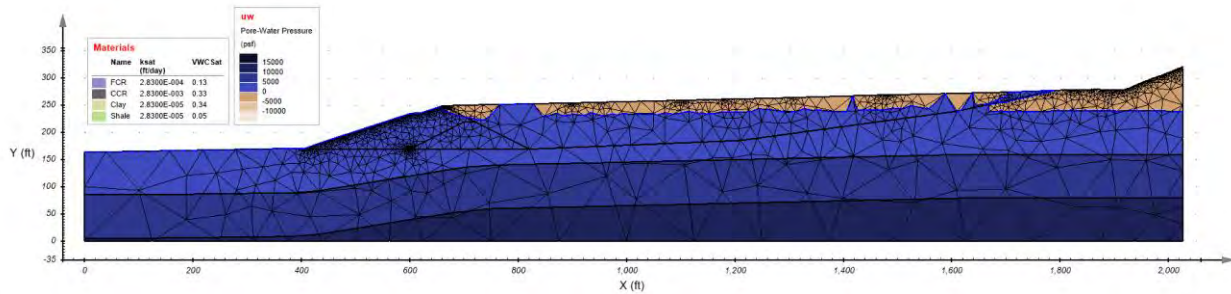


Figure 78. 2 subbasin DePriest repeating 100-year seepage output.

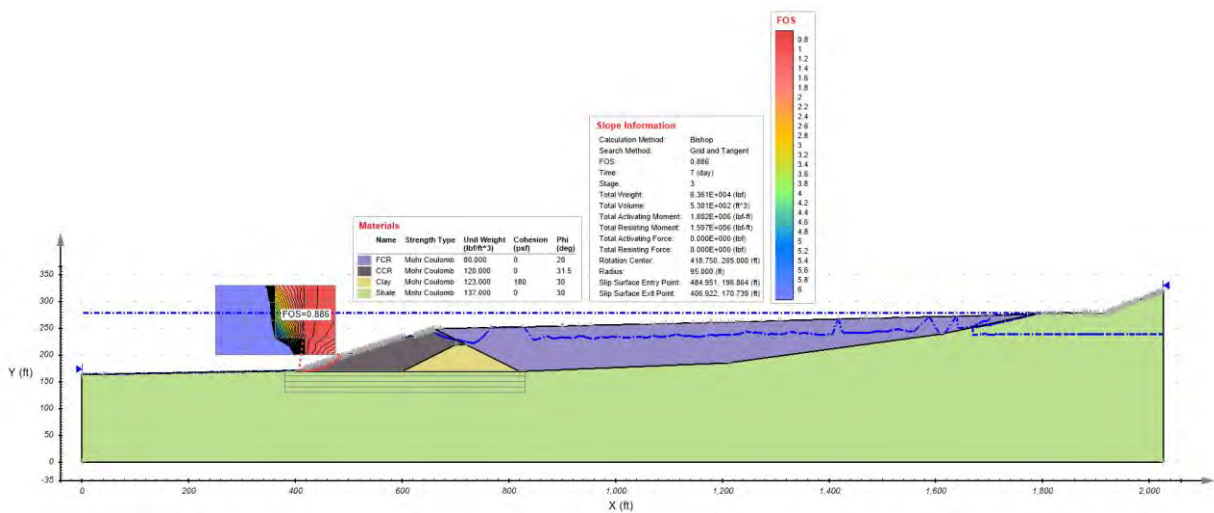


Figure 79. 2 subbasin DePriest deep foundation repeating 100-year.

Table 22. GLD reclamation model results (3 subbasin DePriest).

GLD reclaimed model results (3 subbasin DePriest)						
Location:	Toe	Mid-slope	Crest	Upstream Slope	Deep Foundation	Slope Search
100-year storm	0.995 (B)	1.071	1.614 (B)	N/A	0.937 (B)	1.187 (B)
Repeating 100-year storm	0.919 (B)	0.924	1.341 (B)	N/A	0.900 (B)	1.165 (B)

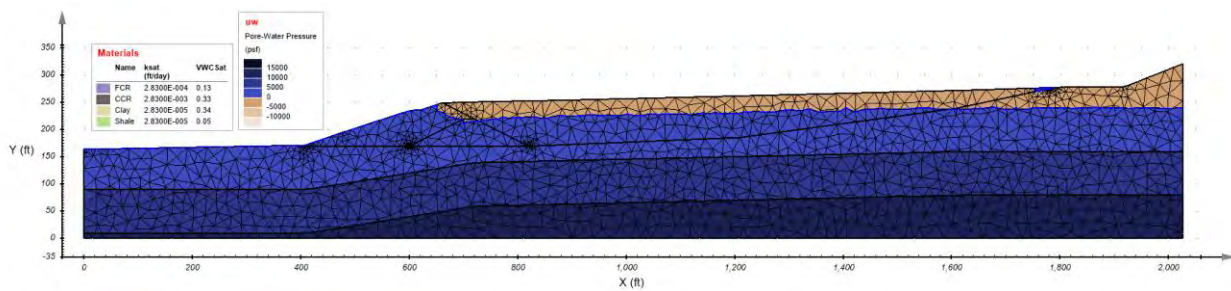


Figure 80. 3 subbasin DePriest singular 100-year seepage output.

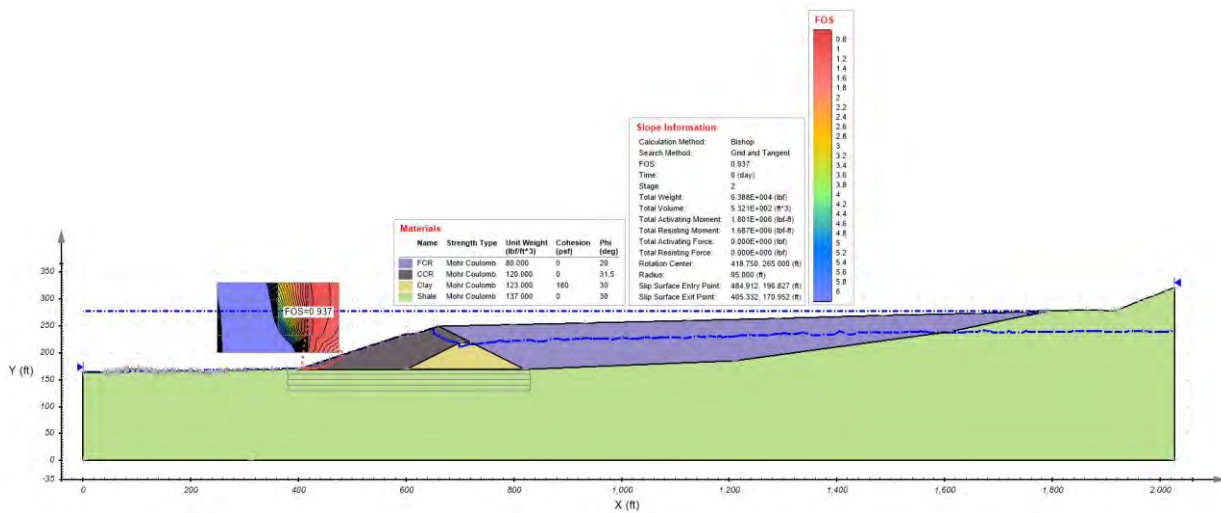


Figure 81. 3 subbasin DePriest deep foundation singular 100-year.



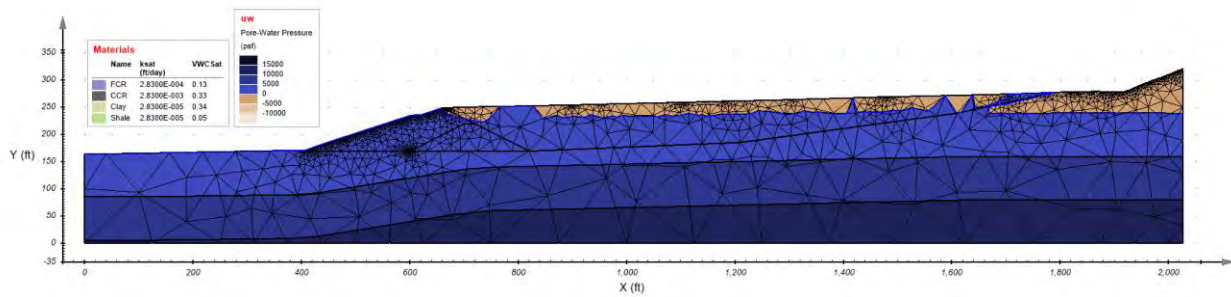


Figure 82. 3 subbasin DePriest repeating 100-year seepage output.

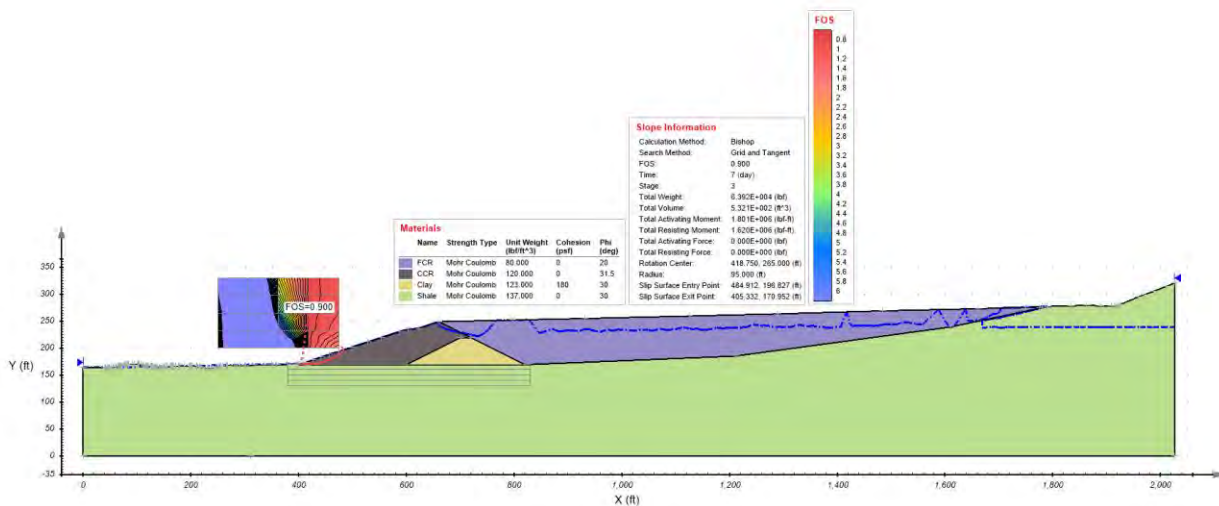


Figure 83. 3 subbasin DePriest deep foundation repeating 100-year.

## Finite Element Modeling for Federal No. 2

The focus of these models outlines the results of coupled seepage and slope stability analysis. All models were conducted along the centerline of the impoundment for the highest summation of forces exerted. Two design storm events were considered in the seepage analysis: a 100-year storm and consecutive 100-year storms, one day apart. The design precipitation event for the area was 5.24 inches in 24 hours, as indicated by from US Department of Commerce (2023) Various failure locations were considered, and the resultant factors of safety were condensed into a table.

### *Federal No. 2 Active Impoundment*

All data used for the Federal No. 2 impoundment was compiled from publicly available data and some documentation from the WVDEP. Data included state boundaries, watershed elements, and contour data. The boundary of the impoundment was added to reduce unnecessary data. Civil 3D was used to compile all data and georeferenced to the datum of Code LL83, EPSG Code 4269 for USGS data. Figure 84 illustrates construction of the correct georeferencing combined into a base map with the reference being set to Code WV83-NF, EPSG Code 26853. Data was color

coordinated for ease of interpretation and manipulation of information: grey is the state boundary, green is the watershed district, light and dark blue are secondary and primary water ways, yellow was used for the contour, and pink was set as the impoundment boundary. A profile view of the existing impoundment was drawn to be imported into PLAXIS LE.

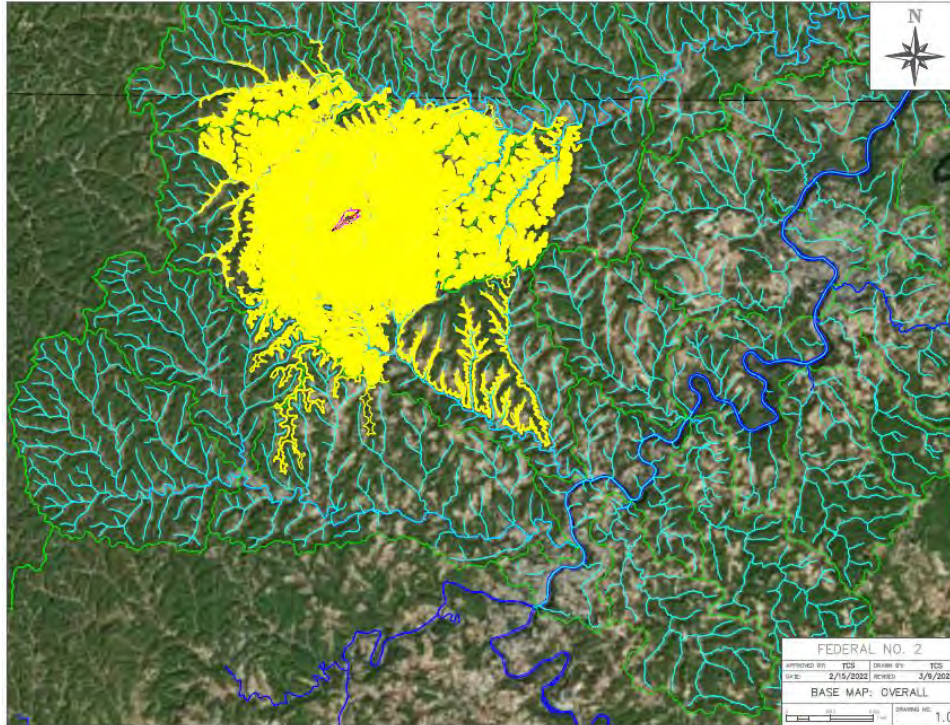


**Figure 84. Overall base map.**

Figure 85 is a view of the existing Federal No 2 impoundment and Figure 86 illustrates the site contours and base map. Figure 87 is the center-line elevation drawing of the impoundment imported into Plaxis LE.





**Figure 85. Zoomed in base map.**



**Figure 86. Base map with contour data.**

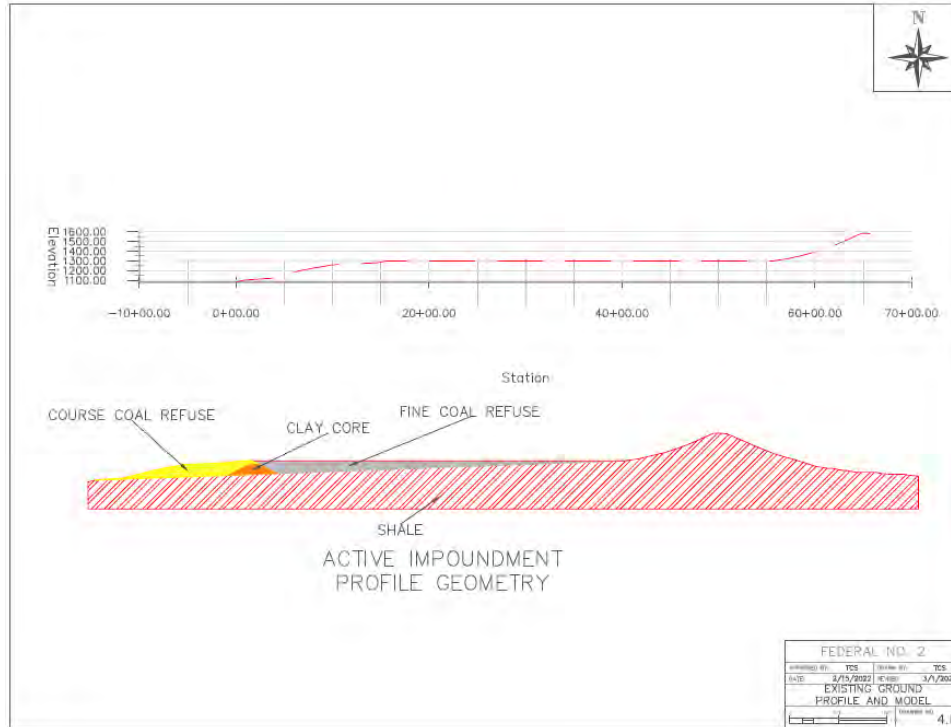


**Figure 87. Federal No. 2 centerline existing ground profile and model.**

**Federal No. 2 Active Impoundment Results**

The active impoundment was evaluated using the slope search method across the entire impoundment. The resultant factors of safety can be listed in Table 23. For the first 100-year storm event the seepage output is illustrated in Figure 83 and the stability analysis using the slope search method identified the lowest Factor of Safety of 1.484 at the downstream toe (Figure 89). As expected, pore water pressure increased (Figure 90) with the additional storm and the overall factor of safety lowered. Shallow failure planes (Figure 91) were generated in the toe of the impoundment, due to the buildup of pore water pressure internal to the downstream slope face.

**Table 23. Active impoundment modeling results.**

Pre-reclamation model results	
Location:	Slope Search
100-year storm	1.484 – 2.868
Repeating 100-year storm	0.977 – 2.735



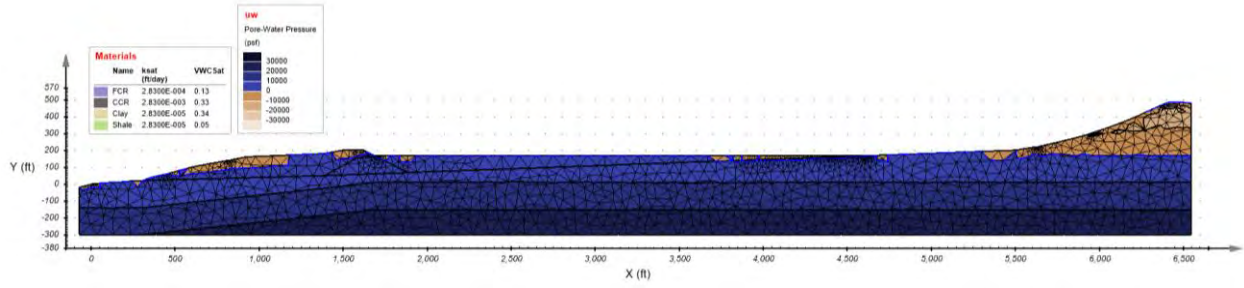


Figure 88. Active Federal No. 2 singular 100-year seepage output.

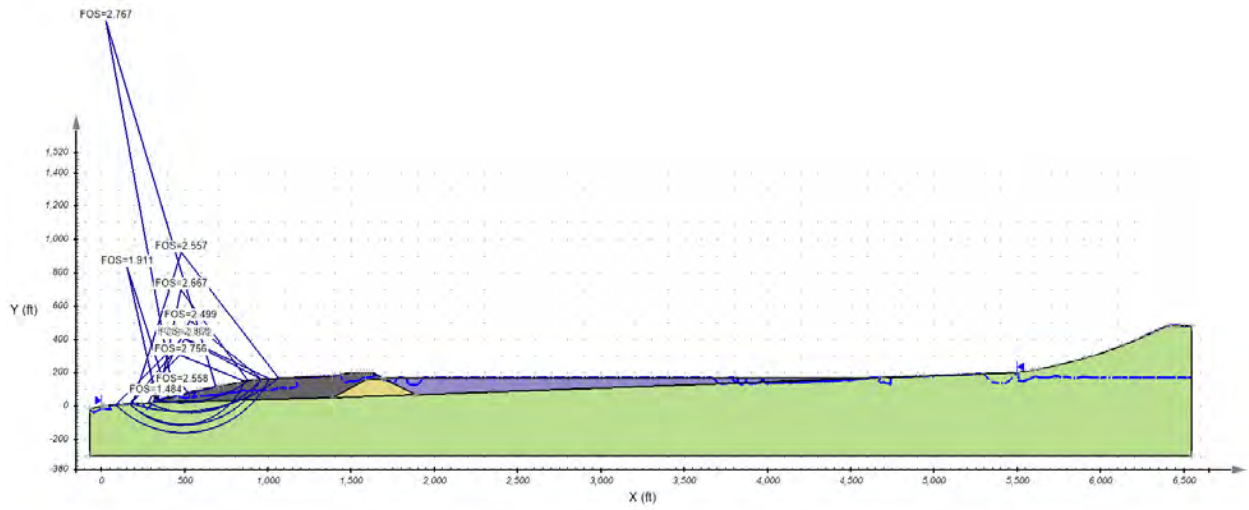


Figure 89. Active Federal No. 2 auto singular 100-year.

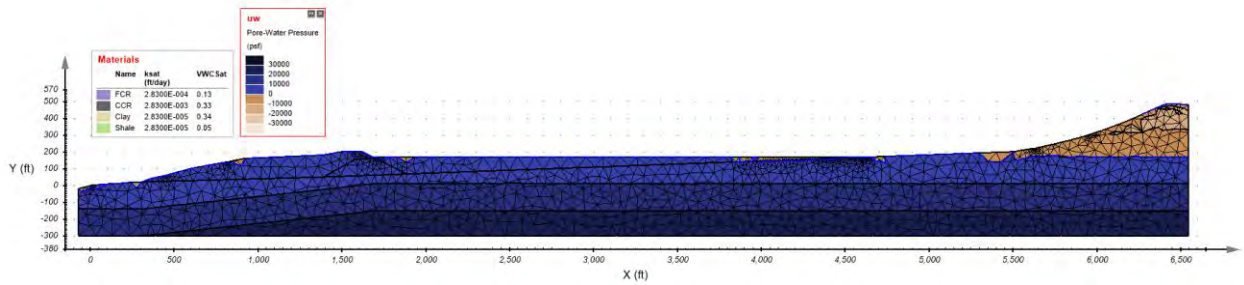
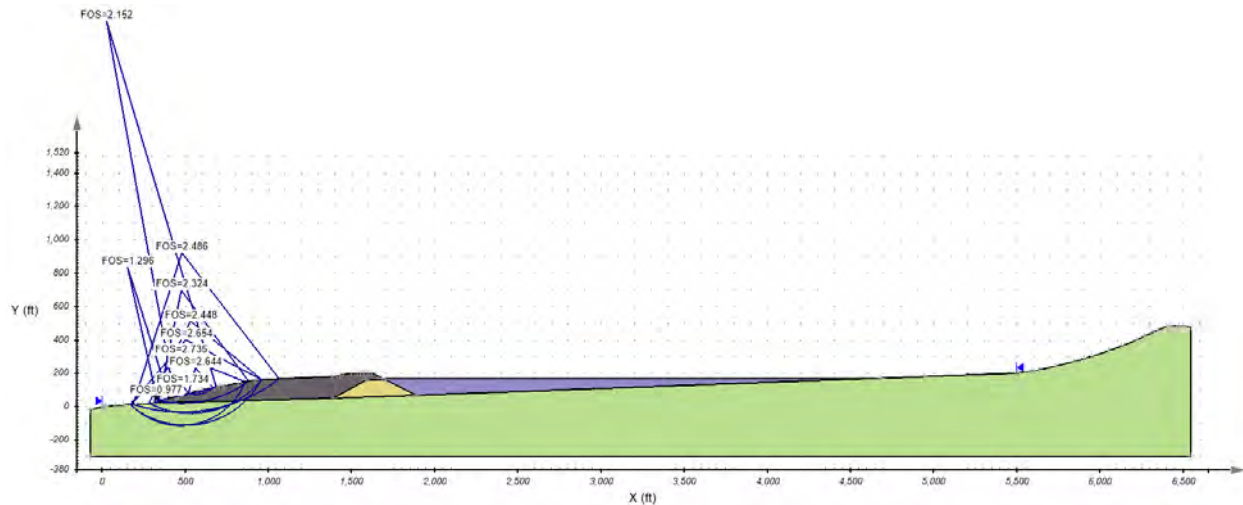


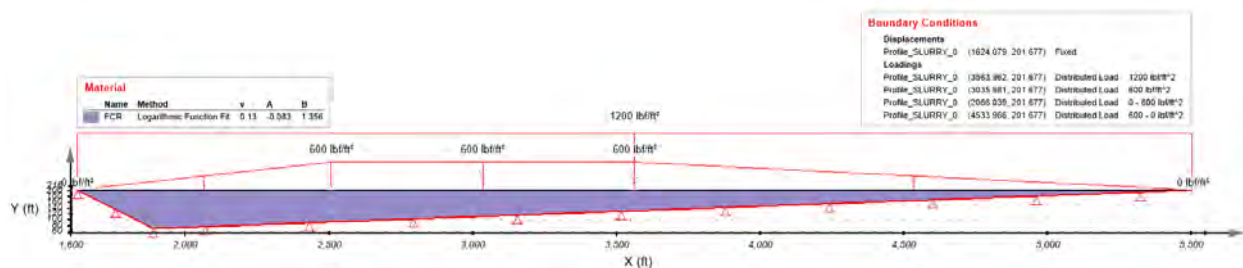
Figure 90. Active Federal No. 2 repeating 100-year seepage output.



**Figure 91. Active Federal No. 2 auto repeating 100-year.**

After conducting the slope stability analysis, consolidation of the refuse material was evaluated to determine the deformation of the FCR under load. Only FCR geometry was evaluated due to the issues experienced in the field with the material. In each model the lower boundaries were fixed point, not allowing deformation past them, mirroring that of the site conditions. The exposed top surface was allowed to displace horizontally and vertically as a free boundary. Groundwater conditions in the model was set at 100 feet. Water was also allowed to drain the model through the bottom upstream face of the refuse shell.

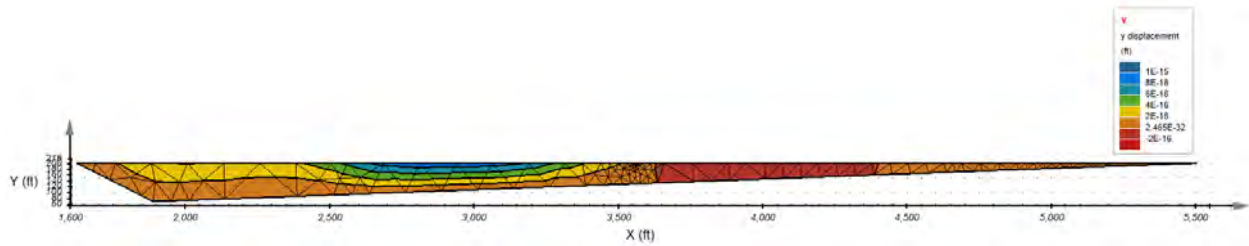
Loads were applied to the model to simulate the addition of mounded material atop the FCR. Two loads were applied to the refuse, a distributed 10-foot-thick layer of CCR and a mounded 5-foot-thick layer of CCR (Figure 92). These loads were the 1,200 lbf/ft<sup>2</sup> and the trapezoidal load of 600 lbf/ft<sup>2</sup>, respectively. Additional models changed the load with the addition of mounded CCR, to a height of 15 and 30 feet. Models were allowed to consolidate and deform over a period of 2000 days, or about 5.5 years.



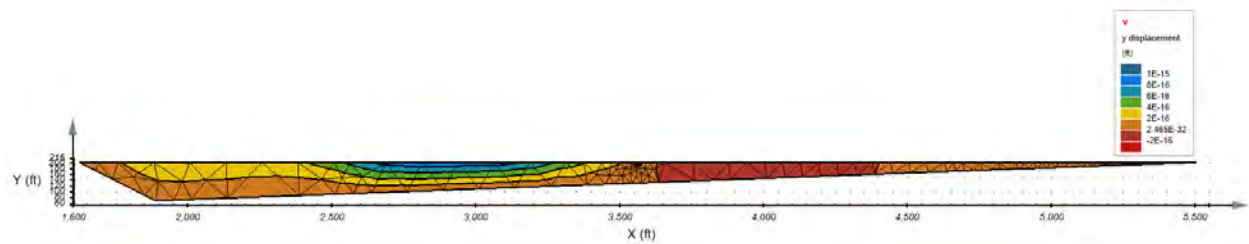
**Figure 92. 5-ft mound load on top of fine coal refuse.**

Figure 93, Figure 94, and Figure 95, show the deformation in the y direction after the application of a 5, 15, and 30 feet of mounded CCR. Results of these models indicate consolidation near the center of the impoundment (3,000 ft upstream) and heave occurring at approximately 4,000 ft.

This deformation is  $1\text{E-}15$  foot consolidation and  $2\text{E-}16$  foot heave, respectively. These results are nearly identical across all three load cases.



**Figure 93. y-displacement for 5-ft mounded after 2,000 days.**



**Figure 94. y-displacement for 15-ft mounded after 2,000 days.**

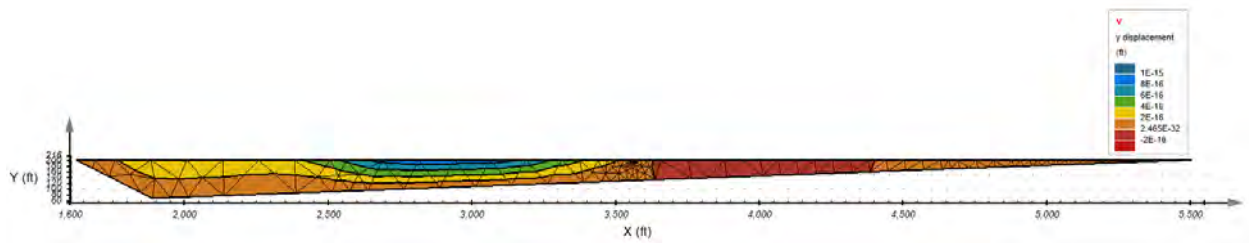


**Figure 95. y-displacement for 30-ft mounded after 2,000 days.**

Additional models were conducted with a pressure head applied to the top right of the model, a length of 15 feet. The pressure head was modeled to imitate that of water runoff from the surrounding hillside and not contained by the perimeter drainage ditch. The pressure heads applied were 5, 15, and 30 feet. The resultant vertical deformation can be seen in Figure 96, Figure 97, and Figure 98, respectively. These models also included a mounded 10-foot-thick layer of CCR.

Results from these loading cases produced nearly identical results across all models. No consolidation was observed across the refuse, however some heaving along the upstream 4,000 foot right side moved up  $4\text{E-}4$  feet.

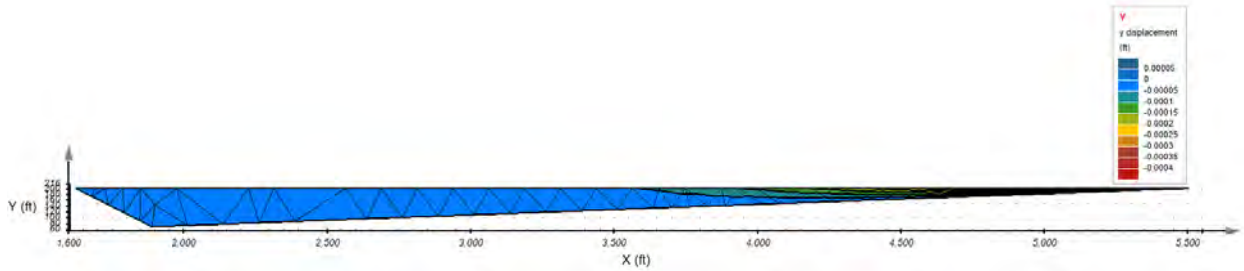


**Figure 96. y-displacement for 5-ft of water head after 2,000 days.**

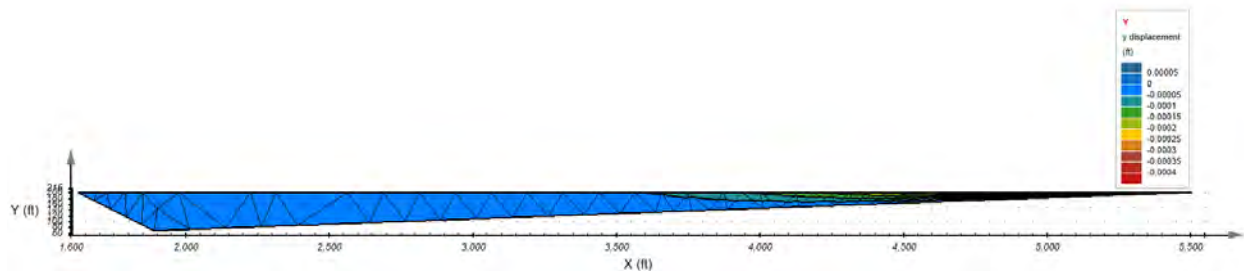


**Figure 97. y-displacement for 15-ft of water head after 2,000 days.**

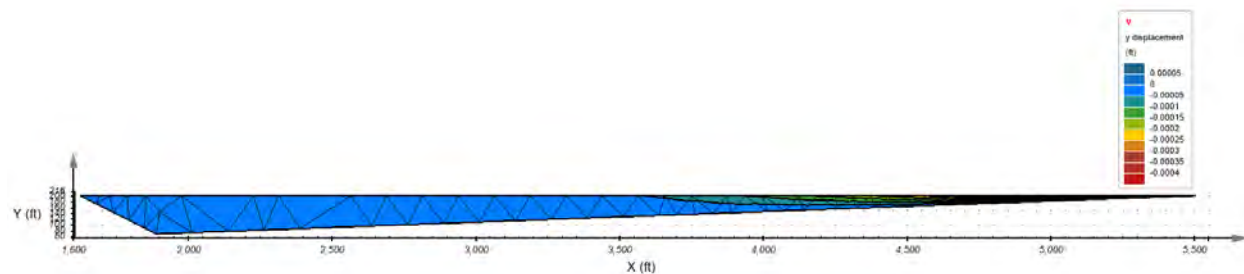


**Figure 98. y-displacement for 30-ft of water head after 2,000 days.**

This concludes with the impounded refuse (FCR and CCR) did not indicate significant vertical movement, either as consolidation or heave. This observation is relevant because after the reservoir volume is filled with CCR, the site should exhibit long-term stability based on a fixed boundary analysis.

#### *Federal No. 2 GLD Reclaimed Impoundment*

After completing the active impoundment and analysis of foundation stability, GLD iterations could be performed on a basis of comparison. Outputs from Carlson were based on a 2-basin design with different allowable areas of disturbance. The difference in the allowable area of disturbance was between the valley ridge (Figure 99), the entire extend of the impoundment's watershed, and the active impoundment (Figure 100), from the headwaters to the crest of the



dam. From these models, an elevation ridge of 1500 feet was established to dictate a desired grading scheme. Centerline profiles were drawn to model in PLAXIS LE.

Three additional cases were based on modified versions of the Carlson models. These models worked to lower the height of the mounded material to 50 feet and maintain the ideology of GLD. Case 3 modeled the Carlson output used in Case 1, lowered to 50 feet. Case 4 and 5 are the application of mounded CCR with a side slope of a 2H:1V (26.6°) and 3H:1V (18.4°), respectively. The profile of all models is illustrated in Figure 101 and Figure 102. The slope search method was then conducted along the dam and along the mounded refuse to determine the resultant factor of safety.

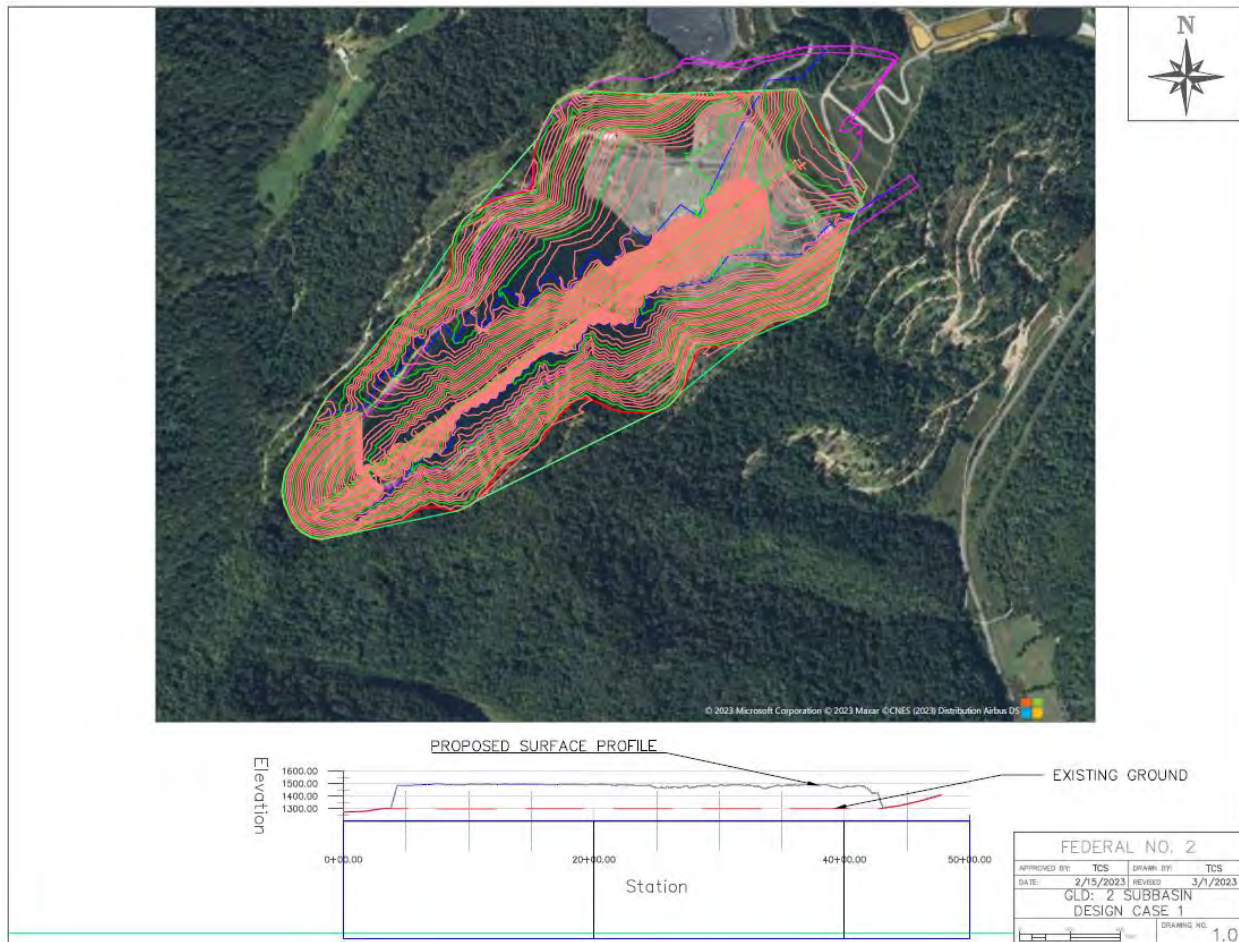


**Figure 99. GLD 2 subbasin ridge design (Case 1).**

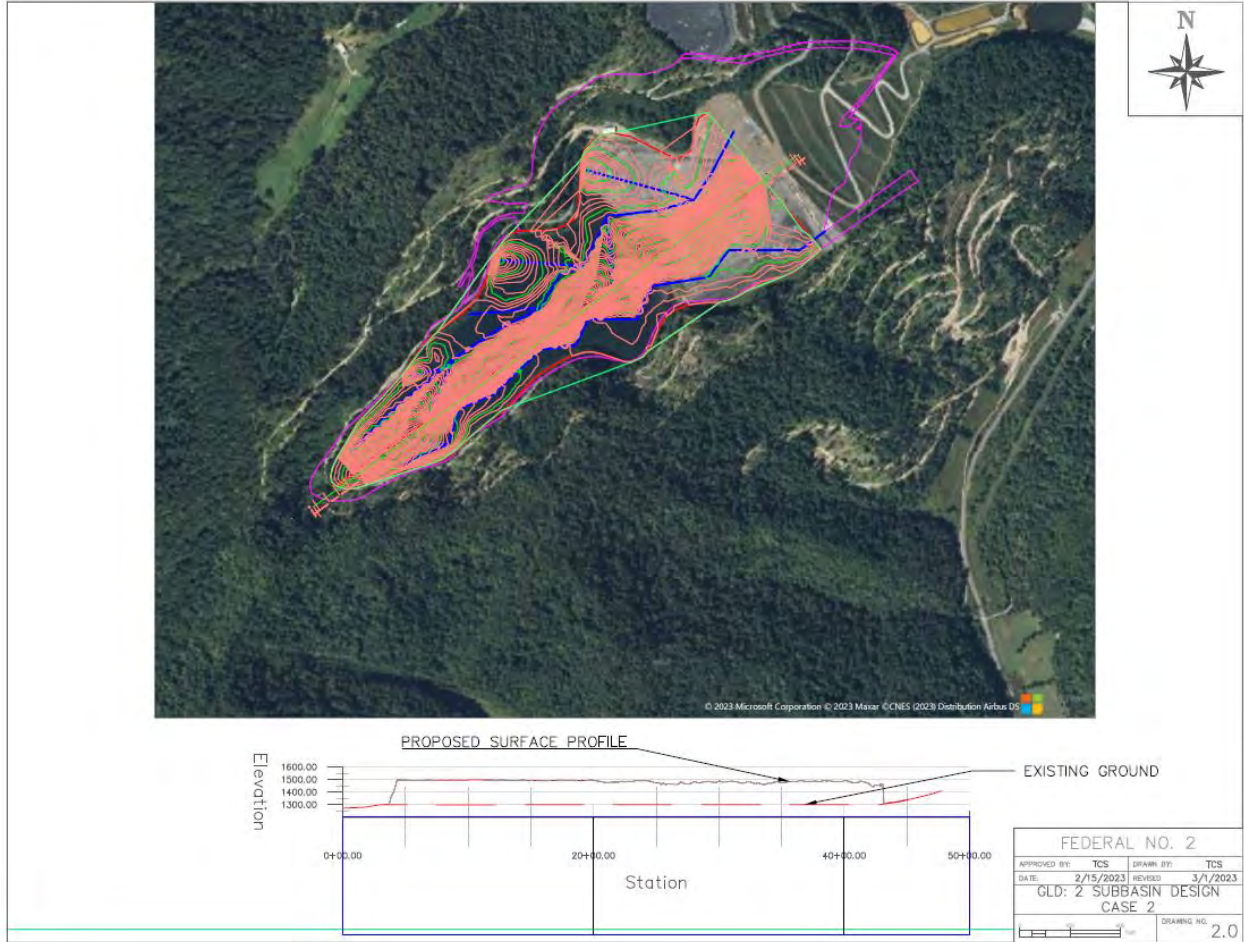


**Figure 100. GLD 2 subbasin impoundment design (Case 2).**

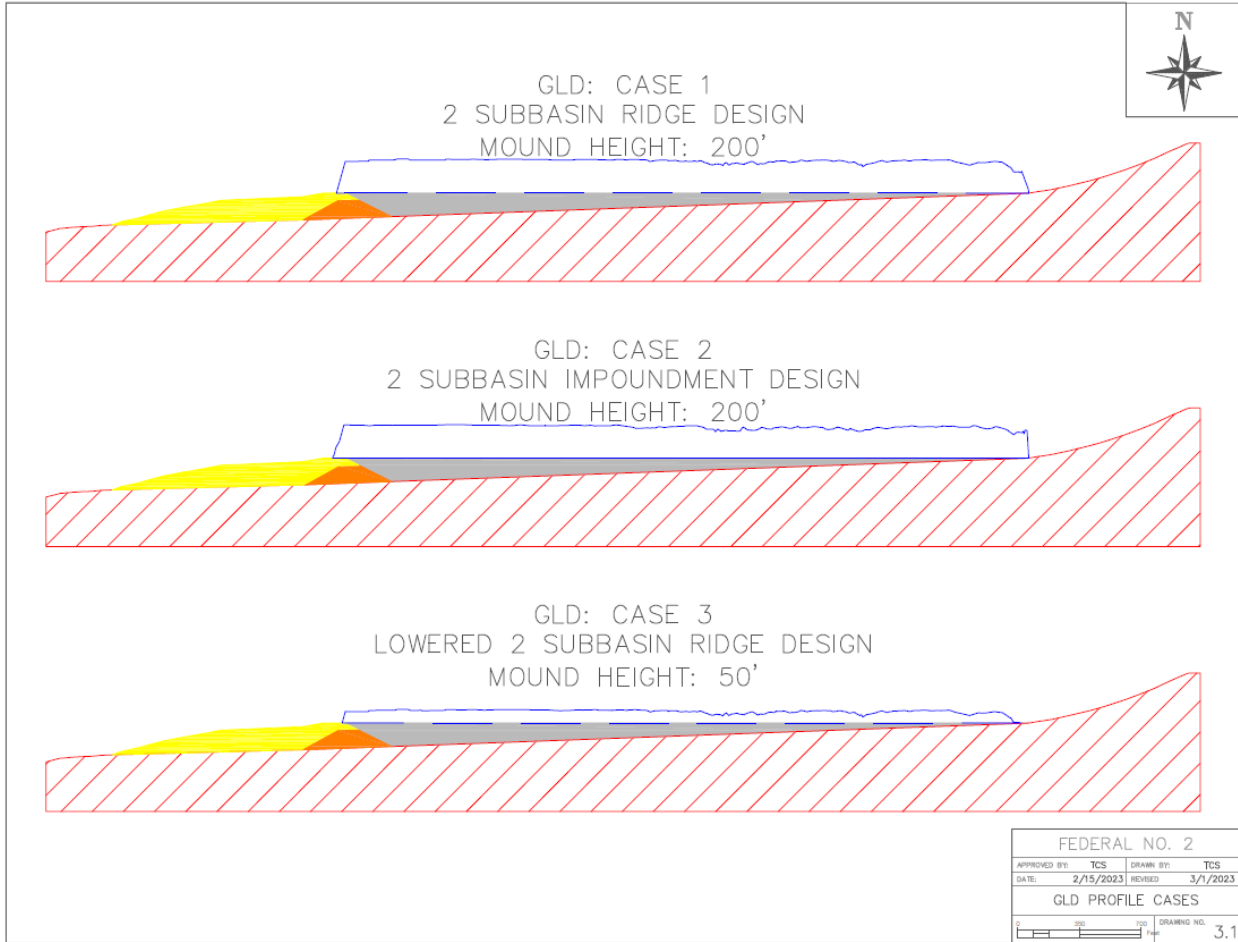


**Figure 101. GLD Profile Cases (Part 1).**

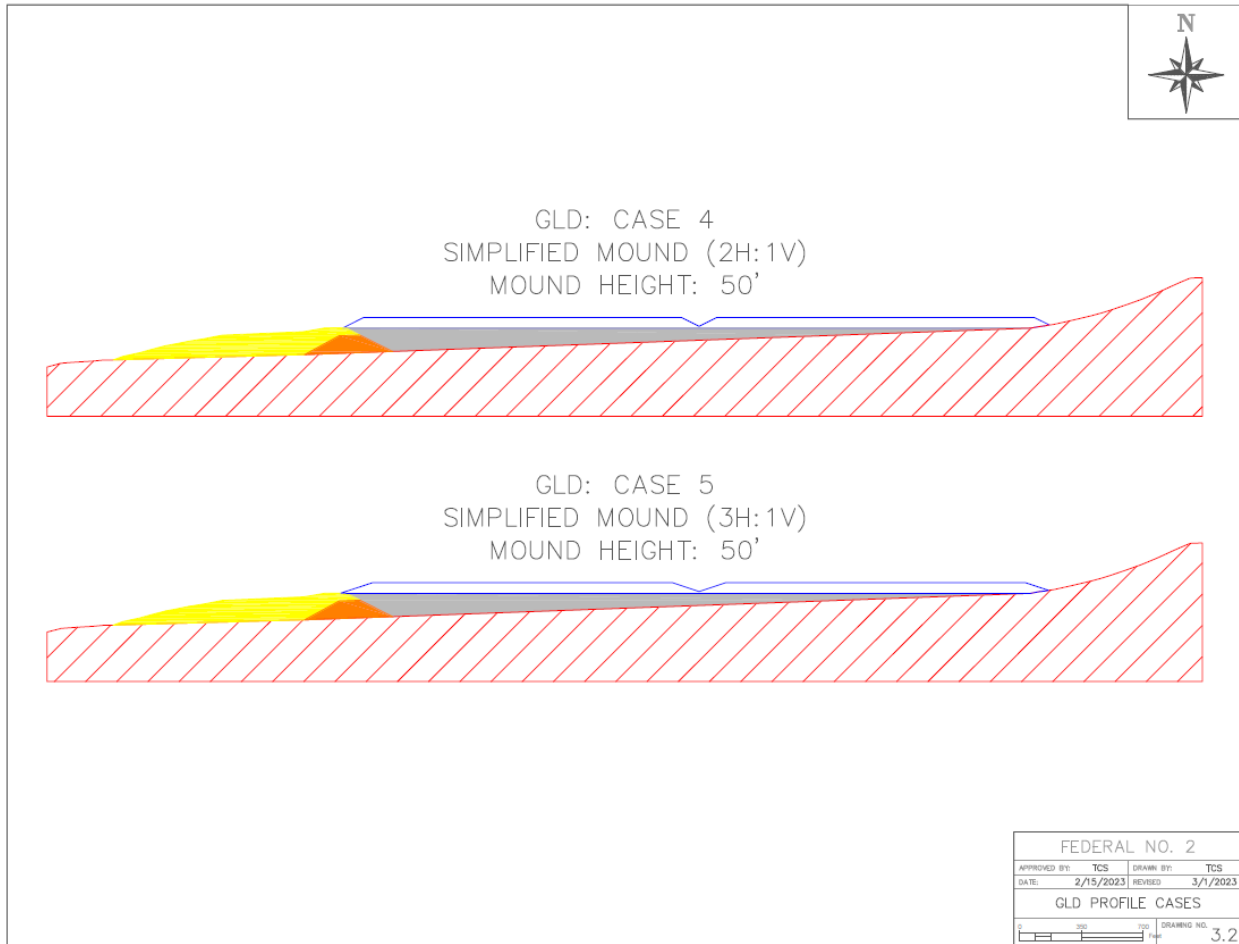


**Figure 102. GLD Profile Cases (Part 2).**

### Federal No. 2 GLD Reclaimed Impoundment Results

The singular 100-year storm seepage outputs for the five cases are illustrated in Figure 103, Figure 107, Figure 111, Figure 115, and Figure 123. The repeating 100-year storm seepage outputs for the five cases are outlined in Figure 105, Figure 109, Figure 113, Figure 119, and Figure 127. The resultant factors of safety for the singular 100-year storm are shown in Figure 104, Figure 108, Figure 112, Figure 116, Figure 117, Figure 118, Figure 124, Figure 125, and Figure 126. The resultant factors of safety for the repeating 100-year storm are shown in Figure 106, Figure 110, Figure 114, Figure 120, Figure 121, Figure 122, Figure 128, Figure 129, and Figure 130. Table 24 through Table 28 provide the summarized data of each modeling case.

The results of the GLD modeling of the Federal No. 2 impoundment set to reduce infiltration along the mounded material added to backfill the slurry. As seen in Case 1 through 3, the complex geometry of the CCR cap reduces infiltration and saturation of the impoundment cap. However, the complex geometry also generated unstable slopes based on the failure observed on the left end of the mounded CCR. Cases 4 and 5 were simplified profiles, which became completely saturated after each storm event. However, slope stability within the mound was maintained. Small failure planes were still experienced along the dam as pore water pressure built up.



**Table 24. Case 1 modeling results.**

GLD 2D Case 1	
<b>Location:</b>	<b>Slope Search</b>
<b>100-year storm</b>	0.635 – 0.956
<b>Repeating 100-year storm</b>	0.635 – 0.956

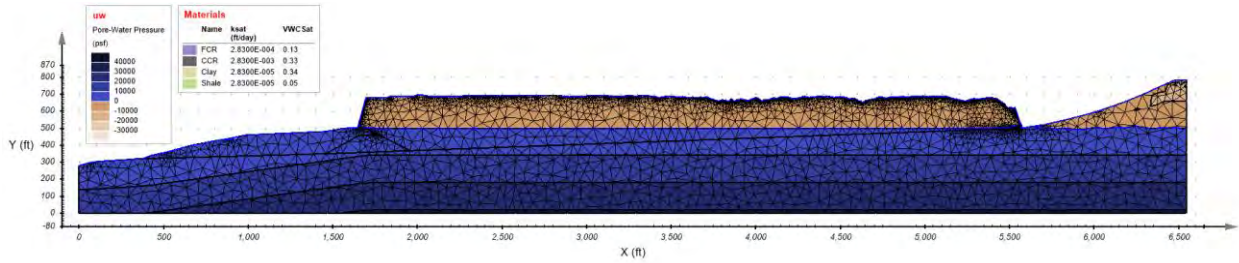


**Figure 103. Case 1 singular 100-year seepage output.**

picture of output from computer modeling

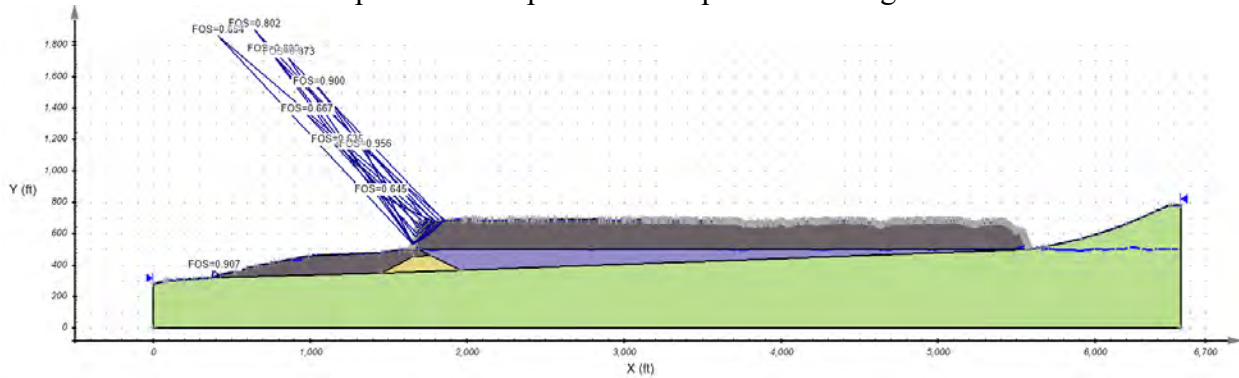


**Figure 104. Case 1 auto singular 100-year.**

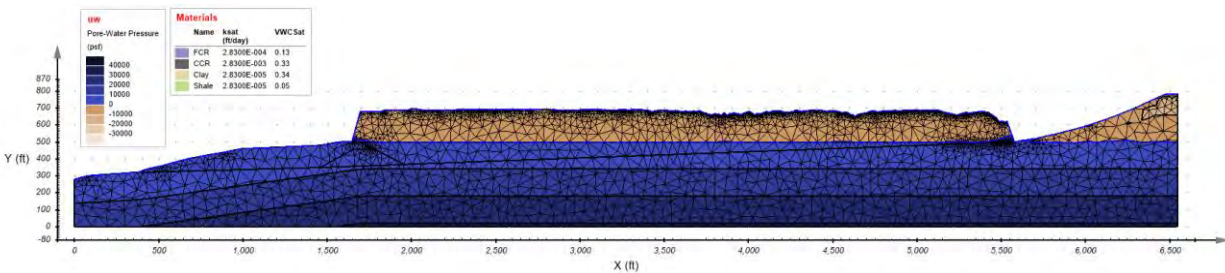


**Figure 105. Case 1 repeating 100-year seepage output.**

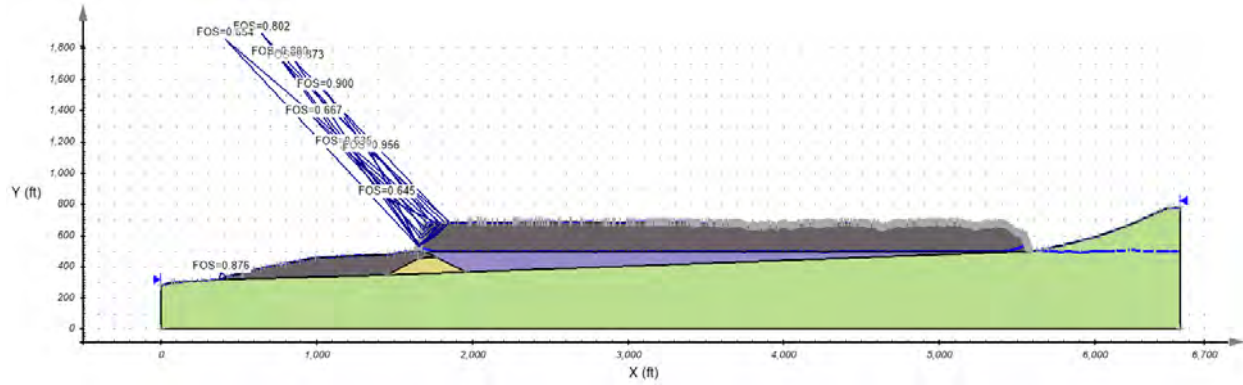


Figure 106. Case 1 auto repeating 100-year.

Table 25. Case 2 modeling results.

GLD 2D Case 2	
Location:	Slope Search
100-year storm	0.435 – 0.839
Repeating 100-year storm	0.435 – 0.839

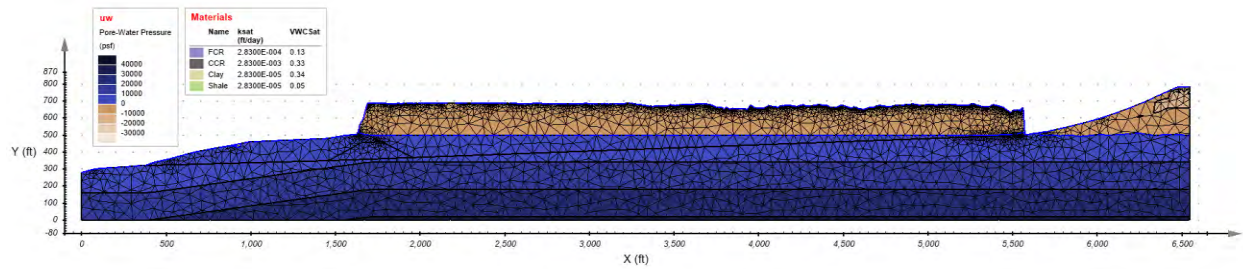


Figure 107. Case 2 singular 100-year seepage output.

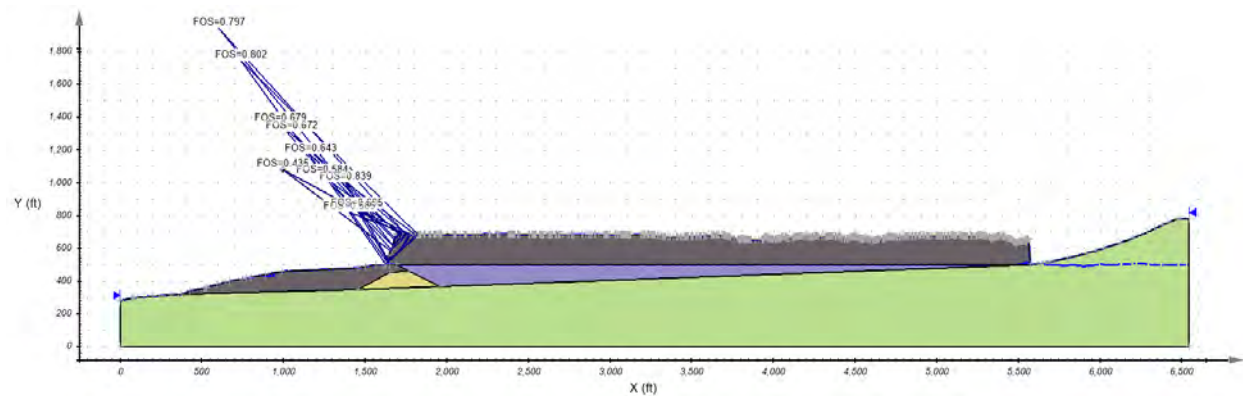


Figure 108. Case 2 auto singular 100-year.

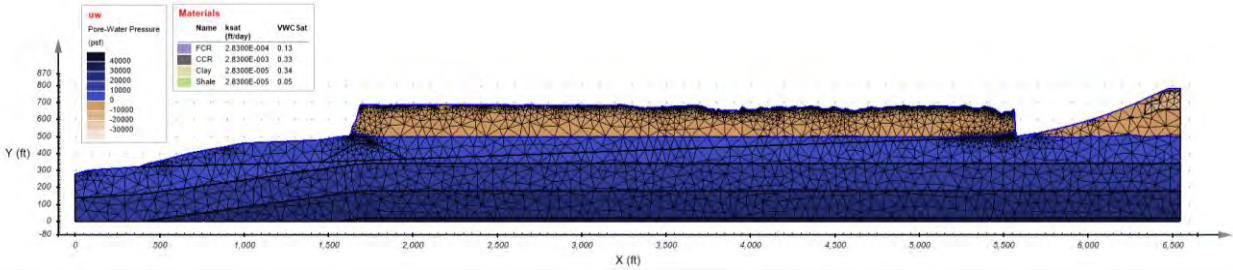


Figure 109. Case 2 repeating 100-year seepage output.

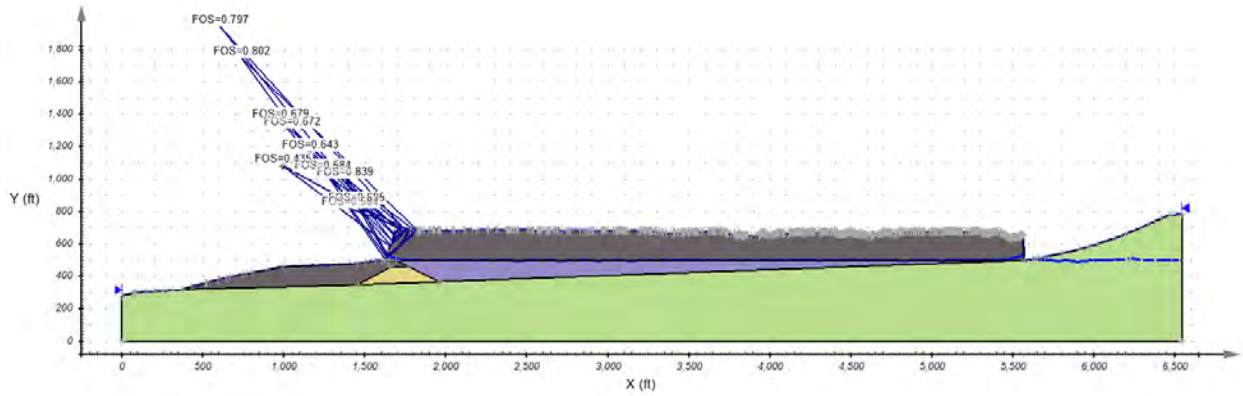


Figure 110. Case 2 auto repeating 100-year.

Table 26. Case 3 modeling results.

GLD Lowered to 50'	
Location:	Slope Search
100-year storm	0.472 – 1.322
Repeating 100-year storm	0.404 – 1.322

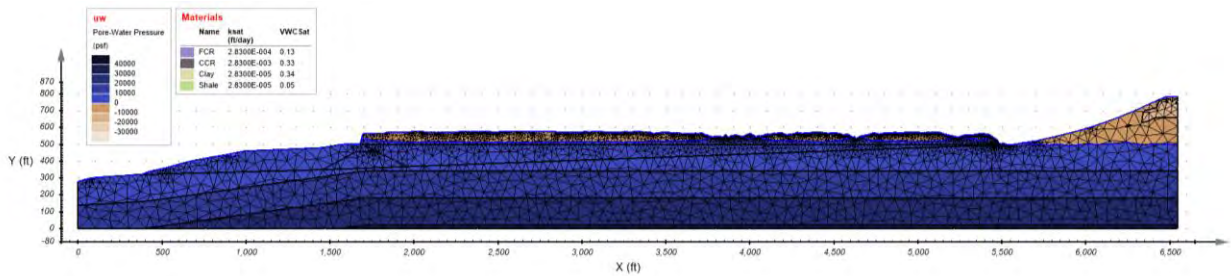


Figure 111. Case 3 singular 100-year seepage output.



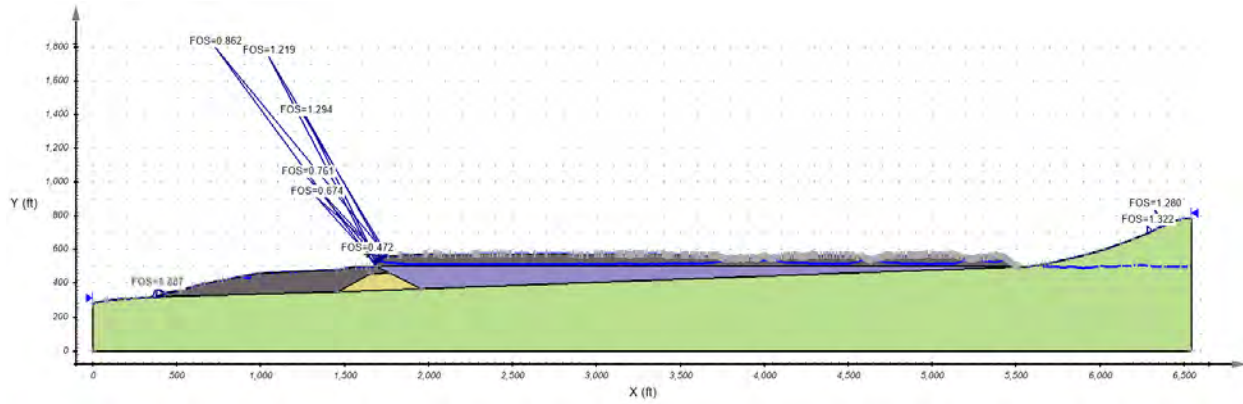


Figure 112. Case 3 auto singular 100-year.

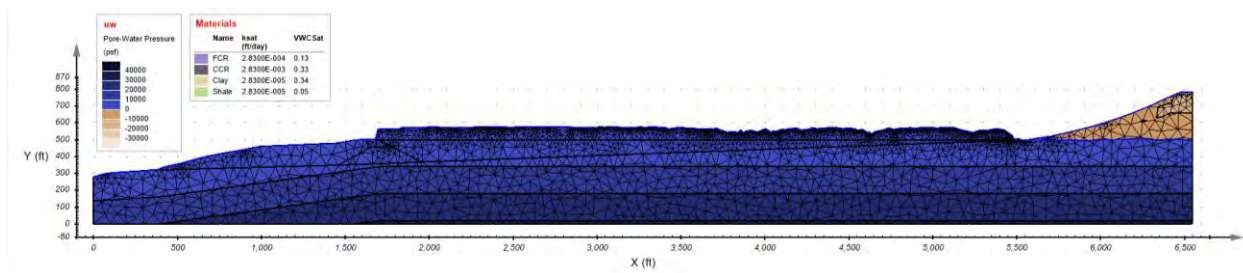


Figure 113. Case 3 repeating 100-year seepage output.

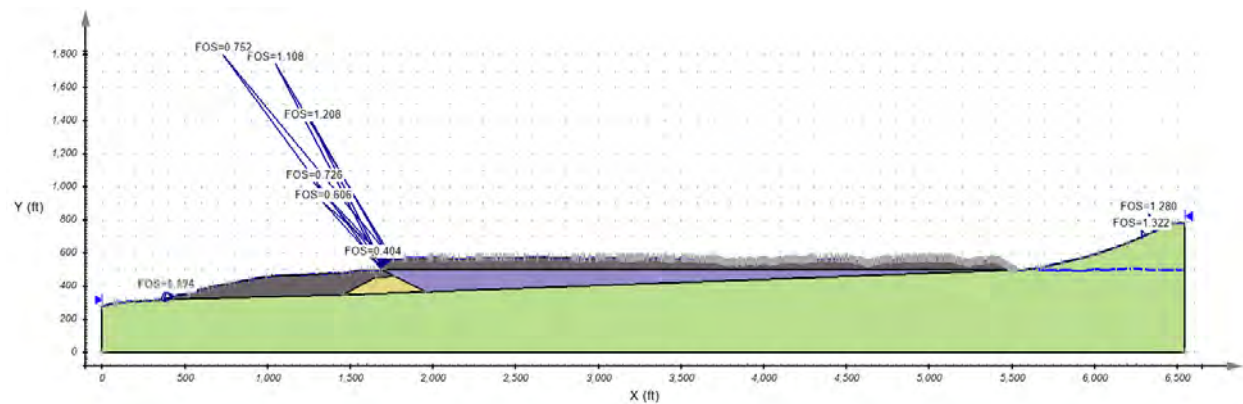


Figure 114. Case 3 auto repeating 100-year.

Table 27. Case 4 modeling results.

2 Mounds (2H:1V)			
Location:	Slope Search	Slope Search along mound	Slope Search along dam
100yr storm	0.895 - 1.330	1.128	0.895
Repeating 100yr storm	0.881 - 1.405	0.874	0.881



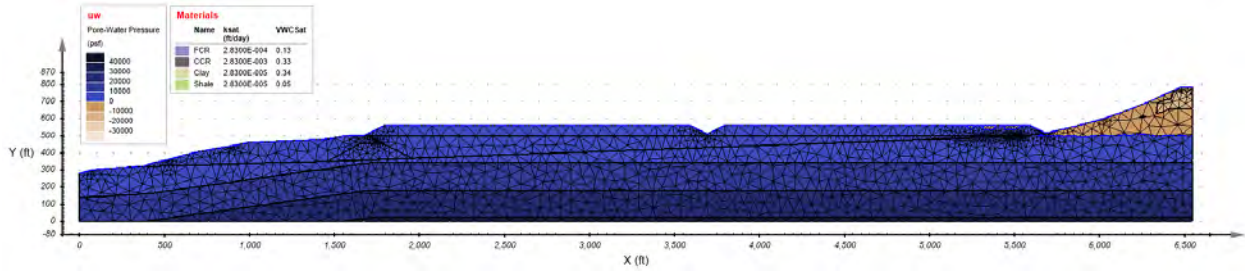


Figure 115. Case 4 singular 100-year seepage output.

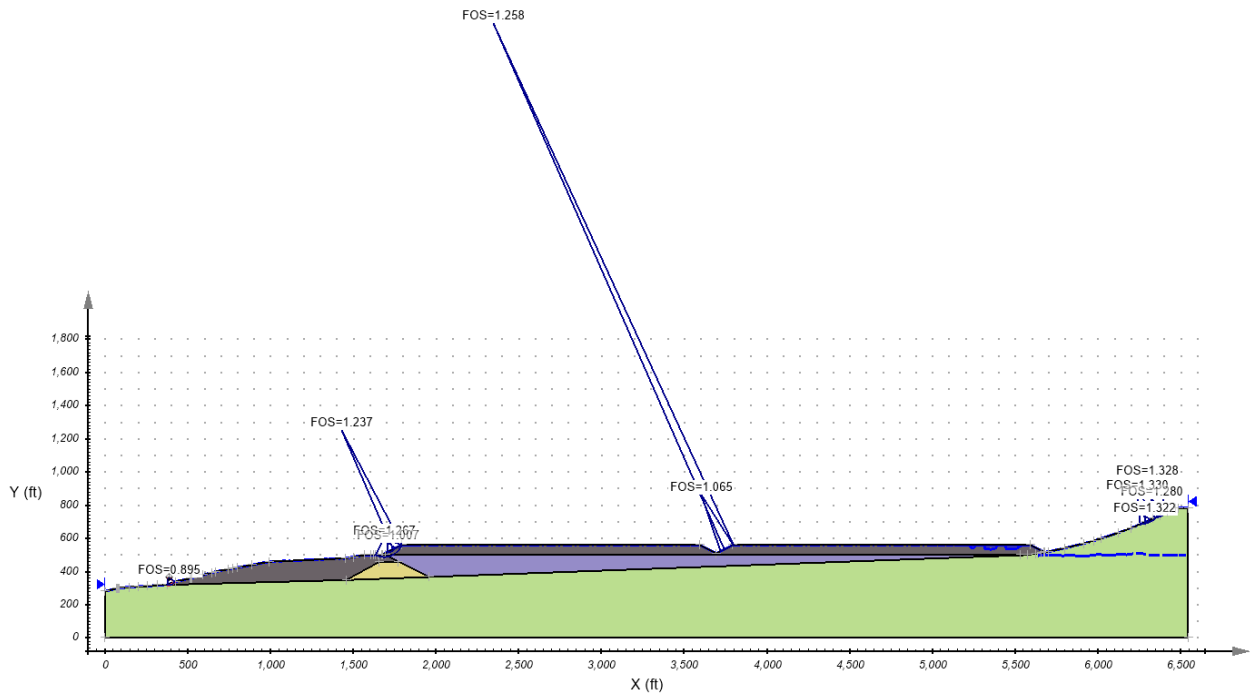


Figure 116. Case 4 auto singular 100-year.

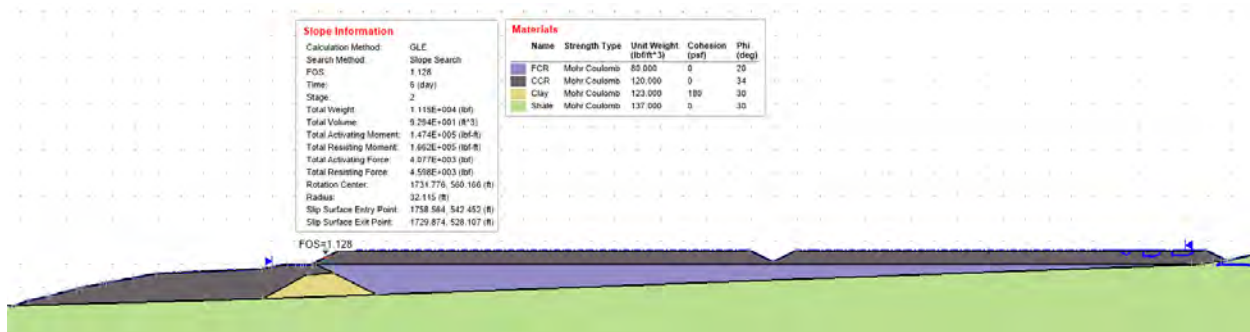


Figure 117. Case 4 auto singular 100-year along mound.

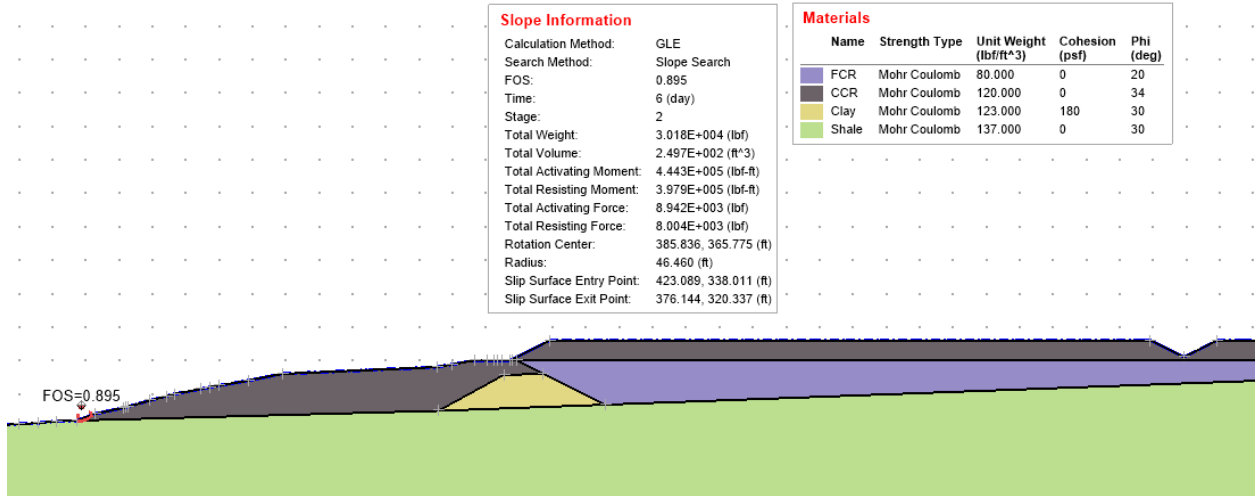


Figure 118. Case 4 auto singular 100-year along dam.

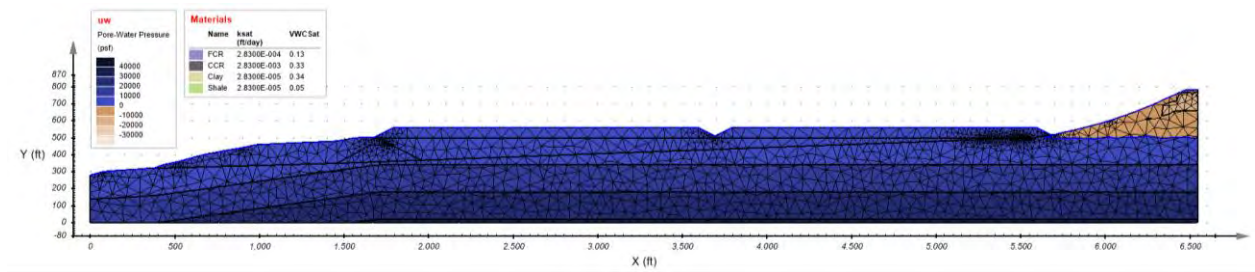


Figure 119. Case 4 repeating 100-year seepage output.

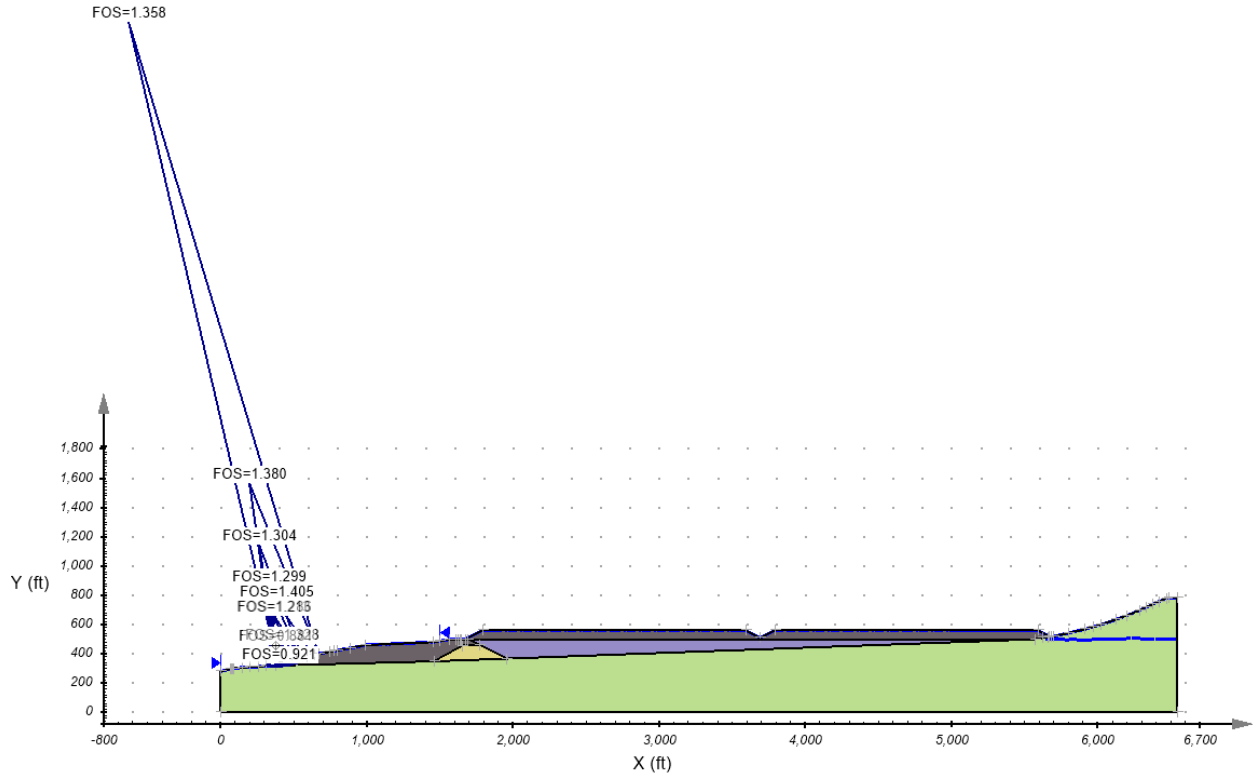


Figure 120. Case 4 auto repeating 100-year.

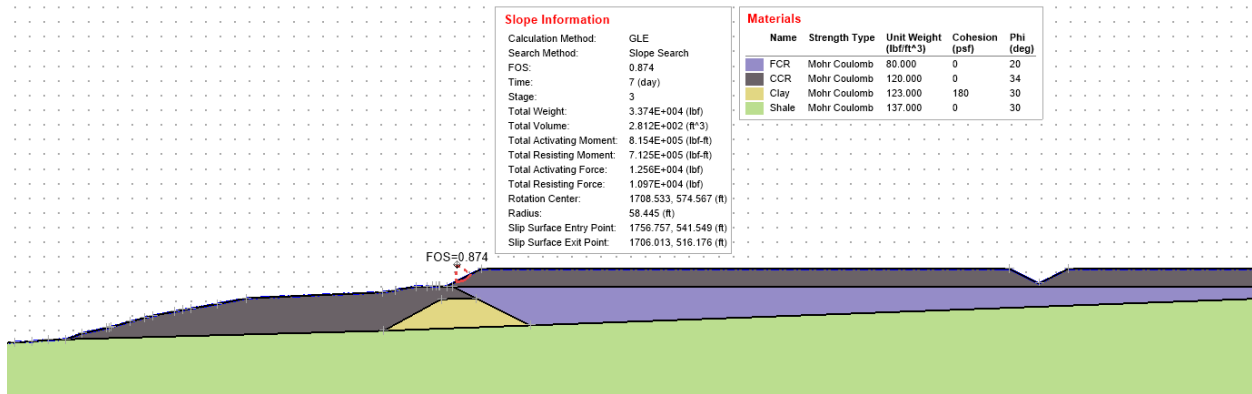


Figure 121. Case 4 auto repeating 100-year along mound.

picture of output from computer modeling

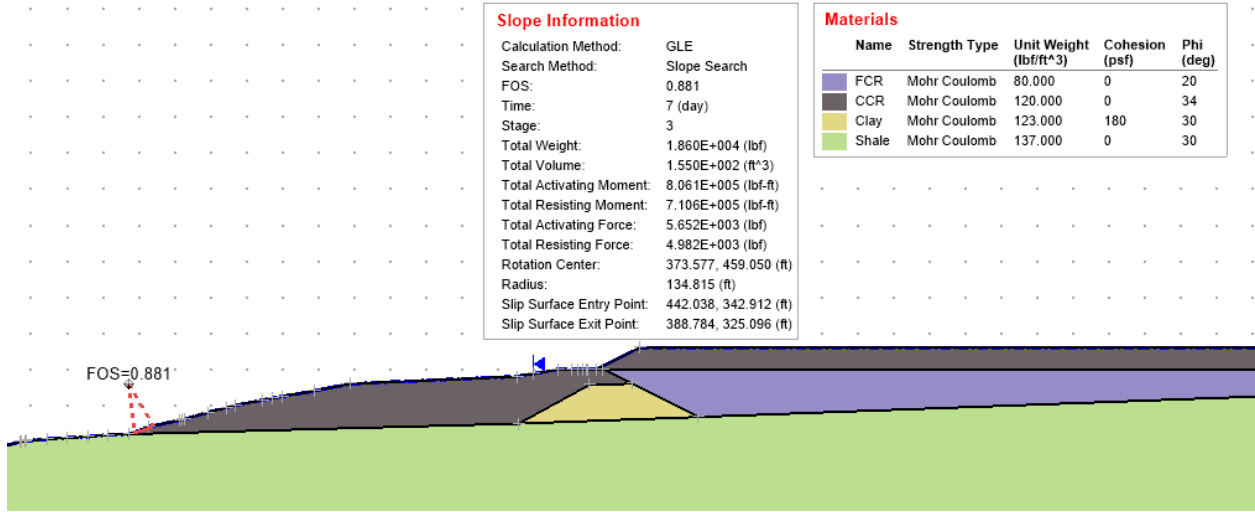


Figure 122. Case 4 auto repeating 100-year along dam.

Table 28. Case 5 modeling results.

2 Mounds (3H:1V)			
Location:	Slope Search	Slope Search along mound	Slope Search along dam
100yr storm	0.895 - 1.416	1.498	0.895
Repeating 100yr storm	0.876 - 1.394	1.239	0.876

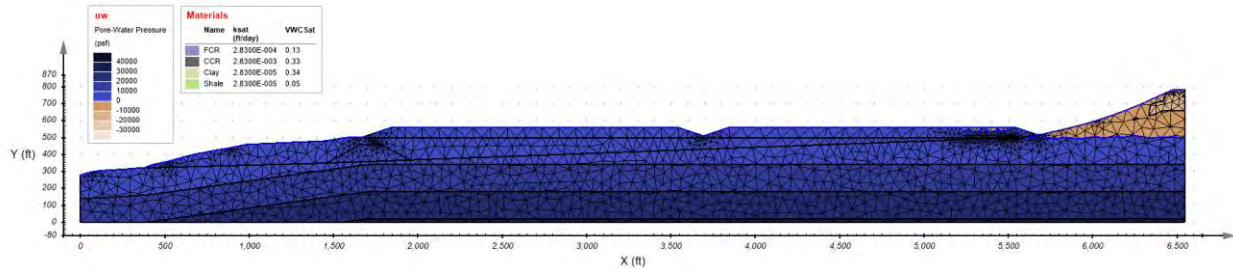


Figure 123. Case 5 singular 100-year seepage output.



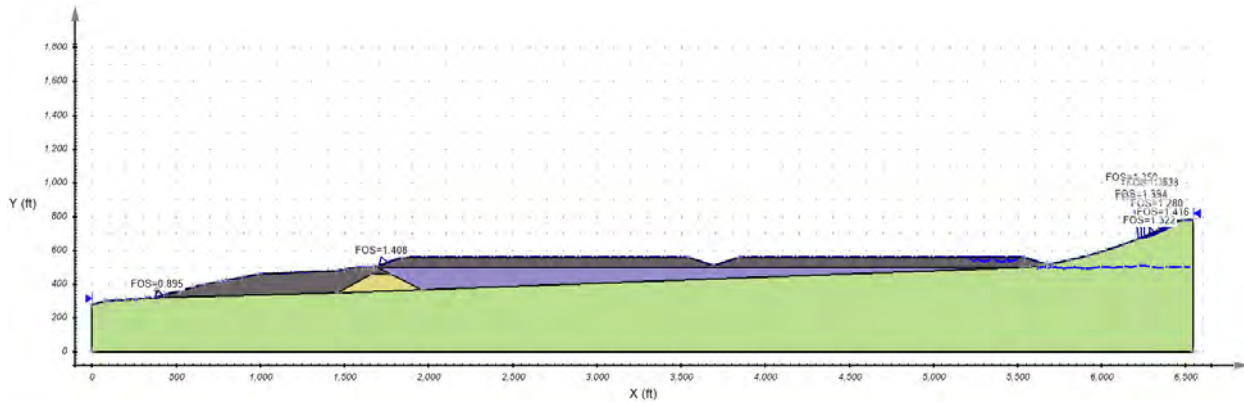


Figure 124. Case 5 auto singular 100-year.

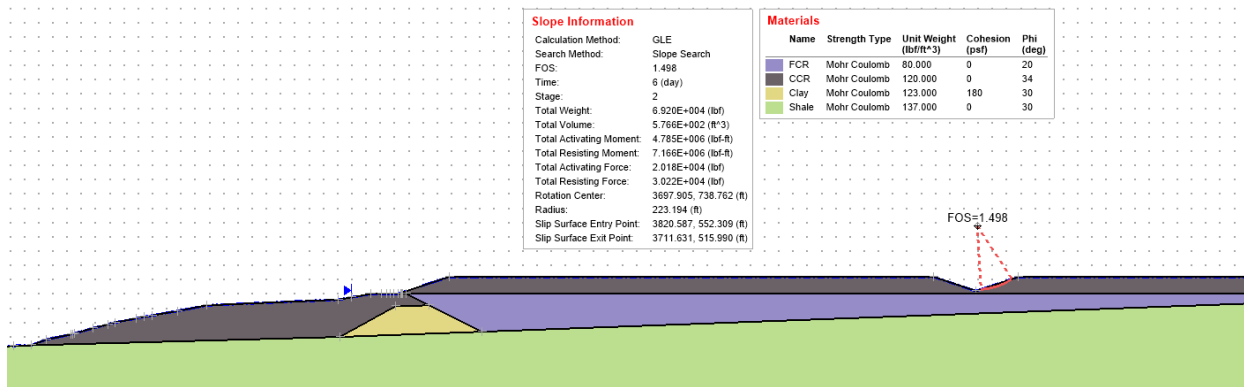


Figure 125. Case 5 auto singular 100-year along mound.

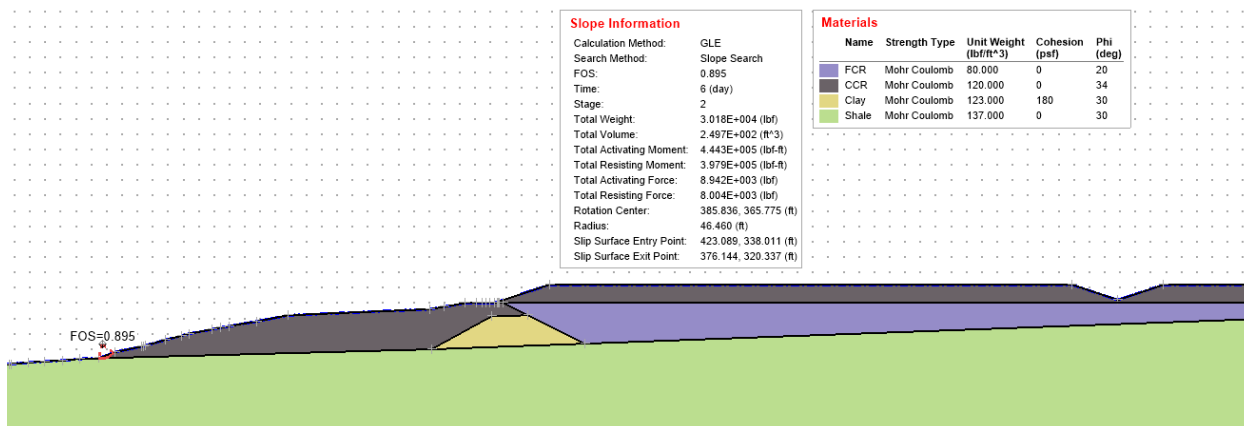


Figure 126. Case 5 auto singular 100-year along dam.

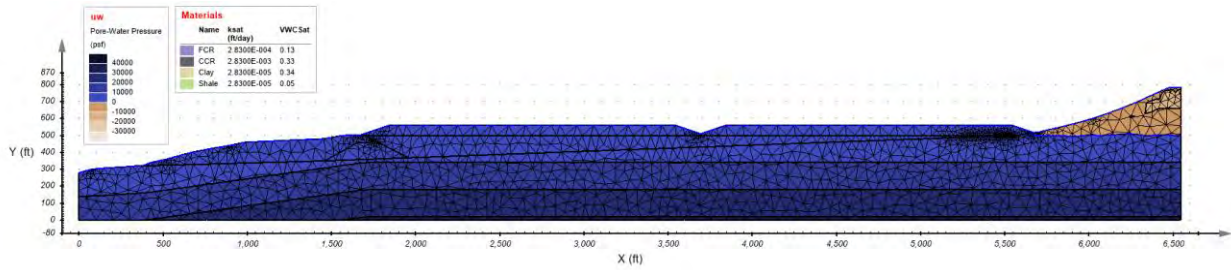


Figure 127. Case 5 repeating 100-year seepage output.

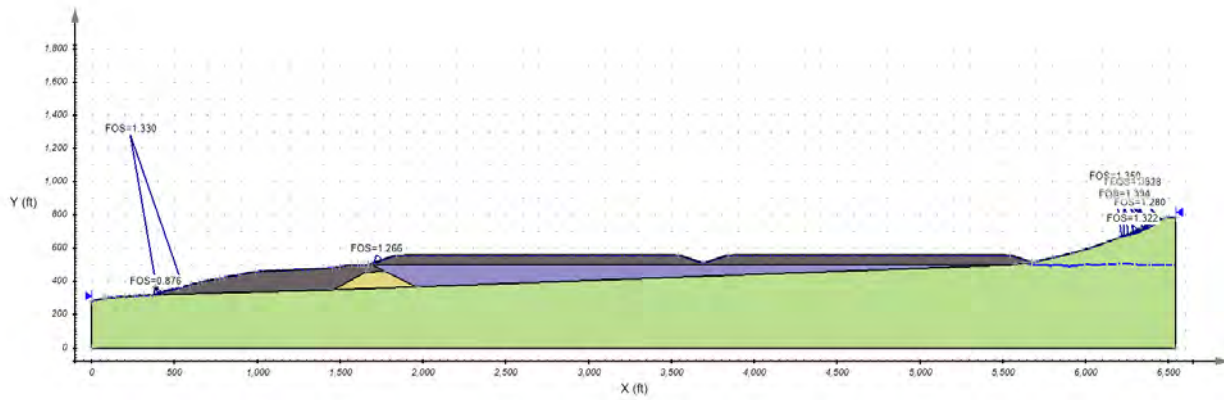


Figure 128. Case 5 auto repeating 100-year.

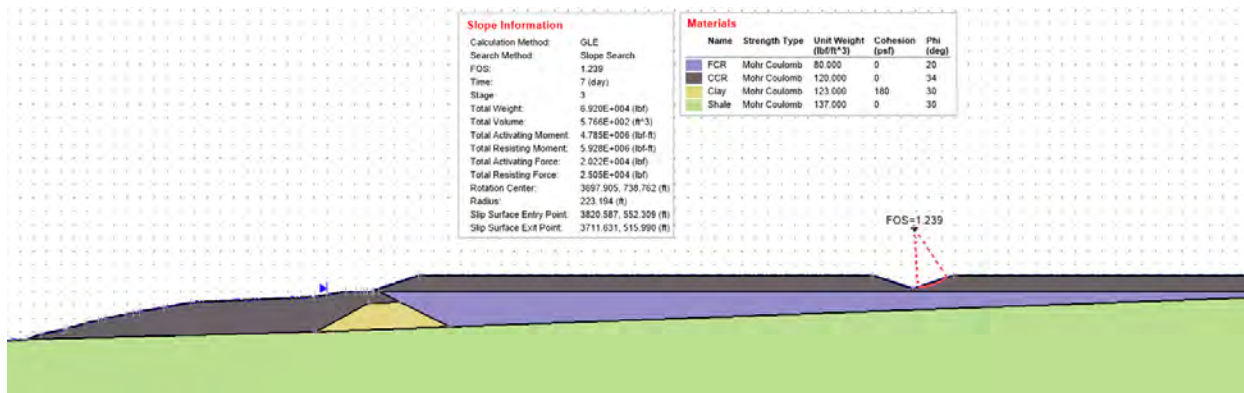
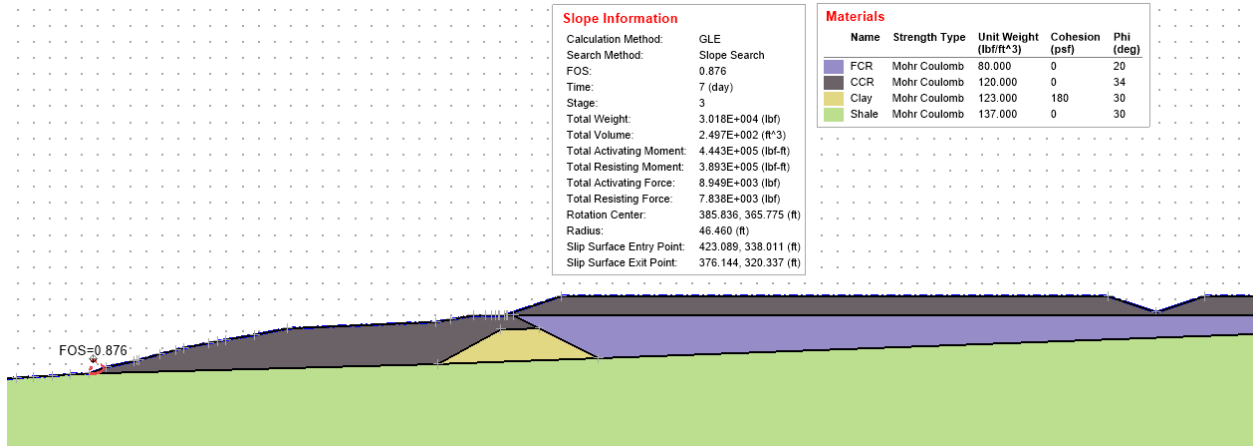


Figure 129. Case 5 auto repeating 100-year along mound.



**Figure 130. Case 5 auto repeating 100-year along dam.**

## Geomorphic reclamation and evaluation for Century Impoundment

The conceptual geomorphic landform designs and hydrologic analysis results are presented in the following sections.

### *One-basin impoundment designs*

The one-subbasin impoundment designs, I-Def-1 (Figure 131, Figure 132) and I-DP-1 (Figure 133, Figure 134), were characterized by one main channel and two tributaries. The tributaries were added to the main channel in each case to satisfy the target drainage density of 80 to 120 ft/ac and 47.74 to 76.26 ft/ac, respectively. In both cases, the main channel drains to an outlet located at the existing sedimentation pond (Figure 131, Figure 133).

I-Def-1 had a total channel length of 3,409 ft, where the main channel length was 1,805 ft, and the tributaries were 1,037 ft (main-R1) and 567 ft (main-L1). The overall drainage density for the I-Def-1 design was 100.26 ft/ac, satisfying the target value which ranged from 80 to 100 ft/ac.

I-DP-1 total channel length was 2,117 ft, where the main channel was 1,331 ft, and the tributaries main-R1 and main-L1 were 436 ft and 351 ft long, respectively. The overall drainage density for I-DP-1 was 62.27 ft/ac, also satisfying the target range of 47.74 to 76.26 ft/ac. Additional information about the 1-basin designs is summarized in Table 29.

The hillside slope sizes for both models were mostly under 35%, with only 1% of the areas presenting slopes between 35% and 50%.

**Table 29. Summary of designs for 1 subbasin in the impoundment area.**

Criteria	I-Def-1	I-DP-1
Area (ac)	34	34
Drainage density (ft/ac)	91.84 to 100.28	61.44 to 62.28
Total channel length (ft)	3,409	2,117
Sinuosity	< 1.2 to >1.5	< 1.2 to >1.5
Bankfull width (ft)	0.28 to 10.56	1.33 to 6.36
Bankfull depth (ft)	0.03 to 0.84	0.01 to 0.85
Flood prone width (ft)	0.59 to 11.59	0.26 to 19.50
Channel slope (%)	1.9 to 15.9	2.0 to 24.8
Hillslope (%)	0.1 to 41.4	0.0 to 49.4

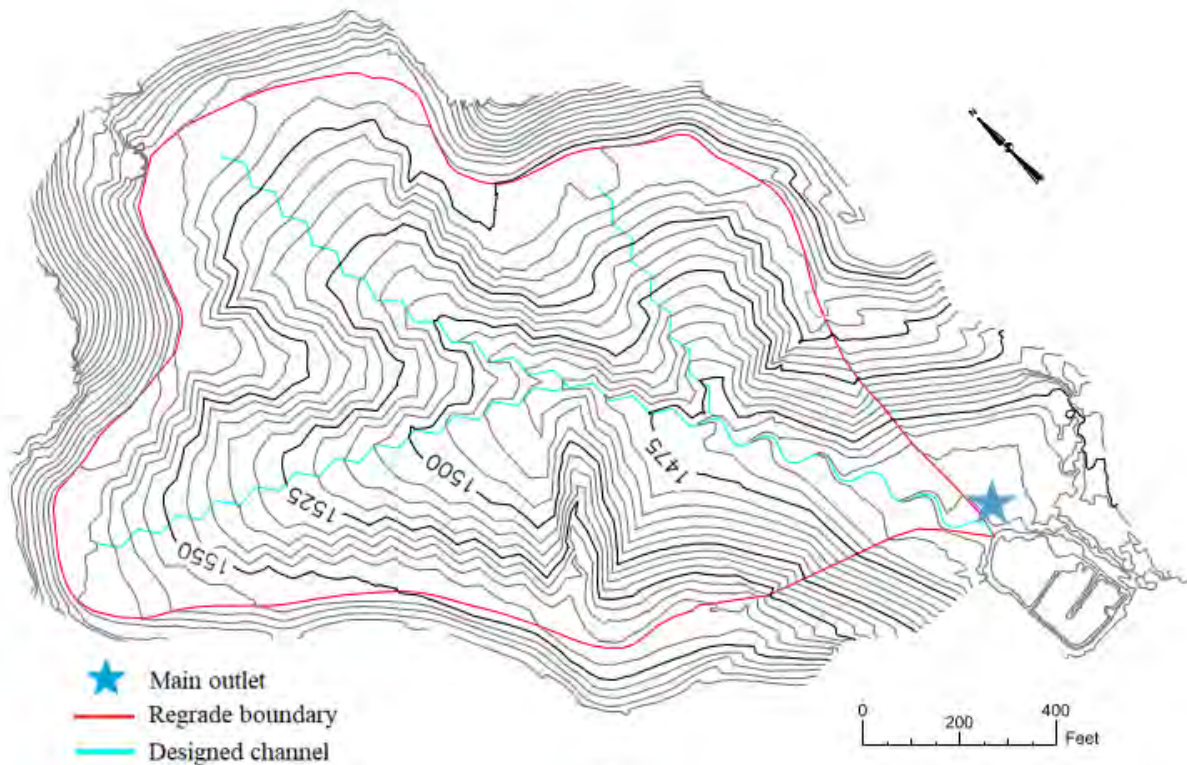


**Figure 131. I-Def-1 designed contour lines.**



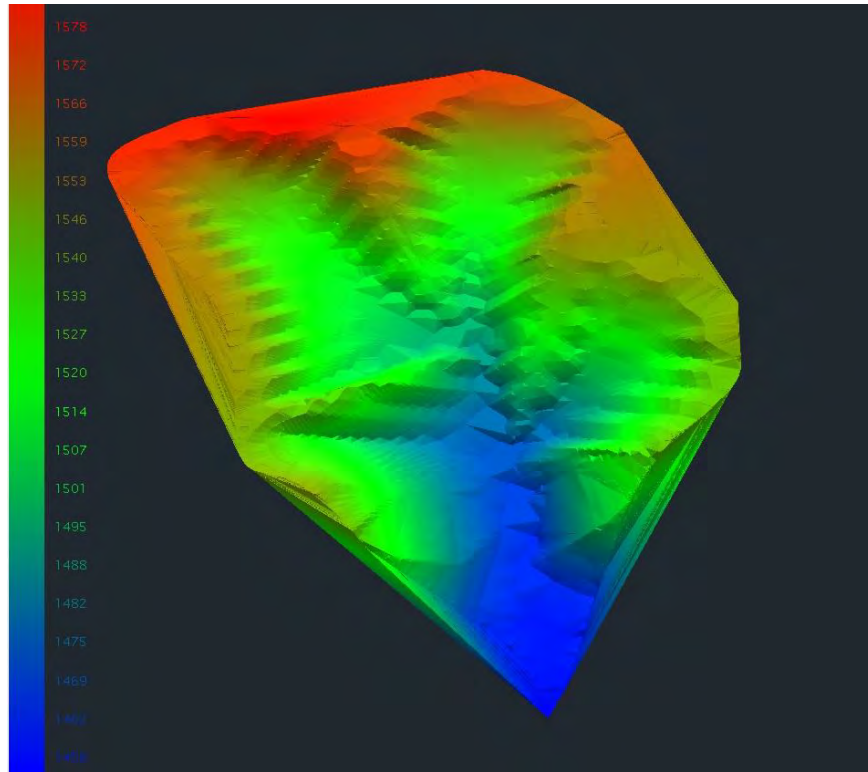


**Figure 132. Three-dimensional geomorphic design: I-Def-1.**

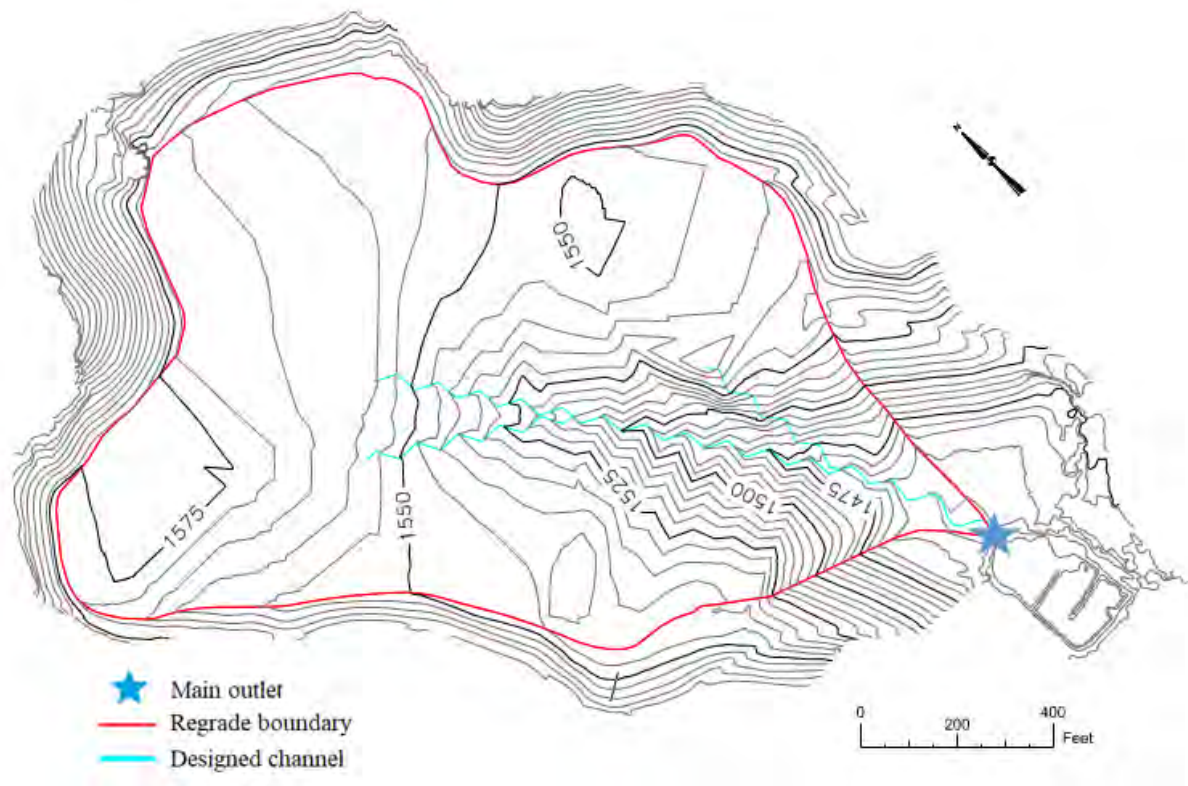


**Figure 133. I-DP-1 designed contour lines.**

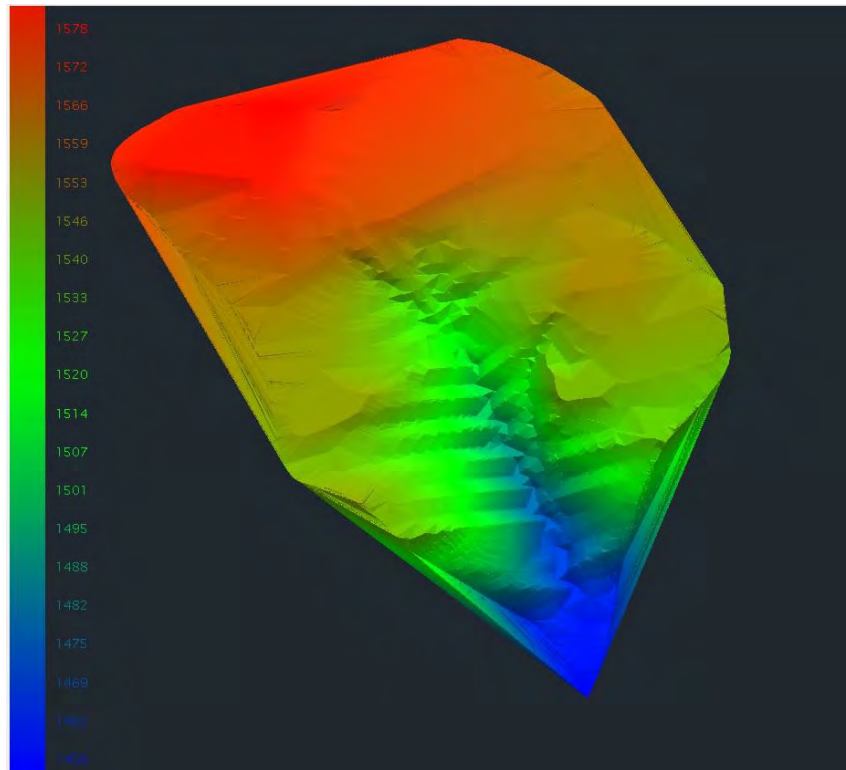


**Figure 134. Three-dimensional geomorphic design: I-DP-1.**

### *Two-basin impoundment designs*

On the two-basin designs, the impoundment area was divided into two subbasins, one at the east (17.2 acres) and the other at the west side of the impoundment (16.8 acres), roughly following the water tracking for the as-built impoundment model. Both subbasins drained to the same point at the sedimentation pond.

Both methods, I-Def-2 and I-DP-2, were characterized by one main channel in each subbasin. I-Def-2 had a total channel length of 3,710 ft, where the east main channel was 1,874 ft and the west main channel was 1,836 ft. The overall drainage density for the I-Def-2 model was 109.12 ft/ac, in accordance with the target range of 80 to 100 ft/ac (Figure 135, Figure 136).

The eastern channel for the I-DP-2 model was 1,067 ft long, while the western channel was 1,036 ft long. The total channel length for this model was 2,103 ft. The overall drainage density for the I-DP-2 was 61.84 ft/ac, also falling within the target range of 47.74 to 76.26 ft/ac for its design criteria (Figure 137, Figure 138). Table 30 presents additional information about these models.

Although some extreme hillslope sizes such as 80.1% (I-Def-2) were observed, most of the area in the designs presented slopes bigger than 50%. Eighty-seven percent of I-Def-2 area and 96% of I-DP-2 presented slopes ranging between 0% and 35%.

**Table 30. Summary of designs for 2 subbasins in the impoundment area.**

Criteria	I-Def-2	I-DP-2
Total area (ac)	34	34
Drainage density (ft/ac)	109.04 to 109.24	61.65 to 62.05
Total channel length (ft)	3,710	2,103
Sinuosity	<1.2 to >1.5	<1.2 to >1.5
Bankfull width (ft)	0.8 to 7.05	0.19 to 6.99
Bankfull depth (ft)	0.08 to 0.56	0.02 to 0.60
Flood prone width (ft)	1.74 to 13.89	0.41 to 13.76
Channel slope (%)	1.8 to 11.9	2.1 to 12.0
Hillslope (%)	0.4 % to 80.1	0.1% to 68.2

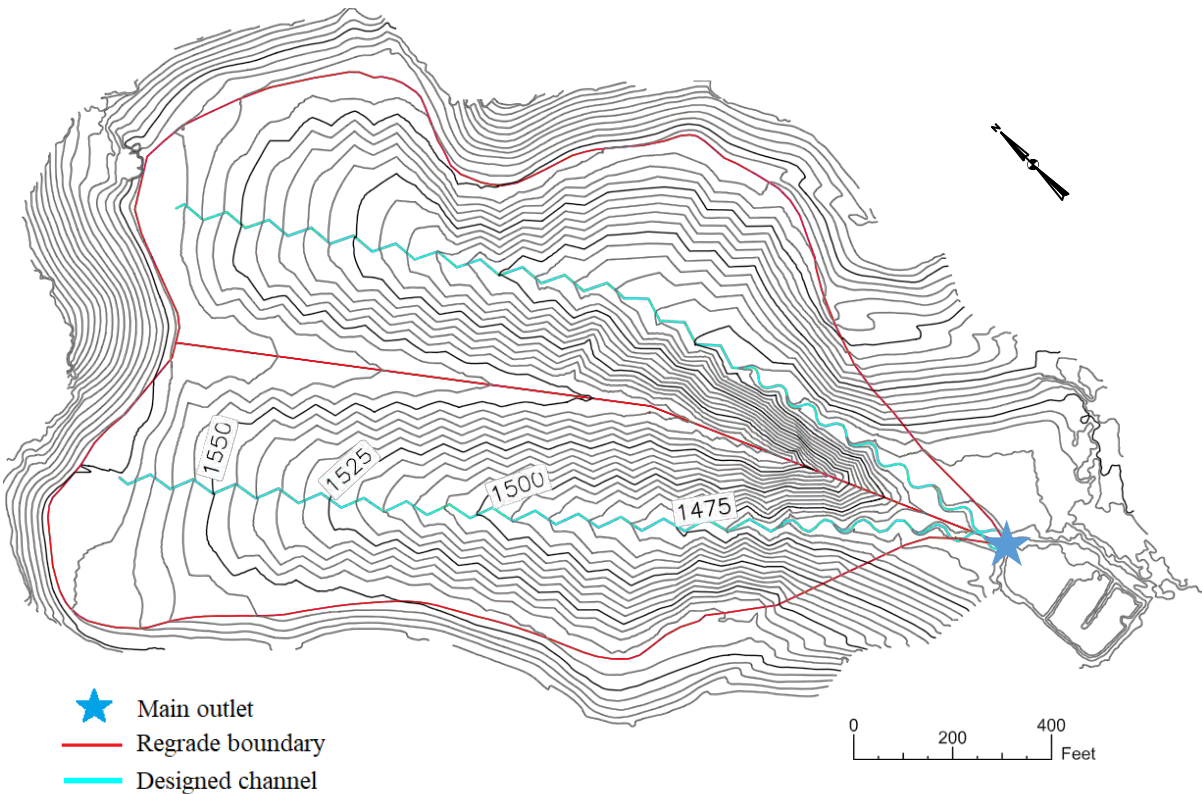


**Figure 135. I-Def-2 designed contour lines.**



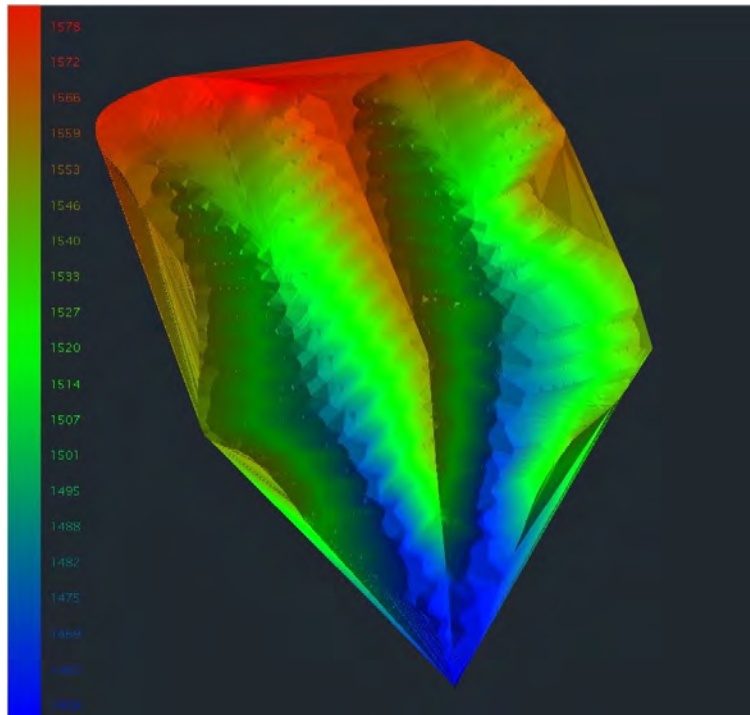


**Figure 136. Three-dimensional I-Def-2 design view.**

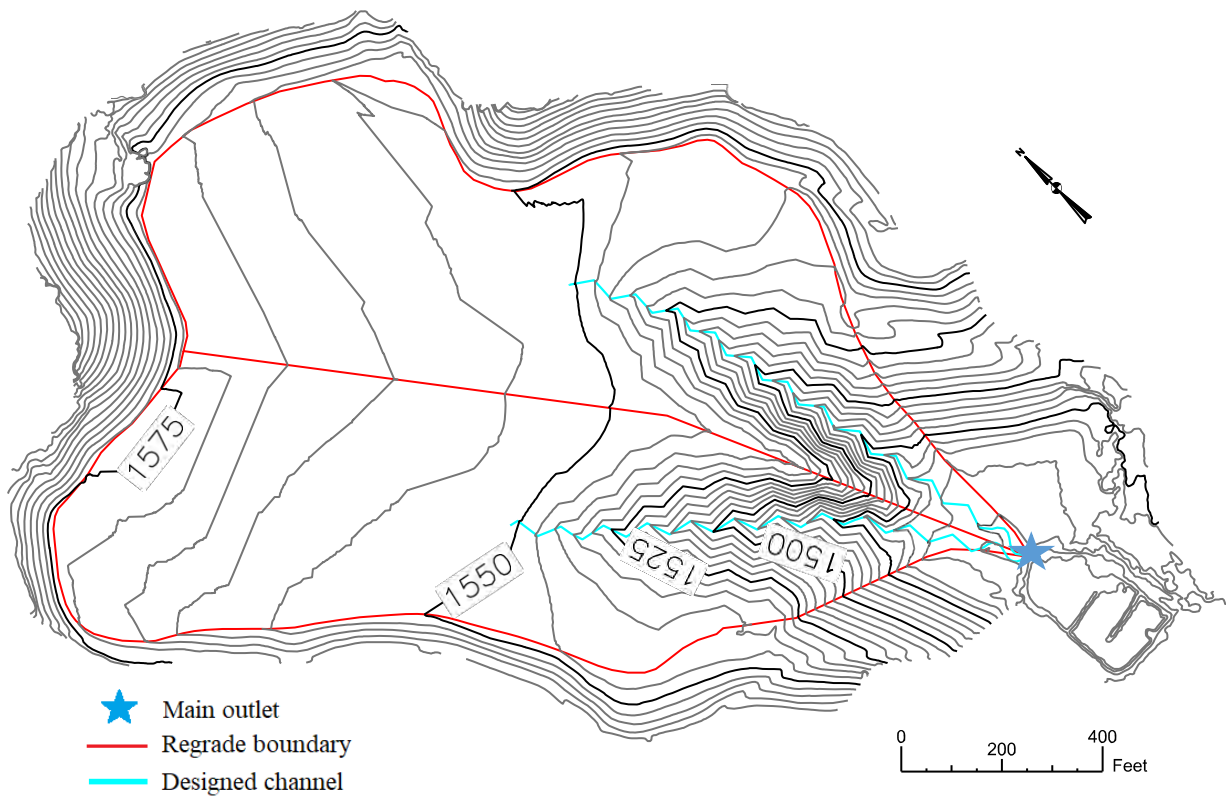


**Figure 137. I-DP-2 designed contour lines.**

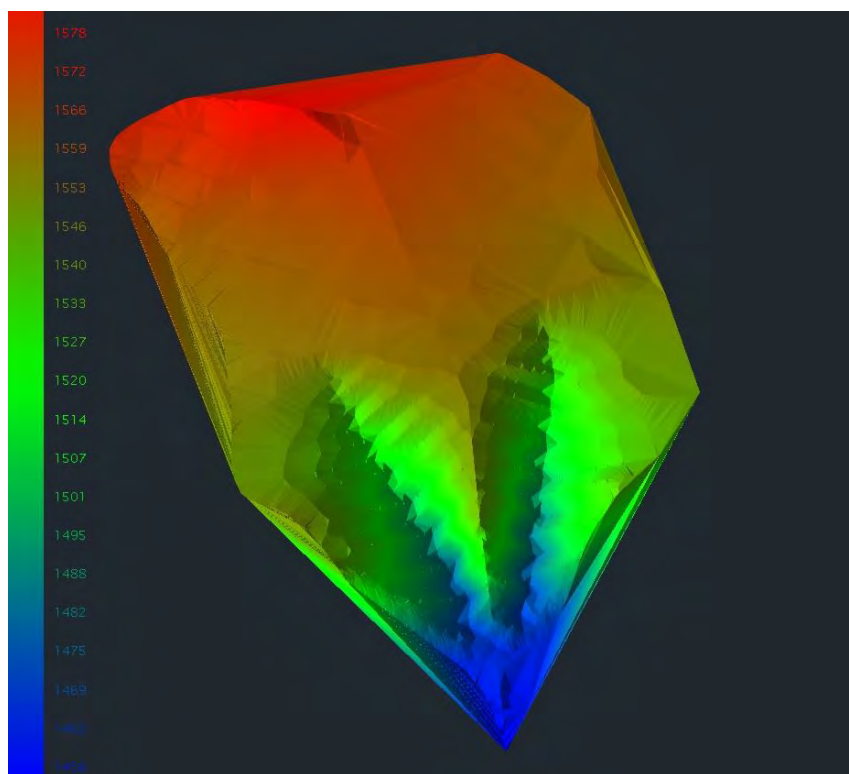


**Figure 138. Three-dimensional I-DP-2.**

*Three-subbasin impoundment designs*

For the three-subbasins analysis, the impoundment area was divided into three subbasins as shown on Figure 9c. The 8.8 ac. subbasin was modeled first, then the 9.6 ac followed by the 15.6 ac one. The two smaller subbasins drained to existing channels at each side of the impoundment in both 3-basins models (Figure 139, Figure 141).

For the I-Def-3 model the 8.8 ac, and the 9.6 ac subbasins were characterized by one single channel of 882 ft and 965 ft, respectively. The 15.6 ac. subbasin was characterized by one main channel and one tributary which drained to the main outlet at the bottom of the impoundment (Figure 139, Figure 140). The main channel ran from the west to the bottom of the watershed and was 1,058 ft long. The tributary was located at the left margin of the main channel and was 503 ft long. The overall drainage density for this model was 100.25 ft/ac. Ninety-two percent of the area of I-Def-3 presented a maximum slope of 20%. Table 31 shows other result values for I-Def-3 design criteria.

I-DP-3 was basically characterized by the same configuration as I-Def-3: two channels at the top, draining to the side channels, and one main channel with one tributary at the bottom subbasin. However, the bottom subbasin for this model presented a contours configuration with a peak at the west side in which the water would not drain to any of the defined channels (Figure 141, Figure 142). This configuration would make the water pond on the northwest part of the subbasin and ultimately run to the side channels defined for the 9.6 ac subbasin. As this is not the ideal configuration for the water flow, this model was not considered for further analysis.

**Table 31. Summary of results for 3 subbasins in the impoundment area.**

Criteria	I-Def-3
Total area (ac)	34
Drainage density (ft/ac)	80.29 to 100.44
Total channel length (ft)	3,408
Sinuosity	<1.2 to >1.5
Bankfull width (ft)	0.0 to 6.71
Bankfull depth (ft)	0.0 to 0.59
Flood prone width (ft)	0.0 to 13.21
Channel slope (%)	0.4 to 12.0
Hillslope (%)	0.4 to 41.4

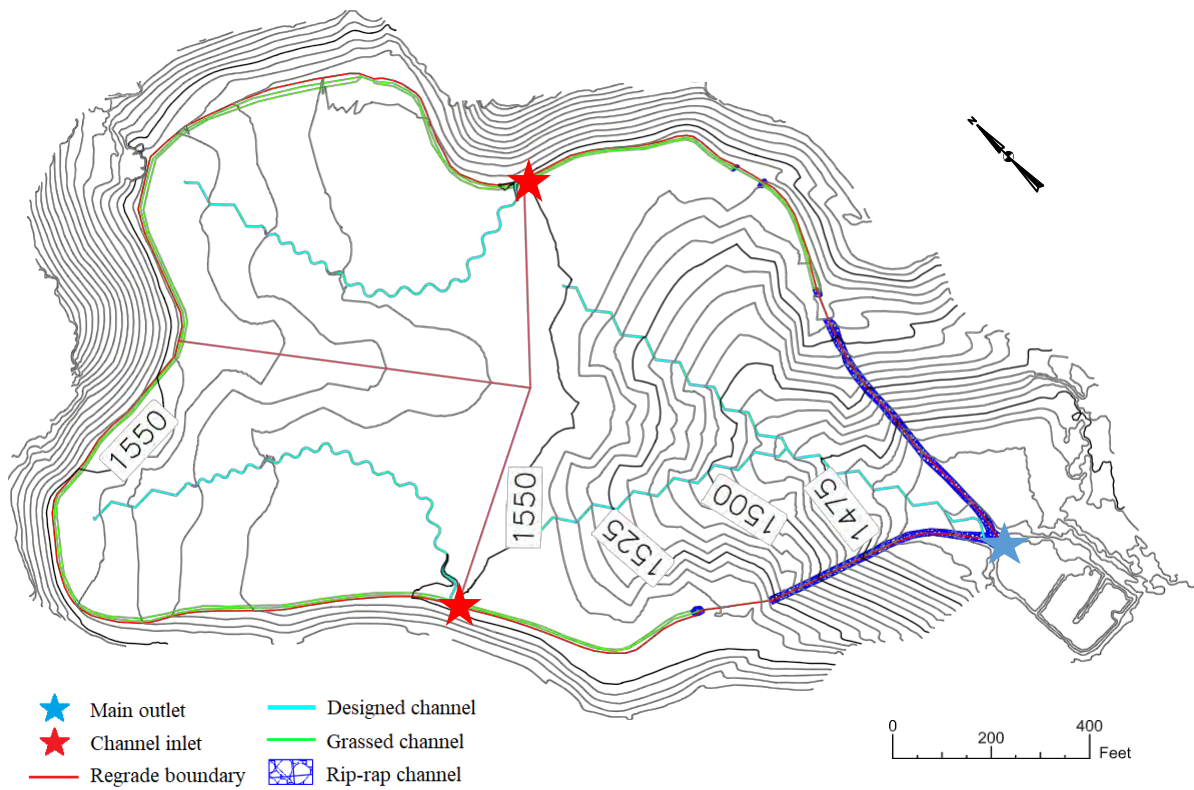


**Figure 139. I-Def-3 designed contour lines.**

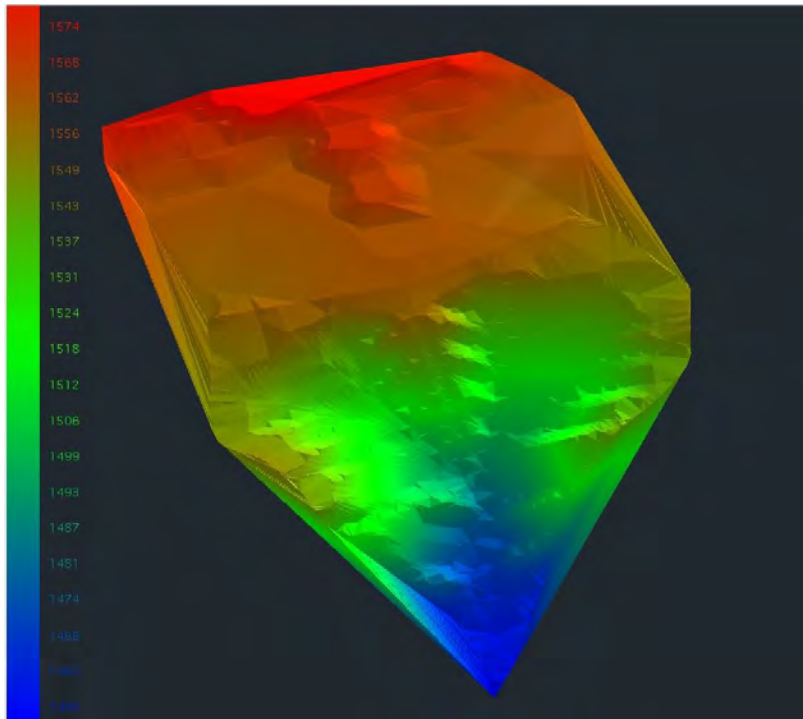


**Figure 140. Three-dimensional I-Def-3 design view.**

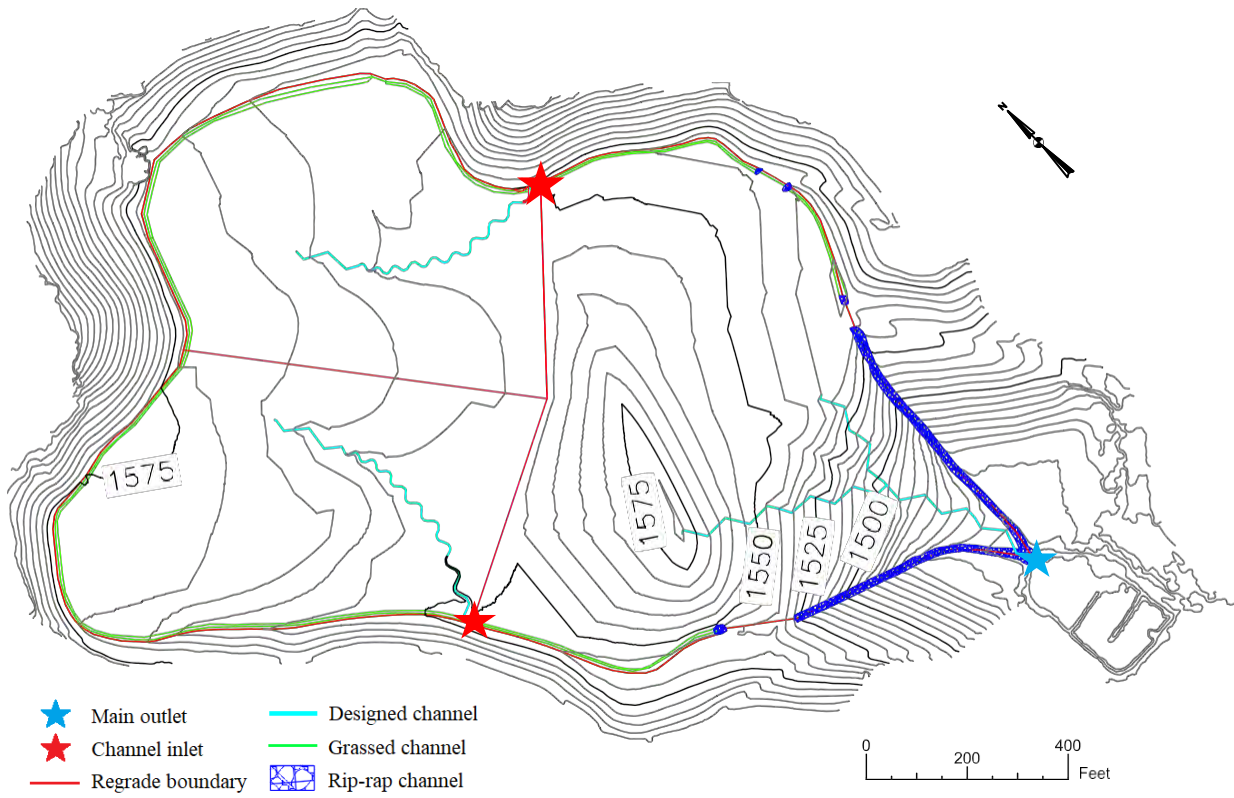


**Figure 141. I-DP-3 designed contour lines.**



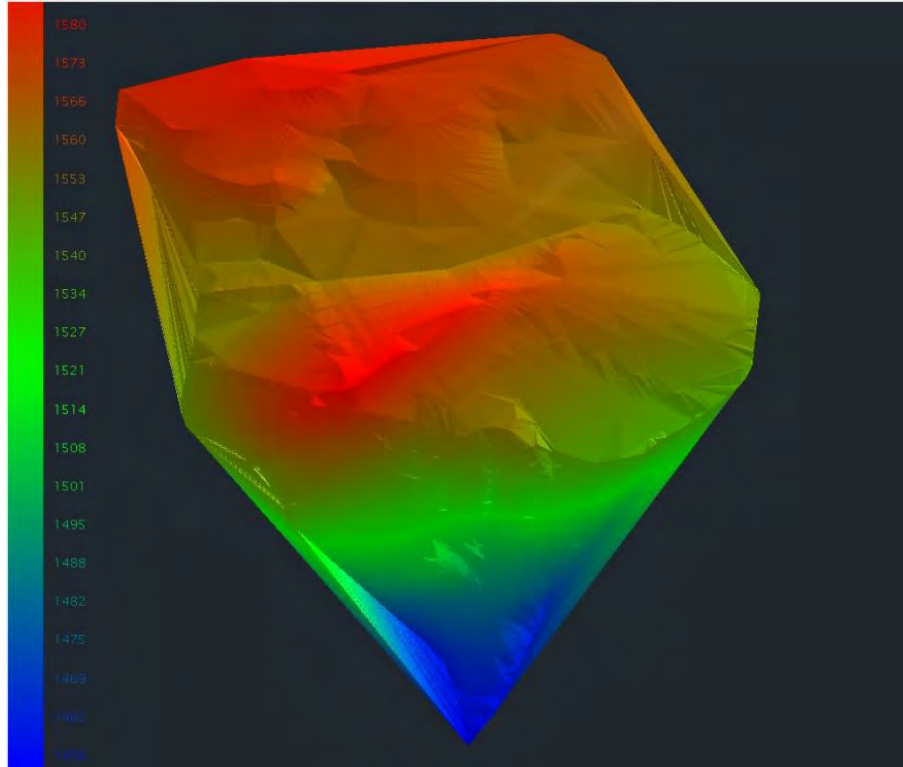


**Figure 142. Three-dimensional I-DP-3 design view.**

### *Watershed designs*

The watershed designs included areas outside of the impoundment area, totaling 90 ac. The area was not divided in subbasins for the regrade analysis. A main channel and several tributaries were necessary to reach the target drainage density for each design criteria (Figure 143 - Figure 146). The W-Def-1 design was composed of one main channel and five tributaries. The total channel length was 8,615 ft, where 2,356 ft was the main channel. The tributaries length varied from 696 ft to 1,185 ft. The overall drainage density for this model was 95.76 ft/ac. The W-DP-1 design had one main channel 1,998 ft long, and four tributaries varying from 566 ft to 1131 ft. The total channel length of 5,191 ft and a drainage density of 57.7 ft/ac.

These models showed a larger range in slope sizes. The maximum slope size for W-Def-1 was 64.8%. Slopes over 50% represented 0.4% of the W-Def-1 area. The maximum slope for W-DP-1 was 73.8%. W-DP-1 showed 3.6% of the area with slopes bigger than 50%. For both designs most of the slopes were less than 35% (Table 32).

**Table 32. Summary of designs for the watershed-based designs.**

Criteria	W-Def-1	W-DP-1
Total watershed area (ac)	90	90
Drainage density (ft/ac)	81.12 to 111.83	53.67 to 70.33
Total channel length (ft)	8,615	5,191
Sinuosity	<1.2 to 1.16	<1.2 to 1.19
Bankfull width (ft)	0.11 to 17.26	0.00 to 17.17
Bankfull depth (ft)	0.01 to 1.54	0.00 to 1.42
Floodprone width (ft)	0.23 to 33.60	0.01 to 33.42
Channel slope (%)	5 to 25.4	1.8 to 29.2
Hillslope (%)	0.9 to 64.8	0.5 to 73.8

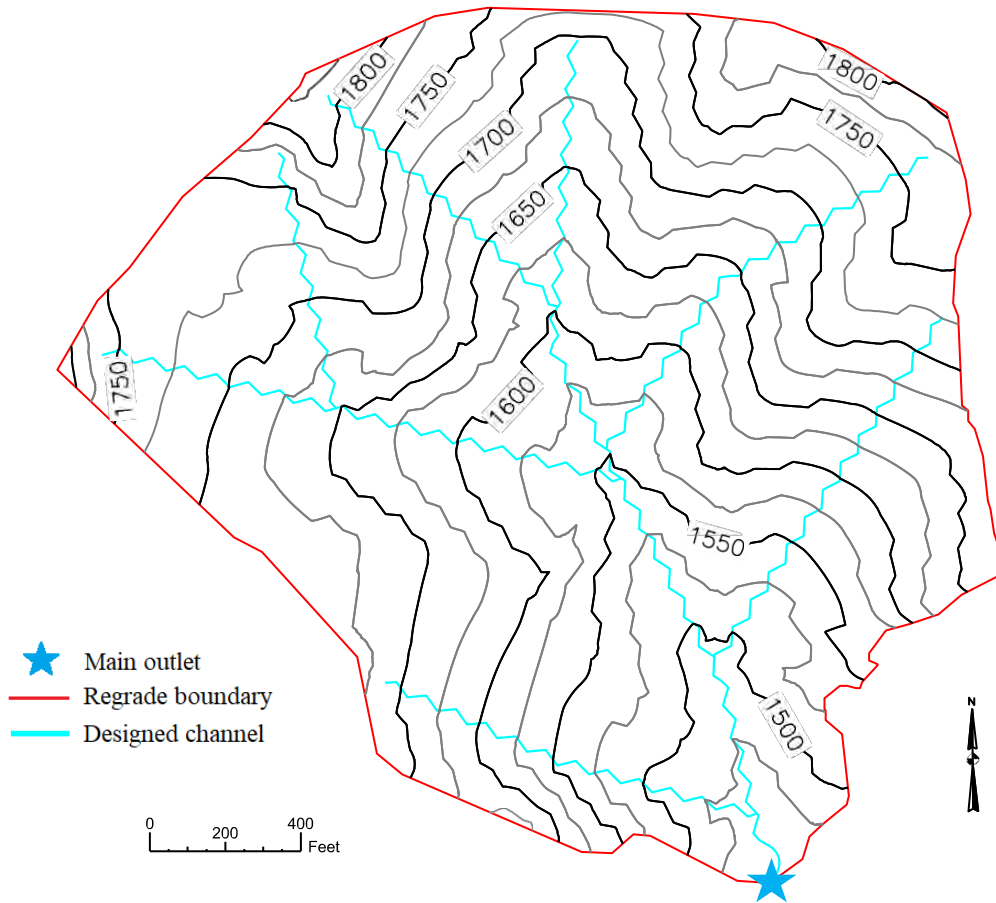


**Figure 143. W-Def-1 designed contour lines.**

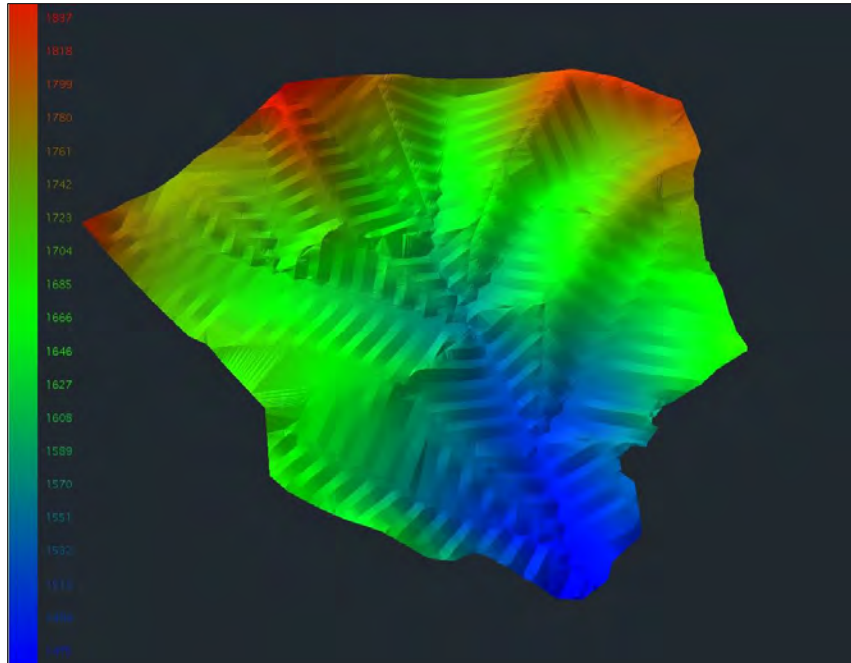


**Figure 144. Three-dimensional W-Def-1 design view.**

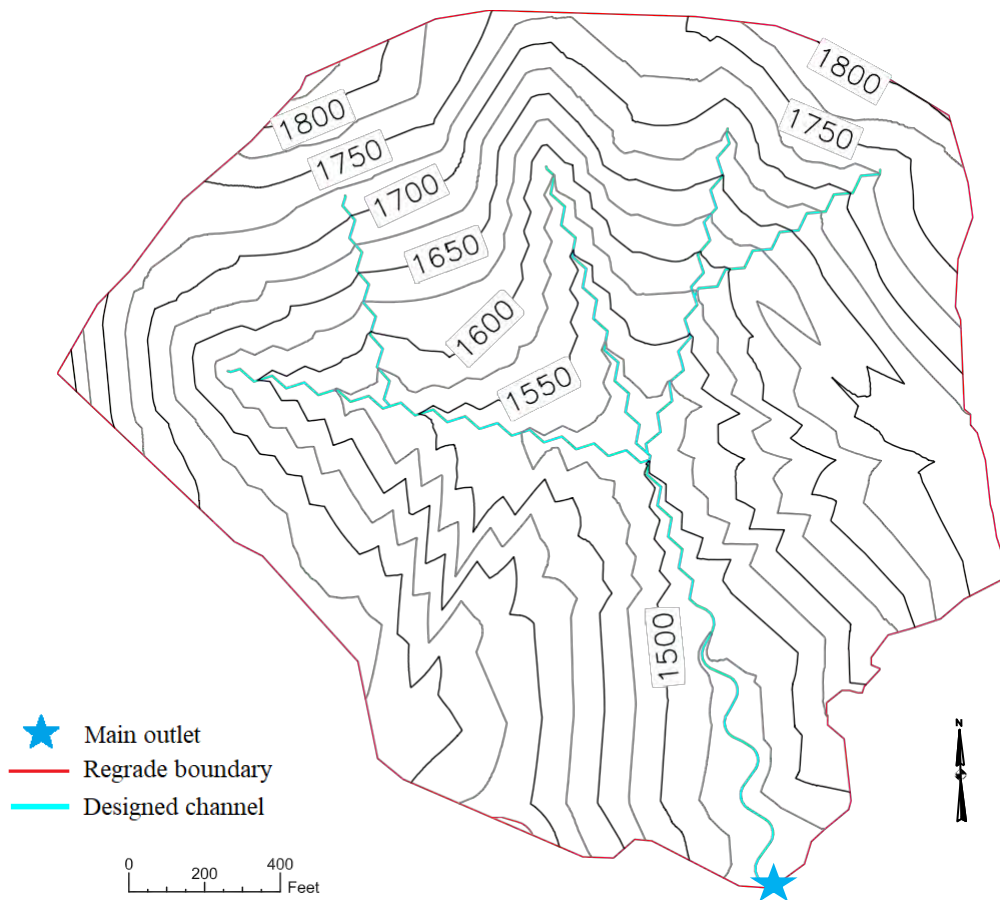


**Figure 145. Three-dimensional W-DP-1 design.**

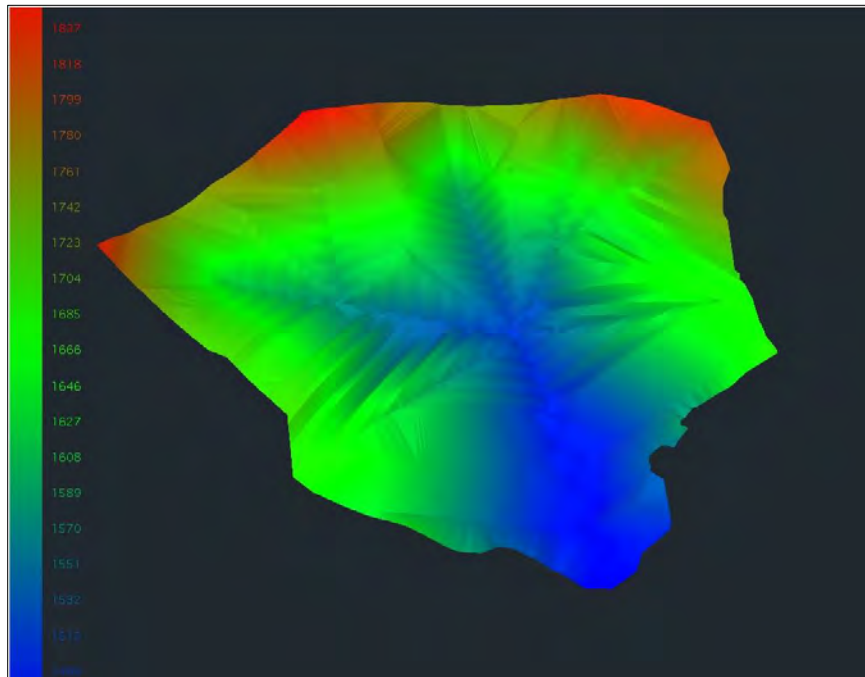


**Figure 146. Three-dimensional geomorphic design: W-DP-1**

### *Hydrologic analysis*

The hydrographs for 100-yr and 500-yr storm events are presented for the designed models and the baselines at Figure 147 through Figure 150 and are summarized on Table 33 and Table 34. The geomorphic designs increased the peak runoff and decreased the time to peak in all cases for the two rainfall intensities analyzed.

For the 100-yr storm, the impoundment models presented an increase at the peak runoff that ranged from 9.4% (I-DP-1) to 23% (I-Def-3). The time to peak presented some reductions that ranged from 1.2 min (I-DP-1) and 10.8 min (I-DP-3). The 500-yr storm analysis showed that the peak discharge for the impoundment designs increased in a range of 9.2% (I-DP-1) to 23.2% (I-Def-3), following the same pattern and order of magnitude as the 100-yr storm. The time to peak in the 500-yr storm was reduced in an order of 1.2 min to 10 min.

The whole watershed geomorphic models presented a lower runoff variation than the impoundment area ones. When compared to the as built baseline, the maximum peak runoff observed for a 100-yr storm intensity was 281.34 cfs for W-Def-1, which is only 2.4% bigger than the baseline. W-DP-1 presented an increased on peak runoff of only 0.8%. The variations for the 500-yr storm were of the same magnitude as the 100-yr storm, varying from 0.7% (W-DP-1) to 2.3% (W-Def-1). No difference was observed in the time to peak between the geomorphic models for the watershed area and the as-built baseline for any rainfall intensity analyzed.

Bigger differences were observed when comparing the watershed models to the woods baseline: W-Def-1 had the runoff increased in 13.3%, while W-DP-1 had the runoff increased in 11.5%. The time to peak had a reduction of 1.2 min for both models when compared with the woods baseline. Increase in runoff and decrease in time to peak are expected when comparing the



models to the woods baseline once forested areas present higher infiltration rates and consequently lower runoff rates than more compacted areas, as is the case of the impoundment. The soil profile in the woods environment also contributes to delay the runoff velocity, reflecting in a delayed peak (Bedient *et al.*, 2013).

**Table 33. Hydrologic analysis summary results for impoundment designs.**

	100-yr, 24-h			500-yr, 24-h		
	Qp (cfs)	Time to peak (hr)	Runoff vol. (ac-ft)	Qp (cfs)	Time to peak (hr)	Runoff vol. (ac-ft)
I-Def-1	116.06	12.16	9.84	155.94	12.16	13.36
I-DP-1	105.19	12.22	9.85	141.4	12.2	13.37
I-Def-2	118.15	12.16	9.85	158.61	12.16	13.37
I-DP-2	117.40	12.16	9.85	157.65	12.16	13.37
I-Def-3	118.34	12.12	9.85	159.47	12.12	13.36
I-DP-3	-	-	-	-	-	-
As-built	96.18	12.24	9.83	129.45	12.22	13.36

*Note: I-DP-3 was excluded from hydro analysis due to problems at regrade modeling results discussed in section 4.3.*

**Table 34. Hydrologic analysis summary results for watershed area designs.**

	100-yr, 24-h			500-yr, 24-h		
	Qp (cfs)	Time to peak (hrs)	Runoff vol. (ac-ft)	Qp (cfs)	Time to peak (hrs)	Runoff vol. (ac-ft)
W-Def-1	281.34	12.18	23.9	384.91	12.18	32.97
W-DP-1	276.78	12.18	23.9	379.06	12.18	32.98
As-built	274.62	12.18	23.9	376.28	12.18	32.98
Woods	248.25	12.20	22.48	345.08	12.20	31.37

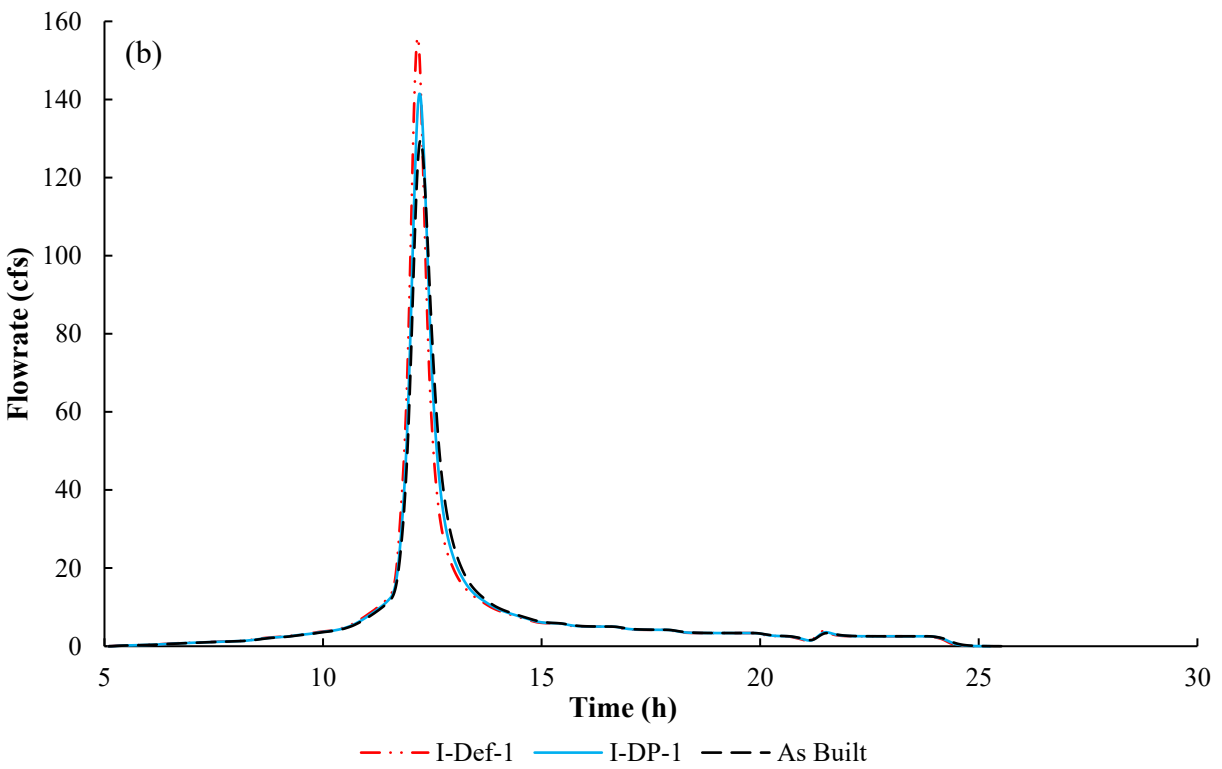
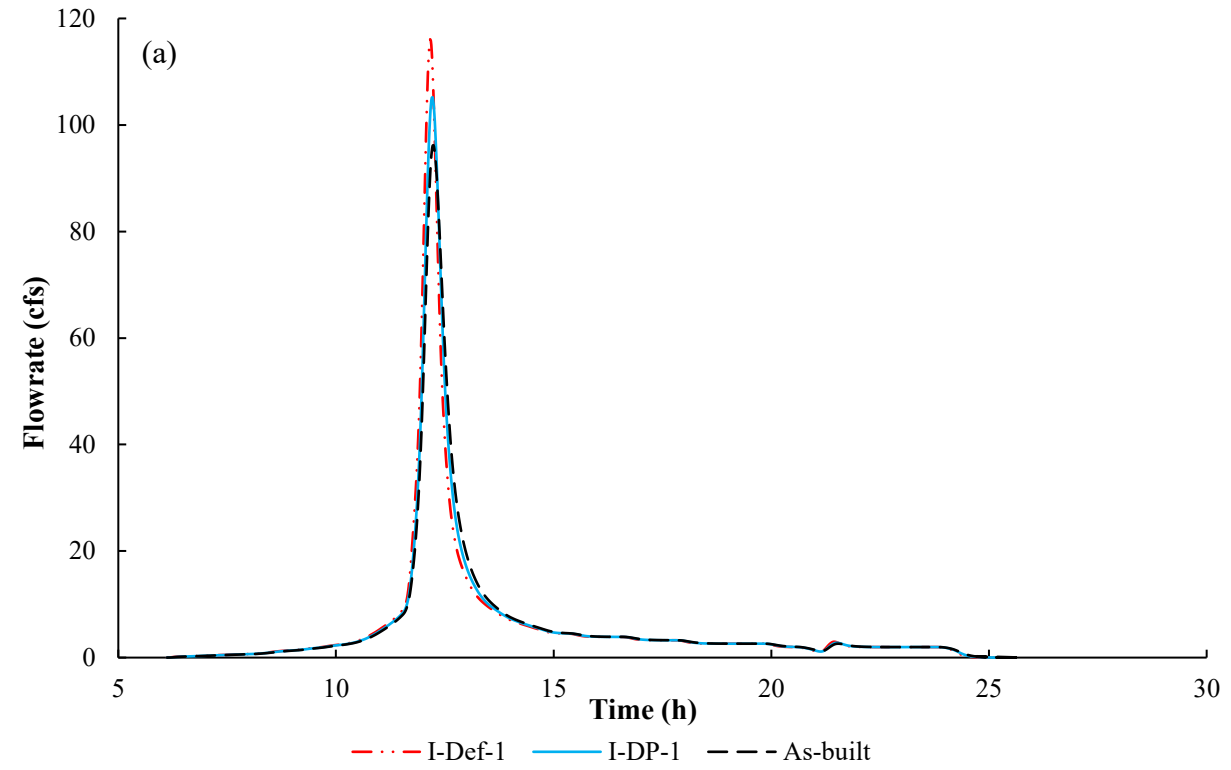


**Figure 147. Runoff hydrograph for impoundment area design considering 1 subbasin. (a) 100-yr storm; (b) 500-yr storm.**

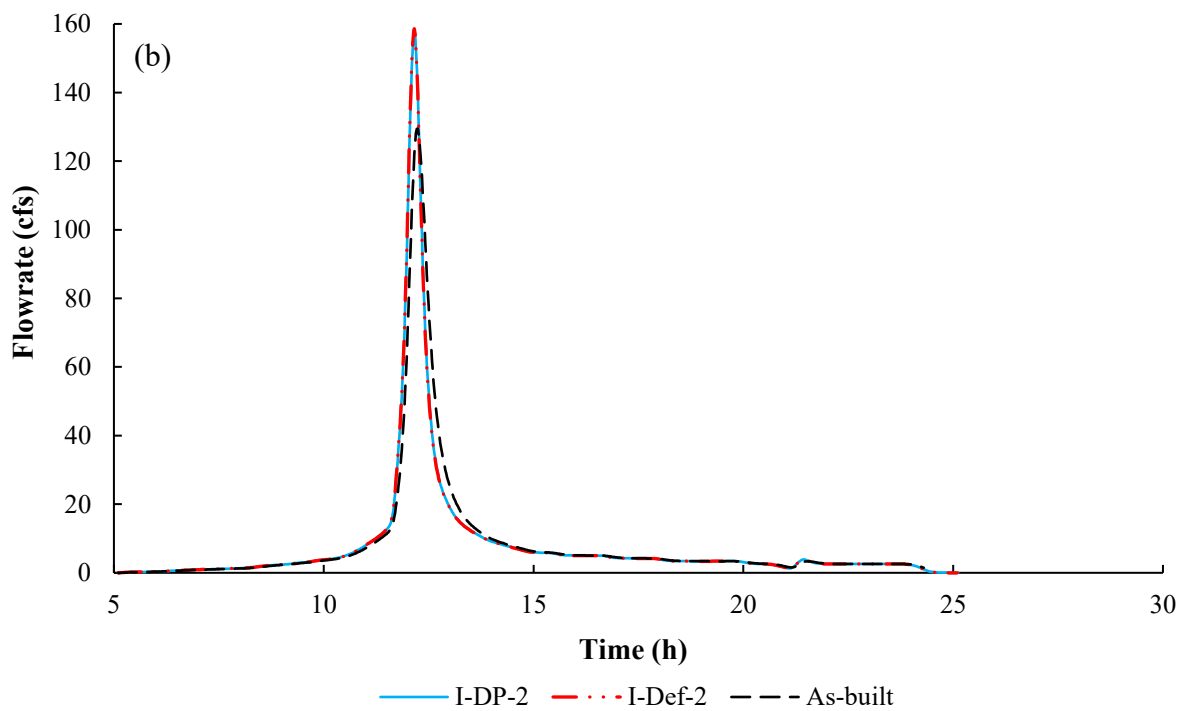
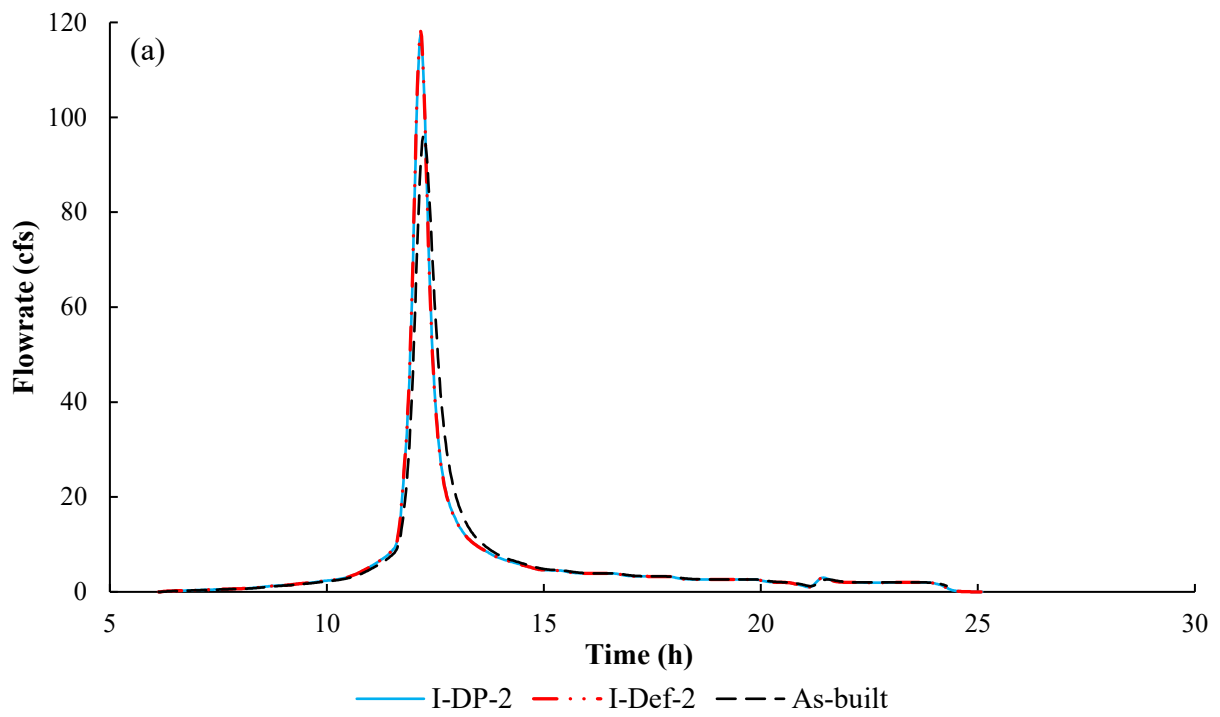


**Figure 148. Runoff hydrograph for the impoundment area design considering 2 subbasin. (a)100-yr storm; (b) 500-yr storm.**

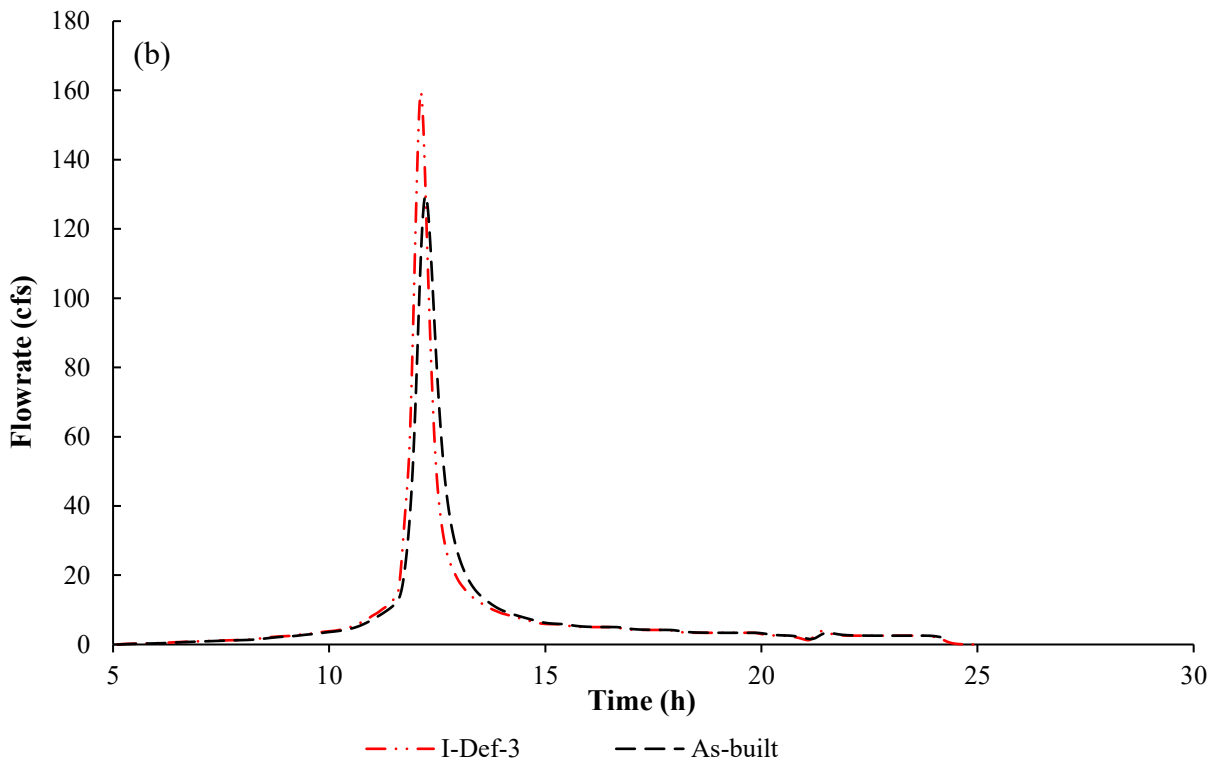
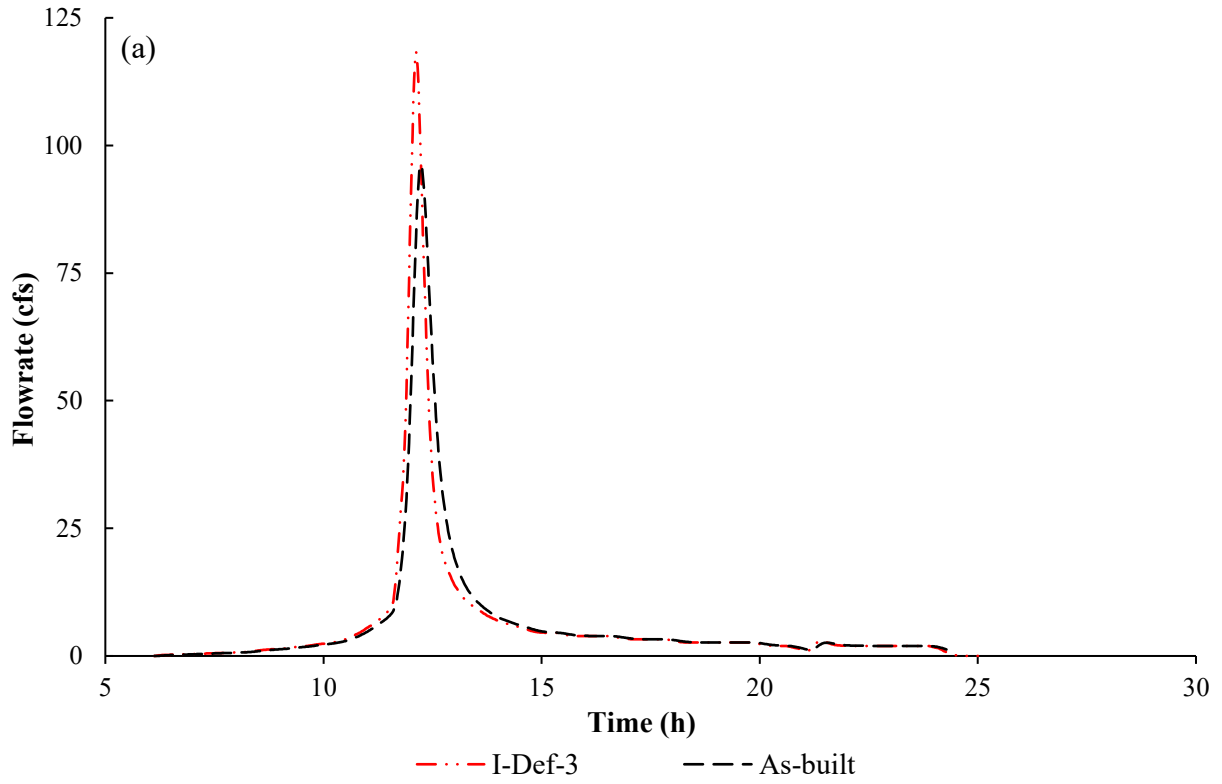


**Figure 149. Runoff hydrograph for the impoundment area design considering 3 subbasins. (a) 100-yr storm; (b) 500-yr storm.**



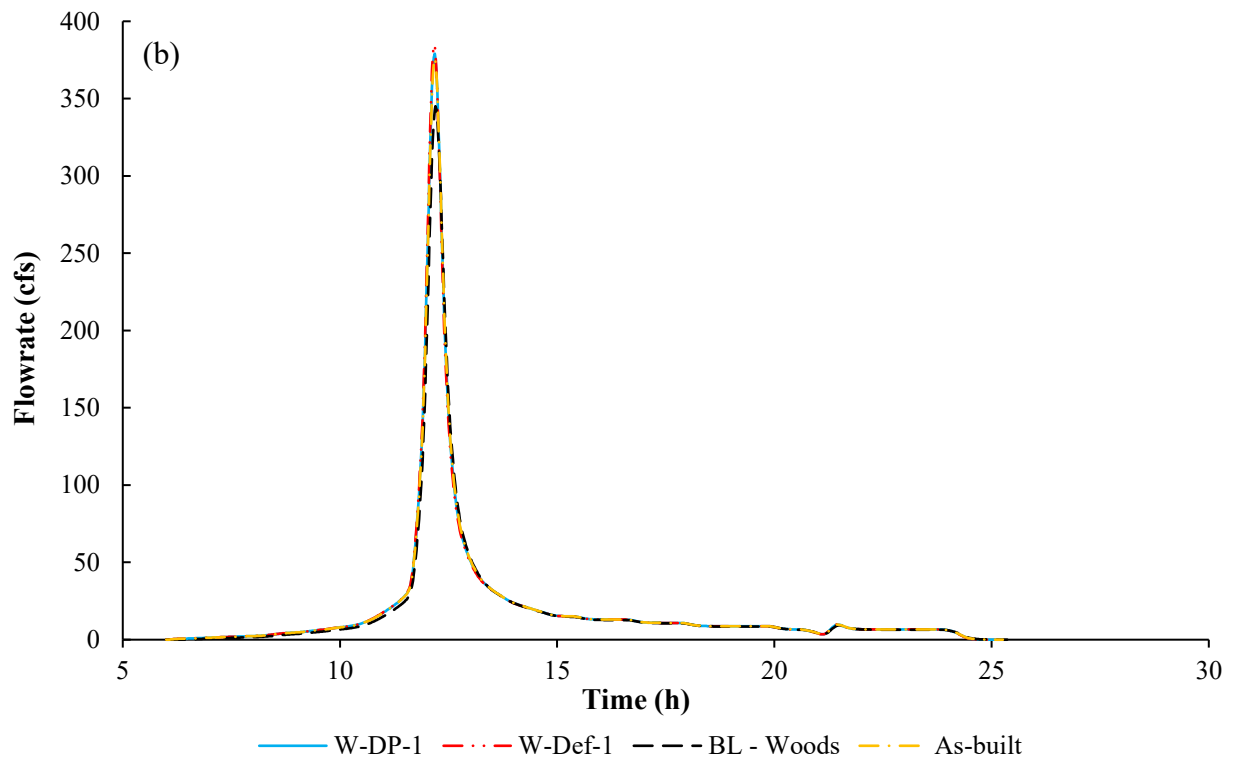
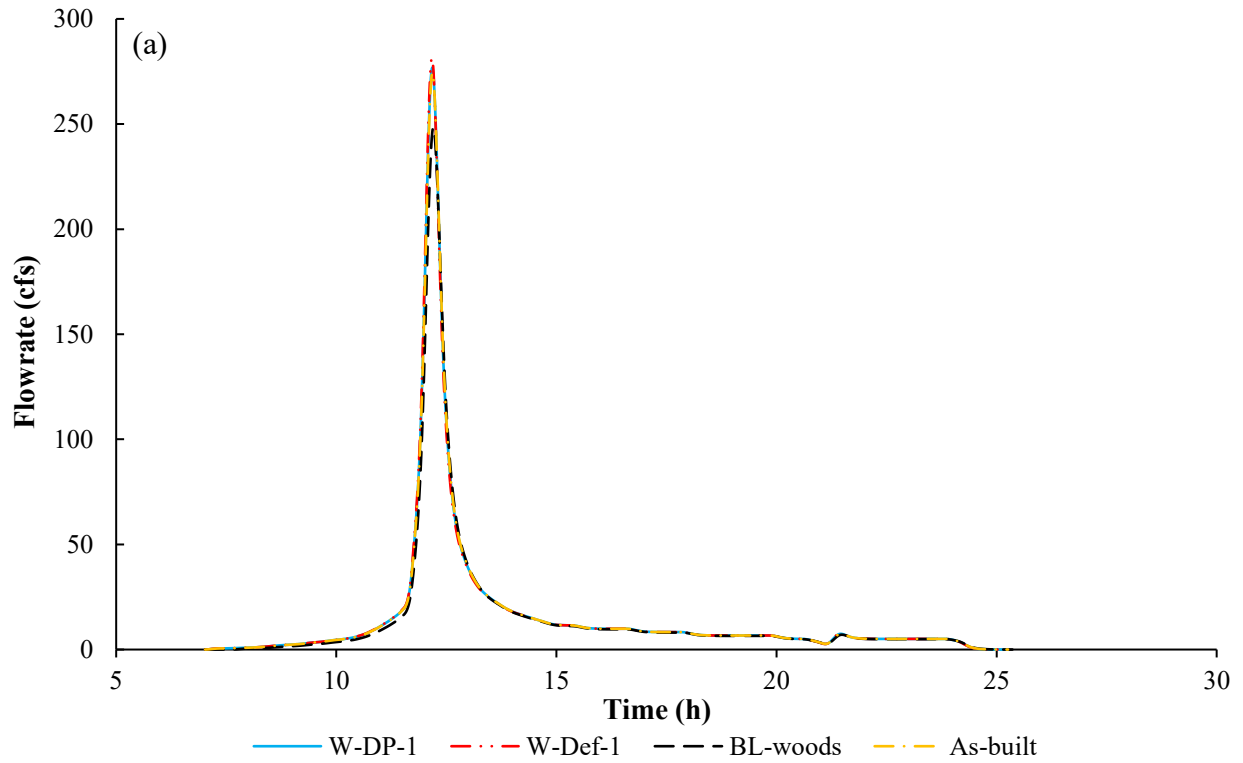


**Figure 150. Runoff hydrograph for design considering the whole watershed area. (a) 100-yr storm; (b) 500-yr storm.**

## Discussion

The geomorphic design approach for impoundment reclamation has the objective of creating slopes and a drainage network that mimics the balanced pre-disturbed landscape aspect. By achieving these objectives, the reclaimed impoundment would achieve long-term stability, with reduction of surface erosion and sediment transport, infiltration and environmental contamination risks due to AMD production, and breakthroughs (DePriest, 2012; Michael *et al.*, 2013).

From the results, we observed increases on the peak flow for all designs compared to the baselines. The time to peak flow and runoff duration were reduced for the designs. These variations indicate a faster runoff flow. These variations occurred due to the larger availability of channels (drainage density) compared to the baselines, improving runoff dissipation. However, little change was noticed in runoff volume. It can be explained by the small size of the watershed analyzed, which does not reflect the small changes in flux. Also, the Curve Number method, here used to calculate runoff, associates all rainfall losses with one term: Initial abstraction ( $I_a$ ).  $I_a$  is correlated with soil and cover parameters, through the curve number, by the empirical Equations 3 and 4 (USDA, 1986). Once the same curve number was used for GLD models and baselines, the losses for both cases had the same value.

$$I_a = 0.2S \quad (\text{Eq. 3})$$

$$S = \frac{1000}{CN} - 10 \quad (\text{Eq. 4})$$

where:

$I_a$  = Initial abstraction

$S$  = Potential maximum retention after runoff begins

CN = Curve number

The results here presented are a conceptual assessment and need complementary analysis to confirm its applicability. From this first analysis, we could notice that:

- The models that used the DePriest *et al.* (2015) input settings presented a tendency to create crests inside the basin that could deviate the water flow from the designed channel. This tendency was observed on the 1-basin and 3-subbasin impoundment models (I-DP-1 and I-DP-3), with the last one showing to be more evident. This configuration creates an undesired flow on the existing channels, which ultimately can create an overflow in these channels.
- The main outlet location for all models was chosen according to the current channel configuration built on the site. Keeping this configuration for the GLD models as proposed here requires the deconstruction of part of the embankment. Once the embankment fills the purpose of stabilizing the non-cohesive slurry material, alterations to its structure would not represent a geotechnically stable model and present a breakthrough hazard (NRC, 2002). To solve this matter, future work will analyze the stability of newly proposed models where the outlets are located at the crest of the embankment on each side, as shown in Figure 151. Changes on the outlet location also would probably reduce the steep slopes observed in the models, once they are mostly

located on the surrounds of the embankment area, where the biggest difference in height is observed.

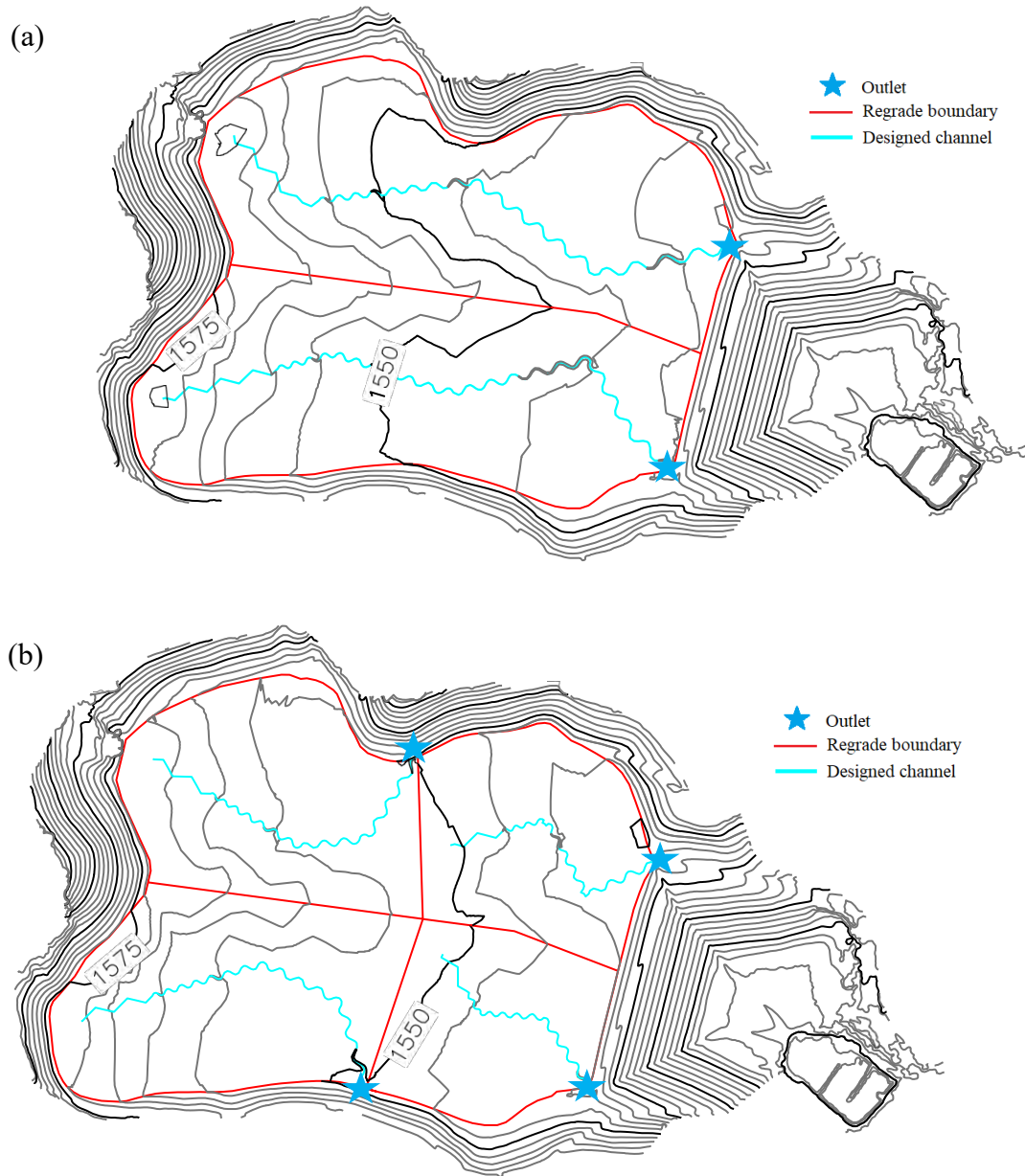


**Figure 151. Alternative designs keeping embankment structure. (a) 2-subbasins; and (b) 4-subbasins.**

- Erosion rates of the proposed models need to be accessed and compared to the traditional reclamation method and the original topography (e.g., Sears *et al.*, 2018). Erosion can decrease land value and slope stability. Also, soil transported by erosion can carry contaminants, which is a particular concern for contaminant-rich soils areas such as reclaimed impoundments.

- Infiltration rates should be determined. As discussed before, the method used for runoff calculation does not account for infiltration in each individual case. Infiltration is related to groundwater seepage, having influence on slope stability and contaminant transport (DePriest, 2012).
- Comparisons between existing and designed surface (earthwork amounts) can be an important parameter of costs and feasibility and should be considered for future work. Costs related to structure removal, earthmoving and revegetation make up for the majority of direct costs of reclamation (OSMRE, 1987). It is desired that the GLD approach keep costs competitive with the conventional design (Hopkinson *et al.*, 2017). Therefore, it would be important to assess the cut-and-fill balance to study the feasibility of the application of the GLD method. Besides costs, this assessment would be especially useful when considering the whole watershed models, once these models include the hillsides, undisturbed area. The surface comparison would measure the alterations to be done in these undisturbed areas. Once the GLD approach aims to bring disturbed landscapes to look and behave close to undisturbed ones, a scenario where the surrounding mountains had to be largely changed is not coherent.

## **Geomorphic reclamation and evaluation for Federal Mine No. 2**

### *Conceptual Reclamation Designs*

#### Uniform-200

Results showed that adding mounded material as high as 200 ft. with an elevation of 1,500 ft. to simulate the elevations of ridgelines surrounding the impoundment created a contour configuration with low elevations at the headwater (Figure 10b and Figure 131a). This region associated with low elevations would result in water ponding and with high elevations surrounding, water would not drain to the created channels. In the event of water ponding, water might infiltrate through the mounded material in an attempt to drain, ultimately resulting in an unstable design. Moreover, the  $D_d$  of the first and second sub-basins were 77 and 84 ft./ac., respectively, which does not comply with the preferred range of 120 ft./ac.  $\pm$  20% for both sub-basins (Tables 3 and 4).

Results from the slope stability analysis completed on this model suggested that the complex geometry generated unstable slopes. A failure plane was observed near the headwater end of the mounded material. According to the analysis, 3H:1V slopes provide the best slope stability across all modeling parameters [36]. Therefore, a 3:1 slope was recommended as the maximum slope grade to be used in subsequent designs in this work. The seepage analysis performed by Smith [36] showed that backfilling the slurry impoundment with mounded material can reduce water infiltration when it is as high as 50 feet or higher, thus boosting the stability of the built design [36].

This design was not evaluated for cut and fill and hydrologic analysis because it did not meet water drainage and slope stability requirements. However, findings from the design were considered when creating the four subsequent GLD designs. The following points were considered based on highlights from this design (Uniform-200) for subsequent designs.



- Main channels in both sub-basins need more tributaries to be built in to meet the target  $D_d$  of 120 ft./ac.  $\pm$  20%,
- Slope modification is required along the extent of the impoundment. The best slope stability across all modeling parameters can be managed following a slope grade of 3H:1V [36],
- Design adjustments should be made when adding the mounded material at the headwater to avoid water ponding and, thus, water infiltration [36],
- The height of the mounded material should be kept below 200 ft. (at least 50 ft. or higher) to reduce water infiltration and thus support the structural stability of the design [36],

### Uniform-50

Due to the varying reservoir width, the mounded material was created with a slope of 3:1 or less (a slope angle range of  $16^\circ$  to  $18^\circ$ ) across the extent of the reservoir. In this design, the  $D_d$  of the first and second sub-basins were increased by 35% and 29%, respectively, compared to the model (Uniform-200) by adding five tributaries to the first sub-basin and six tributaries to the second sub-basin (Table 35 and Table 36). Therefore, the target  $D_d$  of 120 ft./ac.  $\pm$  20% was satisfied. The  $D_d$  of the first and second sub-basins were 104 and 108 ft./ac., respectively. When the height of the mound material was reduced to 50 ft. with an elevation of 1,350 ft., in addition to the created tributaries on each side of the two main channels, contour configurations with high elevations were formed. The elevations of the generated contours were approximately 1,390 ft. and were built as small mounds on top of larger sloping hills (Figure 152b). The elongated shape and the varying width of the reservoir were the main two reasons for the creation of the small mounds.

### Uniform-90

This model had a mid-ridge line designed at 90 ft. in this design. Results indicated an approximately uniform contour configuration compared to the previous two designs (Figure 152c). The mounded material was created with a slope ranging between 4:1 and 3:1 (slope angle range of  $10^\circ$  to  $18^\circ$ ) as a result of the varying reservoir width. The  $D_d$  of the first and second sub-basins were increased by 32% and 21%, respectively, compared to the model (uniform-200) by adding five tributaries to the first sub-basin and five tributaries to the second sub-basin (Table 35 and Table 36).

### Two-elevated Areas (T-E)

In this model, the total length of the main channel ( $L_{MC}$ ) designed for the first sub-basin was 4,832 ft., while the total channel length ( $L_T$ ) was 9,675 ft., resulting in a  $D_d$  of 99 ft./ac. The  $L_{MC}$  designed for the second sub-basin was 4,771 ft., and the  $L_T$  was 8,450 ft., resulting in a  $D_d$  of 97 ft./ac. (Table 35 and Table 36). As a result of moving the main channels further from the center of the reservoir, in addition to the elongated shape of the reservoir, some complicated contour configuration was created at the headwater (Figure 152d). The resulting contour configuration had a low elevation, which may result in ponding. Even though the water in this area will find a way to end up in the created channels, some might migrate through the backfilling, which is

known to work against the stability of the design as the slope and seepage stability analysis showed in the model (Uniform-200) (Smith, 2023).

### Conventional

The main channel in this model was designed on the perimeter of the reservoir. The  $L_{MC}$  for sub-basins 1 and 2 were 4,026 ft. and 3,745 ft., respectively, which is equal to  $L_T$ . No tributaries were included in this design (Table 35 and Table 36). The main channels in this design have shorter lengths compared to the length of main channels in other designs because sinuosity is approximately 1 in this conventional approach (Figure 152e).

### Conventional-GLD

The backfill gradually slopes toward the beach of fines close to the dam with a smooth contour configuration that mimics natural terrain (Figure 152f). Main channel 1 was designed on the perimeter except for the curved location near the outlet. For the first sub-basin,  $L_{MC}$  was 4,503 ft., which is equal to  $L_T$  because no tributaries were added to main channel 1 (Table 35 and Table 36). In contrast,  $L_{MC}$  designed for the second sub-basin measured 4,404 ft., which was also similar to  $L_T$  for the same reason.  $D_d$  of the first and second sub-basins were 96 and 102 ft. ac., respectively. The targeted  $D_d$  was satisfied even though no tributaries were added to any of the two main channels, and that is due to the smaller area of disturbance (89.66 ac.).

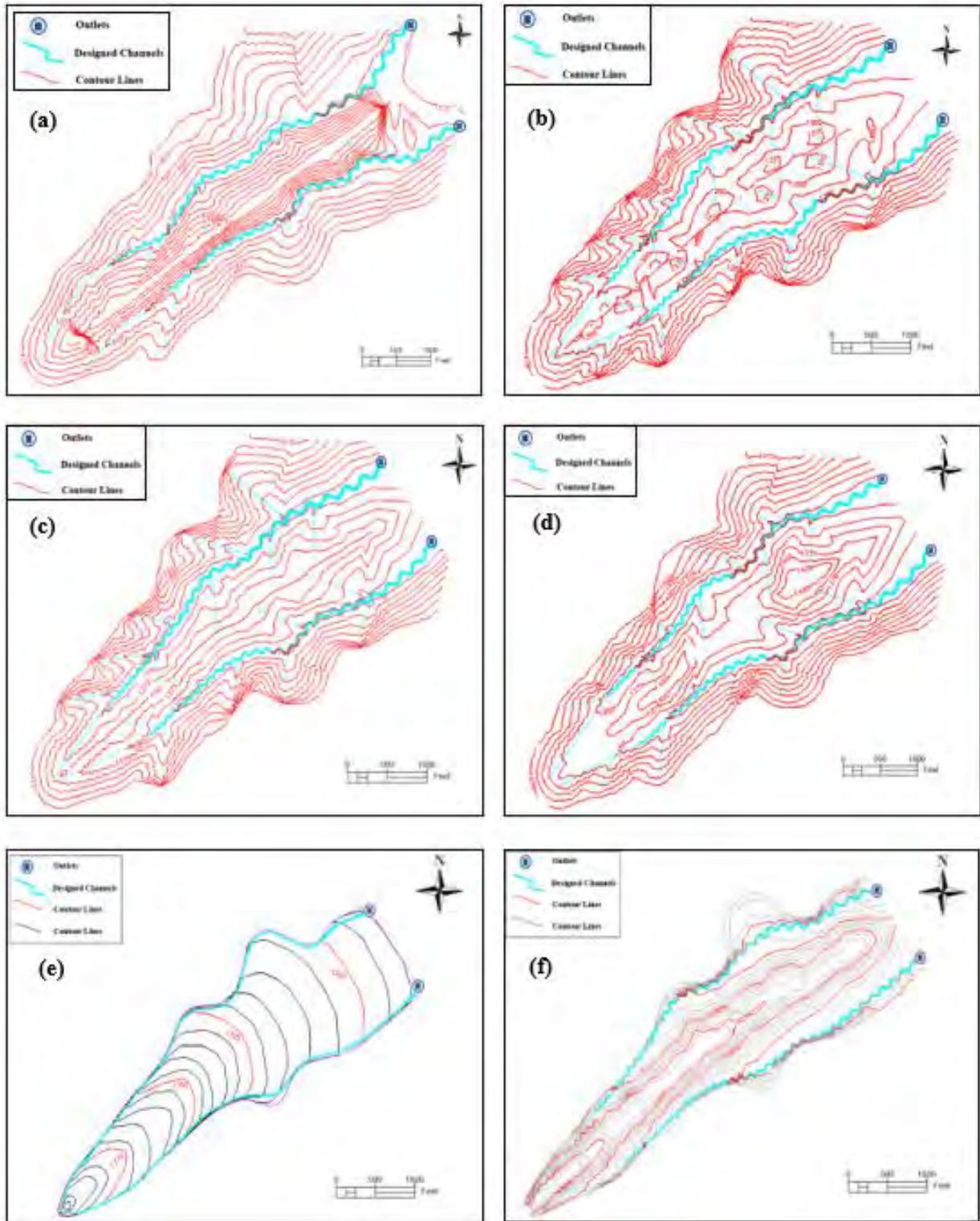


Figure 152. Designed surface with contour elevations in ft.: a) Uniform-200, b) Uniform-50, c) Uniform-90, d) T-E, e) Conventional, and f) Conventional-GLD.

**Table 35. Design characteristics for sub-basins 1 for all created designs.**

Results	Uniform-200	Uniform-50	Uniform-90	T-E	Conventional	Conventional-GLD
Area, $A$ (ac.)	110.7	97.57	97.57	97.57	46.68	46.68
Drainage density, $D_d$ (ft./ac.)	77	104	102	99	-	96
Head elevation, $E_H$ (ft.)	1,420	1,397	1,397	1,400	1,390	1,390
Base elevation, $E_B$ (ft.)	1,282	1,280	1,280	1,280	1,278	1,278
Main channel length, $L_{MC}$ (ft.)	5,406	4,761	4,761	4,832	4,026	4,503
Total channel length (ft.)	8,537	10,183	9,960	9,675	4,026	4,503
Sinuosity	1.15 to 1.24	1.15 to 1.24	1.15 to 1.24	1.15 to 1.24	1	1.15 to 1.24
Bankfull width, $W_B$ (ft.)	0.3 to 18.1	0.2 to 19.2	0.0 to 19.2	0.3 to 17.0	-	1.06 to 13.5
Bankfull depth, $D_B$ (ft.)	0.03 to 1.5	0.02 to 1.5	0.0 to 1.5	0.03 to 1.4	-	0.11 to 0.8
Flood-prone width, $W_F$ (ft.)	0.55 to 35.9	0.39 to 33.9	0.0 to 33.9	0.6 to 33.1	-	2.28 to 23.8
Flood-prone depth, $D_F$ (ft.)	0.06 to 3.6	0.04 to 3.6	0.0 to 3.6	0.06 to 3.4	-	0.26 to 2.13

- Not applicable

**Table 36. Design characteristics for sub-basins 2 for all created designs.**

Results	Uniform-200	Uniform-50	Uniform-90	T-E	Conventional	Conventional-GLD
Area, $A$ (ac.)	85	86.7	86.7	86.7	42.98	42.98
Drainage density, $D_d$ (ft./ac.)	84	108	102	97	-	102
Head elevation, $E_H$ (ft.)	1,440	1,400	1,401	1,396	1,386	1,386
Base elevation, $E_B$ (ft.)	1,300	1,282	1,279	1,279	1,278	1,278
Main channel length, $L_{MC}$ (ft.)	4,929	4,781	4,781	4,771	3,745	4,404
Total channel length, $L_T$ (ft.)	7,107	9,367	8,881	8,450	3,745	4,404
Sinuosity	1.15 to 1.24	1.15 to 1.24	1.15 to 1.24	1.15 to 1.24	1	1.15 to 1.24
Bankfull width, $W_B$ (ft.)	0.00 to 17.9	0.25 to 16.0	0.21 to 16.02	0.00 to 18.11	-	0.00 to 11.3
Bankfull depth, $D_B$ (ft.)	0.00 to 1.12	0.02 to 1.3	0.02 to 1.28	0.00 to 1.13	-	0.00 to 0.9
Flood-prone width, $W_F$ (ft.)	0.01 to 31.6	0.53 to 31.2	0.45 to 31.97	0.00 to 31.98	-	0.00 to 21.9
Flood-prone depth, $D_F$ (ft.)	1.75 to 2.15	0.06 to 3.2	0.05 to 3.2	0.00 to 2.86	-	0.00 to 2.23

- Not applicable

### *Slope Analysis*

In this analysis, slopes were quantified by area. In GLD designs that had a big disturbance area (roughly 184 ac.) (Uniform - 50, Uniform - 90, and T-E), approximately 24 to 32% of the hillside slope was built with a slope of 2:1. However, 14 to 16% of the hillside slopes were built with a slope of greater than 2:1. T-E had a 54% area of 3:1 slope, which includes the reservoir limit and surrounding ridgelines (elevation = 1,340 ft.). Part of the two elevated areas in this design was built with a slope of 2:1. Reservoir limit, mid-ridgeline, and surrounding ridgelines (elevation = 1,340 ft.), which make up 57 to 60% of the area for models Uniform - 50 and Uniform - 90, are all areas of slope 3:1 or less (Table 37).

Conventional and Conventional-GLD had 50 to 54% of a 3:1 slope area that includes the reservoir limit and surrounding ridgelines (elevation = 1,340 ft.). The hillside in these two models was not altered through the design process, and it is 41% area of a 2:1 slope. Around 5% of the hillside is built with a slope greater than 2:1 slope (Table 37).



**Table 37. Slope analysis of six created designs.**

<b>Model</b>	<b>% area of slope 3:1 or less</b>	<b>% area of slope 3:1 to 2:1</b>	<b>% area of slope greater than 2:1</b>
Uniform - 50	60	24	16
Uniform - 90	57	29	14
T-E	54	32	14
Conventional-GLD	54	41	5
Conventional	54	41	5

*Material Movement*

The main focus of comparison in the earthwork estimation task is the filling zones, as piles of CCR located in the site will be used for backfilling purposes. T-E required the most fill material ( $7.8 \times 10^6$  yd<sup>3</sup>); the two built elevated areas needed the most material (blue hatches Figure 153c). Uniform-90 required the second-highest filling ( $7.5 \times 10^6$  yd<sup>3</sup>) (Figure 153b and Table 38). However, Conventional-GLD required the least fill ( $3.3 \times 10^6$  yd<sup>3</sup>) (Figure 153e) compared to all the designs. Even though Conventional and Conventional-GLD were built following the same plan that the WVDEP intends to follow, the design that was created using the GLD approach (Conventional-GLD) required less fill material compared to the other design, which was built manually following the conventional approach (Conventional). The GLD approach decreased the required fill material by 8.4%, which can be interpreted by the natural contour configuration generated using the GLD approach compared to the conventional design.

**Table 38. Earthmoving quantities summary.**

<b>Design Name</b>	<b>Total Cut (yd<sup>3</sup>)</b>	<b>Total Fill (yd<sup>3</sup>)</b>
Uniform-50	$1.6 \times 10^6$	$5.9 \times 10^6$
Uniform-90	$1.7 \times 10^6$	$7.5 \times 10^6$
Two-elevated	$0.87 \times 10^6$	$7.8 \times 10^6$
Conventional	$1.26 \times 10^6$	$3.5 \times 10^6$
Conventional-GLD	$1.59 \times 10^6$	$3.3 \times 10^6$

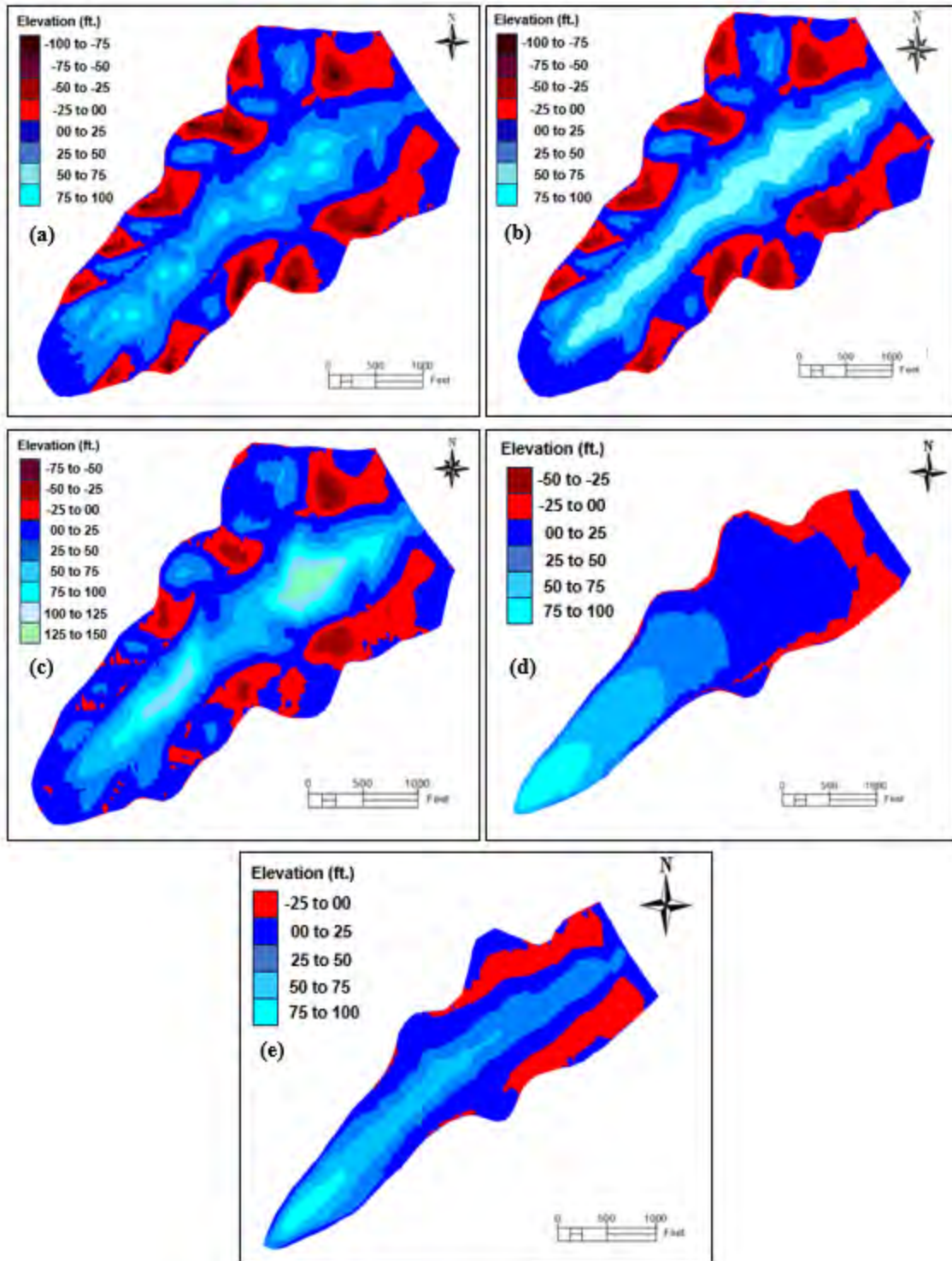


Figure 153. Cut (red hatches) and fill zones (blue hatches): a) Uniform-50, b) Uniform-90, c) T-E, d) Conventional, and e) Conventional-GLD.

*Hydrologic Response Evaluation*

The geomorphic approach decreased the peak discharge and increased the time to peak in all the created designs for both of the analyzed storm events (100 and 500-year storm events) when compared to the conventional approach (Figure 154 and Table 39). For sub-basin 1, the decrease in peak runoff discharge ranges from 12.7% (T-E) to 17.7% (Conventional-GLD) for the 100-year storm event. The decrease in peak runoff discharge ranged from 13.9% (T-E) to 18.4% (Conventional-GLD) for sub-basin 2 for the same storm event. Time to peak ranged from 8 (T-E) to 13.4 min (Conventional-GLD) and 8 (T-E) to 10.8 min (Conventional-GLD) for sub-basins 1 and 2, respectively.

Trends were similar for the 500-year event; the decrease in peak runoff discharge ranges from 12.6% (T-E) to 17.6 (Conventional-GLD) in the analysis of the first sub-basin. There was a range of increments in peak time between 8 (T-E) and 13.4 min (Conventional-GLD). For the same storm event, peak runoff discharge decrease ranged from 13.9% (T-E) to 16% (Conventional-GLD) in the analysis of the second sub-basin. Whereas the peak time increments ranged from 15 (T-E) to 19 min (Conventional-GLD). Sediment transport and surface erosion are reduced when the designed models intend to simulate the balanced landscape aspect of pre-disturbed areas (Hancock et al., 2020, GeoFluv, n.d.). Model (Conventional) resulted in the highest peak runoff with some reduction in the time to peak (Table 39), which can be explained by the less meander channel configuration that has a sinuosity of approximately 1 created following the conventional method of reclamation.

**Table 39. Hydrologic analysis summary 100-year, 24-hr. storm event: sub-basins 1 and 2, and 500-year, 24-hr. storm event: sub-basins 1 and 2.**

Designs	100-year, 24-hr. storm event		500-year, 24-hr. storm event	
	Q <sub>p</sub> (cfs)	T <sub>p</sub> (hr.)	Q <sub>p</sub> (cfs)	T <sub>p</sub> (hr.)
	Sub-basin 1		Sub-basin 1	
Uniform-50	133.11	12.92	190.48	12.90
Uniform-90	136.91	12.88	195.92	12.86
Two-elevated	137.08	12.86	196.16	12.84
Conventional	154.59	12.72	221.06	12.70
Conventional-GLD	131.29	12.94	187.89	12.92
	Sub-basin 2		Sub-basin 2	
Uniform-50	145.45	12.78	208.05	12.78
Uniform-90	146.80	12.77	210.04	12.76
Two-elevated	148.11	12.76	211.82	12.75
Conventional	168.82	12.62	241.29	12.60
Conventional-GLD	142.50	12.80	208.00	12.79

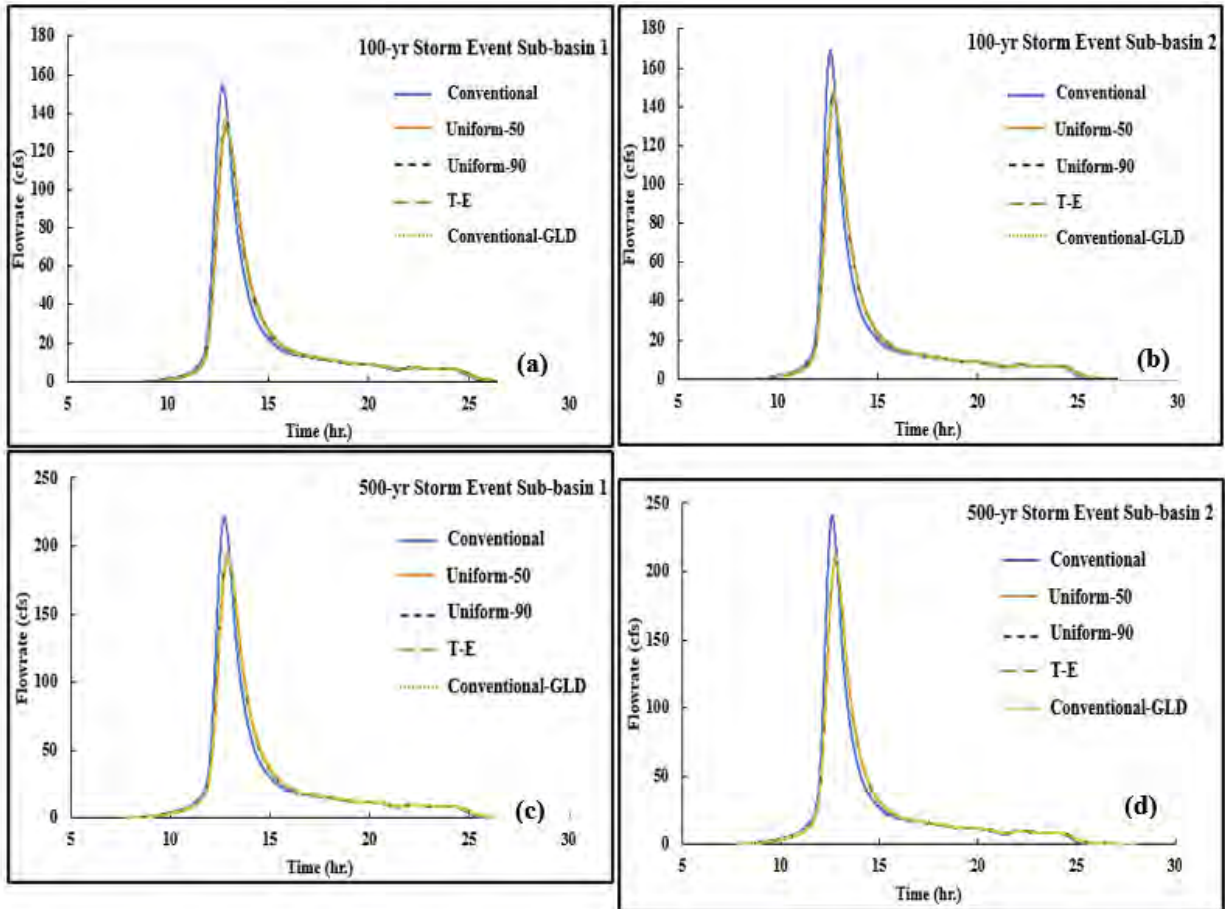


**Figure 154. Runoff hydrographs: 100-year storm event a) sub-basin 1 and b) sub-basin 2 and for the 500-year storm event c) sub-basin 1 and d) sub-basin 2.**

## CONCLUSION

### Coal impoundment site evaluation

From each site visit, the observed issues were documented and summarized into Table 40. It was observed that historical reclamation designs and practices work at maintaining a steady slope but are hydraulically imbalanced. Sites more recently reclaimed experience fewer issues but are not defect free. In the years after closure, the unchecked wet zones and differential settlement of the cap, lead to more issues. After losing the ability to retain water, erosion is raised due to the reduced infiltration promoting runoff to an under designed drainage system.

Notable findings include the following:

1. Wet zones and differential settlement were the lead causes in all site erosion issues,
2. Uneven finish grading, and potential localized differential settlement, was observed with ponded water in low spots,
3. All sites exhibited saturated caps and caused runoff during precipitation events,



4. Observed runoff channelized at the lowest grade point on the impoundment to the installed drainage ditches or formed erosion ditches,
5. Drainage ditches were often filled with sediment sometime after the 5-year reclamation.
6. Vegetation and ground cover within the impoundment was that of a marsh,
7. The cap used at each site was effective in preventing the migration of fine coal refuse (FCR) particles through the structure,
8. Sediment buildup, erosion, or dense vegetation was observed in all natural contact ditches. Only grouted riprap contact ditches were alleviated of these issues.

Recommendations for these observations would be subsurface drainage consisting of a corrugated pipe with a geosynthetic to prevent the transportation of fines. Mounded material placed along the cap would also reduce the saturation of the refuse by promoting runoff. Any infiltrated water would have a more delayed release than that of a saturated impoundment. Additional drainage and more robust construction of contact ditches around the perimeter are needed to divert and release water, preventing re-saturation of refuse.

**Table 40: Observations across site visits.**

Permit No.:	O002684	O101086	O002184	O301286	R070700	S20198 8	S003576	S024076
Name	Energy Marketing North Hollow Impoundment	Building Run Slurry Impoundment	Rockcamp Branch #1 Coal Refuse Impoundment	Peerless Eagle Freshwater Impoundment	#1 Refuse Area/Site A Impoundment	Knight Ink No. 1 Mine Pit	Cowen Trench Area	North Point Surface Impoundment
Status	Capped	Active	Capped	Active	Capped	Capped	Abandoned	Capped
Wet zones, standing water	X	X	N.O.	X	X	X	X	X
Unconnected drainage	N.O.	N.O.	X	X	X	X	X	X
Sediment in drainage system	N.O.	N.O.	X	N.O.	X	X	X	X
Exposed refuse	N.O.	X	N.O.	N.O.	X	N.O.	X	N.O.
Slurry area erosion	N.O.	X	X	N.O.	X	N.O.	N.O.	N.O.
Differential settlement/ uneven grading	X	X	X	N.O.	X	X	X	X
Wetland vegetation	N.O.	N.O.	X	X	X	X	X	X

Note: N.O. = not observed

## Finite Element Modeling of Century Impoundment

From the modeling of the three different cases, findings used to improve the modeling and reclamation process include the following:

- Material properties were determined based on literature: The CCR internal angle of friction ranged 31.5° to 34°. The 31.5° value was used for worst-case scenario conditions,
- The material hydraulic conductivity, both FCR and CCR, from the permit file were too high and caused rapid pool drawdown; refined values based on literature were used,
- The General Limit Equilibrium (GLE) calculation method was used because it produced higher resultant factors of safety with convergence between force and moment equilibrium than Bishop's method,
- The grid and tangent method had edge effects and limited the analysis,
- The automated slope method analyzed the overall stability of the structure to locate the failure surfaces,
- An analysis using the automated slope search method to identify weak regions and a more detailed analysis using grid and tangent method may improve modeling considerations,
- The worst-case loading condition is a saturated zone located at the reclaimed dam crest elevation. Analysis of recurring storm events for Pre-reclamation, WVDEP reclaimed, and GLD options showed most ranges of FS < 1.5,
- All WVDEP and GLD reclaimed models experienced toe failures under saturated conditions from the 100-year and recurring 100-year storm events.

Advancements made in the modeling criteria shall be as follows:

- The internal angle of friction for CCR shall be increased to 34°.
- The hydraulic conductivity values of the FCR and CCR shall be changed to better reflect site conditions, cited from the literature used in Hegazy et al (2004).
- General limit equilibrium (GLE) method will be used in conjunction with the automated slope search method to evaluate failure locations across the structure.

## Geomorphic reclamation and evaluation for Century Impoundment

GLD has shown potential for mine land reclamation applications. This study evaluates the application of GLD principles to a slurry impoundment reclamation. Eight conceptual landform designs were created for the impoundment area ( $n = 6$ ) and watershed scale ( $n = 2$ ). Different channel configurations were analyzed using two different inputs dataset (DePriest *et al.* 2015 and Default). The hydrologic response was compared with the traditional reclamation method showing variation in peak flow rate, time to peak, and runoff duration. No large variation in runoff amounts were observed.

The models that used the DePriest *et al.* (2015) inputs (I-DP-1, I-DP-2, and W-DP-1), showed a smaller variability in hydrologic response compared to the as-built baseline. It can be attributed to the use of criteria values that were measured in Appalachia region and may better represent the study area conditions than the default values, which were measured at southwestern, United

States. The GLD application for coal slurry impoundment reclamation needs further analysis including slope stability, erosion rates, infiltration, and earthwork amounts.

## **Geomorphic reclamation and evaluation for Federal Mine #2**

Historically, slurry impoundments have resulted in human and environmental crises, and regulations have been created to address this issue. Reclamation has, therefore, been integrated into the process of impoundment construction and closure for post-mining land use (Greenberg, 2017). In natural watersheds, stream profiles tend toward concave shapes over time, and their gradients tend to be steeper at the headwater and flatten out as they approach the mouth. Stream plan forms might be sinuous or braided as a result of both the stream gradient and flow (discharge) (Schor and Gray, 2007). Fluvial geomorphic techniques shape the land to facilitate natural erosion under defined climatic conditions, soil types, and slopes present at any site. Landform designs based on geomorphic principles are known to discharge water corresponding to the surrounding natural environment through drainage systems, as opposed to hard engineering solutions, which rely on drop-down structures and rock-lined drainage systems (Lacy, 2019). Current research aims to design a reclamation scheme for a coal mine slurry impoundment located in northern WV, USA. A blending of the constructed topography and the contours around the reservoir was intended to be achieved through the GLD approach. A series of geomorphic designs for the coal slurry impoundment were completed.

Taking a comparative look at the geomorphic designs that were evaluated, the change in elevation of the created mid-ridgeline did not influence the peak runoff discharge significantly, and that is due to two reasons. First, the GLD approach creates a uniform contour configuration that mimics natural terrain, which in terms would not create a big difference in the average slope of the ground comparing all the designs to each other even though the elevation of the created mid-ridgeline varies from one design to another. The second reason is that the SCS method considered in this study for the evaluation of the hydraulic response employs the curve number to determine the infiltration loss. Since the curve number in all designs has the same value, the time of concentration would then have the most significant impact on the calculation and evaluation of peak discharge. The average ground slope was determined based on the ground slope of the furthest path that a raindrop would take to reach an outlet. Since the average ground was not changing considerably from one design to another, the difference in the peak runoff discharge was not substantial. Additionally, model (conventional) resulted in the highest peak runoff with some reduction in the time to peak, which can be explained by the less meander channel configuration design (sinuosity is approximately 1) and the steep slope of the ground, which was created following the conventional method of reclamation.

Extending the area of disturbance to the surrounding ridgeline that has high elevations did not have a substantial influence on the results of the hydraulic response, and that is because the surrounding area is naturally weathered and has a contour configuration similar to what Natural Regrade would generate. The extended disturbance area also required more filling material to satisfy the created contour elevations.

Following the GLD approach, the elongated shape, and the non-uniform width of the reservoir, approximately (250 ft. min.) at the headwater and (1425 ft. max.) close to the dam, resulted in the continuous creation of complicated contour configurations at the headwater (e.g., models



Uniform-200 and Two-elevated) or along the extent of the reservoir in some cases (e.g., model Uniform-50).

DePriest et al. (2015) demonstrated that if minimizing impact area is a concern, then design stability might be an issue. In this study, the area of disturbance of 89.66 ac., considered in models (conventional and conventional-GLD), allowed for some flexibility to achieve the 3H:1V slope design as long as the mid-ridgeline height is approximately 50 ft. However, when the mid-ridgeline is elevated to 1,390 ft. (height 90 ft.) or higher, the area of disturbance should be extended to achieve a stable design with a slope of 3:1 or 2:1 within the reservoir area. This finding is consistent with the findings of other previous studies completed for valley fills in the Appalachian region (Michael et al., 2015). Nevertheless, extending the disturbance area increased hillside areas with a slope of greater than 2:1 by 11%, when compared to what is already built on the ground, and that might create instability in the hillsides.

Based on the results of this study, the following recommendations were made:

- Extending the area of disturbance to the surrounding ridgeline that has high elevations might create some hillside slope instability, have no significant influence on flow rate peaking time, require more filling material, and require the addition of tributaries to the main channels to meet the target. Therefore, a small disturbance area covering the reservoir is recommended.
- If the area of disturbance was to exceed the area of the reservoir, tributaries should be added to satisfy the drainage density of the area.
- Following the GLD approach to reclaim the reservoir area, including surrounding ridgelines of elevation = 1,340 ft., would create uniform contour lines that could result in less amount of backfilling material needed for the design compared to the conventional reclamation approach.
- If the geomorphic approach were to be followed, it is recommended to build drainage channels aligned with the perimeter of the reservoir, as pushing the channels further might create a contour configuration with elevations lower than the channel elevations at the headwater, resulting in water ponding.
- The flow of water over channels is much faster than over hillslopes since vegetation and pores in the ground slow down saturated overland flow (Anderson and Anderson, 2010). Based on the results of the hydrologic analysis, it is recommended to create meander channels even if the conventional approach were to be followed because it would contribute to decreasing the peak runoff discharge and increasing the time to peak, resulting in less erosion carried by runoff. More research is needed to confirm this point.

In the future, the effect of slope shape on mass stability and rainfall erosion resistance could be investigated through conceptual and mathematical models e.g., the SIBERIA landscape evolution model by which erosion can be overviewed, visualized, and quantified. Thus, soil displacement, loss, and deposition during a defined storm event can be determined. Additionally, Different channel configurations can be tested by developing a design where high or elevated areas are scattered along the impoundment area. This configuration would allow for the creation of one main channel with tributes going through the elevated areas. Then, the hydrologic response can be tested for the designed configuration by considering one big basin. Confirmation of the input parameter through field experiments should also be considered.

## REFERENCES

- About us – geofluv land reclamation natural regrade.* (n.d.). Retrieved March 21, 2024, from <https://www.geofluv.com/about-us/>
- Anderson R. S, & Anderson S. P. (2010). *Geomorphology: the mechanics and chemistry of landscapes*. Cambridge University Press, 2010.
- Bedient, P. B., Huber, W. C., & Vieux, B. E. (2013). *Hydrology and floodplain analysis* (5th ed.). Prentice Hall.
- Blacksville, West Virginia weather.* (n.d.). BestPlaces. Retrieved March 21, 2024, from [https://www.bestplaces.net/weather/city/west\\_virginia/blacksville](https://www.bestplaces.net/weather/city/west_virginia/blacksville)
- Buckley, C., Hopkinson, L., Quaranta, J., Mack, B., Ziemkiewicz, P. (2013). Investigating design parameters in the design of West Virginia valley fills to support application of geomorphic landform design principles. In *Environmental Considerations in Energy Production*, J.R. Craynon, ed. Society for Mining, Metallurgy, and Exploration (SME), Englewood, CO, 405-414.
- Bugosh, N. (2004) “Carlson Software’s Natural Regrade Module: Computerizing the Fluvial Geomorphic Approach to Land Reclamation.”
- D’Appolonia Consulting Engineers (2009) *ENGINEERING AND DESIGN MANUAL COAL REFUSE DISPOSAL FACILITIES*. U.S. Department of the Interior, Mining Safety and Health Administration.
- Dalen, S. 2021. Erosion and sediment controls on mine refuse impoundments. Graduate Theses, Dissertations, and Problem Reports. 8066. <https://researchrepository.wvu.edu/etd/8066/>
- DePriest, N. 2012. Comparison of Groundwater Seepage Modeling in Approximate Original Contour and Geomorphic Valley Fill Design. Graduate Theses, Dissertations, and Problem Reports. *Graduate Theses, Dissertations, and Problem Reports*. 470. <https://researchrepository.wvu.edu/etd/470>
- DePriest, N., Hopkinson, L., Quaranta, J., Sears, A., Russell, H. Snyder, M., O’Leary, E., Eddy, J., Mack, B., and Hause, J. (2014). Developments in valley fill reclamation in Central Appalachia: the design of stable and sustainable landforms. *Advances in Geomorphic Reclamation at Coal Mine Sites. A Technical Interactive Forum and Field Tour*. Office of Surface Mining Reclamation and Enforcement. May 20-22. Albuquerque, NM. 6 pp.
- DePriest, N. C., Hopkinson, L. C., Quaranta, J. D., Michael, P. R., & Ziemkiewicz, P. F. (2015). Geomorphic landform design alternatives for an existing valley fill in central Appalachia, USA: Quantifying the key issues. *Ecological Engineering*, 81, 19–29. <https://doi.org/10.1016/j.ecoleng.2015.04.007>
- FEMA. 2020. WVV 1ft contours GDB. Accessed November 1, 2022. [https://data.wvgis.wvu.edu/pub/Clearinghouse/Elevation/QL2Lidar/2\\_CountyBundles\\_Q\\_L2\\_Lidar\\_Products/Contours/Barbour\\_Contours\\_GDB\\_clipped\\_FEMA\\_2018-20\\_WV\\_SouthCentral/](https://data.wvgis.wvu.edu/pub/Clearinghouse/Elevation/QL2Lidar/2_CountyBundles_Q_L2_Lidar_Products/Contours/Barbour_Contours_GDB_clipped_FEMA_2018-20_WV_SouthCentral/)
- Genes, B.E., T.O. Keller, and J.P. Laird (2000). “Steady State Liquefaction Susceptibility of High Hazard Upstream-Constructed Coal Refuse Disposal Facilities,” *Proceedings, Tailings Dams 2000*, Las Vegas, ASDSO/USCOLD, pp. 47-58.

- Greenberg, P. (2017). Disproportionality and resource-based environmental inequality: An analysis of neighborhood proximity to coal impoundments in appalachia. *Rural Sociology*, 82(1), 149–178. <https://doi.org/10.1111/ruso.12119>
- Hancock, G. R., Duque, J. F. M., & Willgoose, G. R. (2020). Mining rehabilitation – Using geomorphology to engineer ecologically sustainable landscapes for highly disturbed lands. *Ecological Engineering*, 155, 105836. <https://doi.org/10.1016/j.ecoleng.2020.105836>
- Hancock, G. R., Duque, J. M., & Willgoose, G. R. (2019). Geomorphic design and modelling at catchment scale for best mine rehabilitation – The Drayton mine example (New south wales, australia). *Environmental Modelling & Software*, 114, 140–151. <https://doi.org/10.1016/j.envsoft.2018.12.003>
- Hegazy, Y. A., Cushing, A. G., and Lewis, C. J. (2004). “Physical, mechanical and hydraulic properties of coal refuse for slurry impoundment design.” *D’Appolonia Engineering*, Monroeville, PA.
- Hopkinson, L. Sears, A.E., Snyder, M., O’Leary, E., DePriest, N., Quaranta, J., and Ziemkiewicz, P. (2015). Simulating the hydrologic response when streams are incorporated in valley fill design. Paper submitted to *Journal of Mining, Reclamation, and Environment* 30(5-6): 422-437
- Hopkinson, L. C., Lorimer, J. T., Stevens, J. R., Russell, H., Hause, J., Quaranta, J. D., & Ziemkiewicz, P. F. (2017). Geomorphic landform design principles applied to an abandoned coal refuse pile in central appalachia. *Journal American Society of Mining and Reclamation*, 2017(2), 19–36. <https://doi.org/10.21000/JASMR17020019>
- Ismael, M., Abdelghafar, K., Sholqamy, M., & Elkarmoty, M. (2021). Performance prediction of hydraulic breakers in excavation of a rock mass. *Rudarsko-Geološko-Naftni Zbornik*, 36(4), 107–119. <https://doi.org/10.17794/rngn.2021.4.9>
- Jedari, C., Drumm, E.C. and Palomino, A.M. (2022) “Approximation of the Time Rate of Consolidation for Hydraulically Placed Fine Coal Refuse Using a Variable Coefficient of Consolidation Method,” *International Journal of Geomechanics*, 22(1). Available at: [https://doi.org/10.1061/\(asce\)gm.1943-5622.0002241](https://doi.org/10.1061/(asce)gm.1943-5622.0002241).
- Lacy, H. (2019). *Mine landforms in Western Australia from dump to landform design: Review, reflect and a future direction*. 371–384. [https://doi.org/10.36487/ACG\\_rep/1915\\_30\\_Lacy](https://doi.org/10.36487/ACG_rep/1915_30_Lacy)
- Lorimer, J. T. (2016). *Geomorphic landform design principles applied to an abandoned coarse coal refuse pile on steep terrain in central Appalachia*. M.S., West Virginia University.
- Martín-Duque, J.F., Sanz, M.A., Bodoque, J.M., Lucía, A., and Martín-Moreno, C. 2010. Restoring earth surface processes through landform design. A 13-year monitoring of a geomorphic reclamation model for quarries on slopes. *Earth Surf. Process. Landforms*. 35. 531–548. <https://doi.org/10.1002/esp.1950>
- Michael, P. R., Richmond, M. W., Lane, D. L., and Superfesky, M. J. 2013. Preventing breakthroughs of impounded-coal-waste-slurry into underground mines. West Virginia Mine Drainage Task Symposium. March 26-27, Ramada Inn, Morgantown, WV. <https://wvmdtaskforce.files.wordpress.com/2016/01/13-michael-paper.pdf>

- National Oceanic and Atmospheric Administration (NOAA). Precipitation Frequency Data Server. Accessed October 27, 2022. <https://hdsc.nws.noaa.gov/pfds/>
- National Research Council (NRC). 2002. Coal Waste Impoundments: Risks, Responses, and Alternatives. Washington, DC: The National Academies Press. <https://doi.org/10.17226/10212>
- Office of Surface Mining Reclamation and Enforcement (OSMRE). U.S. Department of the Interior. 1987. Handbook for Calculation of Reclamation Bond Amounts.
- O’Leary, E.E. (2014). Floodplain Mapping in Response to Surface Mine Reclamation. Thesis. Morgantown, WV: WVU.
- Pf data server-pfds/hdsc/owp*. (n.d.). Retrieved March 21, 2024, from <https://hdsc.nws.noaa.gov/pfds/>
- Quaranta, J. D., Hopkinson, L., Ziemkiewicz, P. (2013). Comparison of groundwater seepage modeling in approximate original contour and geomorphic valley fill design. In *Environmental Considerations in Energy Production*, J.R. Craynon, ed. Society for Mining, Metallurgy, and Exploration (SME), Englewood, CO, 246-254. ISBN: 978-0-87335-380-9.
- Raji, S. A., Zava, A., Jirgba, K., & Osunkunle. (2017). Geometric design of a highway using Autocad Civil 3d. *Journal of Multidisciplinary Engineering Science and Technology*, 4(6), 7415-7421.
- Rodrigues, A. (2022). "Evaluating potential soil amendments and geomorphic methods for mine land reclamation". Graduate Theses, Dissertations, and Problem Reports. 11524. <https://researchrepository.wvu.edu/etd/11524>
- Russell, H., "Soil and Slope Stability Study of Geomorphic Landform Profiles versus Approximate Original Contour for Valley Fill Designs" (2012). *Graduate Theses, Dissertations, and Problem Reports*. 4914. <https://researchrepository.wvu.edu/etd/4914>
- Russell, H., Quaranta, J. D. (2013). Slope stability analysis of geomorphic landform profiles versus approximate original contour applied to valley fill designs. In *Environmental Considerations in Energy Production*, J.R. Craynon, ed. Society for Mining, Metallurgy, and Exploration (SME), Englewood, CO, 415-423.
- Santos, I.L., L.C. Hopkinson, J.D. Quaranta, L. Cyphers, and P. Ziemkiewicz. (2023). Field testing of geomorphic landform design features in Central Appalachia. *Reclamation Sciences*, 1: 2-12. DOI: 10.21000/RCSC-202200006.
- Schor HJ, & Gray DH. (2007). *Landforming: an environmental approach to hillside development, mine reclamation and watershed restoration*. John Wiley & Sons.
- Sears, A. E. (2012). The Integration of Geomorphic Design into West Virginia Surface Mine Reclamation. Graduate Theses, Dissertations, and Problem Reports. 4916. <https://researchrepository.wvu.edu/etd/4916>
- Sears, A., Bise, C., Quaranta, J.D., Hopkinson, L. (2013). Methodology for geomorphic landform design of valley-fills in Appalachia surface mine reclamation. In *Environmental Considerations in Energy Production*, J.R. Craynon, ed. Society for Mining, Metallurgy, and Exploration (SME), Englewood, CO, 397-404.



- Sears, A. E., Bise, C. J., Quaranta, J. D., & Hopkinson, L. C. (2014). Field and modeling study for stream mitigation on surface mine sites in West Virginia. *Mining Engineering*, 66(5), 48–53.
- Sears, A.E., L.C. Hopkinson, J.D. Quaranta. 2018. Predicting erosion at valley fills with two reclamation techniques in mountainous terrain. *International Journal of Mining, Reclamation and Environment*. 34(4): 223-237. DOI: 10.1080/17480930.2018.1516938
- Silva, A. R. (2023). *Evaluating potential soil amendments and geomorphic methods for mine land reclamation*. M.S., West Virginia University
- Sinclair, H. 2014. An introduction to Earth Surface Process. *Earth Syst. Environ.*  
<https://doi.org/10.1016/B978-0-12-409548-9.05903-0>
- Smith, Titus C., "Condition and Modeling Assessment of Geomorphic Landform Design on Coal Refuse Impoundments" (2023). Graduate Theses, Dissertations, and Problem Reports. 11725.
- Snyder, M. W. 2013. Hydrologic Response of Alternative Valley Fill Reclamation Designs. Graduate Theses, Dissertations, and Problem Reports. 399.  
<https://researchrepository.wvu.edu/etd/399>
- Stawovy, J., “Strength Properties of Coal Slurry Impoundment Materials under Monotonic Stress Conditions.” MSCE Theses, West Virginia University, 2011.
- Tailor D, & Shrimali NJ. (2016). Surface runoff estimation by SCS curve number method using GIS for Rupen-Khan watershed, Mehsana district, Gujarat. *J Indian Water Resour Soc*, 36: 1–5.
- Technical Innovation and Professional Services (TIP). 2010. CAD 301: Carlson Mining; Field, Hydrology and Natural Regrade for Permitting and Reclamation. U.S. Dept of interior, Office of Surface Mining Reclamation & Enforcement.
- Thompson, Derrick. Trihydro. 2021. Applying Geomorphic Reclamation to Mine Sites and Disturbed Lands. Accessed November 6, 2022. <https://www.trihydro.com/news/news-details/2020/07/22/applying-geomorphic-reclamation-to-mine-sites-and-disturbed-lands>
- Tolikonda, R., and Quaranta, John, D., “Environmental factors affecting geotextile filter design in coal refuse impoundments,” *International Journal of Mining, Reclamation and Environment*, DOI:10.1080/17480930.2011.603511, August 2011.
- Tolikonda, Rajesh, “Nonwoven Geotextile Filtration Performance with Coal Refuse.” MSCE Thesis, West Virginia University, 2010.
- U.S. Energy Information Administration. 2022. Coal explained. Accessed November 11, 2022. <https://www.eia.gov/energyexplained/coal/>
- U.S. Office of Surface Mining Reclamation and Enforcement, Pittsburgh, PA 15220, Michael, P. R., Hopkinson, L. C., DePriest, N., & Quaranta, J. D. (2015). Methodology for applying geomorphic reclamation to excess spoil fills in west virginia. *Journal American Society of Mining and Reclamation*, 4(1), 57–72. <https://doi.org/10.21000/JASMR15010057>
- United States Department of Agriculture (USDA), Natural Resources Conservation Service. 2004. National Engineering Handbook, title 210–VI. Part 630, chapter 10. Accessed November 06, 2022.  
<https://directives.sc.gov.usda.gov/OpenNonWebContent.aspx?content=17752.wba>

- United States Department of Agriculture (USDA), Natural resources conservation service, Conservation Engineering Division. 1986. Urban hydrology for small watersheds (TR-55). Technical Release 55, June. Accessed November 1, 2022.  
<https://www.hydrocad.net/pdf/TR-55%20Manual.pdf>
- United States Department of Agriculture (USDA), Natural resources conservation service. 2019. Web Soil Survey. Accessed November 1, 2022.  
<https://websoilsurvey.sc.egov.usda.gov/App/WebSoilSurvey.aspx>
- United States Department of Agriculture (USDA), Natural Resources Conservation Service. 1985. Eng. Simplified dam-breach routing procedure (TR-66). Technical Release 66, September. Accessed November 06, 2022.  
<https://directives.sc.egov.usda.gov/OpenNonWebContent.aspx?content=22165.wba>
- US Department of Commerce, National Oceanic and Atmospheric Administration, National Weather Service (2023) *PF Data Server-PFDS/HDSC/OWP*. Available at:  
<https://hdsc.nws.noaa.gov/hdsc/pfds/>.
- Web soil survey—Home*. (n.d.). Retrieved March 21, 2024, from  
<https://websoilsurvey.nrcs.usda.gov/app/>
- WVDEP. 2018. Energy Marketing Slurry Impoundment – Permit 0-26-84. Office of abandoned mine lands and reclamation. Division of land restoration.
- WVDEP. 2020. Energy Marketing Slurry Impoundment Permit: 0-26-84 Reclamation as-built. - Office of abandoned mine lands and reclamation. Union District, WV.
- WVDEP. 2022. Personal communication with the author.
- Zeng, X., Goble, JA and Fu L., (2008), “Dynamic properties of coal waste refuse in a tailings dam”, ASCE Geotechnical Special Publication No., 181, 1-14

## Geomorphic Landform Design to Optimize Impoundment Closure

### Technical Transfer Products

#### Publications

- Hopkinson, L., T. Smith, S. Dalen\*, E. Wimer\*\*, B. Watters\*, J. Quaranta. 2023. Exploring erosion of reclaimed coal refuse impoundments. *Environmental Connection: The Official Publication of the International Erosion Control Association*. 18(3): 12-14. (peer reviewed)
- Jawad, Z., J. Quaranta, L. Hopkinson. Geomorphic methods as a reclamation approach for a coal mine slurry impoundment. To be submitted for peer review by May 2024.

#### Poster Presentations (Presenter in bold)

- **Jawad\***, Z., L. Hopkinson, J. Quaranta. 2023. Geomorphic methods as a reclamation approach for a coal mine slurry impoundment. All Voices as One Conference, September 21. West Virginia University.

#### M.S. Theses and Ph.D. Dissertation

- Rodrigues Silva, Amanda, "Evaluating potential soil amendments and geomorphic methods for mine land reclamation" (2022). Chapter 3. *Graduate Theses, Dissertations, and Problem Reports*. 11524. <https://researchrepository.wvu.edu/etd/11524>
- Smith, Titus C., "Condition and Modeling Assessment of Geomorphic Landform Design on Coal Refuse Impoundments" (2023). *Graduate Theses, Dissertations, and Problem Reports*. 11725. <https://researchrepository.wvu.edu/etd/11725>
- Jawad, Zainab. Dissertation. Chapter 2. Geomorphic methods as a reclamation approach for a coal mine slurry impoundment. (*Expected 2025*).



## Geomorphic Landform Design to Optimize Impoundment Closure

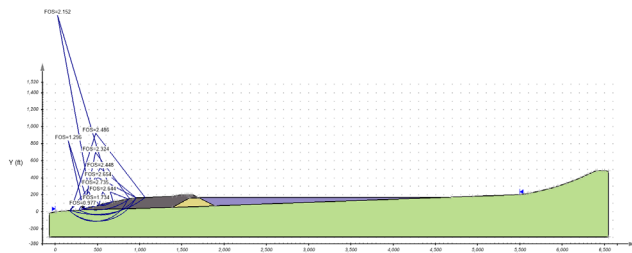
**Authors:** John Quaranta and Leslie Hopkinson  
**Affiliation:** West Virginia University, Morgantown, WV

### Project Description and Objectives:

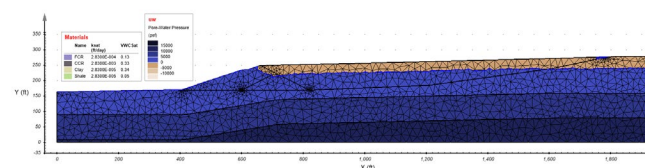
Restoration of abandoned mine lands from bond forfeited mining permits and pre-law sites is ongoing in Appalachia and across the United States. One potential reclamation technique to reclaim these areas is geomorphic landforming also termed geomorphic landform design (GLD). The geomorphic approach attempts to approximate the long-term, steady state landform condition, leading to reduced erosional adjustment as compared to standard engineered designs. The objectives of this research were to apply geomorphic landform design principles to investigate closure design alternatives.

### Applicability to Mining and Reclamation:

This research investigated GLD principles for impoundment reclamation. These areas have unique and challenging long-term structural stability elements, public safety hazards and failure outcomes, and environmental legacy issues.



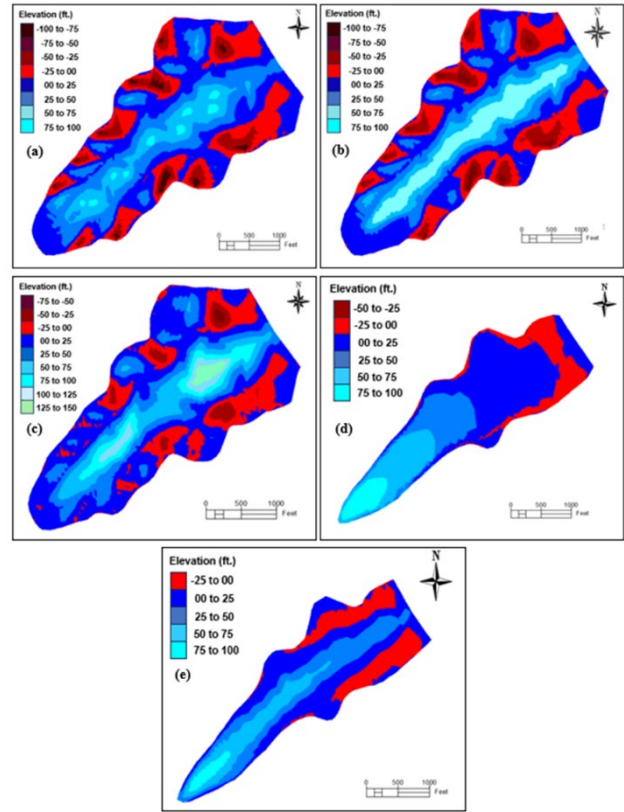
Slope stability testing was completed.



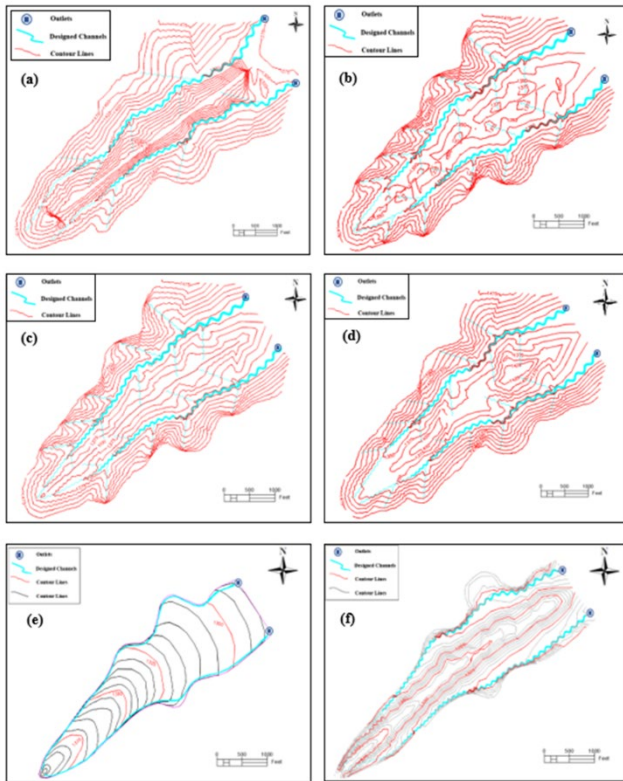


Highlights:

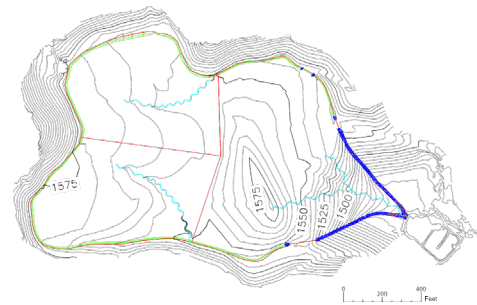
- Six reclaimed refuse impoundments, one active freshwater impoundment, and one active impoundment were visited to observe site conditions.
- Conceptual geomorphic landform design iterations were created for two impoundments. Slope and seepage analysis was completed. The design iterations were evaluated for hydrologic response.



Cut (red hatches) and fill zones (blue hatches) of design iterations for Federal Mine #2: a) Uniform-50, b) Uniform-90, c) T-E, d) Conventional, and e) Conventional-GLD.



Design iterations for Federal Mine #2: a) Uniform-200, b) Uniform-50, c) Uniform-90, d) T-E, e) Conventional, and f) Conventional-GLD.



Preliminary geomorphic design iteration of Century impoundment with multiple sub-basins.

Fact Sheet Contact Information

PRINCIPAL INVESTIGATOR (PI):

John Quaranta, jdquaranta@mail.wvu.edu  
304-293-9942, West Virginia University

PROJECT TECHNICAL REPRESENTATIVE (PTR):

Self, Stefanie, Sself@osmre.gov  
Office of Surface Mining Reclamation and Enforcement



# Geomorphic Methods as a Reclamation Approach for a Coal Mine Slurry Impoundment

Zainab Jawad<sup>1</sup>, Leslie Hopkinson<sup>2</sup>, John Quaranta<sup>2</sup>

<sup>1</sup>Graduate Research Assistant, Wadsworth Department of Civil & Environmental Engineering, West Virginia University, Morgantown, WV.

<sup>2</sup>Associate Professor, Wadsworth Department of Civil & Environmental Engineering, West Virginia University, Morgantown, WV.

## Background

- Coal Refuse impoundments are coal waste collection basins located between adjacent mountains built by damming rocks and coarse coal refuse generated during mining. The coal mining industry uses coal refuse impoundments for the disposal of fine coal refuse slurry (Daniels et al., 2018).
- Fine coal refuse is associated with weak strength and relatively low permeability. Due to the low permeability of the material, excessive pore-water pressure would easily build up and further reduce shear strength (Yu et al., 2019).
- It is possible in some cases that the fine-grained coal refuse could turn into a viscous fluid which could build pressure against the dam containing it, resulting in dam failure. For that reason, slurry impoundments pose a threat to communities (Yu et al., 2019).
- Consequently, regulations have been created to govern impoundment construction and closure and integrate reclamation in the process.
- Geomorphic landform design (GLD) is considered a promising reclamation approach that is gaining acceptance and could outcompete conventional reclamation procedures (Bugosh, 2004).

## Goal and Objectives

**Research Goal:** Apply the GLD principles to the coal mine slurry impoundment structure at Federal No.2 Coal Mine located in West Virginia to generate a design that is stable, hydrologically balanced, aesthetically appealing, and cost-effective.

### Research objectives:

- Create a reclamation design for the slurry impoundment structure.
- Determine whether changing the elevation of a mid-ridgeline extending across the impoundment would affect the peak runoff that would accumulate over time.
- Create a representative layout of the reclamation plan that the West Virginia Department of Environmental Protection (WVDEP) intends to follow to reclaim the slurry impoundment structure.
- Compare the created designs in terms of material movements and hydrologic response.

## Methods

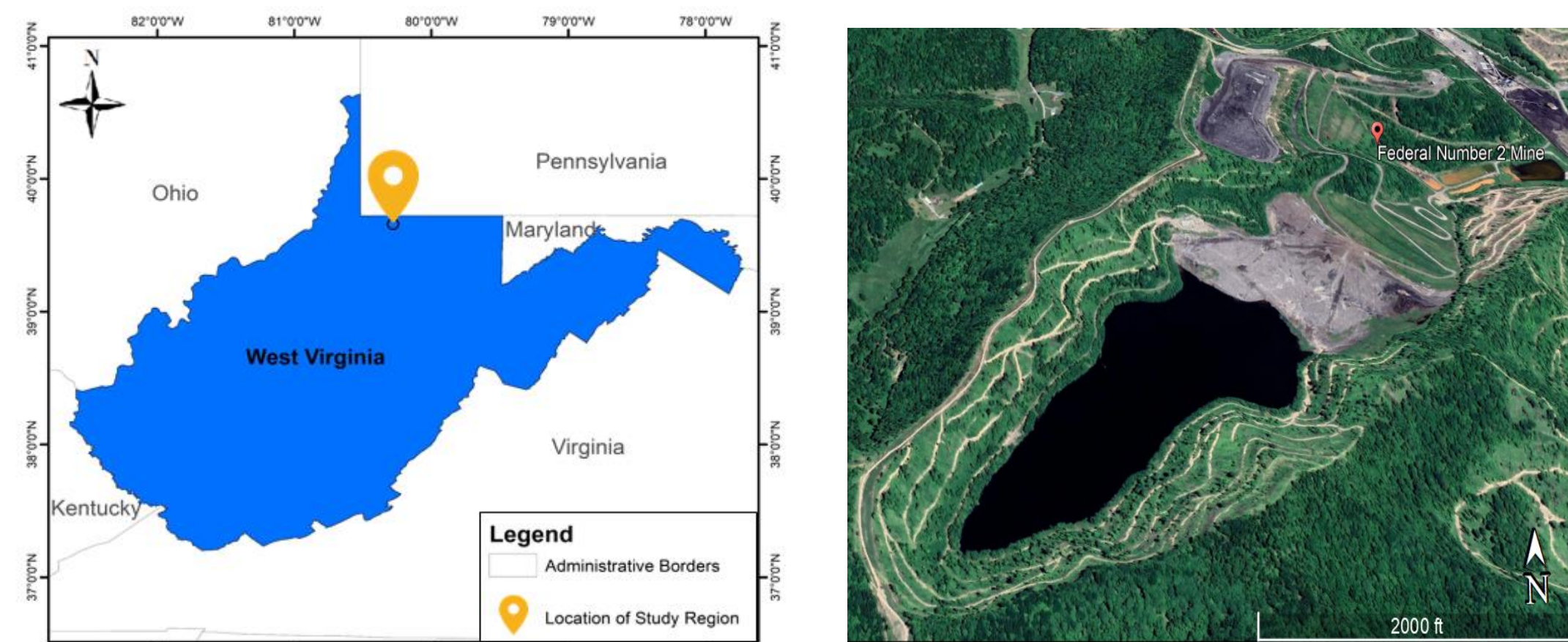


Figure 1: Study Area - Federal No. 2 Coal Mine located near Blacksville in Monongalia County, West Virginia

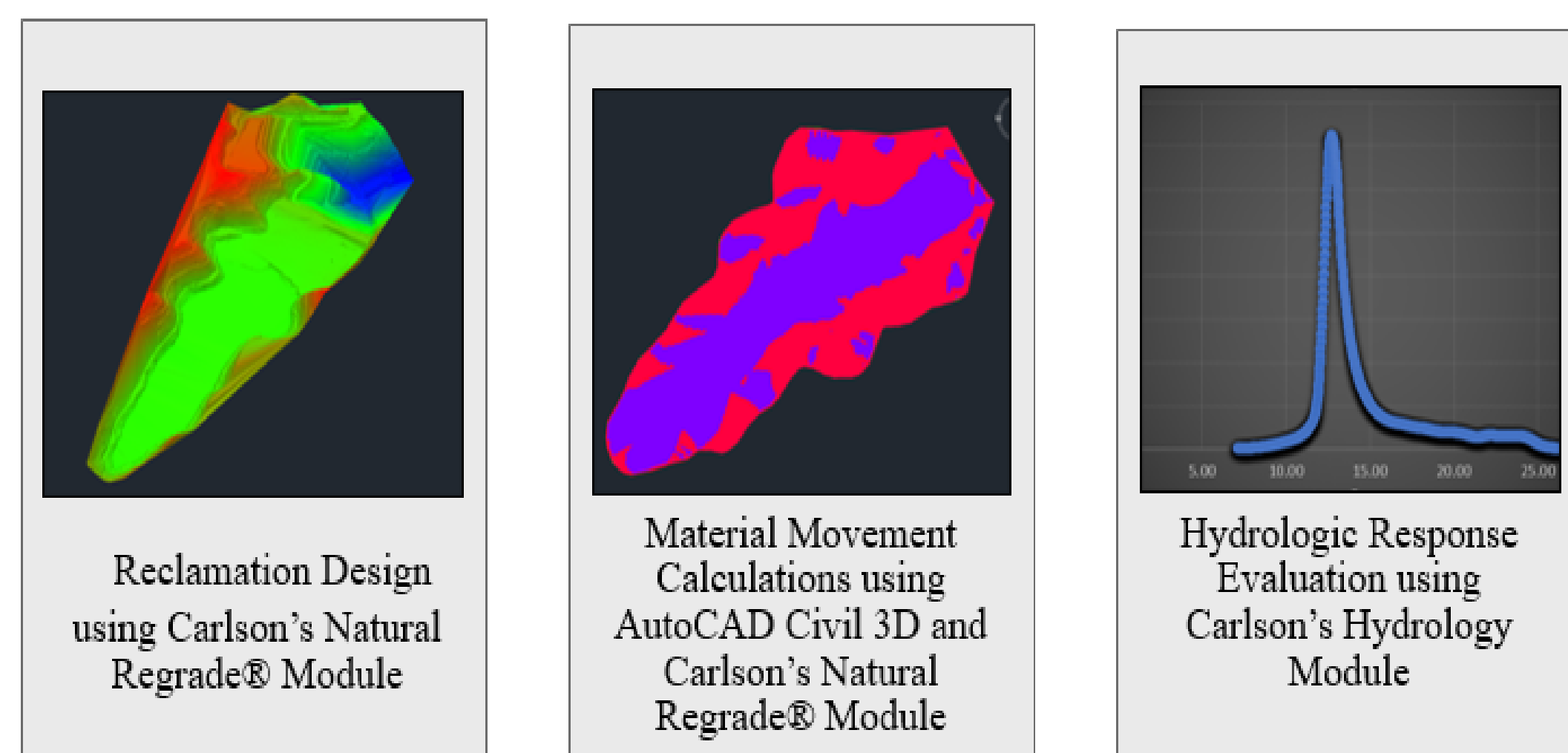


Figure 2: Tasks and Methods Used to Achieve the Goal of the Research Work

## Acknowledgment

The work described in this publication was supported by Grant/Cooperative Agreement Number S21AC10058 from the Office of Surface Mining, Reclamation, and Enforcement. Its contents are solely the responsibility of the authors and do not necessarily represent the official views of the OSM. This work is also in collaboration with the West Virginia Department of Environmental Protection, Office of Special Reclamation.

## Results: Conceptual Reclamation Designs

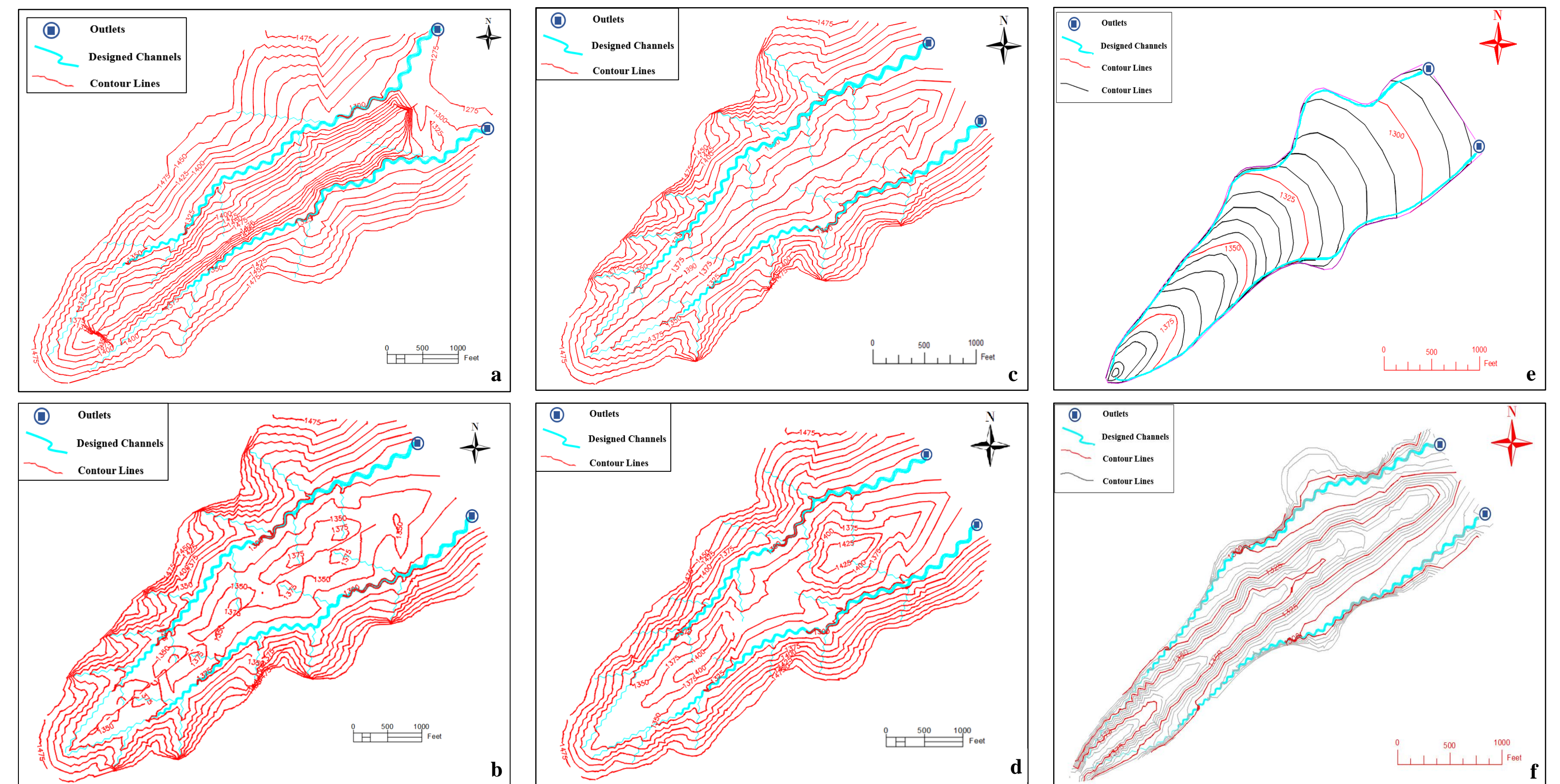


Figure 3: Contour Lines of Created Conceptual Reclamation Designs

Table 1: Designs Description Summary

Design Iterations	Name	Description	Ground Slope	Elevations of Mounded Material
a	U-200	Uniform elevation of mounded material across the extent of the impoundment	1.73H:1V	1,500 ft.
b	U-50	Uniform elevation of mounded material across the extent of the impoundment	3H:1V	1,350 ft.
c	U-90	Uniform elevation of mounded material across the extent of the impoundment	3H:1V	1,390 ft.
d	T-E	Two elevated areas and a saddle	2H:1V and 3H:1V	1,400 ft. – 1,425 ft. and a saddle of 1350 ft.
e	WVDEP	Mounded material slopes down toward the dam; its elevation decreases from 1,390 ft at the headwater to 1,300 ft. at the dam	3H:1V	1,390 ft. and 1,300 ft.
f	WVDEP-NR	Mounded material slopes down toward the dam; its elevation decreases from 1,390 ft at the headwater to 1,300 ft. at the dam	3H:1V	1,390 ft. and 1,300 ft.

## Results: Material Movement and Hydrologic Response

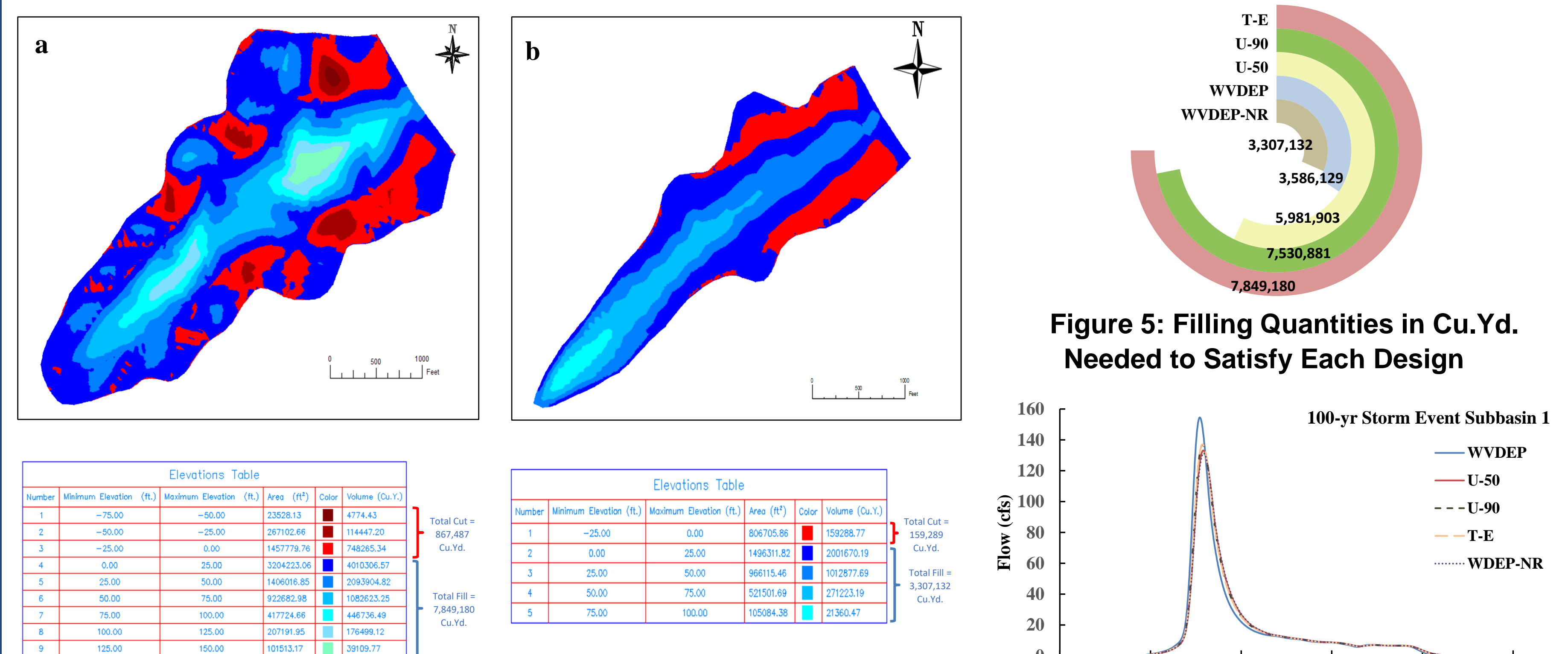


Figure 4: Cut and Fill Zones: a) T-E Model, b) WVDEP-NR Model

Figure 5: Filling Quantities in Cu.Yd. Needed to Satisfy Each Design

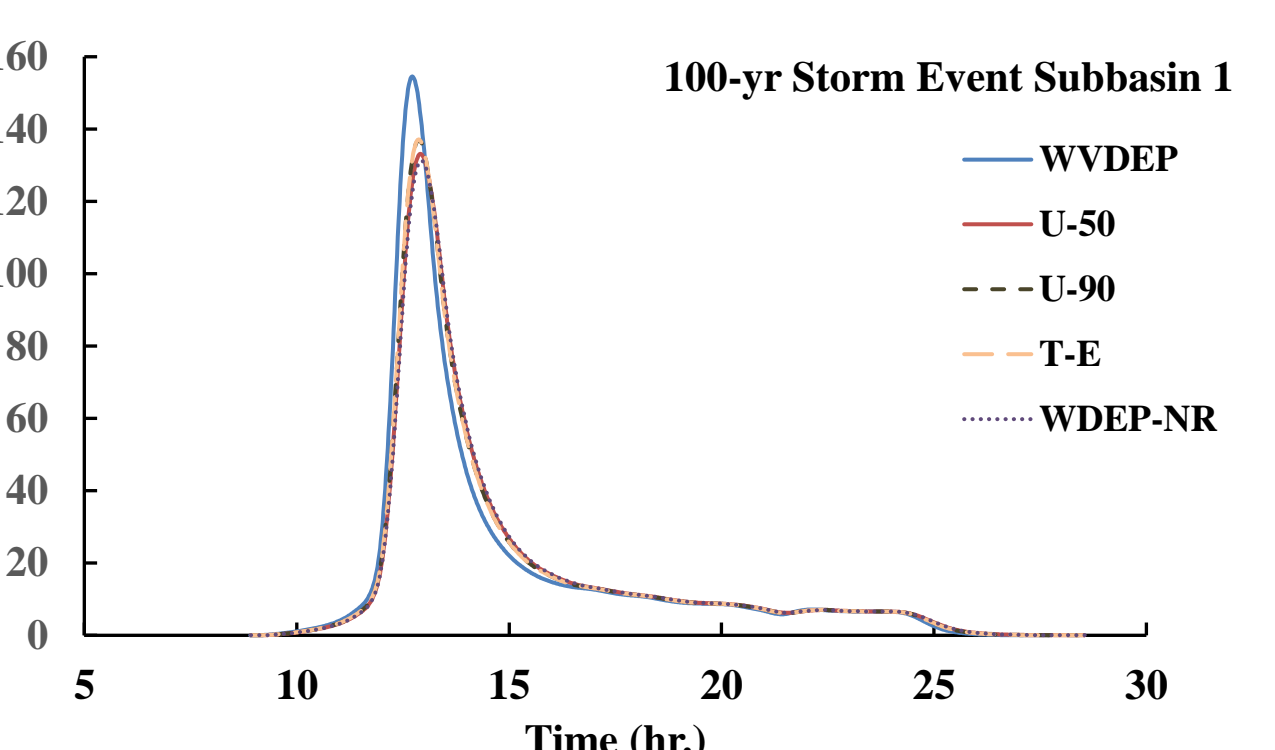


Figure 6: Runoff hydrograph for One Subbasin for the 100-year storm event

## Conclusions

The geomorphic reclamation approach to reclaim the reservoir area generated uniform contour lines with transition in slopes from convex to concave results in natural appearing landscapes. The generated uniform contour lines resulted in less backfill material needed for the design compared to the conventional reclamation approach, which may result in some cost savings. Significant differences in the peak runoff discharge among designs were not observed.

## Future Work

The effect of slope shape on mass stability and rainfall erosion resistance could be investigated through conceptual and mathematical models e.g., the SIBERIA landscape evolution model by which erosion can be overviewed, visualized, and quantified. Thus, soil displacement, loss, and deposition during a defined storm event can be determined.

## References

- Bugosh, N. (2004, April). Computerizing the fluvial geomorphic approach to land reclamation. In 2004 National Meeting of the American Society of Mining and Reclamation and the 25th West Virginia Surface Mine Drainage Task Force (pp. 240-258). Lexington, KY: ASMR.
- Carlson®, (2022). "Carlson® Natural Regrade® Manual." Carlson®: Software for Land Development Professionals.
- Daniels, W. L., Stewart, B. R., & Zipper, C. E. (2018). Reclamation of coal refuse disposal areas. Yu, H., Zeng, X., & Michael, P. R. (2019). Geotechnical properties and flow behavior of coal refuse under static and impact loading. Journal of Geotechnical and Geoenvironmental Engineering, 145(7), 04019024.